Monitoring Nociception by Analyzing Gene Expression Changes in the Central Nervous System of Mice

Dissertation

zur

Erlangung der naturwissenschaftlichen Doktorwürde

(Dr. sc. nat)

vorgelegt der

Mathematisch-naturwissenschaftlichen Fakultät

der

Universität Zürich

von

Igor Asner

von

St. Cergue VD

Promotionskomitee

Prof. Dr. Peter Sonderegger

Prof. Dr. Kurt Bürki

Prof. Dr. Hanns Ulrich Zeilhofer

Dr. Paolo Cinelli (Leitung der Dissertation)

Zürich, 2010

Table of content

Table of contents

Table of contents

Table of contents

Curriculum vitae

Igor Asner

Date of Birth : May 31st, 1980
Citizenship : Switzerland
Marital status : Single, no children

Professional Experience

01/ 2006 – Today **PhD Student in Biology**
Institute for Laboratory Animal Science, University of Zurich
Supervisor: Prof. K. Bürki and Dr. Paolo Cinelli

Research Theme: Monitoring of nociception by measuring gene expression in the central nervous system of mice

05/ 2007 – 08/2008 **Freelance scientific clinical trial collaborator**
BioPartners GmbH
Supervisor: Dr. C. Savoy, CSO

Function: Presentation and figure preparation for Phase III clinical trial reports on the sustained-release recombinant Human Growth Hormone
Experience with ICH/GCP guidelines and clinical trial operations

06/ 2006 – Today **Tutor, Introductory Course in Laboratory Animal Science (Module 1)**
Institute for Laboratory Animal Science, University of Zurich
Supervisor: Dr. H-P. Käsermann

10/ 2004 – 07/ 2005 **Secondary School Biology and Mathematics teacher**
Collège des Coudriers, Geneva

09/ 2004 – 12/ 2004 **Collaborator on the "Quality of Life Assessment for Elderly People with Dementia" research project**
Psychology Faculty, University of Geneva
Supervisor; Prof. N. Von Steinbüchel, University of Geneva
Function: Interviews of patients living with dementia

08/ 2003 – 10/ 2003 **Freelance journalist**

09/ 2002 – 04/ 2004 **Diploma Student in Biology**
Neuroscience Institute, Swiss Federal Institute of Technology in Lausanne
Supervisor: Prof. P. Aebischer and Prof. W. Pralong

Research Theme: Establishment of a cell line for the in-vitro study of the GDNF receptor

Education

01/ 2006 – Today **PhD in Biology**
University of Zurich, Switzerland

09/ 2002 – 04/ 2004 **Diploma in Biology**
University of Geneva and Swiss Federal Institute of Technology in Lausanne, Switzerland

09/ 1998 – 06/ 2002 **Licence of Science in Biology**
University of Geneva, Switzerland

09/ 1995 – 06/ 1998 **High school education**

International School of Ferney-Voltaire, France

Scientific Baccalauréat, specialisation in Biology
KMK German Language Diploma, Advanced Level
General Certificate of Secondary Education: English, English Literature and Mathematics

Languages

French:	Mother tongue
English:	Excellent
German:	Excellent
Croatian:	Excellent

Publications

"Genetic vasectomy - Overexpression of Prm1-EGFP fusion protein in elongating spermatids causes dominant male sterility in mice" Sabine Haueter, Miyuri Kawasumi, Igor Asner, Urszula Brykczynska, Paolo Cinelli, Stefan Moisyadi, Kurt Bürki, Antoine H.F.M. Peters, Pawel Pelczar, Genesis 2010

"Analysis of physiological and behavioural parameters in mice after toe clipping as newborns" D. C. Schaefer, I. N. Asner, B. Seifert, K. Bürki, and P. Cinelli, Laboratory Animals. Lab Anim. 2010 Jan;44(1):7-13

"Detection of pain in laboratory animals via gene expression?" I. Asner, P. Cinelli, 3R-Info Bulletin, February 2009

To my family…

Summary

Monitoring pain in laboratory animals is essential from an animal welfare point of view as experimental procedures often involve surgeries, or other potentially harmful interventions. Moreover, the genetic modifications induced in disease modeling might impair the animal and induce some suffering. Properly treating pain is not only necessary for the animal wellbeing, but also eliminates possible data biases caused by nociception. Inflammation can also influence data and should therefore also be treated appropriately. Laboratory mice instinctively hide all signs of suffering. A routine observation and scoring of pain is therefore very difficult and highly subjective. More precise behavioral tests or measurements of blood corticosterone imply some additional stressful handling, which might further influence the experimental data. In this work, we investigated the feasibility of an innovative monitoring of nociception based on the detection of gene expression level changes in the central nervous system. This method could be applied to sentinel animals to assess the level of pain induced by a specific procedure.

A wide set of elements is necessary for the transduction of the nociceptive message from the periphery to the central nervous system and its integration in brain. Monitoring the expression level changes of the genes encoding elements might help to identify genetic patterns characteristic of longer lasting nociception and might be used to monitor pain. In the first part of this project, we screened the literature and chose a set of 226 genes, which induce altered pain-related behaviors in transgenic animals experiments. We then built a low-density 70mer oligonucleotide microarray, and developed a single-color hybridization and normalization protocol, to detect changes in the expression level of these genes. This protocol could be validated in a gene profiling experiment assessing the expression level differences between the brainstems, cortices and hippocampi of naïve NMRI mice. The normalized fold changes observed had similarity rates ranging from 66.7 to 100% with published whole genome microarray data comparing the expression levels in these parts of the brain. The experiments to measure gene expression changes linked to nociception were performed on NMRI mice, which had been subjected to a telemetric apparatus implantation, which induces a heart rate increase characteristic of pain in the post-operative recovery phase, and on control animals from the same strain, which underwent the same anesthetic and analgesic protocol, without surgery. A two-color microarray experiment was performed on whole brains. This experiment did not lead to any convincing data and was biased by a dye imbalance. A more precise analysis was therefore performed to monitor eventual expression changes in the brainstems, cerebelli, cortices, hippocampi and spinal cords of these animals. For these experiments, we followed the single color hybridization protocol, which we had previously developed. However, these measurements gave only a few artefactual results, which could not be confirmed by Real-Time PCR measurements.

In the second part of the project, a high-throughput Real-Time PCR analysis was performed on the 26 most promising candidate genes, to test if a more sensitive technique would detect some changes that the microarray missed. The experiments were carried out on 6 animals per condition, and the analyzed parts of the central nervous system were the cortex, the brainstem, the hippocampus, and the lumbar dorsal root ganglia. Only one gene showed a significant 2.2 time higher expression in the cortices of the operated animals: the serotonin receptor 5HTr1A. This difference could not be observed in an inflammatory pain model. Taken together, our data shows that the 226 commonly known "pain genes" are therefore poor candidates for the establishment of a routine microarray test to monitor nociception.

In the final part of the project, we performed a whole genome analysis using Affymetrix GeneChip® Mouse Exon 1.0 ST Arrays, on the spinal cords of 6 mice which underwent our surgical protocol and 6 control mice, in order to identify new candidate genes for the monitoring of nociception. After filtering, and a functional classification, we focused on 166 downregulated genes, and 96 upregulated genes, which were mostly involved in cytoskeleton, cell motility, extracellular matrix and inflammation. A Bi-Clustering meta-analysis identified 21 downregulated and 17 upregulated genes, which were involved in axonal sprouting and neuronal rearrangements. Another analysis of the 410 most relevant alternatively spliced genes also revealed that 10% of them were linked to cell motility. Taken together, these data indicate that genes involved in cell migration linked to inflammation, or in neuron movements characteristic of synaptic plasticity show a differential expression or are subjected to alternative splicing, and should be considered as potent candidate genes, for the establishment of a routine microarray tool designed to monitor nociception in the spinal cord of sentinel animals subjected to a potential painful experiment. Recent developments in the microarray technology have increased their sensitivity. Moreover, subtle events such as the alternative splicing underlying nociception in the spinal cord can now also be monitored. These assets open the door to new possibilities in the monitoring of pain.

Zusammenfassung

Die genaue Überwachung von Versuchstieren ist aus Tierschutzgründen sehr wichtig, denn Operationen oder andere schmerzhafte Behandlungen sind Bestandteil vieler Experimente. Zusätzlich können induzierte genetische Veränderungen in Krankheitsmodellen das Tier beeinträchtigen und Leiden verursachen, welches mit Schmerzmitteln behandelt werden sollte. Eine angemessene Schmerzbehandlung ist nicht nur notwendig für das tierische Wohlbefinden, sondern verhindert auch mögliche Datenabweichungen aufgrund von Schmerz und Entzündungsprozessen. Labormäuse verstecken instinktiv sämtliche Anzeichen von Leiden. Die routinemässige Beobachtung und objektive Erfassung von Schmerz ist deshalb sehr schwierig und überaus subjektiv. Genauere Verhaltensexperimente oder die Messung von Corticosteron im Blut sind mit Stress verbunden, was zu einer zusätzlichen Beeinflussung experimenteller Daten führen kann. Im Rahmen dieser Arbeit wurde die Eignung einer neuen Methode zur Schmerzerfassung untersucht, welche auf der Detektion von Veränderungen der Genexpression im Zentralen Nervensystem beruht.

Der Übermittlung eines Schmerzsignals von der Peripherie zum Zentralen Nervensystem und seiner Integration ins Gehirn liegt ein umfangsreiches Zusammenspiel von Signalen zugrunde. Die Überwachung von Änderungen im Expressionsgrad der diesen Signalelementen zugrunde liegenden Genen könnte hilfreich dabei sein, genetische Muster zu identifizieren, welche charakteristisch sind für längerdauernden Schmerz und somit zur Schmerzbeobachtung beitragen könnten.

Im 1. Teil dieses Projekts haben wir zunächst eine Gruppe von 226 Genen identifiziert, welche mit schmerzbedingten Verhaltensweisen in transgenen Tieresperimenten assoziiert werden. Dann konstruierten wir einen „low-density 70mer oligonucleotide microarray“ und entwickelten ein Protokoll für eine 1-Farben Hybridisierung und Normierung um Veränderungen im Expressions-Niveau dieser Gene zu detektieren. Dieses Protokoll konnte in einem Gen-Profiling-Experiment validiert werden, welches Unterschiede im Expressionsgrad zwischen Hirnstamm, Hirnrinde, und Hippocampus dreier naiver NMRI Mäuse analysierte. Die hier beobachteten normalisierten „fold changes“ zeigten Ähnlichkeiten im Bereich von 66.7 bis 100% verglichen mit bereits publizierten Daten aus das ganze Genom erfassenden Microarrays , welche die Expressionsniveaus in gleichen Teilen des Gehirns vergleichen.

Experimente zur Messung von mit Schmerz verbundenen Änderungen in der Gen-Expression wurden mit NMRI Mäusen durchgeführt. Diese Mäuse wurden einer Telemetrie-Chip Implantation unterzogen, welche eine für die post-operative Phase charakteristische Erhöhung der Herzfrequenz hervorruft. Kontroll-Mäuse desselbes Stammes waren ebenfalls Bestandteil dieses Experiments, sie wurden demselben Anästhesie- und Analgesie Protokoll unterzogen, allerdings ohne den operativen Eingriff. Es wurde ein 2-Farben-

Microarray an kompletten Gehirnen durchgeführt. Dieses Experiment führte nicht zu aussagekräftigen Resultaten, deshalb wurde eine präzisere Analyse durchgeführt, um mögliche Expressionsänderungen in Hirnstamm, Kleinhirn, Hirnrinde, Hippocampus und Rückenmark zu erfassen. Bei diesen Versuchen folgten wir einem von uns im Vorfeld entwickelten Ein-Farben Hybridisierungs-Protokoll. Diese Experimente ergaben jedoch nur wenige, artefakt-ähnliche Resultate, welche nicht durch Real-Time PCR Messungen bestätigt werden konnten.

Eine Real-Time PCR Analyse mit hohem Durchsatz wurde im Rahmen des 2. Projektteils mit den 26 vielversprechendsten Kandidatengenen durchgeführt, um herauszufinden, ob eine empfindlichere Messtechnik Veränderungen detektieren könnte, welche eventuell vom Microarray nicht erkannt wurden. Für diese Versuche wurden 6 Tiere pro Bedingung verwendet und es wurden Hirnrinde, Hirnstamm, Hippocampus und die dorsalen Spinalganglien aus dem Lendenbereich untersucht. Nur ein Gen wies eine signifikante, um das 2.2 fache erhöhte Expression in der Hirnrinde der operierten Tiere auf: der Serotonin Rezeptor 5HTr1A. Dieser Unterschied konnte an einem Entzündungsschmerzmodell nicht nachgewiesen werden. Insgesamt gesehen sind die 226 als „Schmerzgene“ bekannten Gene deshalb ungeeignet für die Etablierung eines routinemässig einsetzbaren Microarrays zur Überwachung der Schmerzwahrnehmung.

Im letzten Teil dieses Projekts verwendeten wir Affymetrix GeneChip Mouse Exon 1.0 ST Arrays zur Analyse des gesamten Genoms des Rückenmarks von 6 Mäusen, welche dem Operations-Protokoll unterzogen wurden, sowie 6 Kontrollmäusen, mit dem Ziel neue Kandidatengene zur Überwachung der Schmerzwahrnehmung zu identifizieren. Nach vorangegangener Filtierung und funktioneller Klassifizierung konzentrierten wir uns auf 166 herunter- sowie 96- nach oben regulierte Gene, welche hauptsächlich Bestandteil sind von Zytoskelett, Zellbeweglichkeit, Extrazellulärer Matrix und Endzündungsprozessen. Eine „Bi-Clustering“ Meta-Analyse führte zur Identifizierung von 21 nach unten und 17 nach oben regulierten Genen, welche eine Rolle spielen bei der Ausbreitung von Axonen und bei neuronaler Neuanordnung. Zusätzlich erbrachte eine Analyse der 410 relevantesten alternativ gespleissten Gene, dass 10% von ihnen mit Zellbeweglichkeit in Verbindung stehen. Insgesamt zeigen diese Daten, dass Gene, welche mit entzündungdbedingter Zellwanderung oder mit für synaptische Plastizität charakteristische neuronale Bewegung in Verbindung stehen, eine unterschiedliche Expression aufweisen oder alternativem Spleissen unterzogen werden. Sie sollten deshalb als mögliche Kandidatengene für die Etablierung eines routinemässig-anwendbaren Microarray in Erwägung der Schmerz-Wahrnehmung unter Verwendung des Rückenmarks von Sentineltieren vor einem potenziell Schmerzhaften Versuch herangezogen werden könnten

1 Introduction

Genes dictate a wide variety of biological processes, and their role is constantly better understood. Since Mendel's observations of inherited traits and phenotypes, a lot of progress has been made. Many diseases or predispositions have been linked to specific mutations and the general knowledge on genes is refined every day. The development of transgenic technology has allowed to knock-out or overexpress genes in cells to precisely study their function. The generation of transgenic animal models took research further by allowing the assessment of a gene's relevance in a complete organism, and has opened the door to the study of the in-vivo consequences of a genetic modification. In parallel, genomic studies have also shown that genes are not static and do not have a constant expression level. Their expression can be repressed or enhanced by external or internal stimuli, and dictate a complex interplay of cellular processes, which are highly sensitive and adaptable. Understanding how the expression of genes specific to the central nervous system is altered in precise physiological, psychological, and behavioral conditions is a vast research domain, which could lead to the development of new diagnostic tools for complex processes such as pain and stress, which are difficult to measure objectively in laboratory animals.

1.1 Pain and nociception

The International Association for the Study of Pain (IASP) defines pain as an unpleasant sensory and emotional experience associated with actual or potential tissue damage, or described in terms of such damage. This word can describe a physical discomfort, or an emotional distress, and often a painful situation arises from the combination of these two components. In research, pain is described a sensory message, which warns an organism of a potential danger linked to an eventual injury or damage (Scholz and Woolf, 2002). Due to their unpleasant characteristics, painful experiences are memorized and play an important role in the learning processes of vertebrates. Pain avoidance is essential for the survival of species, as it brings animals to run away from their predators and to avoid potential harmful situations.

It has been shown that the development of an animal's behavior can be influenced by painful stimuli. Male rats exhibit longer latencies than untreated control animals at the tail flick test, a common test for thermal pain, when they have been exposed to repeated morphine injections as pups (P1-P7) (Bhutta et al., 2001) They also show less locomotor activity than control animals, when they have been subjected as pups to repeated formalin injections causing inflammatory pain (P1-P7) (Bhutta et al., 2001). Lidow et al have also demonstrated that short-term exposure of rats neonates to an

inflammatory pain induced by a single carrageenan injection in the hindpaw induces long-term alterations in the withdrawal responses of this hindpaw to noxious heat and mechanical stimulation that persist in adult animals (Lidow et al., 2001). By performing wheat germ agglutinin-horseradish peroxidase stainings in the dorsal horns of adult rats, which had been subjected to a complete Freund's adjuvant injection in the left hindpaw, Ruda et al. were able to show permanent segmental changes in primary nociceptive afferent axons, linked to this inflammatory treatment. The adult animals showed a significantly higher density of terminal stainings in the left dorsal horn than in the right one, in the lumbar and sacral region of the spinal cord. They also responded more rapidly to the formalin test (Ruda et al., 2000). Taken together, these studies show that painful stimulations experienced during development can induce anatomical and physiological changes, which can explain persistent altered reactions linked to pain in the adulthood.

Pain is a subjective sensation and is therefore difficult to study objectively. It is a complex experience. Not only does it involve the transduction of noxious stimuli, but it also triggers an emotional reaction. Personal and social empathic experiences shape everyone's perception of pain (Akitsuki and Decety, 2009). Moreover, recent studies have shown that hormone balances and gender influence the way pain is experienced by an individual. Women have generally a higher risk of developing chronic pain (Paller et al., 2009), and both male and female gonadal steroids are key factors in the gender differences in pain perception (Mensah-Nyagan et al., 2009; Paller et al., 2009). Because of all these aspects, the assessment and the monitoring of pain is very difficult. In 2008, the Kyoto Protocol of IASP Terminology defined nociception as the "the neural processes of encoding and processing noxious stimuli" (Loeser and Treede, 2008). Because nociception relies on a series of physiological parameters, it is possible to study it objectively. Understanding the key mechanisms of nociception might provide further insights in pain processes and perception.

1.1.1. Nociceptive neurons and mechanoceptors

Two main groups of afferent sensory neurons, which differ in their size and conduction velocity, have been described: the neurons with A-fibers, and the neurons with C-fibers. These two categories also differ in their cytology. A-fibers have first been described as having light somatas with a lot of neurofilaments, and C-fibers as having dark and smaller somatas, with less neurofilaments (Lawson, 1979; Lawson and Biscoe, 1979; Lawson and Waddell, 1991). Early studies had already described two types of sensations caused by an external stimulation: a localized, distinct pricking sensation, which was attributed to A fibers mechanoceptors, and an unpleasant dull and diffuse sensation, which resulted from the stimulation of C-fibers nociceptive neurons (Collins et al., 1960; Landau and Bishop, 1953). The A-fibers were shown to be myelinated, to have the largest diameter and to

produce a rapid response, whereas the C fibers were described as non myelinated, with a small diameter and induced a slower response when stimulated. Later studies have refined these findings.

Three types of sensory neurons have been described, according to the conduction velocity of their fibers: the Aα/β-, the Aδ- and the C- fibers (Figure 1). In their study of sensory neurons innervating mouse skin, Kotzenburg et al. (1997) have shown that Aβ- fibers could be divided in two categories: the rapidly adaptive fibers (RA), which respond fast to a constant mechanical stimulation, and the slowly adaptive (SA) fibers, which show delayed discharges after similar stimulations. In adult outbred mice, the conduction velocity of RA fibers of the Saphenous nerve was 13.6 m/s, whereas for SA fibers, it had a value of 15.5 m/s. Aδ- fibers could also be divided in two categories: D hair fibers, which have a conduction velocity of 4.8 m/s and which responded to a von Frey filament stimulation of 1mN, and the high threshold mechanoceptors (MA), which respond to a stimulation of 5.6 mN and have a slower conduction velocity (7 m/s). A noxious heat stimulation revealed that MA Aδ- fibers have a mean threshold of 42.5°C and an average discharge of 15.8 action potentials per stimulus, whereas C fibers have a mean threshold of 37.6°C and an average discharge of 22 action potential per stimulus (Koltzenburg et al., 1997). Other studies have shown that neurons with Aδ- fibers can be divided into two subsets. The neurons with type I Aδ- fibers, which have a thermal threshold of 52°C and are insensitive to capsaicin, an irritant compound frequently used in pain research. Neurons with type II Aδ- fibers of 45°C and are responding capsaicin, just like neurons with C-type fibers (Nagy and Rang, 1999).

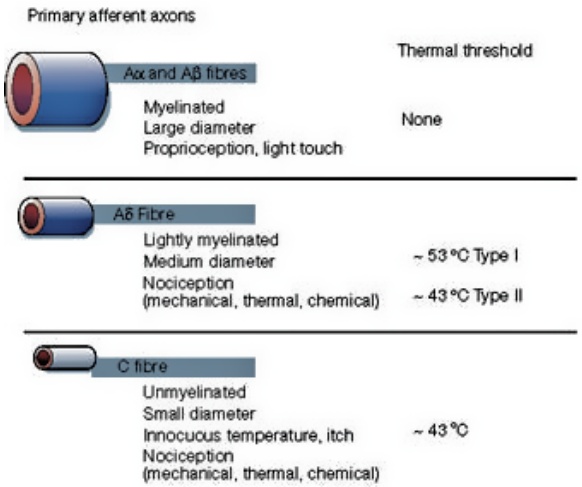

Figure 1: Adapted from Julius, D. Nature 413, 203-210 (Julius and Basbaum, 2001). The 3 types of sensory neurons and their respective thermal threshold

A common misinterpretation in pain research, is the assumption that only C- and Aδ- fibers have nociceptive properties (Julius and Basbaum, 2001). The reality is in fact more complicated. In-vivo intracellular voltage recording studies made in dorsal root ganglia neurons of young guinea pigs have demonstrated that 42% of A fibers nociceptive neurons have a conduction velocity in the Aβ range (Djouhri et al., 1998), and similar data observed in cats (Koerber et al., 1988) or rats (Ritter and Mendell, 1992) show the existence of nociceptive, and non-nociceptive fibers of the Aα/β-, the Aδ- and the C-type.

Although C fibers are commonly thought to be only transducing nociceptive signals, low threshold mechanoceptors (LTM) C-fibers, which respond to low intensity mechanical stimuli have also been identified (Bessou et al., 1971; Djouhri et al., 1998). Djhouri et al have demonstrated by analyzing intracellular voltage recordings from the somata of Guinea Pig's DRG neurons, that LTM C-fibers make up 8% of all C-fibers in the guinea pig, the rest being nociceptive fibers. In their study, the main difference between these fibers could be seen in the duration their respective action potentials. Indeed, nociceptive C-fibers neurons had longer lasting action potentials and after hyperpolarizations than LTM C- fibers (Djouhri et al., 1998).

The amplitude of somatic action potentials has been shown to be generally greater in C- fibers than in A- type fiber neurons (Bessou et al., 1971). However, in the Aα/β-, the Aδ- or the C- fibers, the nociceptive units always have significantly larger somatic action potential overshoot phases than low-threshold mechanoreceptors. The overshoot phase is the phase during which the action potential reaches its highest amplitude (Djouhri and Lawson, 2001). There are therefore differences between nociceptive fibers and mechanoceptors, which are true for all three categories of fibers.

Taken together, these studies show that the key difference between C- and A- fibers is their proportion of nociceptive neurons over low threshold ones. Basically, the highest proportion of nociceptive neurons is found amongst C-fiber type neurons. Aδ- fiber type neurons have a lower proportion of nociceptive neurons than C fiber-type ones, but this proportion is still higher than amongst Aα/β- fiber type neurons. This explains why C-fibers and Aδ-fibers are preferably seen as the neurons involved in nociception. However, regardless of which CV type they belong to, nociceptive neurons have higher thermal and mechanical thresholds than LTM, and once this threshold is reached, they fire longer action potentials than LTMs followed by a prolonged after-hyperpolarization phase. Each nerve has a different proportion of Aα/β-, Aδ- and C- type fibers, and amongst each of these types, the proportion of LTM and nociceptive neuron varies (Koltzenburg et al., 1997). These gradations in the ratio of nociceptive neurons versus LTM in each CV type of

neurons (and consequently in each nerve), the fundamental activation and firing differences between nociceptive neurons and LTM, as well conduction velocities differences between Aα/β-, Aδ- and C- type fibers, allow a fine tuning of the sensory messages, which range from normal to painful sensations.

In normal conditions, the threshold of a stimulus applied at the periphery has to be high enough to trigger the activation of nociceptive neurons and the subsequent transduction of pain messages. However various factors, such as inflammation, injuries or malfunctions of the Central Nervous System (CNS), or neural plasticity can lead to changes in the pain signal activation threshold, and to neuropathic pain in the most severe cases (Scholz and Woolf, 2002). It is therefore essential to understand the various mechanisms which trigger and influence nociception.

1.1.2. Activation of nociceptive neurons at the periphery

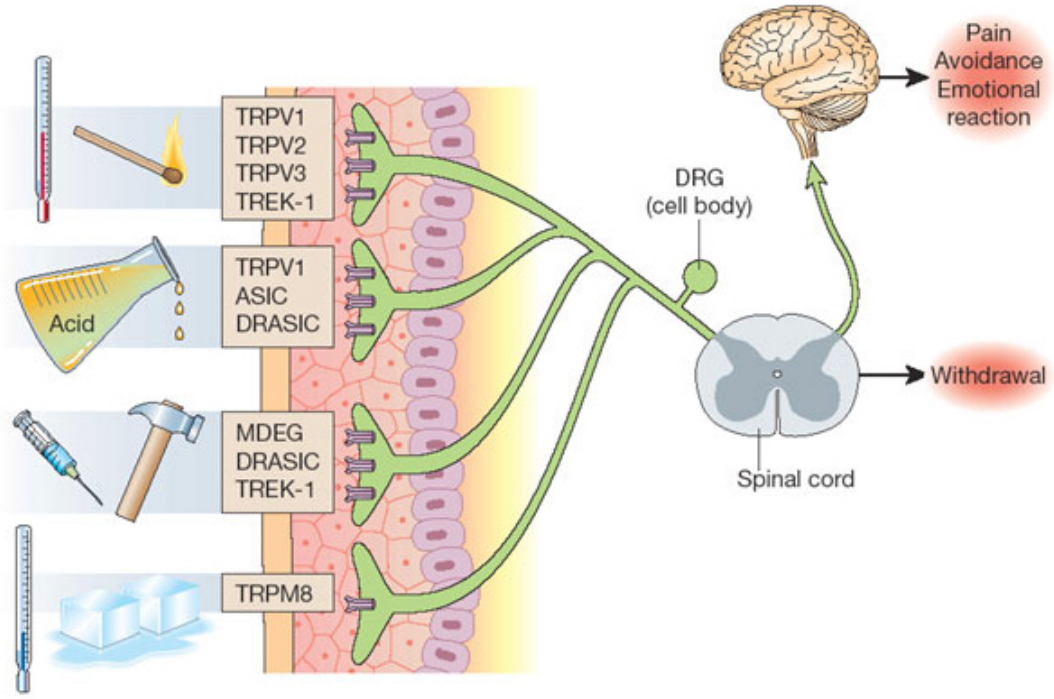

Figure 2: Modified from Scholz, (Scholz and Woolf, 2002). Nociception mechanisms. At the periphery, a stimulus such as noxious heat, acidic stress, mechanical stress or noxious cold activates specific receptors. If the stimulus reaches a certain threshold, it activates nociceptive neurons, which will transmit the message through the dorsal root ganglias to the CNS. In the spinal cord, the message is processed into an immediate reflex reaction, and transmitted by the spinothalamic and the spinoparabrachial ascending pathways to the brain, to elicit a sensory and emotional reaction, and to possibly activate the descending inhibiting pathways.

An interesting ability of nociceptive neurons is their ability to detect a variety of systems at the periphery. In that sense, they differ from sensory neurons of the olfactory or visual system, which only detect one type of stimulus and

activate neurons through G-protein coupled receptors (Kato and Touhara, 2009; Shichida and Morizumi, 2007). Nociceptive neurons can be activated by noxious heat, noxious cold as well as pressure, mechanical stress, or chemical assaults, and must therefore have a wide variety of receptors and transduction molecules that allow them to respond to each of these stressors, as seen on Figure 2.

1.1.2.1 Response to noxious heat

A key molecule in the stimulation of nociceptive neurons by noxious heat is the vanilloid receptor VR1, which has first been described and cloned as the capsaicin receptor. Sequence analyses have shown that this receptor is an 838 amino acids long, hydrophilic protein, with 6 transmembrane domains, and an amino-terminal hydrophilic segment (432 amino acids) containing a proline-rich region followed by three ankyrin repeats. This structure is similar to transient receptor potential channels (Caterina et al., 1997), (TRP channels), a family of channels, which has been shown to be activated by G protein coupled or tyrosine kinase receptors, which activate phospholipase C (Julius and Basbaum, 2001).

Further studies have shown that this receptor is not only activated by noxious heat and by capsaicin, but also by protons (Tominaga et al., 1998; Welch et al., 2000). In their work, Tominaga et al have shown that the rat VR1 receptor has a thermal threshold of 43°C, which coincides with the thermal threshold of Aδ- and C- fibers. Interestingly, extracellular Ca^{2+} is necessary for the cell desensitization mediated by the interaction of capsaicin or protons with the VR1 receptor. However, the desensitization, which is caused by a heat activation of the VR1 receptor, is not calcium dependent. These observations suggest that the action mechanisms of capsaicin and heat on the VR1 receptor are different. However, capsazepine, a competitive antagonist of capsaicin blocks capsaicin-, heat- as well as proton-evoked current. This means that the action mechanism of capsaicin and heat are nevertheless similar to some degree (Tominaga et al., 1998). Welch et al have taken this work further by inducing expression of different mutated rat VR1 receptors isoforms in Xenopus laevis oocytes to analyze them by patch clamp. They were able to show that that 3 amino acid residues localized near the pore of the VR1 contribute to the activation pathway by capsaicin, as a mutation in this site modifies the response to this compound without altering the receptor's sensitivity to heat or protons (Welch et al., 2000).

In vivo studies of knockout mice, which do not express the VR1 receptor, brought the knowledge on heat-evoked nociception further. These mice have 3 times less heat sensitive C-fibers. Extracellular recordings performed on lumbar spinal cord neurons showed that $VR1^{-/-}$ mice show similar responses to mechanical stimuli, but altered responses to noxious heat. Interestingly, behavioral studies showed that these mice reacted to temperatures in the

range of the threshold of the VR1 receptor, but not to temperature higher than 50°C. However, measurements performed on cultured DRG neurons from these mice showed that neurons have defects in low-threshold but not in high-threshold heat-evoked currents (Caterina et al., 2000). This might be explained by the existence of another heat-activated receptor, the vanilloid receptor-like 1 (VRL-1), which also has a TRP structure. To perform functional studies of this receptor, its expression has been induced in Xenopus oocytes and HEK293 human embryonic kidney cells. VRL-1 appears to have a thermal threshold of 52°C, and is not activated by capsaicin or protons. Histological studies of adult rat spinal cords and sensory ganglia have shown that VRL-1 is expressed in a subset of Aδ- fibers. This could explain why the type Aδ- fibers have a thermal threshold of 52°C. Northern Blot analyses revealed that VRL-1 messenger RNA is expressed in tissues other than sensory ganglia and spinal cord, including lung, spleen, intestine, and brain (most subregions), which means that VRL-1 may be activated by stimuli other than noxious heat outside of the CNS (Caterina et al., 1999).

1.1.2.2 Response to noxious cold

Two important channels in the nociceptive neurons activation by noxious cold are the transient receptor potential melastin 8 channel (TRPM8) and the transient receptor potential ankyrin 1 (TRPA1). Patch clamp recordings have shown that TRPM8 enables the detection of temperatures that encompass all of the innocuous cool (15–28°C) and part of the noxious cold (8–15 °C) range (McKemy et al., 2002). Knockout TRPM8$^{-/-}$ show less behavioral responses linked to cooling sensations. is a TRPM8 agonist, which induces "wet dog shakes" and "jumping" behaviors when injected i.p. in wildtype (wt) mice. TRPM8$^{-/-}$ mice showed none of these behaviors after an ilicin injection, and TRPM8$^{-/+}$ mice jumped significantly less than wt ones (Colburn et al., 2007). By comparing the firing rates of cultured skin neurons subjected to decreasing temperatures, Bautista et al showed, that TRPM8$^{-/-}$ mice exhibit less firing from C-fibers, as well as a lower basal firing rate. The same analysis conducted on Aδ- fibers showed that these fibers also react to cold, with about 4.5 times more Aδ- fibers firing observed in wt mice than in TRPM8-/- mice (Bautista et al., 2007). Other studies have shown, that TRPM8 activation by cold can have an analgesic effect on mice, which were subjected to a formalin injection in the hindpaw. This could not be seen in TRPM8-/- mice (Dhaka et al., 2007). Taken together, these results show that TRPM8 is essential for the transduction of noxious cold, but is also an essential player of the analgesic effect linked to cooling.

The research done TRPA1 has not provided such clear results on its involvement in noxious cold sensation. Intracellular calcium imaging experiments have shown TRPA1 is found in a subpopulation of sensory neurons, in which it is co-expressed with VR1 but not with TRPM8 (Story et al., 2003). Patch clamp measurements have demonstrated that the threshold of

activation of TRPA1 is 17°C (Sawada et al., 2007). On the other hand, recent studies on TRPA1 deficient mice have shown that this gene is essential for mechanoception. TRPA1$^{-/-}$ mice had a normal sensitivity to acute cold, but their C-fiber nociceptors had action potential firing rates 50% lower than those in wt C-fibers across a wide range of force intensities. Their A -fiber mechanonociceptors only had reduced firing after stimulations at high intensity forces (Kwan et al., 2009).

1.1.2.3 Response to mechanical stress

An important familiy of ion channels involved in the detection of mechanical stress is the Degenerin / Epithelial Sodium channel (DEG/ENaC). The members of this family have two transmembrane domains and a large extracellular loop. These domains form homomeric or heteromeric channels that are blocked by amiloride, a common sodium channel blocker, and have been shown to be permeable to sodium (Corey and Garcia-Anoveros, 1996; Garcia-Anoveros and Corey, 1996). This family of genes is expressed in a wide variety of organisms, ranging from nematodes to mammals (Garcia-Anoveros et al., 1995). BNC1 is a member of the DEG/ENaC, which has been identified in peripheral mechanosensory terminals of DRG neurons and has been shown to respond to acidic stimuli (Garcia-Anoveros et al., 2001; Lingueglia et al., 1997). The generation of a BNC$^{-/-}$ mouse showed however that this receptor is activated by mechanical stress, as these knockout mice have a reduced sensitivity to hair movement (Price et al., 2000). Another interesting gene of the DEG/ENaC family, which has been shown to be involved in mechanoception, is the Dorsal Root Acid Sensing Ion Channel (DRASIC), which has first been identified as an H^+ gated channel (Waldmann and Lazdunski, 1998). However, DRASIC null mice had an increased sensitivity to light touch, but showed a delayed response to noxious pinch, acid or noxious heat. It has been since then postulated that his channel is a part of a heteromultimeric complex, which has a different composition among functionally distinct sensory neurons (Price et al., 2001). An interesting feature of the DEG/ENaC genes expressed in the CNS is that they seem to be involved in mechanoception, mechanical stress and acid-induced nociception. On the other hand, TRPA1 has been shown to be involved in mechanoception and noxious cold stimulation (Kwan et al., 2009). This tends to show, that one channel can be involved in various functions, depending on the type of sensory neuron it is expressed and which type of complex it is part of.

Another important element for mechanoception and pain related to mechanical stress is extracellular ATP. Ion gated voltage channels, which are activated by ATP (P2X receptors) as well as G-protein coupled ATP receptors (P2Y receptors) have been identified in rat sensory neurons (Burnstock, 1981; Krishtal et al., 1988). Nakamura et al. provided valuable information on the role of these receptors in mechanosensitivity. By inducing expression of P2Y1 receptor in Xenopus laevis, they were able to show that a mechanical

stimulus caused an autocrine release of ATP by the transfected oocyte, and a subsequent activation of the P2Y1 receptor, which leads to a 350nA current (Nakamura and Strittmatter, 1996). The same mechanism might activate P2Y receptors at sensory nerve terminal endings, and might be involved in mechanoception and nociception.

1.1.3 Nociceptive message processing in the Spinal Cord

The cell bodies of nociceptive neurons are located in the dorsal root ganglia, and the first synapse in the transmission of a nociceptive message is in the dorsal horn of the spinal cord. The dorsal horn contains 2 principal structures: the marginal zone (lamina I) and the substantia gelatinosa (lamina II) (Lawson et al., 1997; Willis, 2007). Spinal electrophysiological recordings performed on rat lamina I neurons have shown that 74% of the neurons of this region are nociceptive specific. 18% of these neurons react to various noxious stimuli, and have therefore been characterized as polymodal nociceptive (HPC). The other 26% have a wide dynamic range (WDR), and respond to noxious as well as benign stimuli. In the lamina V, which is a deeper region of the spinal cord, the majority of the neurons show a WDR. However, the WDR neurons of the lamina I have a higher threshold of excitation than the ones from lamina V, This tends to show, that lamina I WDR neurons are involved in nociception, whereas lamina V neurons are mostly involved in the transmission of innoxious stimuli (Seagrove et al., 2004).

1.1.3.1 The lamina I and the ascending pathways

Lamina I neurons project mainly in a contralateral way to various sites in the brain: the periaqueductal grey matter (PAG), the lateral parabrachial area, the nucleus of the solitary tract and the medullary reticular formation (Burstein et al., 1990a; Burstein et al., 1990b; Todd, 2002; Todd et al., 2000). Immunocytochemistry studies have shown 80% of the lamina I neurons, which project to the thalamus, the periaqueductal grey matter, the parabrachial area as well as to the caudal ventrolateral medulla, express the neurokinin 1 receptor (NK1) (Marshall et al., 1996; Todd et al., 2000). Substance P binds the NK1 receptor and leads to the internalization of this receptor. It has been shown, that rat lamina I neurons show an internalization of the receptor, as well as dendritic reorganization after an acute noxious stimulation. This indicates, that the NK1 receptor positive neurons, which project to higher centers, are involved in the transmission of a nociceptive signal (Mantyh et al., 1995).

Intrathecal injections of a Substance P-Saporin conjugate leads to a selective ablation of the lamina I neurons. The conjugate is internalized by NK1-expressing lamina I neurons, and once in the cell, Saporin blocks protein

synthesis, which ultimately induces cell death. Rats, which have been treated that way exhibit significantly decreased responses to an intraplantar capsaicin injection. The mechanical and thermal hyperalgesia induced by this treatment is also diminished in the treated animals. 28 days after the injection, the treated rats exhibited a 75% decrease in the nocifensive behavior induced by a unilateral injection of capsaicin into the hindpaw (Mantyh et al., 1997). These results show the relevancy of the lamina I ascending pathways to the brainstem, as well as the importance of these pathways in the integration of the nociceptive message, and the generation of both a behavioral and an affective response to the stimulus.

1.1.3.2 The lamina II and the descending pathways

Histological studies of rat lumbar spinal cord have shown clear differences between the structures of the lamina I and II. While the former contains neurons with long axons, which project to higher CNS centers, the latter is formed of small neurons with intrinsic projections and local terminations (Todd, 2002; Woolf and Fitzgerald, 1983). However, the lamina II neurons appear to play a central role in pain modulation, as they receive two main inputs: one coming from the periphery conveyed through nociceptive neurons, and another coming from the brain through inhibitory descending pathways. Intracellular recordings in adult rat spinal cord slices have demonstrated that both Aδ- and C-fiber afferents release synaptic transmitters that elicit fast glutamate excitatory post synaptic potentials neurons in Lamina II neurons (Yoshimura and Jessell, 1989a, b). Another important molecule involved in the modulation of nociception at the lamina II level is GABA. Histological studies on rats have shown that laminae I-III have a high density of GABA immunoreactive neurons. Two weeks after unilateral sciatic nerve injury, no more GABAergic neurons could be seen. The deficit could be observed in the spinal dorsal horn both on the ipsilateral and the contralateral sides to the injured member. Moreover, a behavioral analysis of these animals indicated that they exhibit thermal hyperalgesia (Moore et al., 2002). More recent studies on rats have however demonstrated that here is no loss of neurons from laminae I–III in similar nerve injures models model, and that the animals exhibit allodynia even if no neuronal death was observed in the dorsal horn (Polgar et al., 2005; Polgar and Todd, 2008).

The main descending inhibitory pathways, which modulate pain at the lamina II level, involve the noradrenergic and the serotonergic system. Noradrenergic neurons projecting from the nucleus ceruleus form synaptic contacts with lamina II neurons (Westlund et al., 1982). Histological studies have indicate that most dorsal horn axons possessing the α_{2C} adrenergic receptor are excitatory spinal interneurons, which form synaptic connections with lamina II neurons. (Olave and Maxwell, 2003), and in-vivo whole cell patch clam recordings performed on rat spinal cords suggest that noradrenaline has two effects the lamina II. On one hand, it induces a

hyperpolarization of the excitatory interneurons, which inhibits the transduction of the nociceptive message, and thereby reduces the noxious stimuli-induced excitatory-post synaptic current measured on the lamina II neurons. On the other hand, it produces an antinociceptive effect by acting directly on the postsynaptic lamina II neurons through the α_{2C}-adrenergic receptor, which induces a G-protein-mediated activation of K+ channels receptors and leads to an outward current (Sonohata et al., 2004).

Serotonergic neurons coming from the raphe magnus in the brainstem have projections which form synaptic contacts with lamina I and lamina II neurons (Morales et al., 1998). Contradictory observations have been made on the effects of serotonin on the dorsal horn neurons. Whole-cell recordings from substantia gelatinosa neurons in spinal cord slices from ovariectomized rats which exhibit hyperalgesia, have shown that serotonin inhibits afferent C-fibers presynaptically through the HT_{1A}-Like Receptor, which subsequently leads to a reduction of the excitatory post-synaptic current measured on the lamina II neurons, and an analgesic effect on the animals (Ito et al., 2000). On the other hand, an excitatory pronociceptive effect of the 5HT3 receptor has been identified in electrophysiological studies. A significant decrease in the electrically evoked responses of dorsal horn neurons of rats subjected to the formalin test could be observed after a treatment with the selective 5HTr3 antagonist ondansetron. This suggests, that this receptor is normally involved in the maintenance of the nociceptive message (Green et al., 2000). Taken together, these findings indicate that the serotonergic descending pathway can modulate nociceptive messages in various manners, depending on which serotonin receptor is involved.

1.1.4 Pain processing and integration in the Brain

1.1.4.1 The Pain Matrix

In humans, the responses to pain sensation involve a complex network which is commonly referred to as the "Pain matrix", and is largely distributed in the brain. The neuroanatomical structure of this network can be divided into the sensory-discriminatory and the affective-cognitive-evaluative components. The sensory-discriminatory areas are the primary (S1) and the secondary (S2) somatosensory cortex, the posterior parts of the insula and the thalamus. The areas involved in the affective-cognitive-evaluative processes are the anterior part of the insula, the anterior cingulated cortex (ACC) and the prefrontal cortex (PFC) (Albe-Fessard et al., 1985). A meta-analysis of brain imaging data obtained by positron emission tomography (PET) and functional magnetic resonance (FMRI) performed on healthy subjects and on patients suffering from chronic pain has shown that the pain matrix cannot always be so clearly defined. While the main regions involved in acute pain perception are the S1, S2, insula, the ACC, the prefrontal cortex (PFC), and the thalamus, other regions such as the basal ganglia, cerebellum, amygdala, the

hippocampus, and the areas within the parietal and temporal cortices can also show some activity depending on the state and the condition of the tested individual (Apkarian et al., 2005). These areas are illustrated in Figure 3.

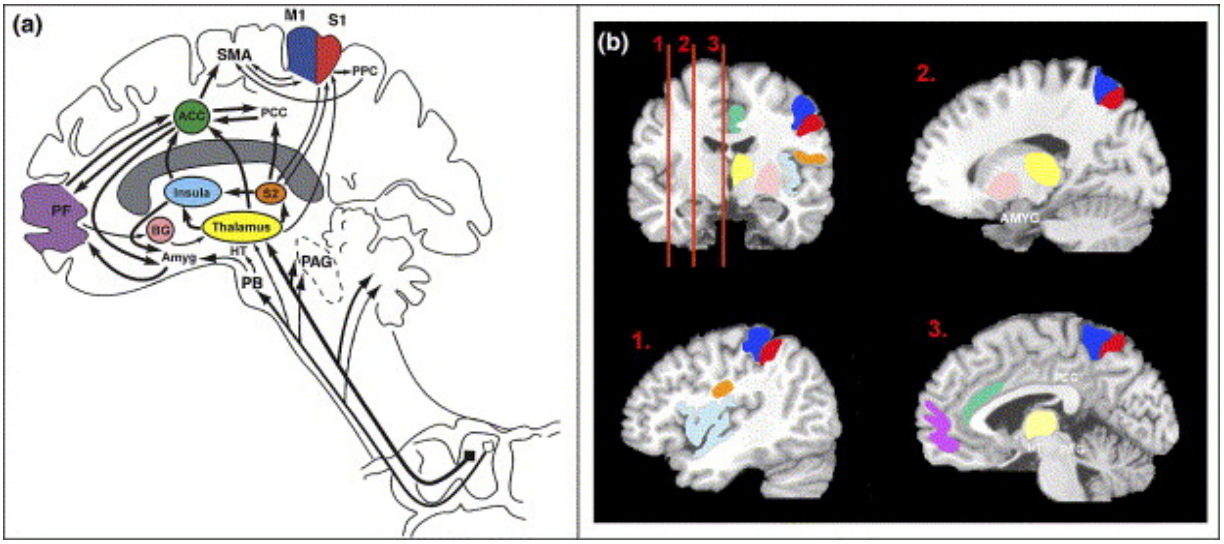

Figure 3: From Apkarian, (Apkarian et al., 2005). Cortical and sub-cortical regions involved in pain perception, and the integration of the nociceptive message. The locations of brain regions are color-coded in the scheme drawing and in an example MRI. (a) Scheme shows the regions, their inter-connectivity and afferent pathways. (b) The areas corresponding to those shown in the schematic are shown in an anatomical MRI, on a coronal slice and three sagittal slices as indicated on the coronal slice. The pain matrix areas are the secondary somatosensory cortices (S1, S2, red and orange), anterior cingulate (ACC, green), insula (blue), thalamus (yellow), and prefrontal cortex (PF, purple). Other regions indicated on this figure include: primary and supplementary motor cortices (M1 and SMA), posterior parietal cortex (PPC), posterior cingulate (PCC), basal ganglia (BG, pink), hypothalamus (HT), amygdala (AMYG), parabrachial nuclei (PB), and periaqueductal gray (PAG).

Positron emission tomography (PET) recordings studies have shown, that immersing the hand of a patient in ice water is a painful stimulus, which produces significant increases in regional cerebral blood flow (rCBF) within the contralateral secondary somatosensory (S2) and insular cortex, bilaterally in the thalamus and cerebellum, and medially in the cerebellar vermis. The patients also grade the stimulus as being unpleasant. When the patients receive an intravenous injection with Fentanyl, a μ-opioid receptor agonist, the grades they give to the stimulus indicate that they do not perceive it as painful, and their PET recordings reveal that all their cortical and subcortical responses to noxious cold are reduced. However, the same recordings performed on patients, who are subjected to unpleasant vibration on their forearm indicate an activation of the primary S1 cortex, which remains unaffected by a treatment with Fentanyl. The treated patients also continue to grade their stimulation as painful (Casey et al., 2000). These findings indicate that different painful stimuli activate different components of the pain matrix.

Chronic pain states can also provide valuable information on brain areas involved in the processing of a nociceptive message. FMRI studies performed on brains of patients suffering from postherpetic neuralgia (PHN) have shown that spontaneous pain, induced by this condition, activates affective and sensory-discriminative areas, such as the thalamus, the S1 and S2, insula and the ACC as well as areas involved in emotion, hedonics, reward, and punishment such as the central striatum, the amygdala, the orbital frontal cortex, and the ventral tegmental area. The patients were treated with lidocaine patches, and brain FMRI recordings were performed to check whether this treatment could decrease the activity recorded in these areas. Interestingly, the sensory and affective activations could only be inhibited after 6h of treatment, while the activity in the striatum and amygdala – which are reward-related regions – decreased only after 2 weeks of treatment (Geha et al., 2007). This data shows, that chronification processes activate sensory regions, but also elicit emotional responses, which are differently integrated, and cannot be simply reversed with the same treatment. It can be hypothesized that the chronification of pain induces changes in the brain pain-related circuitry. The participation of hedonic/reward sub-cortical areas increase with time, while the sensory-representational cortical areas could be gradually less involved, making the condition perhaps more sub-conscious and impacting on motivational drives (Geha et al., 2007).

1.1.4.2 Activation of the descending pathways

The periaqueductal gray-rostral ventromedial medulla (PAG-RVM) activation system of the descending pathways has been widely studied. The PAG receives inputs from limbic forebrain structures such as the ACC, the amygdala (AMY), the dorsomedial nucleus of the hypothalamus, and the medial prefrontal cortex (MPC), and projects to the RVM in the brainstem. In the RVM, structures such as the raphe magnus and the adjacent reticular formation project to the dorsal horn, and therefore play a pivotal role in pain modulation (Fields, 1985, 2000; Hermann et al., 1997). Early experiments have shown that it is possible to perform an exploratory laparotomy in rats, without using any chemical anesthetics after stimulating the PAG (Reynolds, 1969). Since then, it has been shown that the PAG-RVM system is involved in analgesia mediated by cannabinoids (Hohmann et al., 2005), opioids (Loyd and Murphy, 2009; Yaksh et al., 1976) and by cyclooxygenase inhibitors (Leith et al., 2007). Figure 4 illustrates the various inputs and outputs of the PAG-RVM system.

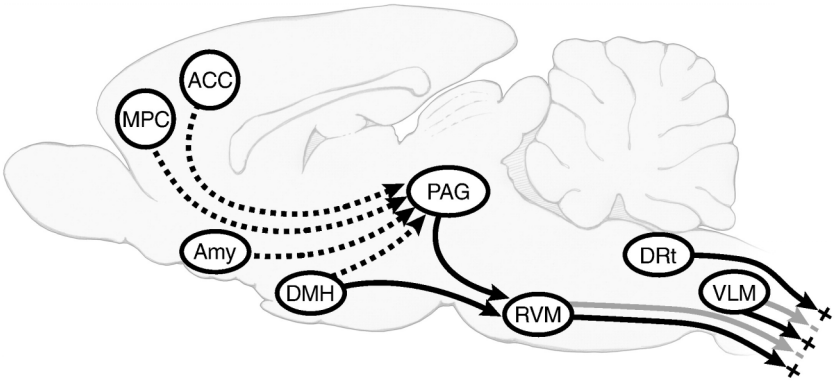

Figure 4: Scheme representing PAG-RVM system in a midline cut of the mouse brain. The PAG-RVM system exerts bidirectional control over dorsal horn nociceptive processing, and the DRt and VLM in the caudal medulla. The PAG receives important direct and indirect inputs from limbic forebrain areas including anterior cingulate cortex (ACC), amygdala (AMY), dorsomedial nucleus of the hypothalamus (DMH), and medial prefrontal cortex (MPC). It projects to the RVM, which integrates the response, and can lead to a inhibitory or stimulating effect. The dorsal reticular nucleus of the caudal medulla (DRt) and the ventrolateral quadrant of the caudal medulla (VLM) are also involved in descending modulating pathways. The DRt is thought to be facilitating, and VLM primarily inhibitory, although it may, like the RVM, have both an inhibitory and facilitatory influence.

Depending on the conditions, the RVM is able to trigger analgesia or hyperalgesia. In-vivo recordings of the activation of RVM neurons in rats and observations of a tail flick reflex after a noxious heat stimulus revealed that this structure contains "on-cells"and "off-cells" which have different firing profiles. The on-cells are excited and their firing increases after the noxious stimulus. For the off-cells, on the other hand, a decrease in the firing is measured after the stimulus; this indicates that these cells are then inhibited. There is clear segregation between these two cell populations along the mediolateral axis of the RVM (Fields et al., 1983), but further recordings in the spinal cords have shown that both cell types project to the laminae I, II and V of the spinal cord, which are precisely the areas which receive inputs from sensory and nociceptive neurons (Fields et al., 1995). A third group, the "neutral cells" did not respond to noxious stimuli, or gave variable responses. These 3 cell types respond differently to iontophoretic applications of morphine. The on-cells are inhibited, but the off-cells and the neutral cells do not exhibit any clear changes. However, if morphine is applied locally, the on-cells get depressed, whereas the "off-cells" get continuously activated. The firing of the neutral cells remains unaffected by either morphine application types (Heinricher et al., 1992). This data suggests that these 3 cell types contribute differently to the descending pathways and to pain modulations.

Iontophoretic applications of bicuculline methiodide, a GABA a receptor antagonist, in the RVM of rat suppressed the tail flick reflex, and reduced the firing of off-cells. The activity of on- and neutral cells however remained unchanged by this treatment. This suggests that GABA inhibition of off-cells is

essential for the tail flick reflex (Heinricher et al., 1991; Heinricher and Kaplan, 1991). Moreover, rat RVM infusion with a selective μ-opioid agonist inhibited on cells, which led in most cases to a subsequent activation of off-cells correlated with a suppression of the heat-evoked tail flick (Heinricher et al., 1994). Taken together, these data suggest that on-cells are inhibitory GABA-ergic interneurons, which form synaptic contacts with off-cells. The on-cells start fire upon activation of the μ-opioid receptor, release GABA and subsequently inhibit the constitutive firing of the off-cells, which leads to analgesia. Given that both cell types project to the dorsal horn, a complex interplay of inhibition and activation can directly and indirectly modulate nociception at the RVM- and spinal-levels. The firing profile and role of neutral cells is to date less understood. Histological studies of the rat have shown that these cells are serotonergic, which is not the case of on- or off-cells (Potrebic et al., 1994), which tends to show, that they are also involved in pain modulation.

1.1.5 Inflammatory pain

Inflammation is a process, which is closely linked to injuries. Cells of the immune system infiltrate the site, in order to protect the organism from a possible infection. This process involves the interplay of a wide variety of cytokines, chemokines, growth factors and other diffusible components, which contribute to pain and tend to elicit hyperalgesia. It has for instance been shown in the rat that an intraplantar injection of CFA triggers a reduction of the latency in the hotplate test as well as the mechanical threshold in the Von Frey filaments tests. The inflammation induced by the CFA induces a significant elevation of the TNF-α, interleukine1β (IL-1β) and NGF at the site of injection. Interestingly, intraplantar TNF-α injections induce short, dose-dependent increases in thermal and mechanical sensitivity, which can also lead to an increase of the IL-1β and NGF concentration at the site of injection. The hyperalgesia can be significantly attenuated by prior administrations of anti-NGF antiserum (Woolf et al., 1997). This data shows that soluble factors alone can lead to a sensitization, which is similar to the one observed during a complete inflammatory process involving cell infiltration. Similarly, it has been shown in mice that intraperitoneal injections of zymosan and acetic acid induced a writhing behavior characteristic of pain. This response decreased when a lavage of the peritoneal cavity, which eliminates macrophages and resident mast cells, was performed prior to the injection, and increased when the mice were pre-treated with thioglycolate, a compound, which enhances the responses of macrophages. Interestingly, a pre-treatment with an anti-interleukin-8 serum partially inhibited the writhing behavior, but on the other hand a combined injection with a TNF-α, IL-1β and interleukin-8 induced the writhing (Ribeiro et al., 2000).

Neutrophils are the first cells, which are detected at the injury site. They produce chemokines, which mediate the infliltration of the site by other

leukocytes (Antony et al., 1985). Chemokine receptors are G-protein coupled, and are not only expressed in cells from the immune system. Indeed, chemokines and their receptors are found in the CNS, and are even essential for the development of the brain, as shown by the early lethality and the severe deficit in the brain development of transgenic mice, which do not express the stromal cell derived factor 1 and its receptor CXCR4 (Ma et al., 1998). While neutrophils and macrophages trigger neuroinflammation at the periphery, glial cells are responsible for the same process in the CNS. It has been demonstrated histologically that rats, which have been subjected to a plantar injections of formalin or zymosan – 2 compounds causing mechanical allodynia - exhibited a higher rate of glial activation and IL-1β in their spinal cords, 1 to 6 hours after the treatment (Sweitzer et al., 1999).

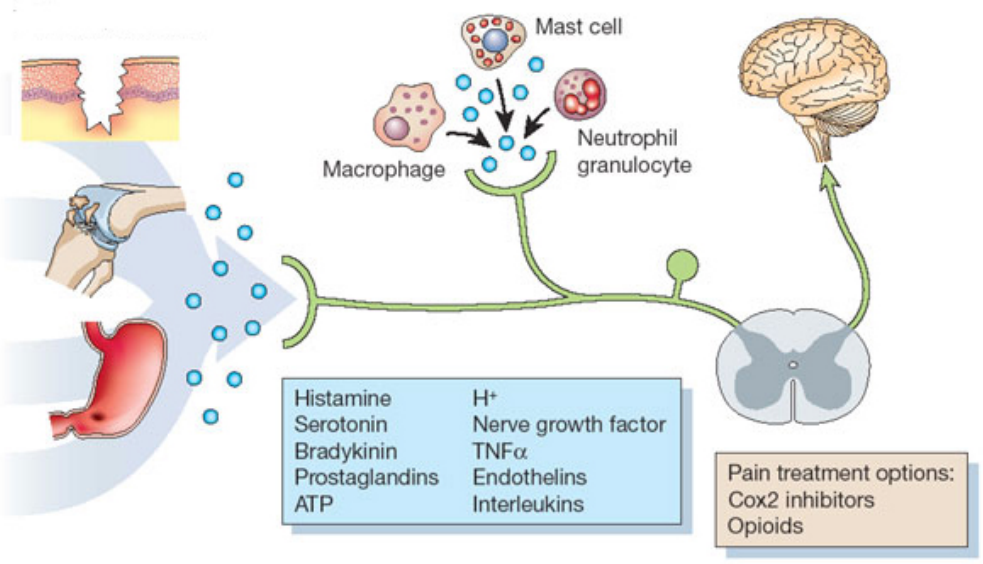

Figure 5: Modified from Scholz, J. (Scholz and Woolf, 2002). Inflammatory Pain processing. When an injures occurs at the periphery, Cells from the immune system infiltrate the site, and release chemokines, cytokines and other soluble substances necessary to the coordination of the inflammatory reaction. These substances lower the activation thresholds of nociceptive neurons, and lead to an increased pain sensation for the subject, to stimulus, which would not be noxious under normal conditions.

The mitogen-activated protein kinases (MAPKs) seem to play an important role in pain sensitization during inflammation. This family of proteins contains 3 main subgroups: the extracellular signal regulated kinases (ERKs), the p38 kinases, and the c-Jun N-terminal kinases (JNK), which represent 3 different signaling cascade responding to a range of extracellular stimuli, and leading to transcriptional and non-transcriptional regulation (Johnson and Lapadat, 2002). ERK kinases are for instance involved in Bradykinin mediated hypersensitivity. Bradykinin is a vasodilatator peptide, which is produced after a tissue injury, contributes to inflammation by increasing vascular permeability, and is also involved in pain sensitization (Couture et al., 2001).

The Bradykinin receptor B_2 is a G-coupled receptor, which is expressed on DRG neurons (Wang et al., 2005). In situ hybridization studies coupled with immunohistochemistry and patch clamp recordings have been made in rats, and have shown that the B_2 receptor, and the protein kinases A and Cδ are coexpressed in lamina II neurons. By interacting with those receptors, Bradykinin activates the two previously mentioned kinases, which then recruit ERK kinases to lead to an increase of AMPA and NMDA receptor-mediated current. This process therefore facilitates glutamatergic post-synaptic responsiveness, and ultimately leads to hyperalgesia (Kohno et al., 2008).

The p38 kinases also play a central role in pain processes linked to inflammation, and are activated by the Nerve Growth Factor (NGF), IL-1β and TNF-α among other factors (Widmann et al., 1999). Ji et al. have shown in rats, that p38 is expressed in C-fiber neurons, and contributes to thermal hyperalgesia caused by the inflammation induced by a CFA intraplantar injection. NGF levels increase during the inflammation at the site of the injury. It gets retrogradely transported to the cell body, where it activates p38, which enhances the translation and transport of the VR1 (TRPV1) receptor towards the periphery, a process, which maintains a hypersensitivity to heat. An intrathecal injection of a selective p38 inhibitor (SB203580) prior to the CFA injection inhibits this mechanism, and reduces the thermal hyperalgesia observed after the injection (Ji et al., 2002; Woolf et al., 1994). Given that the VR1 receptor is also activated by H^+, this regulation might therefore also contribute to sensitivity to the acidic stress induced by the H^+ release at injury site during inflammatory processes (Scholz and Woolf, 2002).

Another cascade, which leads to an increased sensitivity to pain, involves p38. The activation of high-threshold C-fibers leads to the release of substance P and glutamate in the dorsal horn, which activate respectively the post synaptic NK1 and NMDA receptors, elicit an increase of the intracellular Ca^{2+} concentration and activate phospholipase A_2 (PLA_2). This enzyme mediates the release of arachidonic acid from cellular membranes, which is then converted into prostaglandins, by cyclooxygenases (COX) (Lazarewicz et al., 1990). Prostaglandins participate to the inflammatory processes, and the subsequent pain by lowering thermal threshold. This can be assessed in a hot plate test. Intrathecal applications of a p38 inhibitor (SD-282) lead to a decrease of the Prostaglandin E_2 (PGE_2) release and of the subsequent thermal hyperalgesia. This means that p38 is involved in PLA_2 mediated inflammatory pain (Svensson and Yaksh, 2002).

The role of the JNK kinases in inflammatory pain is not as clearly defined. It has been shown by immunohistochemistry that a peripheral axotomy of the sciatic nerve in rats induces an activation of JNK, and c-Jun binding to activator protein 1 (AP-1) to induce gene expression. This mechanism might be involved in axonal sprouting, and might be one of the explanations for neuropathic pain (Kenney and Kocsis, 1998).

1.2 Genes involved in pain mechanisms

1.2.1 Transgenic mice and pain

Many knockout mice, which exhibit altered pain behaviors have been generated. Some have been described previously in this introduction, but other animal models, which do not express specific channels, have a modified neuronal activity, and exhibit uncommon responses to pain. They therefore have an important role in pain research.

Voltage gated sodium channels play an essential role in the generation and the propagation of sensory or nociceptive signals. By disrupting the SCN11A gene, Priest et al. have been able to generate NAv1.9 knockout mice. Although patch clamp recordings made on dissociated DRG neurons from these mice revealed no difference in the passive membrane properties and action potential characteristics between the NAv1.9$^{-/-}$ and the wt mice, behavioral tests showed that NAv1.9$^{-/-}$ had a shorter late response to the formalin test then wt animals (Priest et al., 2005).

In other studies, the Cre-loxP system has been used to generate specific knockout mice, which had a deletion of the NAv1.7 in their nociceptive neurons only. These animals had a reduced responsiveness to mechanical stress in the Randall-Selitto test, which was correlated with a reduced electrophysiological response of lamina V neurons after a mechanical stress. Moreover, these animals did not develop any thermal of mechanical hyperalgesia linked to inflammation caused an intraplantar CFA injection Nassar, 2004 #117}. This study could show the essential role of the NAv1.7 channel in nociception and pain, and also explains why humans, which have a mutated NAv1.7 channel appear to be pain insensitive (Cox et al., 2006).

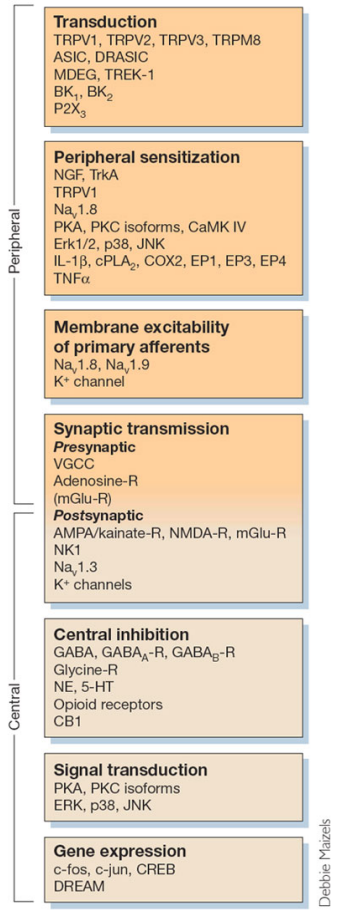

Figure 6: Modified from Scholz, J. Nature Neuroscience 5, 1062 - 1067 (2002) (Scholz and Woolf, 2002). Sum up of the essential genes involved in the generation, transmission, integration and modulation of the nociceptive signal from the periphery to the central nervous system.

Some other proteins than channels have been shown to be essential for a normal transduction of the pain signal. The Downstream Regulatory Element Antagonistic Modulator (DREAM) is a transcription factor that regulates the expression of many genes including c-fos. It was the first identified transcription factor, which could be blocked by Ca^{2+} (Carrion et al., 1998). DREAM$^{-/-}$ mice exhibit a significantly longer delay time in their tail flick response to noxious heat, and the mechanical threshold required to induce withdrawal of the paw after pressure, is significantly higherin these mice than in wt animals. They also show less writhes after intraperitoneal injections of $MgSO_4$, which produces an immediate visceral pain, or of acetic acid, which induces inflammatory pain. Moreover, the DREAM knockout animals have elevated levels of prodynorphin mRNA and dynorphin, which is an endogenous ligand of the κ opiate receptor (Cheng et al., 2002; Costigan and Woolf, 2002). This data shows the variety of elements, which can underlie a single knockout's altered pain behavior phenotype: transcription factors, receptors and ligands.

1.2.2 Pain gene databases

Because many genes seem to induce a pain related phenotype in transgenic or knockout animals, a classification has been necessary. J. Mogil and his team at the Pain Genetics Lab in Canada have established an internationally recognized database of the known "pain genes" (Lacroix-Fralish et al., 2007). To date, the database counts 283 genes, and is regularly updated. To establish this database, they considered 3 criteria of inclusion:

- The mutant animals had to have a null expression of only one gene.
- The mice had to be tested on a behavioral assay of nociception, injury or stimulus induced hypersensitivity or stress-induced inhibition of nociception.
- At least one statistically relevant difference in either direction had to be visible between the mutant and the wild-type mice.

In 2007, the pain gene database contained the categories summed up on Figure 7.

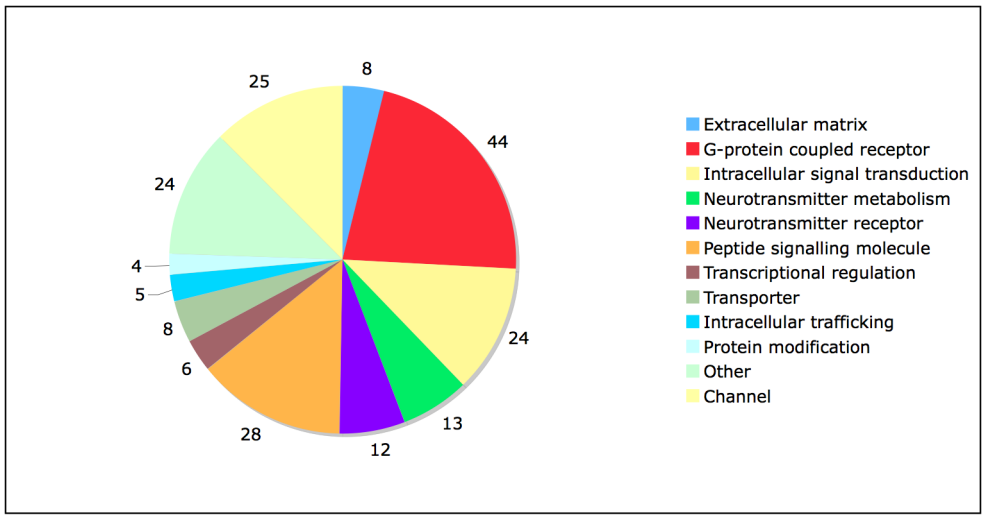

Figure 7: Modified from LaCroix-Fralish et al., 2007 Functional classification of the genes present in the Pain Gene Database.

In a similar way, we have established a list of pain related genes at the beginning this project. A literature search was performed to find potential genes related to pain. The genes, which were included, fulfilled at least one of those criteria:

- A mutant animal for the gene of interest had to have an altered response to a characteristic behavioral test of pain (mechanical, thermal, or inflammatory induced hyperalgesia).
- The gene product induced a modified response to a characteristic behavioral test of pain (analgesia, allodynia or hyperalgesia) if injected into wt animals.

- The gene induced a stress or anxiety phenotype to transgenic animals.

We established a list of 230 genes. Half of them were also in the pain gene database established by J. Mogil's group. The other half were linked to stress and anxiety processes. Here is a description of the main categories we selected:

- Channels and receptors: This category is very wide and counts key players which have a role in the peripheral (such as VR1, DRASIC, etc…) and central (such as GABA receptors, the NAv1.9 channel, etc…) processes of nociception.

- Signal transduction: This category is also very diverse and contains genes such as MAP kinases, p38 kinases and CREB.

- Neuropeptides: For example Subtance P, and other members of the Tachykinin family.

- Oxydative Stress: For example cytochromes .

- Hormone related genes: For example the pro-opiomelanocortin gene gives rise to many splice variants, which encode the various components of the melanocortins family such as the adreno-corticotropic hormone (ACTH).

- Neurotrophins: For example BDNF, and GDNF.

- Heat shock proteins: For example HSP72.

- Cytokines, chemokines and related: For example IL-1β, IL-8 and TNF-α.

The genes previously described in this introduction were all present in our pain genes list. Appendix 1 lists all of these genes with examples of their function, and literature references.

1.2.3 Assessing pain in laboratory mice by monitoring gene expression changes?

Mice live in constant fear of their predators and therefore show little behaviors, which might reveal that they are suffering. In laboratory settings, health observations of the animals depend on scoresheets, which give variable results from one observer to the other. This can be problematic in research, because mice are very commonly used as model animals for diseases and pain must be monitored for animal welfare purposes as well as for experimental reasons. Therefore, other tools have to be used to monitor

pain in laboratory mice, and their development represents a great topic in animal welfare research. One approach to objectively measure pain in laboratory animals, could be to find genes, which show a variation in their expression levels depending on the pain intensity and to test how they behave in known pain models

Recent data have shown that pain does indeed induce specific gene expression changes in defined models. Histological stainings performed in rat spinal cords after an intraplantar formalin injection revealed, that the genes encoding the leukocyte common antigen (LCA/CD45), the MHC class I antigen, and CD11c are both more expressed in the activated microglia 3 days after the injection and reach their peak expression levels after 7 days (Fu et al., 2009).

Performing a nerve injury triggers a hyperexcitability of afferent nociceptive fibers, and is therefore often used in research as a model for chronic pain. In their study, Persson et al have assessed whether this model induces gene expression changes in the DRGs of 5 mice strains. Their microarray analysis revealed that an average of 2552 genes is significantly regulated in DRGs of the tested animals, 3 days after the nerve constriction. However, only 5.6% of these genes had a significant regulation across all the 5 strains, and were correlated to pain behavior such as tactile hypersensitivity. The differential expression between injured and control animals could be validated for 2 genes: the Na^+ channel SCN11, which was correlated with levels of spontaneous pain behavior and Trpm8, which was correlated with heat hypersensitivity (Persson et al., 2009).

In another study, microarray analyses have been performed on dorsal root ganglia of rats, which had been subjected to an intraperitoneal injection of Paclitaxel, a compound used in chemotherapies, which causes painful peripheral neuropathies. The results showed that 38 genes were downregulated and 60 genes were upregulated in the treated animals. Interestingly, 26 of the 60 upregulated genes were linked to inflammation. One of these genes, the matrix metalloproteinase-3 seemed to be responsible for the recruitment and accumulation of macrophages in the DRG of the treated animals, a process, which might induce the neuropathy and the subsequent painful sensation (Nishida et al., 2008).

In humans, gene expression level analyses in the CNS are more difficult, because they require dissection of tissues. However, microarray analyses performed on inflamed oral mucosa tissue samples 3 hours after a tooth removal have revealed, that 25 genes linked to inflammation cascade were upregulated, including IL-6, CCL2 and CXCL2 as well as other cytokines, chemokines and their receptor. These upregulations were correlated with a higher pain sensation reported by the patients (Wang et al., 2009).

Taken together, these results show that nociception and inflammation induce expression level changes in the periphery, as well as in the central nervous system. However, no study has ever been done on the expression profiles of the genes listed in the pain gene database in various pain models, in order to check, whether they present a constant behavior, which might be characteristic of nociception, and could be used to monitor pain objectively.

1.3 Pain models studied in this project

During in the course of this project, we focused on a surgical pain model, but also performed quantitative real-time PCR measurements to study an inflammatory pain model.

1.3.1 Surgical pain model: telemetric apparatus implantation.

A lot of experiments performed on laboratory animals involve surgery. This can be problematic because the results observed might be influenced by the nociceptive processes, which are happening in the animal. It is therefore important to carefully monitor pain in operated animals. In their study on laboratory mice and surgical pain, Arras et al. have demonstrated by using telemetry, that monitoring the heart rate (HR), the electrocardiogram (ECG), the core body temperature (BT) and locomotor activity (ACT) can give precious information on the level of pain experienced by an mouse after surgery (Arras et al., 2007).

In the surgical pain model, eight weeks before the beginning of the experiments, TA10ETA-F20 transmitters (Data Sciences International, St. Paul, MN, USA) are implanted in NMRI mice. After the recovery phase, a laparotomy followed by a vasectomy was performed on the operated animals, and the controls were only anesthetized. Within the operated and control groups, one subgroup received a Caprofen analgesic treatment (Rimadyl™, Pfizer Inc., NY, USA), one subgroup received a Flunixin analgesic treatment (Biokema Flunixine™), and one subgroup received no analgesic treatment. Measurements of the heart rate showed that the operated animals, which did not receive any analgesic treatment had the highest values after the operations. The 2 groups treated with analgesia had values, which were higher than their non-operated controls, but the heart rate of these animals was still lower than the one of the animals, which did not receive any analgesia after surgery. At the end of the first day, HR values of the 2 groups treated with analgesia returned to normal, but the ones of the untreated operated animals remained higher.

Interestingly, when the results were plotted as 12 hours mean values over the 3 days following the surgery, the HR of the operated animals without analgesia appeared to be significantly increased during the first 24 hours, and during

the first dark phase (01-12h post surgery) in the operated animals treated with flunixin. Moreover, the body weight of the operated animals with no pain treatment decreased during in the first 3 days post-surgery, and their food and water consumption also decreased during the first two days after the intervention. During these 2 days the animals of this group had an unstructured territory, with no defined nest and a confused distribution of the nesting material in the habitat. All this data indicate that the animals were experiencing a painful recovery, which was impairing their normal behavior.

An interesting feature of telemetry is the possibility to detect different levels of pain. Indeed, telemetric measurements performed directly after the implantation revealed that the heart rate of the animals was impaired for 3 days (Figure 8) in both the untreated group, and the group treated with flunixin. This tends to show that a highly invasive procedure like a telemetric apparatus implantation causes a higher level of pain than the vasectomy for the animal, and that the heart rate increase cannot be diminished by the use of non-steroidal anti-inflammatory drug (NSAID) (Arras, 2007; Cinelli et al., 2006)

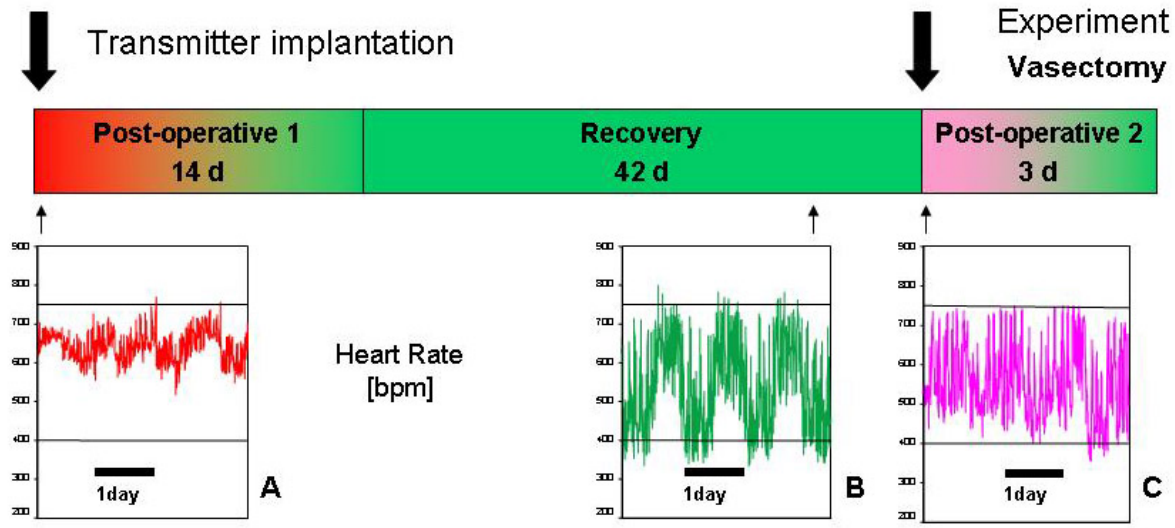

Figure 8: Modified from Arras et al, 2007 (Arras, 2007). Heart rate variations measured by telemetry. **A.** During 3 days after the implantation, the heart rate of the animals is increased. This cannot be prevented by the use of analgesics like flunixin. **B.** After a recovery period of 6 weeks, the heart rate returned to normal. **C.** During 3 days after the vasectomy, the heart rate of the animals is increased. This was also observed during the first 12 hours following the surgery, in the flunixin-treated animals.

1.3.2 Inflammatory pain model: immunization with a BHV-1 virus

Immunizations are routinely performed on laboratory animals, to produce polyclonal antibodies. The common procedure consists in injecting inactivated antigene mixed with CFA, a solution containing mycobacterial cell walls and mineral oils, which enhances the immune response. Further

injections with incomplete Freund's Adjuvant (IFA) are also often performed, to boost the immune response (Stills, 2005). Although adverse effects such as death, immobility, abscesses and necropsy have been reported, no real assessment of the pain level of these animals has been performed (Leenaars et al., 1998). However, as previously addressed in this work, inflammation elicits pain which not only impairs the well being of the animal, but can also bias the outcome of an experiment.

To address these issues, Arras et al. have implanted TA10ETA-F20 transmitters (Data Sciences International, St. Paul, MN, USA) to mice from a strain called 129S/Ev-IFNabRtmAgt, which does not express the α/β interferon receptor (Muller et al., 1994). This strain mounts a strong IgG2a-dominated antibody response but shows no signs of infection, when inoculated with the Bovine Herpes Virus 1 (BHV-1). The animals were randomly divided into 3 groups, which were subjected to 3 different protocols. The first group received a UV-inactivated BHV-1 combined with CFA intraperitoneal injection followed by a booster immunization with IFA 28 days later. The second group was subjected to the same protocol, but was treated with Caprofen once daily during the 3 days which followed the primary immunization, and during one day after the booster injection. The mice from the third group underwent a different protocol. They received an intraperitoneal injection of live BHV-1 virus in cell culture medium. No booster was used in this protocol.

All three protocols were successful for immunizations, as high titers of BHV-1-specific IgG2a and IgG2b were found in every immunized animal. The booster immunizations revealed enhanced the BHV-1 specific IgG1, IgG2a and IgG2b titers. The telemetric measurements were used to detect heart rate changes significant of pain. The animals, which underwent the first immunization protocol, had a significantly elevated heart rate during the first 24 hours. In the second light phase, the elevation did not reach significance. After the booster immunization, the heart rate was also elevated during 24 hours. For the animals, which were subjected the second protocol, a significant increase in the heart rate was observed in the first 24 hours, but the values returned to normal more rapidly, because of the analgesic treatment, and no more increase was detected afterwards. The booster induced a significant increase during the first night only. The animals, which were immunized according to the third protocol, did not exhibit any significant heart rate change (M. Arras, unpublished data).

Measurements performed on the food and water consumption revealed, that it dropped to 80% on the first day following the first immunization protocol, as well as the booster of the fist protocol. However, no significant changes could be observed in the animals, which were subjected to the two other protocols.

Taken together, this data suggests that an immunization with BHV-1 virus in CFA followed by a boosted induces a heart-rate increase, which is related to pain, according to previous studies (Arras, 2007; Arras et al., 2007). The use of

Caprofen reduces the duration of the heart rate increase observed both after the immunization and the booster. Immunization protocols can therefore be an interesting way to study the effects of induced inflammatory pain on an organism.

1.4 Microarray technology

DNA microarrays are widely used today in gene expression analyses. This technology is derived from the 'dot plot' assays, which were developed to analyze cloned DNA sequences using highly radioactive, 32P-labeled DNA or RNA probes (Kafatos et al., 1979). However, the real development of microarrays started when spotting technology was developed enough to enable the switch from membrane to solid surfaces for the spotting of the probes. Schena et al were the first to describe a real microarray protocol. They spotted 48 cDNAs with an average size of 1kb derived from arabidopsis mRNA, on a glas surface. They established a protocol to prepare fluorescent cDNA samples from the total arabidopsis mRNA, by incorporating fluorescein or lissamine. By labeling 2 different samples with either one of the fluorochromes, and by hybridizing an appropriately titrated mix of both samples on the array, they were able to detect fluorescence intensity differences, which were correlated to gene expression differences between the 2 samples (Schena et al., 1995).

This hybridization principle remained virtually identical in most custom-made arrays, even though the technology went through several optimization steps. Nowadays, microarrays can be spotted with either cDNAs or 70mer oligonucleotides, which present the advantage of giving stronger signals and of being less affected by background artifacts (Koltai and Weingarten-Baror, 2008; Lyons, 2003). Moreover, studies have shown that microarray results obtained on slides spotted with 70mer oligos designed to be in the 3' terminal of the genes, were more accurate, and were better correlated to results obtained by real-time-PDR, than results obtained on cDNA-arrays (Zhu et al., 2005). Another important improvement was the development of in-vitro transcription protocols, which allowed the production and use of antisense RNA (aRNA) for the samples. These protocols combine the T7 technology for reverse transcription of the mRNA into double stranded cDNA, which is then transcribed in-vitro into aRNA. Given that the probes spotted on the slide are designed to be in the sense orientation, the hybridization can occur optimally. The biggest advantage of aRNA technology is the higher amount of material, which can be amplified from the total RNA extracted (Wang et al., 2000). This method also presents the advantage of allowing the use of amino-allyl-UTP. These modified UTP integrate in the aRNA molecule like UTP, and N-hydroxysuccinimidyl ester-coupled (NHS-) fluorescent dyes bind to the amino-allyl group during the labeling reaction. This indirect labeling method bypasses the use of bulky fluorescent dyes, which have to be directly during the reverse transcription step in older cDNA microarray sample preparation

protocols and can lead to aberrations. It therefore increases the fidelity of the amplified aRNA sample to the original mRNA extracted. The most common dyes used today for aRNA labeling are NHS-Cy3 and NHS-Cy5 (Holloway et al., 2002).

The slides have also evolved. Glass slides are still the favorite support, because of their low fluorescence, transparency, resistance to high temperature, and their physical rigidity. However a variety of coating techniques have been developed to enhance the binding of the probes. Initially, coating glass slides with poly-L-lysine was highly popular because of the low costs of this technique. These surfaces still give good results and are therefore still used in research (Lyons, 2003). However, more recent studies show that epoxy-coated slides give strong signal, have a better inter- and intra-slide performance (Sauer et al., 2009). In this project, we used SciChip EPOXY slides from Scienion®, coated with a polysiloxane layer, which provides a high density of coupling groups as well as a high homogeneity of the surface functionality

1.4.1 Competitive hybridization protocols

Most custom made microarrays are used for gene expression experiments. The most common protocols consist in competitive hybridizations with of two samples labeled with two different dyes on one slide (see Figure 9 for a scheme). These protocols are derived from the original experiments performed by Schena et al (Schena et al., 1995).

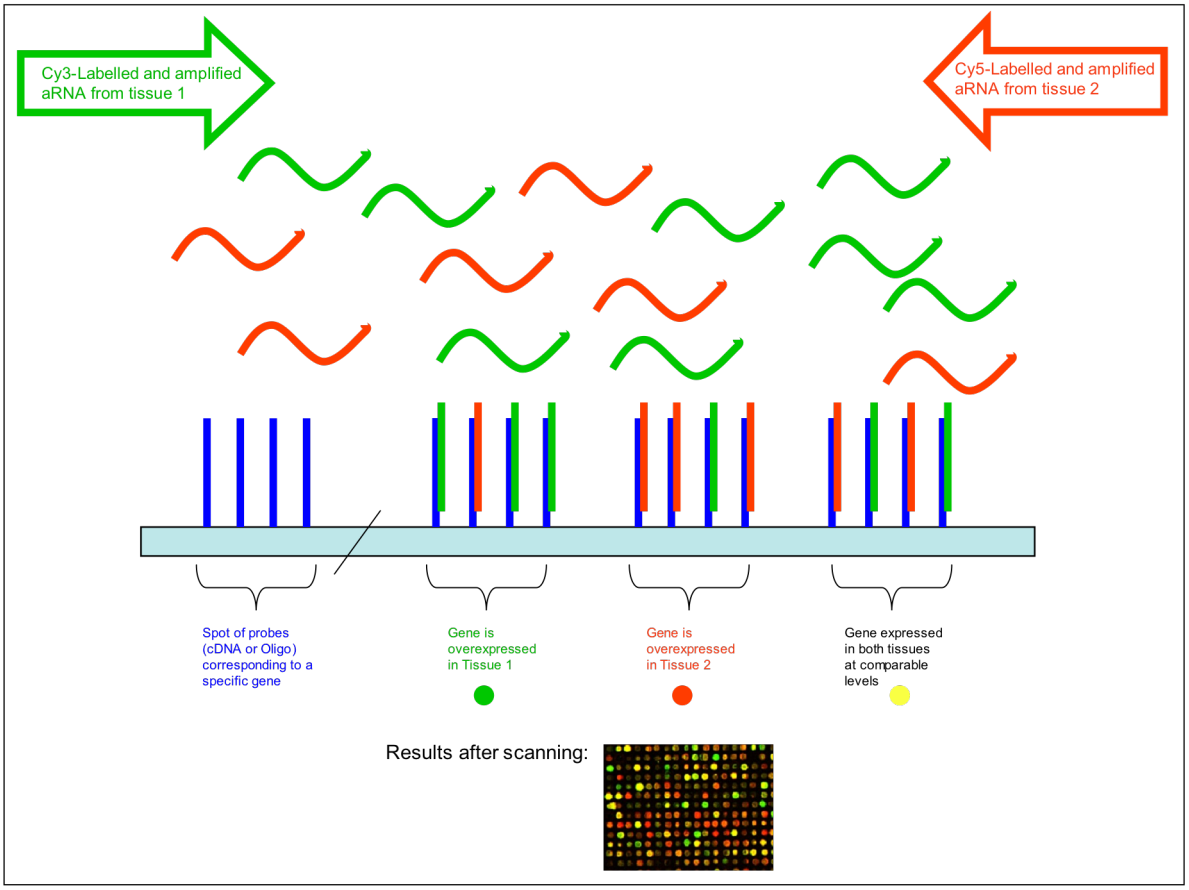

Figure 9: Principle of competitive hybridization of two aRNA samples labeled either with Cy3 or Cy5. If a gene is more expressed in tissue 1, the spot corresponding to that gene will have a stronger Cy3 signal. If a gene is more expressed in tissue 2, the spot corresponding to that gene will have a stronger Cy5 signal. Both signals will be equal if a gene has comparable expression levels in both tissues

In order to observe the gene expression level changes between 2 tissues, the total RNA of both tissues has to be separately extracted, reverse transcribed into cDNA and amplified in aRNA. Each sample is then labeled separately with either Cy3 (emission at 575nm) or Cy5 (emission at 660 nm), which are respectively commonly called the "green" and "red" dyes. A sample mix containing equal amounts of the Cy3- and the Cy5-labelled aRNAs is then hybridized on the chip. The slide is then scanned, to measure the signals intensities coming from the Cy3 and the Cy5 dyes in each spot. Each spot contains the oligonucleotides, which are specific for one gene. Therefore, if a gene is more expressed in the tissue from which the aRNA has been labeled with Cy3, the intensity of the Cy3 signal will be higher than the one coming from Cy5 for the spot representing this gene. The opposite is true, if another gene is more expressed in the tissue from which the aRNA has been labeled with Cy5. This system is widely used in custom-made microarrays, but also in commercially available chips produced by Agilent Technologies (Santa Clara, Ca, USA).

1.4.2 Affymetrix GeneChip® Mouse Exon 1.0 ST Array

Commercially available chips produced by Affymetrix are nowadays widely used to study expression level changes across the whole genome. Recent developments have pushed the technology even further, and allow the monitoring of expression level changes at the exon level, thereby revealing alternative splicing events, which, by recent estimates, affects as many as 94% of all human genes (Pohl et al., 2009; Wang et al., 2008).

The first concept of the exon chip was elaborated by Clark et al. and was designed for humans (Clark et al., 2007). By scanning bioinformatically all the data available in Ensembl, GenScan, Twinscan, SLAM, among others, they defined every region, which corresponded to a putative exon as a Probe Selection Region (PSR). The probes were then designed as 25mer oligonucleotides, so that 90% of all PSRs were covered by a probeset of 4 probes (Figure 10). All PSRs of length greater than 17 nucleotides were covered by at least one probe. In case a PSR was shorter than 25 nucleotides, the probe was designed with a central target sequence, and surrounding genomic sequences filling out the 25mer. The probesets were also designed to take alternative 5' or 3' splice sites into consideration. If there was sequence evidence of overlapping exons with different edges, which suggested alternative and acceptor and donor sites, the exon was divided into multiple PSRs, which took in account the multiple splice variants, and appropriate probesets for each PSR (i.e. splice variants of the exon) were designed.

As for other GeneChip® arrays, the probes were synthesized in situ on a glass surface, according to a proprietary protocol from Affymetrix. The sample preparation was also different than the previously described protocol, it consisted in a total RNA extraction with random hexamer/T7 promoter oligonucleotides as primers followed by a reverse transcription and a second strand synthesis to obtain a double stranded cDNA. From this cDNA a complementary RNA (cRNA) was transcribed in vitro. The cRNA was then again reverse transcribed into cDNA for which the second strand was also synthesized. This cDNA was then fragmented and end labeled with a biotin-conjugated nucleotide analog (DLR-1a; Affymetrix, Inc.)

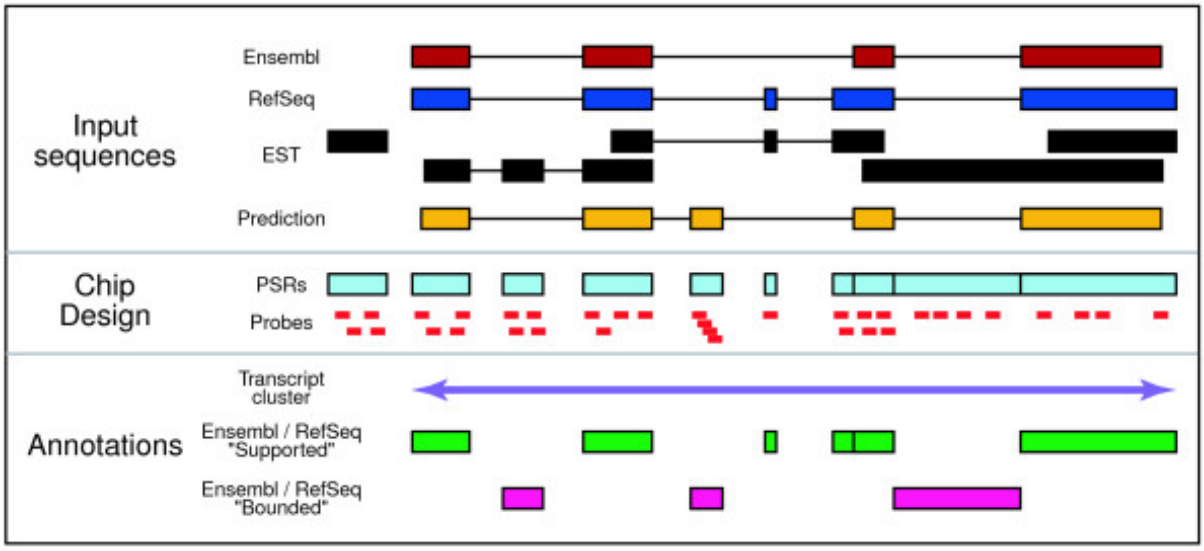

Figure 10: From Clark et al, Genome Biol. 2007; 8(4): R64. The Input sequences were analyzed on a variety of publicly available databases, in order to define all the putative exons – or PSR – of every gene. The probes were then designed, so that 90% of all the PSR had one probeset of 4 probes specific for it.

In order to analyze the signals, they used an algorithm, which normalized exon signals obtained by the 4 probes of a probeset to the signal obtained for the gene as a whole, by all the probes that cover that gene. In their experiments, Clark et al. identified tissue specific exons comparing 16 different healthy human tissues. They were able to validate 86% of the tissue specific exons by real-time PCR (Clark et al., 2007).

The Affymetrix GeneChip® Mouse Exon 1.0 ST Array was developed following the same process for the murine genome. These arrays were used in the final part of this project.

1.5 Project description and relevancy

1.5.1 Rational of the project

Pain is a highly subjective sensory experience, which arises from the combination of physiological and emotional processes. In humans, it is possible to assess the level of pain in most cases, because patients who suffer indicate that they are not feeling well. In animals, the signals an observer has to monitor are different from a species to the other, and can be very difficult to detect. Therefore, the monitoring of nociception could give a more precise and objective estimation of the pain level an animal is experiencing. When a nociceptive message is triggered by an external stimulus and transmitted to the CNS, it activates a wide series of molecules from the nervous and inflammatory systems (Julius and Basbaum, 2001; Scholz and Woolf, 2002). These are all products of genes, or are substrates for proteins, which are encoded by genes. In postoperative phases or longer lasting inflammations,

the painful sensation lasts longer and it seems possible that gene expression changes occur to maintain the noxious signal's transmission and integration, at the various "checkpoints" of the nervous system: the periphery, the DRG, the spinal cord, and within the brain.

Transgenic technology has made it possible to suppress the expression of specific genes in animals, and the studies of knockout mice have indicated mutation or suppression of certain genes can facilitate or inhibit behaviors related to pain (Lacroix-Fralish et al., 2007). These genes therefore probably play an essential role in the generation and transmission of a nociceptive signal. Considering this information, it seems possible, that some of those "pain genes" undergo expression changes, which are essential to maintain longer lasting painful sensation. These expression changes could be measured with microarrays in the brain, the spinal cord, or in the DRGs and could give an objective way to monitor nociception in various lasting pain models.

1.5.2 Aims of the project

This project had the following goals:

- The establishment of a database of the commonly known pain genes.
  - Scanning of the literature on knockout animals and systemic applications to find the most potent candidate genes involved in nociception, fear and anxiety.
  - Establishment of a database of these genes.

- The establishment of a microarray for the analysis of these genes in the CNS, which could possibly be used as a diagnostic tool for nociception and pain.
  - Define RNA extraction and labeling protocols for the optimal study of gene expression in the CNS.
  - Design probes, spotting and hybridization conditions for the microarray analysis of these genes.
  - Define normalizations and data acquisition procedures for the interpretation of the results

- The validation of the microarray protocol for the analysis of the genes in the CNS, by comparing the results obtained in published data.
  - Perform hybridization reactions with various parts of the CNS.
  - Search literature and microarray databases to find data to validate the gene expression changes observed

- Measurements of gene expression changes in the CNS between animals in pain and control animals
  - Perform hybridization reactions with various parts of the CNS of mice in the telemetric apparatus implantation pain model to detect gene

expression changes characteristic of nociception in each of these parts.

- Validation of the data by Real-Time PCR
  - Establish Real-Time PCR conditions for an optimal high throughput analysis of the set of genes, which showed differential expression in the surgical pain model in each analyzed part of the CNS.
  - Compare the behavior of these genes in similar parts of the CNS in mice, which underwent the BHV1-immunization, characteristic of an inflammatory pain model.

- Discover new genes, which might be linked to nociception.
  - Perform a microarray analysis in the CNS at the exon level using Affymetrix GeneChip® Mouse Exon 1.0 ST Arrays to detect new candidate genes, which show gene expression level changes, or alternative splicing modifications linked to the surgical pain model.
  - Define the main new functional categories of genes, which could be possibly used to monitor nociception.

1.5.3 Relevancy of the project for animal welfare

Laboratory animals are widely used in research for experiments, which require painful surgical procedures. Moreover, pain must be considered as an important aspect in research on topics such as inflammation, cancer or infectious diseases. This can be problematic from an experimental point of view, as pain can influence the data observed, but most importantly, it is important that efforts are taken to minimize the animal's suffering during the experiment. Russel and Burch were the first researchers to focus on laboratory animal welfare issues. In their studies from 1952, they defined inhumanity in animal experiments, by grading the level of distress the animals were subjected to. Their work was the stepping stone of the 3R principles: replace, reduce and refine. These rules are still internationally recognized and applied in animal research. In that sense, pain assessments in laboratory animals are very important to ensure that an experiment is not causing some unnecessary suffering to an animal. It is also essential to be able to clearly monitor pain, in order to ensure that stress and pain do not bring bias to the data. For instance, the activation of the nociceptive system could modify the outcome of studies on the central nervous system, as it modifies the neuronal activity. Classical methods for pain assessment such as blood corticosterone measurements imply some extra handling of the animal, which can add some extra stress to the animal and further bias the data (Enthoven et al., 2008; Schmidt et al., 2005). Other methods for pain assessments require behavioral tests performed on cohorts of animals, which cannot be performed routinely during a health check of each animal (Schaefer et al., 2009). It is therefore necessary to develop new diagnostic tools to monitor pain animals. The analysis of the physiological processes underlying

nociception offers a potent new way to assess pain in laboratory animals. However, methods like electrophysiology or patchclamp (Caterina et al., 1997; Djouhri et al., 1998; Priest et al., 2005) demand quite elaborate settings and skills, and can therefore not be used in every day diagnostics.

Mice show moderate behaviors, which might indicate that they are experiencing pain. This feature is an advantage for them to survive in their natural environment, however it renders the assessment of pain very difficult in an experimental setting. Current methods to monitor pain in research facilities rely on observations of the animals and scoresheets annotations, which give variable results from one observer to the other. Moreover, mice will hide their suffering even more, when an observer is in the room. Another way to assess stress and possibly pain is the measurement of blood corticosterone levels (Enthoven et al., 2008; Schmidt et al., 2005). However, this method presents the disadvantage of requiring a handling of the animals, which induces some additional stress and ultimately biases the results.

Monitoring nociception analyzing gene expression changes in the CNS could provide some valuable information on the level of pain experienced by an animal. A microarray analysis, or a series of Real-Time PCR reactions on the appropriate pain genes could be performed on sentinel animals routinely before starting a procedure. This could indicate the pain severity for the animal, and appropriate analgesic measures could then be applied. Moreover, this technique could also be used to monitor the possible level of pain experienced by a transgenic animal, because of the specific mutation or gene deletion it carries. It would allow researchers to take appropriate measures to reduce the suffering of this animal and would therefore contribute greatly to animal welfare.

2. Results

2.1 Low density microarray design

In order to analyze gene expression changes linked to nociception in the central nervous system of mice, we established a low-density microarray. 230 genes were selected according to their relevancy in pain research. The genes had been previously characterized as inducing behaviors characteristic of pain in transgenic animals mouse models in which these genes were either knocked out or overexpressed. Half of the genes we had chosen to study were also listed in a known pain gene database established by Prof. J. Mogil's group in Montreal, Canada (Lacroix-Fralish et al., 2007). The other half consisted in genes associated to stress. The various categories of genes we chose to analyze are listed in table 1. A more detailed list, containing each gene's name and described function, as well as their identifier on the microarray, their accession numbers, and relevant literature references can be found in Appendix 1.

Table 1: Sum up of the genes, which were included in the study and spotted on the microarray. The genes are grouped by function. The positive control genes and the spikes genes were used for normalization purposes. The negative control genes were used to control the relevancy of the hybridization protocols.

Gene Family	Number of genes	Examples
Receptors	97	GABA receptors, Glucocorticoid receptor, Opioid receptors, Serotonin receptors
Signal Transduction	29	Phospholipase C Gamma, MAP kinases, JNK...
Neuropeptides	13	Enkephalin, Neuropeptide Y, Tachykinin…
Oxidative Stress	6	Cytochromes…
Hormone related genes	4	Adrenocorticotropic hormone, Corticotropin releasing hormone binding protein...
Neurotrophins	3	NGF, BDNF…
Heat shock	4	HSP 27, HSP 72…
Channels	3	Sodium channel type IX, Calcium channel P/Q type alpha 1
Cytokine-related genes	14	Interleukin 10, Interleukin 4…
Others	26	Steroidogenic Factor 1, Nociceptin, DREAM…
Positive controls	19	Tubulin, Beta Actin…
Negative controls	11	Bacterial genes, non-genomic randomly generated sequences
Spikes	8	Specific non-genomic sequences used later for normalization

Two types of controls were used for our microarray study. The negative controls were sequences, which are not expressed in the murine central nervous system such as bacterial gene or randomly generated sequences. The positive control genes were ubiquituously expressed (for example: Beta Actin). These genes were expected to have a high signal, and could be used for orientation purposes as well as to monitor the quality of the hybridization reactions.

The slide went through 3 optimization phases. In all designs, the 70-mer oligonucleotide sequences were spotted in triplicates over 4 blocks. Each block was spotted in duplicates in order to have 6 replicates per gene to ensure statistical robustness. The first slide design can be seen in Appendix 2. This version contained only 218 genes. Spots containing Cy3 or Cy5 solely (dye control spots) and empty spots of 3x SSC were used as scanning and orientation controls. In the second design, the spots containing only the dyes were not spotted anymore, to minimize risks of dye carry over during spotting. The positive and negative controls were spotted in the first and last column, as well as in the two middle columns of each block. For orientation purposes, a positive control was spotted at the beginning of each block, followed by 3x SSC. The end of each block contained only 3x SSC. Each block's asymmetry allowed a quick slide orientation of the slide after scanning. A scheme of the second slide design can be seen in Appendix 3. The third design was used for the experiments on parts of the central nervous, and for the validation of the one color hybridization protocol. This batch of slides was spotted with a Genetix contact printer, which allows a fast and reliable slide printing. The spots were spotted horizontally over the blocks, and not in a standard increasing order. This new shuffling separated genes of similar families on different blocks, to ensure that high signals from a certain family of genes were indeed due to each gene, and not to a spotting carry over from one specific member of the family. For blocks 1 and 3, positive controls were spotted in the first and the last lines, as well as in the middle of the blocks next to a line of negative controls. On the other hand, for blocks 2 and 4, negative controls in were spotted in the first and the last lines along with 3xSSC, as well as in the middle of the blocks next to a line of positive controls. The spikes were spotted on the fifth line of the first 2 blocks; the last 2 blocks had 3xSSC spotted instead. Appendix 5 shows graphically how this slide was designed.

2.2 Whole brain microarray experiments

The first set of experiments we performed consisted in analyzing gene expression changes related to nociception in the whole brain of mice. Three NMRI mice were anesthetized with Sevofluorane and underwent a telemetric apparatus implantation, after which they were treated twice daily with an intraperitoneal injection of Flunixin. As controls, 3 NMRI mice underwent the

same anesthesia and analgesia protocol but did not undergo any surgery. After two days, the mice were sacrificed. Their brains were dissected out, and the RNA was extracted, amplified and labeled for microarray hybridization. This analysis was carried out on the first design of the microarray. Figure 1 shows the scanned slides. On each slide a competitive hybridization was carried out: the brain antisense RNA (aRNA) of interst was labeled with Alexa-555 and a Reference mouse brain aRNA, which was identical between each slide was labeled with Alexa-647.

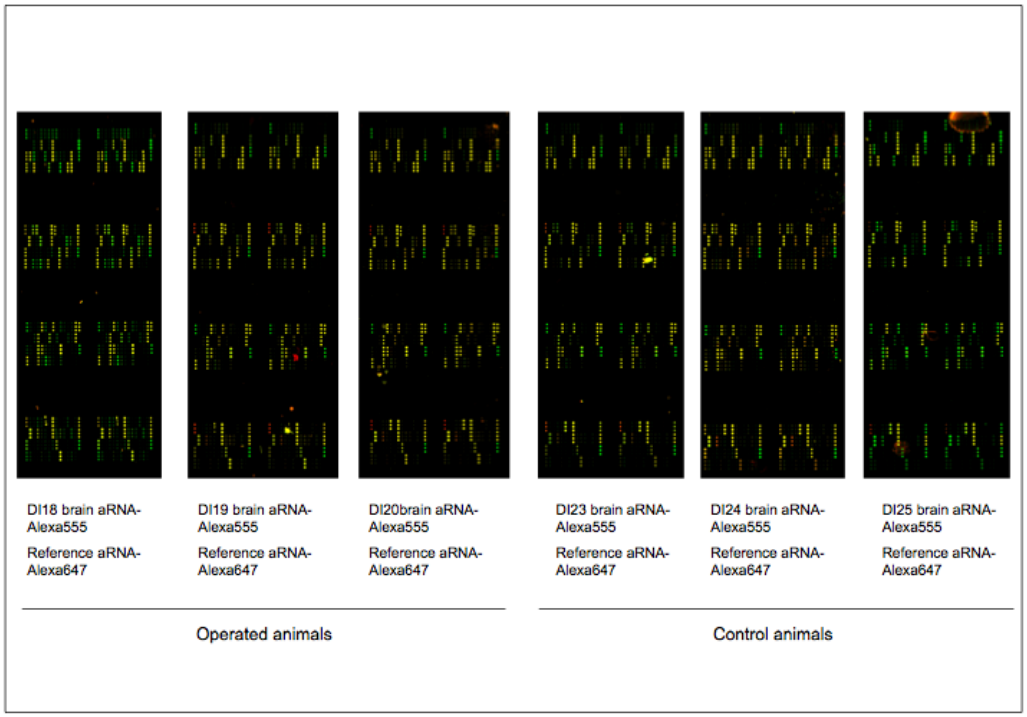

Figure 1: Scanned slides of the whole brain experiment. The slides had been spotted according to the first chip design. Animals 18, 19 and 20 were operated and treated with analgesia. Animals 23, 24, and 25 underwent the same anesthetic and analgesic treatment, with no surgery. On each slide, the brain aRNA of interest is labeled with Alexa-555 and the reference mouse brain aRNA was labeled with Alexa-647. The hybridization quality was good with very little background, well-formed spots, and comparable intensity between triplicates of the same gene. On all slides, most spots appear yellow, suggesting little expression changes between the analyzed brains and the reference brains.

For each slide, scatter plots representing the raw signal intensities in the brain of interest in function of the reference mouse brain signals were calculated (Figure 2). On all slides, the Alexa-555 signals were generally stronger than the Alexa-647 ones, especially for the genes, which had low expression levels. Graphically, each scatter plot was shifted towards the Y-axis representing the Alexa-555 signals. All scatter plots of the raw signals were narrow, and did not indicate big expression changes between the analyzed brains and the reference brains. As expected, the Cy3 and Cy5 signals from the dye control spots were each located on the appropriate side of the scatter plot, but not in a symmetrical way. Both spots had a signal of approximately 10^5 in the appropriate channel. The Cy3 spot had a residual signal of 100 in the red

channel, whereas the residual green signal for the Cy5 spot was of about 1200. This once again indicated a general dye imbalance, with general higher green signals. An analysis of variance (P Value = 0.1) was performed to compare the gene expression changes between the 3 operated animals and the 3 control ones. No gene passed the test, and therefore, no significant gene expression changes could be observed on the raw signals between the brains of the operated animals and the brains of the control animals.

Locally weighted scatter plot smoothing, or Loess, combines linear least square regression with non-linear regression. The advantage of this function is that it normalizes each points of a curve independently, to fit the curve of highest density. It is therefore commonly used as a normalization tool to correct dye imbalances or printing biases, which affect mostly genes with low signal in microarray data. We also applied Loess normalization, which did alter the dye imbalance, and aligned the scatter plots on the midline. However, the asymmetry between the Cy3 and Cy5 control spots remained identical as for the raw values, suggesting that this normalization was not robust enough to completely overcome the general higher green signal. The normalized scatter plots can be seen on Figure 3. As for the raw values, an analysis of variance was performed to compare the gene expression changes between the 3 operated animals and the 3 control ones. In that case too, no significant gene expression changes could be observed when analyzing the normalized values.

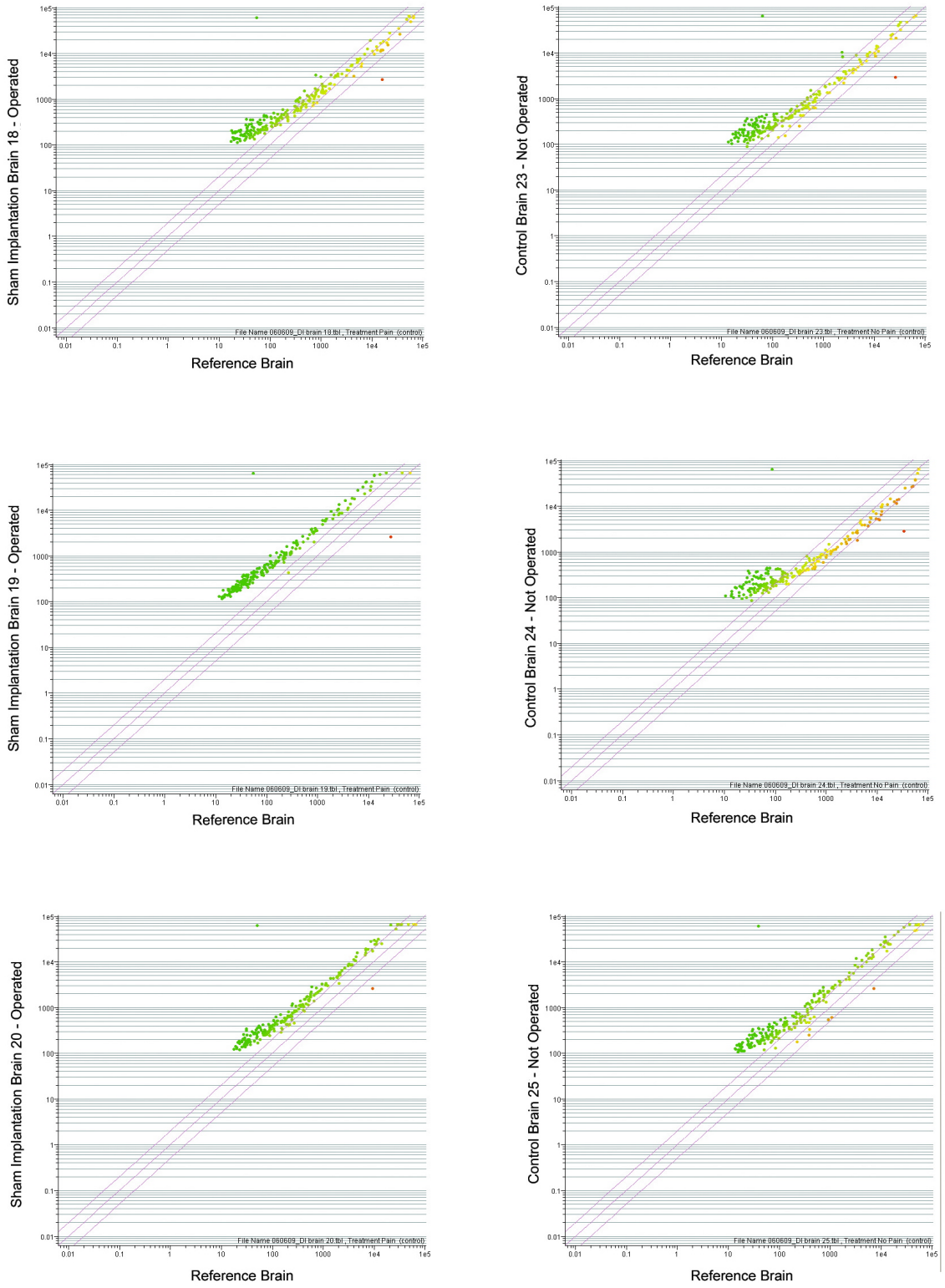

Figure 2: Scatter plots comparing of the Alexa-555 labelled brain of interest's raw signals in function of a reference brain aRNA raw signal. Brains 18, 19, and 20 were dissected from operated mice, and brains 21, 22, 23 were from control animals. The scatter plots are asymmetric, with a general higher green signal. This effect particularly affects the genes with signals lower than 1000. This can be seen by a shift of the plot towards the Y-axis, and a higher residual green signal for the Cy5 control spot than the residual red signal for the Cy3 control spot.

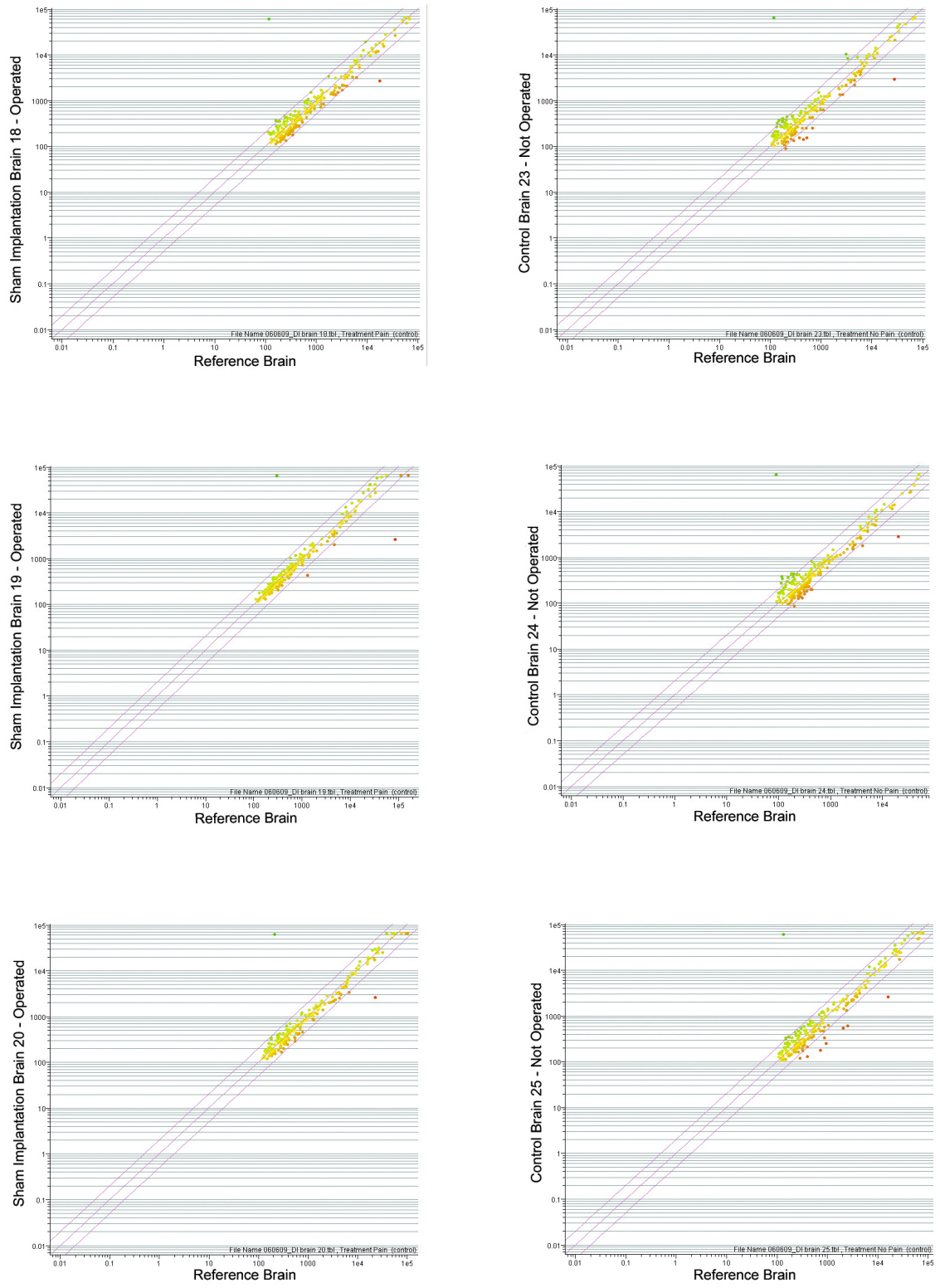

Figure 3: Scatter plots comparing of the Alexa-555 labelled brain of interest's normalized signals in function of a reference brain aRNA normalized signal. Brains 18, 19, and 20 were dissected from operated mice, and brains 21, 22, 23 were from control animals. The Loess normalization partially corrected the dye imbalance. The scatter plots are aligned on the midline. However, the residual green signal of the Cy5 spot still remains higher than the residual green signal of the Cy3 spot. This suggests, that the dye imbalance has not been completely corrected by the Loess normalization.

Equal amounts of brain 19 aRNA labeled with Alexa-555 and reference brain aRNA labeled with Alexa-647 were hybridized on one slide spotted according to the first version of the microarray. On another slide from the same batch, the same amounts of Brain 19 aRNA labeled with Alexa-647 and reference brain aRNA labeled with Alexa-555 were hybridized. The only difference between the two hybridization reactions was the dye swap between the samples. Scatter plots of the raw data were established and indicated a general higher green signal on both slides, evidenced by a dissymmetry between the Cy3 and Cy5 spots (Figure 4). The scatter plots were shifted towards the Y-axis on which the green signals were scaled, regardless of whether it represented aRNA derived from Brain 19 or from the reference mouse brain. This proves that the shift towards the Alexa-555 signals is due to a dye imbalance, and not to a biological event, which leads to a general higher gene expression in one sample.

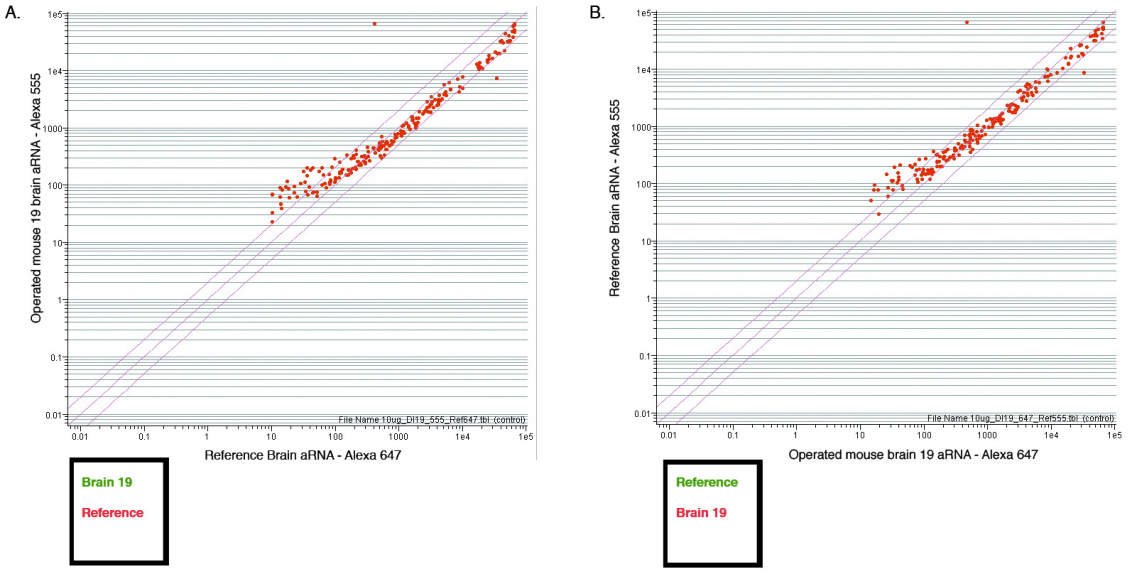

Figure 4: Dye swap experiment. A competitive hybridization of brain 19 aRNA and reference aRNA was performed twice on identical slides. The dyes used for the aRNA labeling were however swapped between these two hybridizations. On scatter plot A, illustrating the first hybridization, the Brain 19 aRNA was labeled with Alexa-555, and the reference brain aRNA was spotted with Alexa-647. On scatter plot B, illustrating the second hybridization, the reference brain aRNA was labeled with Alexa -555 and the Brain 19 aRNA was labeled with Alexa-647. Both plots show an asymmetry between the Cy3 and Cy5 spots, as well as a shift towards the Alexa-647, regardless of which sample was labeled with this dye. This general higher green signal is therefore caused by a dye imbalance, and not by a biological regulation.

2.3 Microarray experiments with specific regions of the central nervous system

In order to have a refined analysis of the genetic regulation processes linked to nociception, we decided to carry a further analysis on parts the central nervous system. To bypass the dye imbalance we observed in previous experiments, and the difficulties linked to the statistical normalization of a low number of genes, we developed a hybridization protocol for single samples labeled with Cy5. The normalization was based on a set of ubiquitously equally expressed positive control genes, and consisted in bringing the signals of this set of genes at equal levels, and further normalize the other genes accordingly. In this experiment, the operated mice underwent the same surgical and analgesic protocol as previously described, and the 3 control animals underwent the same anesthetic and analgesic protocol as the operated animals. After a recovery of 2 days, the animals were sacrificed, and the brainstem, the cerebellum, the hippocampus, the cortex and the spinal cord of each animal were dissected, the RNA extracted, and the mRNA amplified into aRNA, that was labeled with Cy5 for hybridization. After hybridization, each part of the brain was analyzed separately. We analyzed the raw data, as well as the data normalized according to the set of positive genes spotted on our slide. For each part of the central nervous system, scatter plots were established, and the genes were filtered on a volcano plot. This method consists in plotting the genes according to their fold change between the 2 conditions, and their p=values. It is then possible to screen the genes according to their significance and their fold change expression difference. We selected the genes, which had a P Value lower than 0.05 and the fold change higher than 1.5 in one condition or another.

2.3.1 Microarray results in the cortex

In the cortex, no genes could be filtered, either on the raw values or on the normalized values. In both cases, the scatter plots were aligned on the midline, with no significant genes showing a high fold change towards one condition or the other. The scatter plots and the volcano plots can be seen on Figure 5.

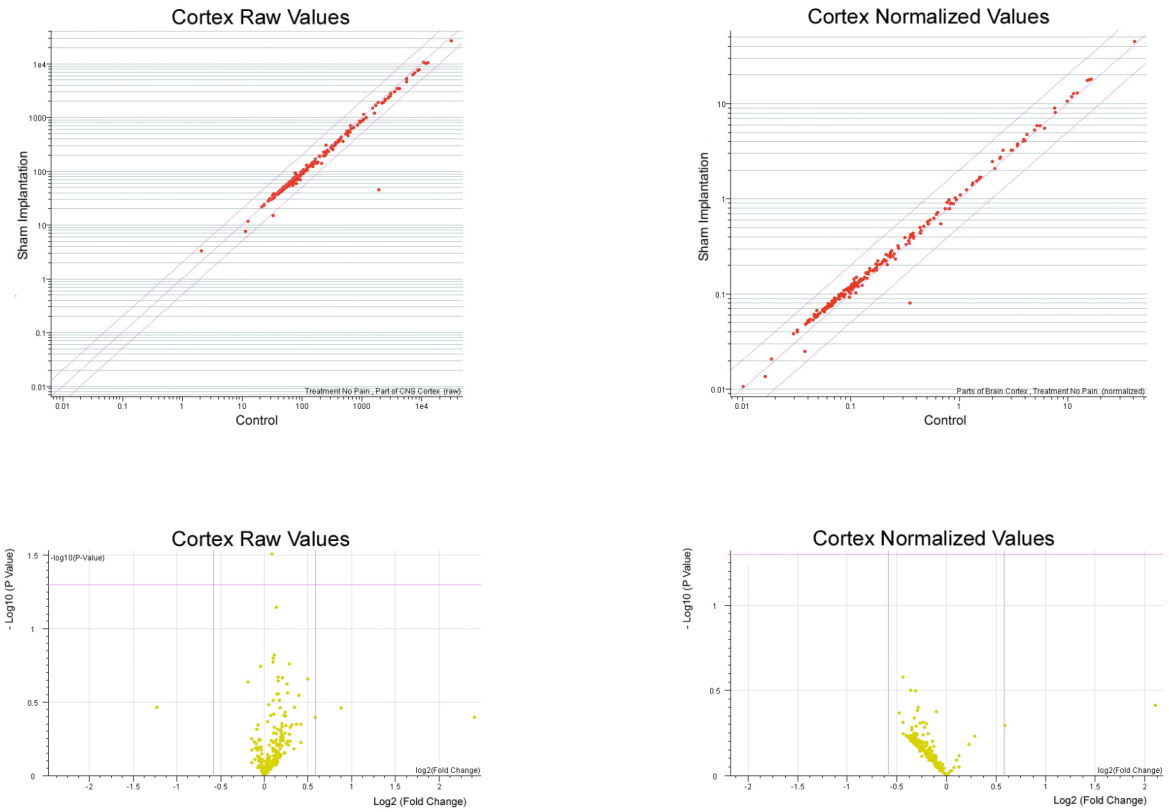

Figure 5: Scatter plots and volcano plots of the genes expression levels changes measured in the cortex. The scatter plots are narrow, aligned on the midline and show no significant difference between the 3 operated animals and the 3 contol ones, both on the raw and normalized values. After a filtering on a volcano plot, no genes have a P Value < 0.05 and a fold change > 1.5.

2.3.2 Microarray results in the brainstem

In the brainstem, the comparison between the animals, which had undergone surgery and the 3 animals, which served as controls revealed some significant gene expression level differences. Both the scatter plots of the raw and normalized values showed no general shift towards one condition (Figure 6). The filtering on a volcano plot of the raw signals unveiled only one gene, which was 1.5 times more expressed in the animals, which had endured pain (Table 2a). This gene is the Neuropeptide Y receptor type 5. The same analysis on the normalized signals revealed that 6 genes had a P Value lower than 0.05 and were more than 1.5 times downregulated in the operated animals (Table 2b). Two of those genes were however negative control genes, which had low expression levels, and were therefore more likely to show fold changes, and appear as false positives in such an analysis.

We performed Real-Time PCR measurements of the regulated genes in order to confirm the results, however no correlation could be established between the microarray measurements and the Real-Time PCR results. The results obtained on the microarray are therefore probably due to artifacts.

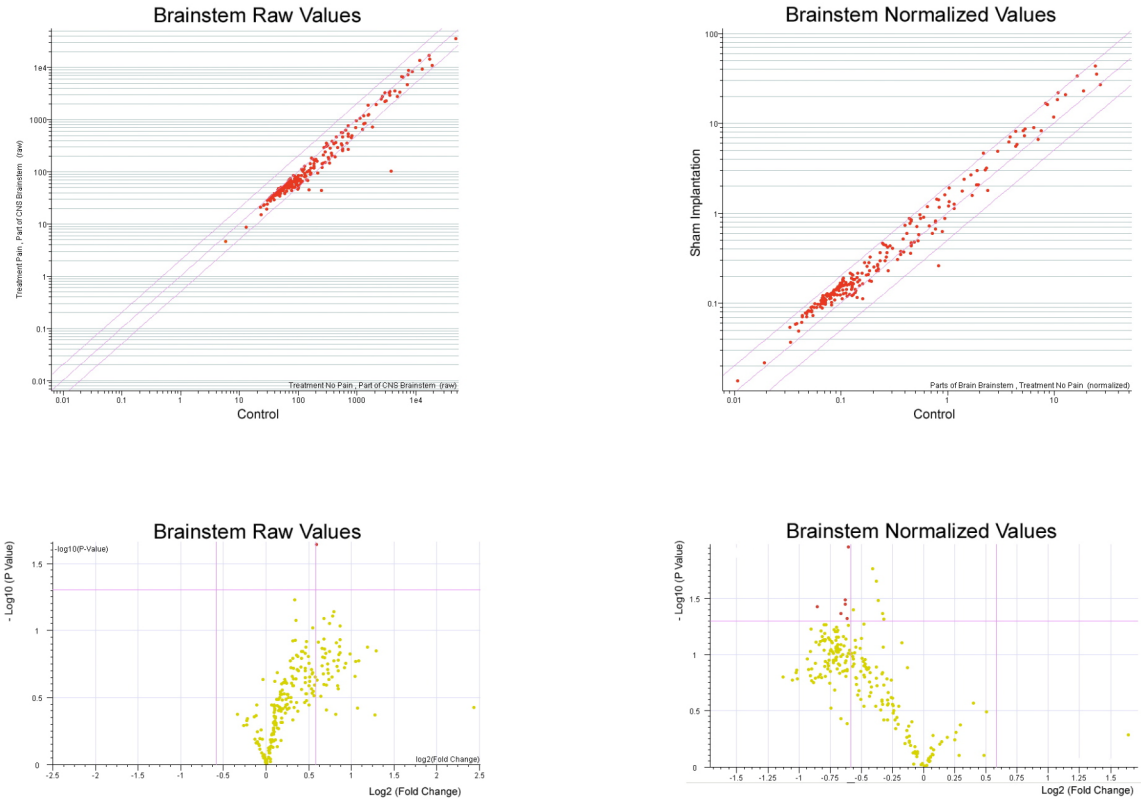

Figure 6: Scatter plots and volcano plots of the genes expression levels changes measured in the brainstem. The scatter plots are aligned on the midline and show significant differences between the 3 operates animals and the 3 control ones, especially on the normalized values. The volcano plots confirmed this tendency. The filtering was performed with a P Value < 0.05 and a fold change > 1.5. For the raw signals, 1 gene was 1.5 times more expressed in the brainstems of the operated animals. For the normalized values, 6 genes were downregulated in the brainstems of the operated animals.

Table 2: Regulated genes in the brainstem filtered on a volcano plot with a P Value < 0.05 and a fold change > 1.5.

2a: Filtering performed on raw signals. There is no correlation between the regulation observed on the microarray and the Real-Time PCR measurements.

Gene Name	Gene ID, NCBI	Real Time PCR			Microarray
		CT Operated	CT Control	Fold Change	Fold Change
Neuropeptide Y receptor type 5 (Npy5r)	NM_016708	Mean=8.83, STD DV= 0.65	Mean=8.87, STD DV=0. 69	1.03	1.5

2b: Filtering performed on normalized signals. There is no correlation between the regulation observed on the microarray and the Real-Time PCR measurements.

Gene Name	Gene ID, NCBI	Real Time PCR			Microarray
		CT Operated	CT Control	Fold Change	Fold Change
Vanilloid-receptor TrpV5	NM_001007572	-	-	-	-1.5
Vanilloid-1 receptor (VR1) Oligo 1	NM_001001445	Mean=6.2, STD DV=0.72	Mean=6.11, STD DV=0.47	-1.07	-1.5
Serotonin receptor: 5-HTr6	NM_021358	Mean=9.32, STD DV=0.41	Mean=9.46, STD DV=0.53	1.1	-1.5
E coli bioA gene	E100000750	-	-	-	-1.55
Randomly generated negative control 4		-	-	-	-1.58
Serotonin receptor: 5-HTr4 Oligo 2	NM_008313	Mean=4.69, STD DV=0.20	Mean=4.96, STD DV=0.61	1.2	-1.81

2.3.3 Microarray results in the cerebellum

The microarray analysis carried out in the cerebellum revealed some differences between the signals measured in the operated animals and in the control ones. The scatter plots for both the raw and the normalized values were aligned on the midline. The spots appeared quite spread between the 2 fold lines indicating that some regulations were present, especially for the normalized values. However, the volcano plot of the normalized values showed that most genes have a high P value. This compromised the significance of the regulations observed (Figure 6). We filtered both the raw and the normalized signals on their respective volcano plots, to select the genes, which have a fold change higher than 1.5 in one condition or another, and a P value lower than 0.05. On the raw values (Table 3a), 15 genes showed a regulation, amongst which 13 were upregulated, and 2 were downregulated in the operated animals. For the normalized values (Table 3b), only one gene showed a differential expression: the Neuropeptide Y receptor type 6, which was 5.5 times more expressed in the animals which endured pain.

We performed Real-Time PCR measurements of most of those genes, to possibly confirm the gene expression changes we had observed either on the raw signals or on the normalized ones. None of the regulations could also be seen in the Real-Time PCR analysis. The gene regulations we observed in the cerebellum were therefore not reproducible.

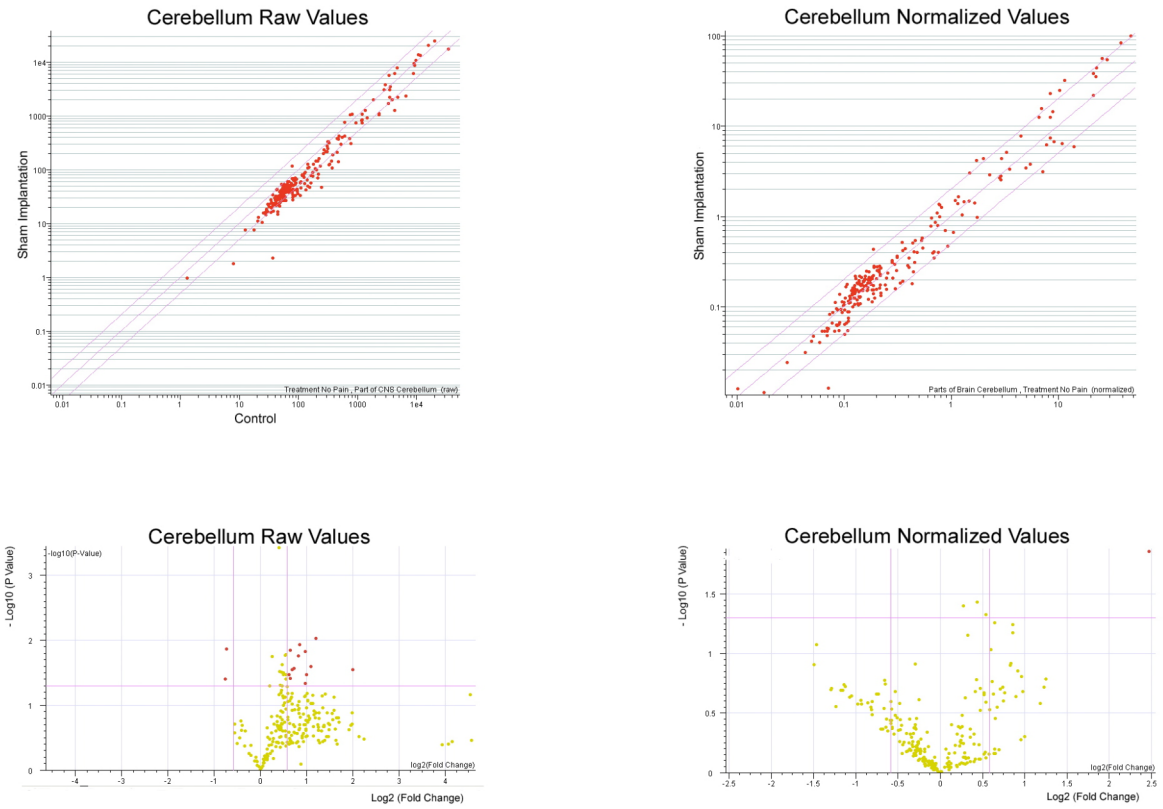

Figure 6: Scatter plots and volcano plots of the genes expression levels changes measured in the cerebellum. The scatter plots are aligned on the midline and quite widely spread, which tends to indicate differences between the 3 operated animals and the 3 control ones, especially. However, the volcano plots showed that the P Value of most genes was high, which indicated that the changes observed were not significant. The filtering was performed with a P Value < 0.05 and a fold change > 1.5. For the raw signals, 15 genes were regulated by nociception in the cerebellum. For the normalized values, only one gene was regulated in the cerebellum of the operated animals.

Table 3: Regulated genes in the cerebellum filtered on a volcano plot with a P Value < 0.05 and a fold change > 1.5.

3a: Filtering performed on raw signals. There is no correlation between the regulations observed on the microarray and the Real-Time PCR measurements.

Gene Name	Gene ID, NCBI	Real Time PCR			Microarray
		CT Operated	CT Control	Fold Change	Fold Change
Neuropeptide Y receptor type 5 (Npy5r)	NM_016708	Mean=11.98, STD DV= 0.2	Mean=12.09, STD DV=0. 11	1.08	4.01
Randomly generated negative control 4		-	-	-	2.31
MAP kinase 1 (=Erk2)	NM_011949	Mean=4.81, STD DV= 0.34	Mean=5.03, STD DV=0.38	1.17	2.13
Somatostatin receptor 1	NM_009216	-	-	-	2.01
Sodium- and chloride-dependent GABA transporter 1	NM_178703	Mean=4.06, STD DV=0.66	Mean=3.93, STD DV=0.61	-1.09	1.97
Guanine nucleotide binding protein, alpha 0	NM_010308	Mean=2.97, STD DV=0.34	Mean=3.03, STD DV=0.28	1.04	1.96
Nerve Growth Factor alpha (NGF)	NM_010915	Mean=3.57, STD DV=0.25	Mean=3.25, STD DV=0.37	-1.25	1.81
Alpha-2C adrenergic receptor	NM_007418	Mean=7.61, STD DV=0.46	Mean=7.79, STD DV= 0.54	1.13	1.77
F2rl2	NM_010170	-	-	-	1.66
Vanilloid-1 receptor (VR1) Oligo 1	NM_001001445	Mean=1.58, STD DV=0.33	Mean=1.69, STD DV=0.21	1.08	1.61
Cytochrome P450 21A1 (CYP21a1)	NM_009995	-	-	-	1.57
NMDA-receptor NMDA1	NM_008169	Mean=8.41, STD DV=0.62	Mean=8.56, STD DV=0.75	1.11	1.57
Serotonin receptor: 5-HTr4(e)	Y09588	Mean=10.29, STD DV=0.57	Mean=10.34, STD DV=0.42	1.03	1.54
Creb3	NM_013497	Mean=3.15, STD DV=0.29	Mean=3.03, STD DV=0.09	-1.09	-1.66
Proopiomelanocortin	NM_008895	Mean=6.82, STD DV=0.13	Mean=7.24, STD DV=0.18	1.34	-1.69

3b: Filtering performed on normalized signals. There is no correlation between the regulations observed on the microarray and the Real-Time PCR measurements.

		Real Time PCR			Microarray
Gene Name	Gene ID, NCBI	CT Operated	CT Control	Fold Change	Fold Change
Neuropeptide Y receptor type 6 (Npy6r)	NM_010935.3	Mean=4.04, STD DV= 0.23	Mean=4.2, STD DV=0. 47	1.11	5.543

2.3.4 Microarray results in the hippocampus

In the hippocampus, the quality of the hybridization was good as evidenced by the scatter plots, which were aligned on the midline and did not show a general shift towards one condition (Figure 7). The volcano plot of the raw signals however revealed that no genes had a fold change higher than 1.5, and a P value lower than 0.5. The same filtering was carried out on the normalized values, and the only gene, which satisfied the criteria, was a negative control gene (randomly generated negative control 4), which was 2.2 times more expressed in the hippocampi of the operated animals. This gene was obviously a false positive, therefore, no significant gene expression differences linked to nociception could be observed in the hippocampus.

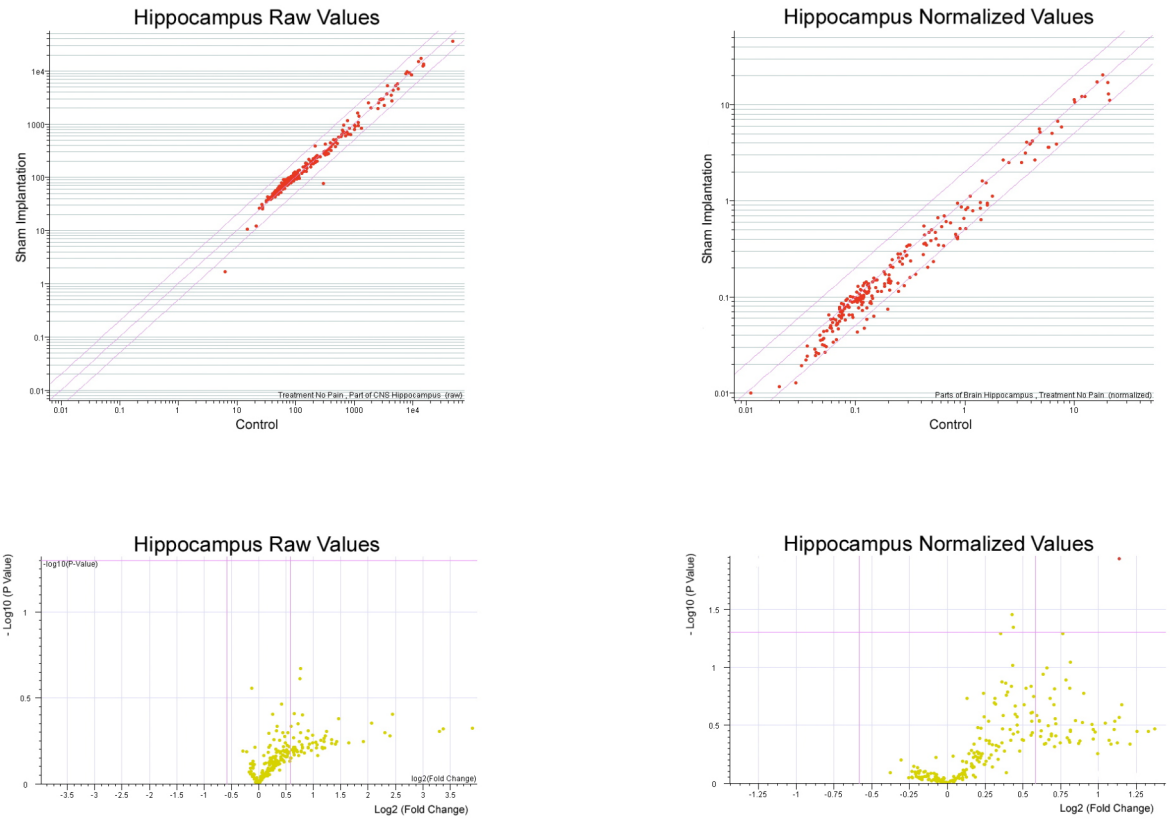

Figure 7: Scatter plots and volcano plots of the genes expression levels changes measured in the hippocampus. The scatter plots were aligned on the midline and showed no significant difference between the 3 operated animals and the 3 control ones, both on the raw and normalized values. After a filtering of the raw signals on a volcano plot, no genes had a P Value < 0.05 and a fold change > 1.5. The same filtering applied to the normalized values revealed one false positive gene, which was 2.2 times more expressed in the operated animals: the randomly generated negative control 4. Therefore, no real significant differences could be observed.

2.3.5 Microarray results in the spinal cord

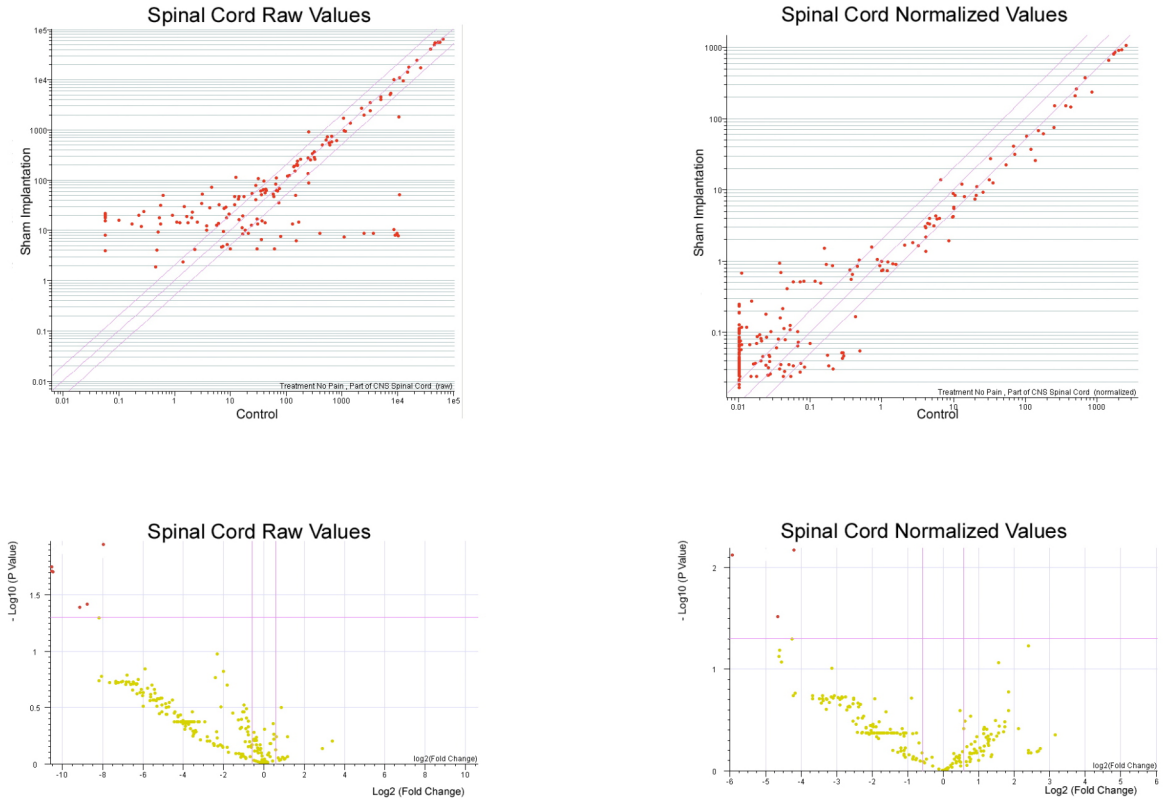

Figure 8 : Scatter plots and volcano plots of the genes expression levels changes measured in the spinal cord. The scatter plots show a lot of genes with signals below 10. These spots are more subject to local background variation, or to biases linked to aRNA amplification from low amounts of total RNA. This appears on the scatter plots as a shift towards one condition or the other for the low intensity genes, and a general flat aspect of the plots, which cannot be corrected with a normalization procedure. A filtering on the volcano plots was nevertheless performed, and showed that 6 genes had a raw signal which were at least 1.5 times downregulated in the operated animals and a P Value lower than 0.05. For the normalized values, 3 genes showed the same features.

A microarray analysis was carried out on the lumbar part of the spinal cord. The scatter plots revealed that the quality of the hybridizations was not optimal. The signals were in the same range as in the other parts of the central nervous system, with the highest values approaching 10^5, however most of the signals of the signals below 100 appeared very spread towards one condition or the other. This tendency does not disappear after normalization. The amount of total RNA extracted from the spinal cord was in average 10 times lower than in the other parts of the CNS. The genes, which had a low expression levels, might have therefore not been sufficiently amplified. This could explain the variability in the low signals. The hybridization quality was however good with little background. A filtering on volcano plot was performed to see if some significant changes could be observed. As

previously, we selected the genes, which have a fold change higher than 1.5, and a P Value lower than 0.05. The scatter plots and the volcano plots can be seen on Figure 8. When analyzing the raw signals, 6 genes appeared highly downregulated in the spinal cords of the operated animals, with fold changes ranging from -245 to -1488. When considering the normalized values, only 3 genes show a significant downregulation ranging from -18 to -62 (Table 4). However, one has to consider, that these genes had very low signals ranging between 0 and 10, and could have been subjected to variability linked to aRNA amplification or background. Because of the critical amount of total RNA and the low signals of the genes, no Real-Time PCR measurements were performed to verify these results.

Table 4: Regulated genes in the spinal cord filtered on a volcano plot with a P Value < 0.05 and a fold change > 1.5.

4a: Filtering performed on raw signals.

Gene Name	Gene ID, NCBI	Fold change in Pain Microarray
ribosomal protein L13 (Rpl13)	NM_016738	-245.10
Endothelin receptor B	NM_007904	-436.68
Serotonin receptor: 5-HTr6	NM_021358	-564.97
MAP kinase 1 (=Erk2): mitogen-activated protein	NM_001038663	-1408.45
Vanilloid receptor-like protein 1 (VRL-1), TrpV2	NM_011706	-1470.59
Peroxisome proliferator activated receptor delta	NM_011145	-1488.10

4b: Filtering performed on normalized signals. There is no correlation between the regulations observed on the microarray and the Real-Time PCR measurements.

Gene Name	Gene ID, NCBI	Fold change in Pain Microarray
GAPDH	NM_008084	-18.349
Opioid receptor sigma 1 (Oprs1)	NM_011014	-25.381
Opioid receptor kappa 3 isoform B (Kor3B)	AF043277	-61.728

2.4 Microarray protocol validation

Given the lack of significant reproducible results of the microarray experiments comparing parts of the central nervous system between operated mice and control ones, we decided to see if some significant results could be observed using the same microarray protocol in another experiment. For the 3 NMRI mice, which had not been operated, we analysed the expression levels of our set of genes between the brainstem, the cortex, and the hippocampus using the same slides and the same hybridization protocol with samples labeled with Cy5 solely. As previously, the raw and normalized data were filtered on a volcano plot, to select only the

genes, which were 1.5 times more expressed in one part of the brain, and had a P value lower than 0.05. The results we obtained were than compared with the ones obtained by Hovatta (Hovatta et al., 2005). In their study, they have assessed the expression profiles of the whole genome in parts of the central nervous sytem of 6 inbred mice strains: 129S6/SvEvTac, A/J, C3H/HeJ, C57BL/6J, DBA/2J, and FVB/NJ. They have worked with Affymetrix Murine Genome U74 Version 2 Arrays, and their results are stored in the GEO dataset, under the following ID number: GDS1406.

2.4.1 Brainstem against cortex hybridizations

This experiment consisted in comparing the expression levels of our set on genes in the brainstems and the cortex of the 3 control mice. The scatter plots of the signals were well aligned on the midline, with some genes showing a significant regulation in the cortex or the brainstem. The normalized values were also well aligned, but tended to show more regulations. Like in the previous experiment, the significant genes were filtered on volcano plots for both the raw, and the normalized values (Figure 9). Only the genes, which showed a 1.5 times regulation in either parts of the brain, and had a P Value of 0.05, were kept. When considering the raw values, 11 genes were significantly regulated, and when considering the normalized values, 6 genes were regulated (Table 5). There was one obvious false positive gene among the 11 regulated genes filtered from the raw signals: the randomly generated negative control 4. Four genes appeared to be regulated both on the raw signals and the normalized ones: the Proteinase-activated receptor 1 and the Heat Shock Protein 70kD, which were more expressed in the Brainstem, and Egr1, and Neuropeptide 1, which were more expressed in the Cortex.

.

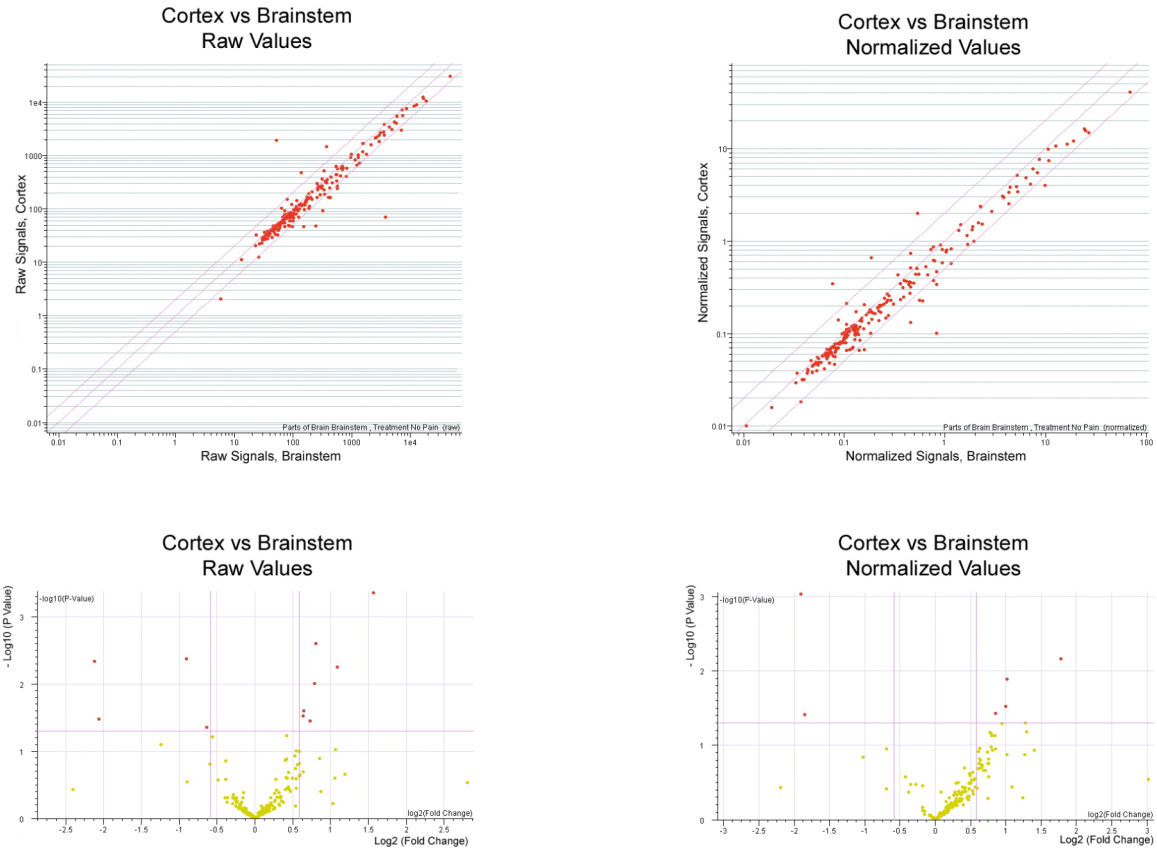

Figure 9: Scatter plots and volcano plots comparing the expression levels on the 230 genes of interest in the cortex and in the brainstem of 3 unoperated NMRI mice. The scatter plots of both the raw and the normalized signals showed genes, which were more regulated in one part of the brain. The volcano plots were used to filter the genes, which had a 1.5 times or higher signal in one part of the brain, and a P Value lower than 0.05. 11 genes were significantly differentially expressed according to the raw signals, and 6 genes were significantly differentially expressed according to the normalized values.

2.4.1.1 Brainstem against cortex hybridizations, raw signals comparisons

To assess the relevance of our results, we checked whether the differential expressions, which we had observed between the brainstem and the cortex, could also be observed in the GEO set n°: GDS1406. We compared the fold changes observed in our experiments with the fold changes of these genes reported for each of the 6 analyzed strains in the GDS1406.

The comparisons with of our raw microarray data with the GDS1406 results for the 129S6/SvEvTac, C3H/HeJ, C57BL/6J and DBA/2J strains were similar. Out of the 11 differentially expressed genes observed in our microarray analysis of the raw signals, 7 showed a similar expression profile in the GDS1409 GEO set, 3 showed a different expression pattern, and 1 was a false positive (randomly generated negative control 4), Therefore, the proportion of regulated genes, which showed a similar behavior on both platforms, was 64%, when comparing our raw results obtained with NMRI mice with the GDS1406 data of either one of the 4 strains mentioned above. In the comparisons with

129S6/SvEvTac, C57BL/6J and DBA/2J, the 3 genes, which showed different regulations between our microarray results and the GDS1409 data set, were Proopiomelanocortin, the 5-HTr5B serotonin receptor, and Neurotrophin-3. In comparisons with C3H/HeJ the 3 genes, which behaved differently on the two platforms were Proopiomelanocortin, the Heat-Shock protein 70kD, and Neurotrophin-3.

In the comparisons of our raw microarray signals with the GEO datasets of the A/J and the FVB/NJ strains, 8 genes showed a similar behavior on both platforms, 2 showed a different behavior, and one was a false positive, (randomly generated negative control 4), for which no data could be found in the GEO data base. Therefore, in these 2 comparisons, the proportion of genes, which showed a similar behavior on both platforms is 73%. In the comparison with the A/J strain, the 2 differently regulated genes were Proopiomelanocortin, and Neurotrophin-3. In the comparison with the FVB/NJ strain, the 2 differently regulated genes were the 5-HTr5B serotonin receptor, and Neurotrophin-3. The comparisons between our raw microarray and the GDS1409 data set for each of the 5 analyzed strains are regrouped in Table 5.

Table 5: Differentially expressed genes between the brainstem and the cortex obtained in the raw data microarray analysis. Comparison of the signals and the fold changes of these genes, with their expression profiles published on the GDS1406 GEO data sets for 6 inbred strain mice.

a. Comparison with the GDS1406 GEO data set for the 129S6/SvEvTac strain: 64% similarity

		Microarray		GDS1406		Microarray	GDS 1406	Comparison
Gene Name	**ID, NCBI**	**Brainstem**	**Cortex**	**Brainstem**	**Cortex**	**FC in Brainstem**	**FC in Brainstem**	**of results**
Proteinase-activated receptor 1 PAR1, F2r	NM_010169	316.9	93.58	108.60	53.11	3.39	2.04	Same
Proopiomelanocortin (POMC)	NM_008895	427.3	163.4	31.68	68.25	2.62	0.46	Different
Tyrosine hydroxylase	NM_009377	561.4	238.9	671.01	80.08	2.35	8.38	Same
Catechol-O-methyl Transferase (COMT)	NM_007744	396	166.3	355.58	108.13	2.38	3.29	Same
Randomly generated negative control 4		25.4	12.44			2.04		No Data
Heat shock protein 70kD protein 5	NM_022310	795.1	407.7	1086.68	636.08	1.95	1.71	Same
Serotonin receptor: 5-HTr5(B)	NM_010483	123.6	71.28	26.52	48.89	1.73	0.54	Different
Neurotrophin-3 (NT-3)	NM_008742	82.61	50.03	8.41	25.15	1.65	0.33	Different
Serotonin transporter (SET)	NM_010484	54.17	33.03	977.44	15.82	1.64	61.80	Same
Egr1 (zif/268)	NM_007913	136.1	478.8	13.31	35.13	0.28	0.38	Same
Neuropeptide Y, Preproneuropeptide Y	NM_023456	364	1'481	146.56	394.60	0.25	0.37	Same

b. Comparison with the GDS1406 GEO data set for the A/J strain: 73% similarity

		Microarray		GDS1406		Microarray	GDS 1406	Comparison
Gene Name	**ID, NCBI**	**Brainstem**	**Cortex**	**Brainstem**	**Cortex**	**FC in Brainstem**	**FC in Brainstem**	**of results**
Proteinase-activated receptor 1 PAR1, F2r	NM_010169	316.9	93.58	33.74	12.63	3.39	2.67	Same
Proopiomelanocortin (POMC)	NM_008895	427.3	163.4	77.93	85.18	2.62	0.91	Different
Tyrosine hydroxylase	NM_009377	561.4	238.9	329.20	78.32	2.35	4.20	Same
Catechol-O-methyl Transferase (COMT)	NM_007744	396	166.3	372.99	171.05	2.38	2.18	Same
Randomly generated negative control 4		25.4	12.44			2.04		No Data
Heat shock protein 70kD protein 5	NM_022310	795.1	407.7	116.83	10.12	1.95	11.54	Same
Serotonin receptor: 5-HTr5(B)	NM_010483	123.6	71.28	76.25	51.84	1.73	1.47	Same
Neurotrophin-3 (NT-3)	NM_008742	82.61	50.03	5.08	32.04	1.65	0.16	Different
Serotonin transporter (SET)	NM_010484	54.17	33.03	743.20	15.50	1.64	47.95	Same
Egr1 (zif/268)	NM_007913	136.1	478.8	278.32	2981.00	0.28	0.09	Same
Neuropeptide Y, Preproneuropeptide Y	NM_023456	364	1'481	113.01	442.62	0.25	0.26	Same

c. Comparison with the GDS1406 GEO data set for the C3H/HeJ strain: 64% similarity

		Microarray		GDS1406		Microarray	GDS 1406	Comparison
Gene Name	**ID, NCBI**	**Brainstem**	**Cortex**	**Brainstem**	**Cortex**	**FC in Brainstem**	**FC in Brainstem**	**of results**
Proteinase-activated receptor 1 PAR1, F2r	NM_010169	316.9	93.58	56.67	17.00	3.39	3.33	Same
Proopiomelanocortin (POMC)	NM_008895	427.3	163.4	53.22	55.44	2.62	0.96	Different
Tyrosine hydroxylase	NM_009377	561.4	238.9	489.09	81.51	2.35	6.00	Same
Catechol-O-methyl Transferase (COMT)	NM_007744	396	166.3	321.28	130.31	2.38	2.47	Same
Randomly generated negative control 4		25.4	12.44			2.04		No Data
Heat shock protein 70kD protein 5	NM_022310	795.1	407.7	934.08	791.69	1.95	1.18	Different
Serotonin receptor: 5-HTr5(B)	NM_010483	123.6	71.28	45.34	32.80	1.73	1.38	Same
Neurotrophin-3 (NT-3)	NM_008742	82.61	50.03	13.07	15.58	1.65	0.84	Different
Serotonin transporter (SET)	NM_010484	54.17	33.03	1017.13	11.73	1.64	86.75	Same
Egr1 (zif/268)	NM_007913	136.1	478.8	212.54	2994.30	0.28	0.07	Same
Neuropeptide Y, Preproneuropeptide Y	NM_023456	364	1'481	92.78	497.32	0.25	0.19	Same

d. Comparison with the GDS1406 GEO data set for the C57BL/6J strain: 64% similarity

		Microarray		GDS1406		Microarray	GDS 1406	Comparison
Gene Name	**ID, NCBI**	**Brainstem**	**Cortex**	**Brainstem**	**Cortex**	**FC in Brainstem**	**FC in Brainstem**	**of results**
Proteinase-activated receptor 1 PAR1, F2r	NM_010169	316.9	93.58	55.19	23.49	3.39	2.35	Same
Proopiomelanocortin (POMC)	NM_008895	427.3	163.4	44.29	85.72	2.62	0.52	Different
Tyrosine hydroxylase	NM_009377	561.4	238.9	348.23	106.01	2.35	3.28	Same
Catechol-O-methyl Transferase (COMT)	NM_007744	396	166.3	346.65	129.68	2.38	2.67	Same
Randomly generated negative control 4		25.4	12.44			2.04		No Data
Heat shock protein 70kD protein 5	NM_022310	795.1	407.7	963.94	412.52	1.95	2.34	Same
Serotonin receptor: 5-HTr5(B)	NM_010483	123.6	71.28	30.11	49.56	1.73	0.61	Different
Neurotrophin-3 (NT-3)	NM_008742	82.61	50.03	5.63	27.20	1.65	0.21	Different
Serotonin transporter (SET)	NM_010484	54.17	33.03	916.24	12.93	1.64	70.89	Same
Egr1 (zif/268)	NM_007913	136.1	478.8	255.72	2684.78	0.28	0.10	Same
Neuropeptide Y, Preproneuropeptide Y	NM_023456	364	1'481	93.76	471.69	0.25	0.20	Same

e. Comparison with the GDS1406 GEO data set for the DBA/2J strain: 64% similarity

		Microarray		GDS1406		Microarray	GDS 1406	Comparison
Gene Name	**ID, NCBI**	**Brainstem**	**Cortex**	**Brainstem**	**Cortex**	**FC in Brainstem**	**FC in Brainstem**	**of results**
Proteinase-activated receptor 1 PAR1, F2r	NM_010169	316.9	93.58	50.80	19.51	3.39	2.60	Same
Proopiomelanocortin (POMC)	NM_008895	427.3	163.4	66.48	63.35	2.62	1.05	Different
Tyrosine hydroxylase	NM_009377	561.4	238.9	339.98	102.20	2.35	3.33	Same
Catechol-O-methyl Transferase (COMT)	NM_007744	396	166.3	342.20	144.31	2.38	2.37	Same
Randomly generated negative control 4		25.4	12.44			2.04		No Data
Heat shock protein 70kD protein 5	NM_022310	795.1	407.7	895.76	687.02	1.95	1.30	Same
Serotonin receptor: 5-HTr5(B)	NM_010483	123.6	71.28	34.65	50.77	1.73	0.68	Different
Neurotrophin-3 (NT-3)	NM_008742	82.61	50.03	4.93	33.24	1.65	0.15	Different
Serotonin transporter (SET)	NM_010484	54.17	33.03	959.89	9.62	1.64	99.78	Same
Egr1 (zif/268)	NM_007913	136.1	478.8	173.78	4276.39	0.28	0.04	Same
Neuropeptide Y, Preproneuropeptide Y	NM_023456	364	1'481	106.28	411.50	0.25	0.26	Same

f. Comparison with the GDS1406 GEO data set for the FVB/NJ strain: 73% similarity

		Microarray		GDS1406		Microarray	GDS 1406	Comparison
Gene Name	**ID, NCBI**	**Brainstem**	**Cortex**	**Brainstem**	**Cortex**	**FC in Brainstem**	**FC in Brainstem**	**of results**
Proteinase-activated receptor 1 PAR1, F2r	NM_010169	316.9	93.58	53.62	19.06	3.39	2.81	Same
Proopiomelanocortin (POMC)	NM_008895	427.3	163.4	210.88	70.09	2.62	3.01	Same
Tyrosine hydroxylase	NM_009377	561.4	238.9	567.42	74.36	2.35	7.63	Same
Catechol-O-methyl Transferase (COMT)	NM_007744	396	166.3	327.75	113.75	2.38	2.88	Same
Randomly generated negative control 4		25.4	12.44			2.04		No Data
Heat shock protein 70kD protein 5	NM_022310	795.1	407.7	1013.70	751.74	1.95	1.35	Same
Serotonin receptor: 5-HTr5(B)	NM_010483	123.6	71.28	37.59	44.11	1.73	0.85	Different
Neurotrophin-3 (NT-3)	NM_008742	82.61	50.03	5.45	15.13	1.65	0.36	Different
Serotonin transporter (SET)	NM_010484	54.17	33.03	1085.01	11.62	1.64	93.41	Same
Egr1 (zif/268)	NM_007913	136.1	478.8	199.17	3856.58	0.28	0.05	Same
Neuropeptide Y, Preproneuropeptide Y	NM_023456	364	1'481	92.44	368.86	0.25	0.25	Same

2.4.1.2 Brainstem against cortex hybridizations, normalized signals comparisons

As mentioned previously, the filtering on volcano plot of the normalized microarray data showed that 6 genes were differentially expressed between the cortex and the brainstem (Figure 9). We compared our signals and fold changes, with the signals obtained on 6 different inbred mouse strains published on the GDS1406 GEO data set. For 5 strains comparison, we obtained 100% similarity between the changes observed on the 2 platforms. The comparison of our data with the GDS1406 data for C3H/HeJ showed that 1 of the 6 differentially expressed gene behaved differently on the two platforms. This gene is the Heat Shock Protein 70kD. We observed a 1.99 times upregulation in the Brainstem, but the GDS1406 dataset reports that the expression levels of this gene are identical in the cortex and the Brainstem. The list of genes, and the comparisons with the GDS1406 dataset for each strain can be seen in Table 6.

Table 6: Differentially expressed genes between the Brainstem and the Cortex obtained in the normalized data microarray analysis. Comparison of the signals and the fold changes of these genes, with their expression profiles published on the GDS1406 GEO data sets for 6 inbred strain mice.

a. Comparison with the GDS1406 GEO data set for the 129S6/SvEvTac strain: 100% similarity

		Microarray		GDS1406		Microarray	GDS 1406	Comparison
Gene Name	**ID, NCBI**	**Brainstem**	**Cortex**	**Brainstem**	**Cortex**	**FC in Brainstem**	**FC in Brainstem**	**of results**
Proteinase-activated receptor 1 PAR1, F2r	NM_010169	0.45	0.13	55.09	19.43	3.42	2.84	Same
Nerve growth factor-specific tyrosine kinase receptor NTRK2, TrkB	NM_008745	0.76	0.38	144.96	5.90	2.02	24.59	Same
Heat shock protein 70kD protein 5	NM_022310	1.14	0.57	1086.68	636.08	1.99	1.71	Same
JNK2 Oligo1	NM_016961	1.68	0.93	573.52	27.97	1.81	20.50	Same
Egr1 (zif/268)	NM_007913	0.18	0.67	282.20	4038.20	0.28	0.07	Same
Neuropeptide Y, Preproneuropeptide Y	NM_023456	0.53	2.00	146.56	394.60	0.27	0.37	Same

b. Comparison with the GDS1406 GEO data set for the A/J strain: 100% similarity

		Microarray		GDS1406		Microarray	GDS 1406	Comparison
Gene Name	**ID, NCBI**	**Brainstem**	**Cortex**	**Brainstem**	**Cortex**	**FC in Brainstem**	**FC in Brainstem**	**of results**
Proteinase-activated receptor 1 PAR1, F2r	NM_010169	0.45	0.13	33.74	12.63	3.42	2.67	Same
Nerve growth factor-specific tyrosine kinase receptor NTRK2, TrkB	NM_008745	0.76	0.38	116.83	10.12	2.02	11.54	Same
Heat shock protein 70kD protein 5	NM_022310	1.14	0.57	926.55	568.09	1.99	1.63	Same
JNK2 Oligo1	NM_016961	1.68	0.93	516.33	29.78	1.81	17.34	Same
Egr1 (zif/268)	NM_007913	0.18	0.67	278.32	2981.00	0.28	0.09	Same
Neuropeptide Y, Preproneuropeptide Y	NM_023456	0.53	2.00	113.01	442.62	0.27	0.26	Same

c. Comparison with the GDS1406 GEO data set for the C3H/HeJ strain: 83% similarity

		Microarray		GDS1406		Microarray	GDS 1406	Comparison
Gene Name	**ID, NCBI**	**Brainstem**	**Cortex**	**Brainstem**	**Cortex**	**FC in Brainstem**	**FC in Brainstem**	**of results**
Proteinase-activated receptor 1 PAR1, F2r	NM_010169	0.45	0.13	56.67	17.00	3.42	3.33	Same
Nerve growth factor-specific tyrosine kinase receptor NTRK2, TrkB	NM_008745	0.76	0.38	103.07	20.35	2.02	5.06	Same
Heat shock protein 70kD protein 5	NM_022310	1.14	0.57	934.08	791.69	1.99	1.18	Different
JNK2 Oligo1	NM_016961	1.68	0.93	543.09	32.31	1.81	16.81	Same
Egr1 (zif/268)	NM_007913	0.18	0.67	212.54	2994.30	0.28	0.07	Same
Neuropeptide Y, Preproneuropeptide Y	NM_023456	0.53	2.00	92.78	497.32	0.27	0.19	Same

d. Comparison with the GDS1406 GEO data set for the C57BL/6J strain: 100% similarity

		Microarray		GDS1406		Microarray	GDS 1406	Comparison
Gene Name	**ID, NCBI**	**Brainstem**	**Cortex**	**Brainstem**	**Cortex**	**FC in Brainstem**	**FC in Brainstem**	**of results**
Proteinase-activated receptor 1 PAR1, F2r	NM_010169	0.45	0.13	55.19	23.49	3.42	2.35	Same
Nerve growth factor-specific tyrosine kinase receptor NTRK2, TrkB	NM_008745	0.76	0.38	171.91	3.42	2.02	50.27	Same
Heat shock protein 70kD protein 5	NM_022310	1.14	0.57	963.94	412.52	1.99	2.34	Same
JNK2 Oligo1	NM_016961	1.68	0.93	545.24	28.49	1.81	19.14	Same
Egr1 (zif/268)	NM_007913	0.18	0.67	255.72	2684.78	0.28	0.10	Same
Neuropeptide Y, Preproneuropeptide Y	NM_023456	0.53	2.00	93.76	471.69	0.27	0.20	Same

e. Comparison with the GDS1406 GEO data set for the DBA/2J strain: 100% similarity

		Microarray		GDS1406		Microarray	GDS 1406	Comparison
Gene Name	**ID, NCBI**	**Brainstem**	**Cortex**	**Brainstem**	**Cortex**	**FC in Brainstem**	**FC in Brainstem**	**of results**
Proteinase-activated receptor 1 PAR1, F2r	NM_010169	0.45	0.13	50.80	19.51	3.42	2.60	Same
Nerve growth factor-specific tyrosine kinase receptor NTRK2, TrkB	NM_008745	0.76	0.38	106.33	7.13	2.02	14.91	Same
Heat shock protein 70kD protein 5	NM_022310	1.14	0.57	895.76	687.02	1.99	1.30	Same
JNK2 Oligo1	NM_016961	1.68	0.93	459.27	30.66	1.81	14.98	Same
Egr1 (zif/268)	NM_007913	0.18	0.67	173.78	4276.39	0.28	0.04	Same
Neuropeptide Y, Preproneuropeptide Y	NM_023456	0.53	2.00	106.28	411.50	0.27	0.26	Same

f. Comparison with the GDS1406 GEO data set for the FVB/NJ strain: 100% similarity

		Microarray		GDS1406		Microarray	GDS 1406	Comparison
Gene Name	**ID, NCBI**	**Brainstem**	**Cortex**	**Brainstem**	**Cortex**	**FC in Brainstem**	**FC in Brainstem**	**of results**
Proteinase-activated receptor 1 PAR1, F2r	NM_010169	0.45	0.13	53.62	19.06	3.42	2.81	Same
Nerve growth factor-specific tyrosine kinase receptor NTRK2, TrkB	NM_008745	0.76	0.38	34.50	26.60	2.02	1.30	Same
Heat shock protein 70kD protein 5	NM_022310	1.14	0.57	1013.70	751.74	1.99	1.35	Same
JNK2 Oligo1	NM_016961	1.68	0.93	384.48	23.23	1.81	16.55	Same
Egr1 (zif/268)	NM_007913	0.18	0.67	199.17	3856.58	0.28	0.05	Same
Neuropeptide Y, Preproneuropeptide Y	NM_023456	0.53	2.00	92.44	368.86	0.27	0.25	Same

2.4.2 Hippocampus vs. brainstem hybridizations

The goal of this experiment was to compare the expression levels of the 230 genes spotted on our chip between the hippocampi and the brainstems of 3 control animals. For both the raw and the normalized values, the scatter plots of signals in these two regions were perfectly aligned on the midline, with genes showing regulations in either the brainstem or the hippocampus (Figure 10). We filtered the signals on a volcano plot to select the genes, which had a 1.5 higher expression in one part of the brain or the other, and a P Value lower than 0.05 (Figure 10). The analysis of the raw signals showed that 10 genes satisfied those criteria. Two of these genes had a more than 2 fold overexpression in the brainstem: Tyrosine Hydroxylase and the Proteinase-Activated Receptor 1. The 8 other genes were upregulated in the hippocampus. Table 7 contains the genes, which are differentially expressed between the brainstem and the hippocampus. The filtering on volcano plots of the normalized data showed that 18 genes show different expression levels in these two parts of the brain (Figure 10). Amongst these genes, 5 were more expressed in the brainstem, and 13 were more expressed in the hippocampus.

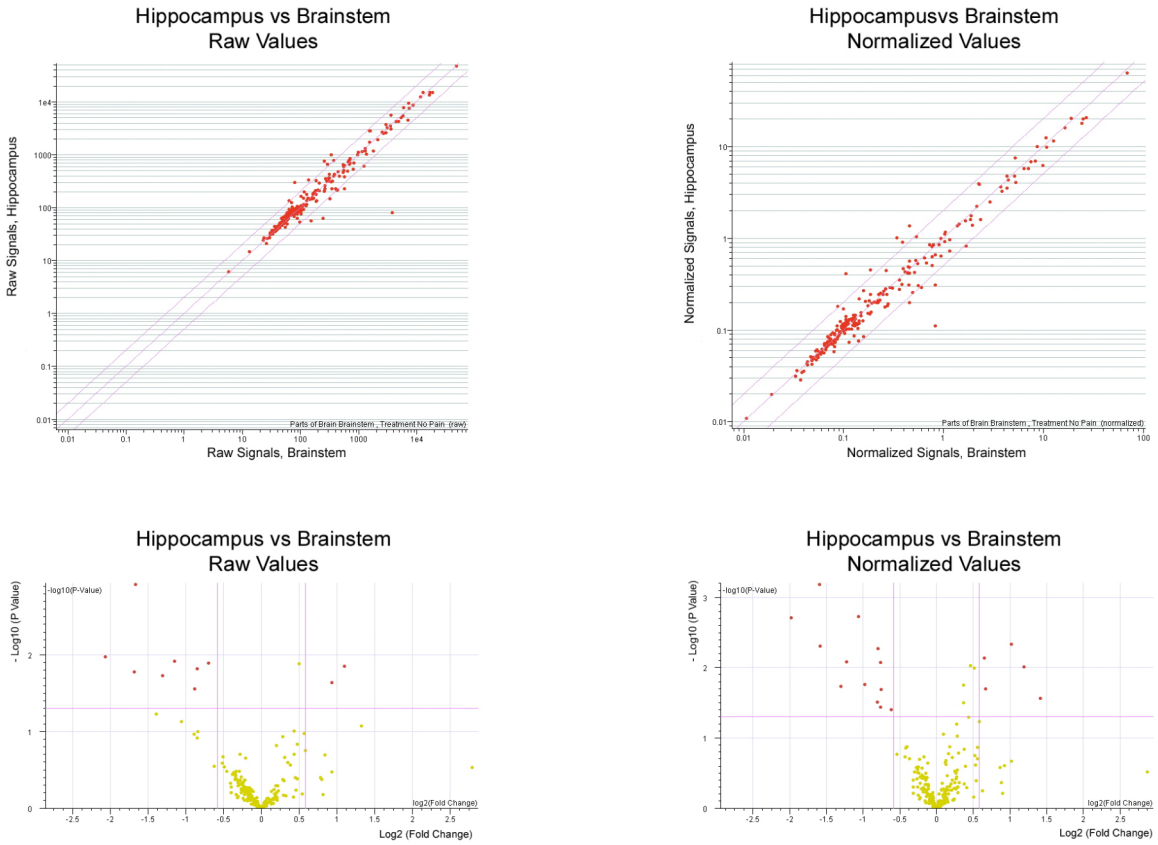

Figure 10: Scatter plots and volcano plots comparing the expression levels on the 230 genes of interest in the hippocampi and in the brainstems of 3 unoperated NMRI mice. The scatter plots of both the raw and the normalized signals show genes, which were more regulated in one part of the brain. The volcano plots were used to filter the genes, which had a 1.5 times or more higher signal in one part of the brain, and a P Value lower than 0.05. The positive genes were highlighted in red. 10 genes were significantly differentially expressed according to the raw signals, and 18 genes were significantly differentially expressed according to the normalized values.

2.4.2.1 Hippocampus against brainstem hybridizations, raw signals comparisons

The filtering of the raw signals on the volcano plot revealed that 10 genes are differentially expressed between the brainstem and the hippocampus (Figure 10). The expression profiles of these genes were compared to the expression profiles observed in 6 different inbred strains, which were published on the GDS 1406 GEO data set. The data we observed had a high similarity with the GEO set data. The GDS1406 set on the C3H/HeJ strain had a 100% similarity with our data. The results obtained for the 129S6/SvEvTac and the A/J strains had 90% similarity with our data. When comparing our data with the GDS1406 values for the DBA/2J and the FVB/NJ strains, the similarity was 80%, and when comparing our data with the results obtained for the C57BL/6J strain, the similarity was 70%.

Our results showed that the Proteinase-activated Receptor 1 (PAR1) was 2.16 times more expressed in the brainstem. A similar observation could only be made in one of the strains analyzed in the GDS1406 dataset: C3H/HeJ. In that

strain, the PAR1 gene was 1.59 times more expressed in the brainstem than in the hippocampus. The five strains analyzed in the GDS1406 dataset showed no difference in the expression levels of that gene between these two regions of the brain.

In the DBA/2J and the FVB/NJ strains, the GDS1406 dataset reported no difference in the expression of the MAPK1 gene between the brainstem and the hippocampus. Our microarray results however showed a 1.79 times higher expression of that gene in the hippocampus. Additionally to this, our measurement made with 2 different oligos for Beta-Actin revealed that the expression level of that gene was about 1.85 times higher in the hippocampus than in the brainstem. This observation could be confirmed in all the strains analyzed in the GDS1406 GEO data set, except in C57BL/6J. In that strain, the expression levels of the Beta-Actin gene were identical in the hrainstem and in the Hippocampus.

The rest of the 10 genes showed similar expression profiles on both platforms, for each strain. The list of differentially expressed genes between the brainstem and the hippocampus, their raw signals, and their fold changes on both platforms can be seen in Table 7.

Table 7: Differentially expressed genes between the brainstem and the hippocampus obtained in the raw data microarray analysis. Comparison of the signals and the fold changes of these genes, with their expression profiles published on the GDS1406 GEO data sets for 6 inbred mice strains.

a. Comparison with the GDS1406 GEO data set for the 129S6/SvEvTac strain: 90% similarity

		Microarray		GDS1406		Microarray	GDS 1406	Comparison
Gene Name	**ID, NCBI**	**Brainstem**	**Hippocampus**	**Brainstem**	**Hippocampus**	**FC in Brainstem**	**FC in Brainstem**	**of results**
Tyrosine hydroxylase	NM_009377	561.4	228.4	671.005	110.235	2.46	6.09	Same
Proteinase-activated receptor 1 PAR1, F2r	NM_010169	316.9	146.6	108.595	84.735	2.16	1.28	Different
Epsin 1	NM_010147	3'550	5'582	1273.095	1904.575	0.64	0.67	Same
MAP kinase 1 (=Erk2): mitogen-activated protein kinase 1, Transcript variant 2	NM_011949	181.7	325.1	39.03	66.09	0.56	0.59	Same
Actin, beta cytoplasmic (ACTB) Oligo 2	NM_007393	1'562	2'849	199.175	318.235	0.55	0.63	Same
Actin, beta cytoplasmic (ACTB)	NM_007393	1'532	2'881	199.175	318.235	0.53	0.63	Same
Neuropeptide Y, Preproneuropeptide Y	NM_023456	364	774.8	146.56	476.415	0.47	0.31	Same
AMPA1 (alpha1) Glutamate Receptor, ionotropic	NM_008165	251.7	765.6	687.6	1734.975	0.33	0.40	Same
AMPA2 (alpha2) Glutamate Receptor, ionotropic	NM_013540	330.7	1'006	247.115	797.485	0.33	0.31	Same
Protein kinase C, gamma (Prkcc)	NM_011102	77.86	304.1	158.59	1532.34	0.26	0.10	Same

b. Comparison with the GDS1406 GEO data set for the A/J strain: 90% similarity

		Microarray		GDS1406		Microarray	GDS 1406	Comparison
Gene Name	**ID, NCBI**	**Brainstem**	**Hippocampus**	**Brainstem**	**Hippocampus**	**FC in Brainstem**	**FC in Brainstem**	**of results**
Tyrosine hydroxylase	NM_009377	561.4	228.4	329.195	105.995	2.46	3.11	Same
Proteinase-activated receptor 1 PAR1, F2r	NM_010169	316.9	146.6	80.665	73.98	2.16	1.09	Different
Epsin 1	NM_010147	3'550	5'582	1374.355	1821.515	0.64	0.75	Same
MAP kinase 1 (=Erk2): mitogen-activated protein kinase 1, Transcript variant 2	NM_011949	181.7	325.1	25.785	47.655	0.56	0.54	Same
Actin, beta cytoplasmic (ACTB) Oligo 2	NM_007393	1'562	2'849	134.435	298.595	0.55	0.45	Same
Actin, beta cytoplasmic (ACTB)	NM_007393	1'532	2'881	134.435	298.595	0.53	0.45	Same
Neuropeptide Y, Preproneuropeptide Y	NM_023456	364	774.8	14.655	169.26	0.47	0.09	Same
AMPA1 (alpha1) Glutamate Receptor, ionotropic	NM_008165	251.7	765.6	737.605	1887.585	0.33	0.39	Same
AMPA2 (alpha2) Glutamate Receptor, ionotropic	NM_013540	330.7	1'006	300.995	882.02	0.33	0.34	Same
Protein kinase C, gamma (Prkcc)	NM_011102	77.86	304.1	154.3	1443.905	0.26	0.11	Same

c. Comparison with the GDS1406 GEO data set for the C3H/HeJ strain: 100% similarity

		Microarray		GDS1406		Microarray	GDS 1406	Comparison
Gene Name	**ID, NCBI**	**Brainstem**	**Hippocampus**	**Brainstem**	**Hippocampus**	**FC in Brainstem**	**FC in Brainstem**	**of results**
Tyrosine hydroxylase	NM_009377	561.4	228.4	489.085	124.6	2.46	3.93	Same
Proteinase-activated receptor 1 PAR1, F2r	NM_010169	316.9	146.6	138.825	87.49	2.16	1.59	Same
Epsin 1	NM_010147	3'550	5'582	1194.395	1871.445	0.64	0.64	Same
MAP kinase 1 (=Erk2): mitogen-activated protein kinase 1, Transcript variant 2	NM_011949	181.7	325.1	33.445	40.915	0.56	0.82	Same
Actin, beta cytoplasmic (ACTB) Oligo 2	NM_007393	1'562	2'849	268.94	364.185	0.55	0.74	Same
Actin, beta cytoplasmic (ACTB)	NM_007393	1'532	2'881	268.94	364.185	0.53	0.74	Same
Neuropeptide Y, Preproneuropeptide Y	NM_023456	364	774.8	92.78	377.62	0.47	0.25	Same
AMPA1 (alpha1) Glutamate Receptor, ionotropic	NM_008165	251.7	765.6	656.78	1728.635	0.33	0.38	Same
AMPA2 (alpha2) Glutamate Receptor, ionotropic	NM_013540	330.7	1'006	294.395	824.735	0.33	0.36	Same
Protein kinase C, gamma (Prkcc)	NM_011102	77.86	304.1	172.26	1487.21	0.26	0.12	Same

d. Comparison with the GDS1406 GEO data set for the C57BL/6J strain: 70% similarity

		Microarray		GDS1406		Microarray	GDS 1406	Comparison
Gene Name	**ID, NCBI**	**Brainstem**	**Hippocampus**	**Brainstem**	**Hippocampus**	**FC in Brainstem**	**FC in Brainstem**	**of results**
Tyrosine hydroxylase	NM_009377	561.4	228.4	348.225	75.745	2.46	4.60	Same
Proteinase-activated receptor 1 PAR1, F2r	NM_010169	316.9	146.6	83.415	78.645	2.16	1.06	Different
Epsin 1	NM_010147	3'550	5'582	1156.1	1971.9	0.64	0.59	Same
MAP kinase 1 (=Erk2): mitogen-activated protein kinase 1, Transcript variant 2	NM_011949	181.7	325.1	37.825	65.025	0.56	0.58	Same
Actin, beta cytoplasmic (ACTB) Oligo 2	NM_007393	1'562	2'849	279.25	284.69	0.55	0.98	Different
Actin, beta cytoplasmic (ACTB)	NM_007393	1'532	2'881	279.25	284.69	0.53	0.98	Different
Neuropeptide Y, Preproneuropeptide Y	NM_023456	364	774.8	11.585	140.635	0.47	0.08	Same
AMPA1 (alpha1) Glutamate Receptor, ionotropic	NM_008165	251.7	765.6	415.77	1258.195	0.33	0.33	Same
AMPA2 (alpha2) Glutamate Receptor, ionotropic	NM_013540	330.7	1'006	199.465	690.82	0.33	0.29	Same
Protein kinase C, gamma (Prkcc)	NM_011102	77.86	304.1	119.29	1528.635	0.26	0.08	Same

e. Comparison with the GDS1406 GEO data set for the DBA/2J strain: 80% similarity

		Microarray		GDS1406		Microarray	GDS 1406	Comparison
Gene Name	**ID, NCBI**	**Brainstem**	**Hippocampus**	**Brainstem**	**Hippocampus**	**FC in Brainstem**	**FC in Brainstem**	**of results**
Tyrosine hydroxylase	NM_009377	561.4	228.4	339.975	115.885	2.46	2.93	Same
Proteinase-activated receptor 1 PAR1, F2r	NM_010169	316.9	146.6	96.3	98.69	2.16	0.98	Different
Epsin 1	NM_010147	3'550	5'582	1384.6	1776.96	0.64	0.78	Same
MAP kinase 1 (=Erk2): mitogen-activated protein kinase 1, Transcript variant 2	NM_011949	181.7	325.1	41.53	45.09	0.56	0.92	Different
Actin, beta cytoplasmic (ACTB) Oligo 2	NM_007393	1'562	2'849	152.22	229.22	0.55	0.66	Same
Actin, beta cytoplasmic (ACTB)	NM_007393	1'532	2'881	152.22	229.22	0.53	0.66	Same
Neuropeptide Y, Preproneuropeptide Y	NM_023456	364	774.8	106.275	454.915	0.47	0.23	Same
AMPA1 (alpha1) Glutamate Receptor, ionotropic	NM_008165	251.7	765.6	501.13	1953.865	0.33	0.26	Same
AMPA2 (alpha2) Glutamate Receptor, ionotropic	NM_013540	330.7	1'006	227.415	808.79	0.33	0.28	Same
Protein kinase C, gamma (Prkcc)	NM_011102	77.86	304.1	199.1	1526.41	0.26	0.13	Same

f. Comparison with the GDS1406 GEO data set for the FVB/NJ strain: 80% similarity

		Microarray		GDS1406		Microarray	GDS 1406	Comparison
Gene Name	**ID, NCBI**	**Brainstem**	**Hippocampus**	**Brainstem**	**Hippocampus**	**FC in Brainstem**	**FC in Brainstem**	**of results**
Tyrosine hydroxylase	NM_009377	561.4	228.4	567.42	122.20	2.46	4.64	Same
Proteinase-activated receptor 1 PAR1, F2r	NM_010169	316.9	146.6	94.69	94.70	2.16	1.00	Different
Epsin 1	NM_010147	3'550	5'582	1281.36	1665.97	0.64	0.77	Same
MAP kinase 1 (=Erk2): mitogen-activated protein kinase 1, Transcript variant 2	NM_011949	181.7	325.1	35.89	39.00	0.56	0.92	Different
Actin, beta cytoplasmic (ACTB) Oligo 2	NM_007393	1'562	2'849	243.38	359.20	0.55	0.68	Same
Actin, beta cytoplasmic (ACTB)	NM_007393	1'532	2'881	243.38	359.20	0.53	0.68	Same
Neuropeptide Y, Preproneuropeptide Y	NM_023456	364	774.8	92.44	414.08	0.47	0.22	Same
AMPA1 (alpha1) Glutamate Receptor, ionotropic	NM_008165	251.7	765.6	540.14	2104.34	0.33	0.26	Same
AMPA2 (alpha2) Glutamate Receptor, ionotropic	NM_013540	330.7	1'006	228.06	730.55	0.33	0.31	Same
Protein kinase C, gamma (Prkcc)	NM_011102	77.86	304.1	169.36	1683.14	0.26	0.10	Same

2.4.2.2 Hippocampus against brainstem hybridizations, normalized signals comparisons

The low-density microarray analysis of the normalized signals revealed that 18 genes were differentially expressed between the brainstem and the hippocampus (Figure 10). In order to validate this data, we compared these observations with the results published for these genes on the GDS1406 GEO data sets of 6 inbred mice. The comparisons of the differently expressed genes fold changes with the ones published for the either the 129S6/SvEvTac or the C3H/HeJ strains revealed 94.4% similarity. When comparing our results with the data observed in A/J mice, the similarity was 88.9%. The comparisons of our data with the results measured in the C57BL/6J strain revealed a similarity of 83.3%, and when compared with the published results for DBA/2J or FVB/NJ, the similarity was 77.8%.

Amongst the 18 differentially expressed genes observed in our analysis, the Proteinase-Activated Receptor 1A showed a different expression profile in the 5 strains analyzed in the GDS1406. According to our results, this gene was 2.28 times more expressed in the brainstem. The GEO set reported similar expression levels of that gene in the brainstem in the hippocampus in all the strains, except C3H/HeJ, in which the gene showed a 1.6 times higher expression level in the brainstem. This result confirmed the data we observed in our microarray for Proteinase-Activated Receptor 1A.

In the low-density microarray normalized results, the Heat Shock Protein 70kD showed a 1.57 times higher expression in the brainstem. The same observation was made in the GDS1406 dataset of the129S6/SvEvTac strain. However, in the other 5 strains from that data set, the gene was almost equally expressed in these two parts of the brain.

Our microarray contained 2 different oligos to measure 2 transcripts variants of the MAP Kinase 1. Our results showed a consistent 1.69 times higher expression of both MAP Kinase 1 transcript variants in the Hippocampus. This observation could be confirmed in the GDS1406 GEO data set for the 129S6/SvEvTac, A/J and C3H/HeJ strains. However, in the 4 remaining strains, this gene was equally expressed in the hippocampus and the brainstem.

The GDS1406 dataset for the C57BL/6J strain revealed 2 differences with our data, which were not present in the datasets of the other strains. In that set, the expression level of the Ubiquitin C gene was comparable in the brainstem and the hippocampus, whereas this gene was 1.59 times more expressed in the Bbainstem according to our microarray data. Similarily, our data showed that beta-Actin was 1.75 times more expressed in the hippocampus, and the GDS1406 data set reported no difference in the expression levels of that gene between in the brainstems and the hippocampi of C57BL/6J mice. The list of differentially expressed genes between the brainstem and the hippocampus, their raw signals, and their fold changes on both platforms can be seen in Table 8.

Table 8: Differentially expressed genes between the brainstem and the hippocampus obtained in the normalized data microarray analysis. Comparison of the signals and the fold changes of these genes, with their expression profiles published on the GDS1406 GEO data sets for 6 inbred mice strains.

a. Comparison with the GDS1406 GEO data set for the 129S6/SvEvTac strain: 94.4% similarity

		Microarray		GDS1406		Microarray	GDS 1406	Comparison
Gene Name	**ID, NCBI**	**Brainstem**	**Hippocampus**	**Brainstem**	**Hippocampus**	**FC in Brainstem**	**FC in Brainstem**	**of results**
Tyrosine hydroxylase	NM_009377	0.825	0.31	671.005	110.235	2.66	6.09	Same
Proteinase-activated receptor 1 PAR1, F2r	NM_010169	0.452	0.198	108.595	84.735	2.28	1.28	Different
JNK2 Oligo1	NM_016961	1.68	0.828	573.52	273.2	2.03	2.10	Same
Ubiquitin C (housekeeping)	NM_019639	9.881	6.217	4654.77	2693.325	1.59	1.73	Same
Heat shock protein 70kD protein 5	NM_022310	1.142	0.729	1086.68	687.29	1.57	1.58	Same
Heat shock protein 72 (HSP72)	NM_008301	0.142	0.218	100.14	197.92	0.65	0.51	Same
MAP kinase 1 (=Erk2): mitogen-activated protein kinase 1, Transcript variant 2	NM_011949	0.262	0.443	39.03	66.09	0.59	0.59	Same
MAP kinase 1 (=Erk2): mitogen-activated protein kinase 1, Transcript variant 1	NM_011949	0.158	0.267	39.03	66.09	0.59	0.59	Same
Mus musculus actin, beta, cytoplasmic (Actb), mRNA	NM_007393	2.284	3.879	199.175	318.235	0.59	0.63	Same
Brain derived neurotrophic factor (BDNF)	NM_007540	0.0979	0.17	246.96	442.755	0.58	0.56	Same
Actin, beta cytoplasmic (ACTB)	NM_007393	2.242	3.922	199.175	318.235	0.57	0.63	Same
Neuropeptide Y, Preproneuropeptide Y	NM_023456	0.532	1.044	146.56	476.415	0.51	0.31	Same
Protein kinase C epsilon type	NM_011104	0.0869	0.182	129.94	349.43	0.48	0.37	Same
Neuropeptide Y receptor type 2 (Npy2r)	NM_008731	0.385	0.901	8.795	83.47	0.43	0.11	Same
Egr1 (zif/268)	NM_007913	0.184	0.454	282.2	574.185	0.41	0.49	Same
AMPA1 (alpha1) Glutamate Receptor, ionotropic	NM_008165	0.336	1.007	687.6	1734.975	0.33	0.40	Same
AMPA2 (alpha2) Glutamate Receptor, ionotropic	NM_013540	0.453	1.371	247.115	797.485	0.33	0.31	Same
Protein kinase C, gamma (Prkcc)	NM_011102	0.105	0.414	158.59	1532.34	0.25	0.10	Same

b. Comparison with the GDS1406 GEO data set for the A/J strain: 88.9% similarity

		Microarray		GDS1406		Microarray	GDS 1406	Comparison
Gene Name	**ID, NCBI**	**Brainstem**	**Hippocampus**	**Brainstem**	**Hippocampus**	**FC in Brainstem**	**FC in Brainstem**	**of results**
Tyrosine hydroxylase	NM_009377	0.825	0.31	329.195	105.995	2.66	3.11	Same
Proteinase-activated receptor 1 PAR1, F2r	NM_010169	0.452	0.198	80.665	73.98	2.28	1.09	Different
JNK2 Oligo1	NM_016961	1.68	0.828	516.325	281.585	2.03	1.83	Same
Ubiquitin C (housekeeping)	NM_019639	9.881	6.217	3898.715	2783.76	1.59	1.40	Same
Heat shock protein 70kD protein 5	NM_022310	1.142	0.729	926.545	762.115	1.57	1.22	Different
Heat shock protein 72 (HSP72)	NM_008301	0.142	0.218	101.895	225.19	0.65	0.45	Same
MAP kinase 1 (=Erk2): mitogen-activated protein kinase 1, Transcript variant 2	NM_011949	0.262	0.443	25.785	47.655	0.59	0.54	Same
MAP kinase 1 (=Erk2): mitogen-activated protein kinase 1, Transcript variant 1	NM_011949	0.158	0.267	25.785	47.655	0.59	0.54	Same
Mus musculus actin, beta, cytoplasmic (Actb), mRNA	NM_007393	2.284	3.879	134.435	298.595	0.59	0.45	Same
Brain derived neurotrophic factor (BDNF)	NM_007540	0.0979	0.17	202.165	461.74	0.58	0.44	Same
Actin, beta cytoplasmic (ACTB)	NM_007393	2.242	3.922	134.435	298.595	0.57	0.45	Same
Neuropeptide Y, Preproneuropeptide Y	NM_023456	0.532	1.044	113.005	376.765	0.51	0.30	Same
Protein kinase C epsilon type	NM_011104	0.0869	0.182	132.075	566.39	0.48	0.23	Same
Neuropeptide Y receptor type 2 (Npy2r)	NM_008731	0.385	0.901	14.655	169.26	0.43	0.09	Same
Egr1 (zif/268)	NM_007913	0.184	0.454	278.315	431.37	0.41	0.65	Same
AMPA1 (alpha1) Glutamate Receptor, ionotropic	NM_008165	0.336	1.007	737.605	1887.585	0.33	0.39	Same
AMPA2 (alpha2) Glutamate Receptor, ionotropic	NM_013540	0.453	1.371	300.995	882.02	0.33	0.34	Same
Protein kinase C, gamma (Prkcc)	NM_011102	0.105	0.414	154.3	1443.905	0.25	0.11	Same

c. Comparison with the GDS1406 GEO data set for the C3H/HeJ strain: 94.4% similarity

		Microarray		GDS1406		Microarray	GDS 1406	Comparison
Gene Name	**ID, NCBI**	**Brainstem**	**Hippocampus**	**Brainstem**	**Hippocampus**	**FC in Brainstem**	**FC in Brainstem**	**of results**
Tyrosine hydroxylase	NM_009377	0.825	0.31	489.085	124.6	2.66	3.93	Same
Proteinase-activated receptor 1 PAR1, F2r	NM_010169	0.452	0.198	138.825	87.49	2.28	1.59	same
JNK2 Oligo1	NM_016961	1.68	0.828	543.09	253.375	2.03	2.14	Same
Ubiquitin C (housekeeping)	NM_019639	9.881	6.217	5348.915	3400.735	1.59	1.57	same
Heat shock protein 70kD protein 5	NM_022310	1.142	0.729	934.075	930.24	1.57	1.00	Different
Heat shock protein 72 (HSP72)	NM_008301	0.142	0.218	95.435	228.575	0.65	0.42	Same
MAP kinase 1 (=Erk2): mitogen-activated protein kinase 1, Transcript variant 2	NM_011949	0.262	0.443	33.445	40.915	0.59	0.82	Same
MAP kinase 1 (=Erk2): mitogen-activated protein kinase 1, Transcript variant 1	NM_011949	0.158	0.267	33.445	40.915	0.59	0.82	Same
Mus musculus actin, beta, cytoplasmic (Actb), mRNA	NM_007393	2.284	3.879	268.94	364.185	0.59	0.74	Same
Brain derived neurotrophic factor (BDNF)	NM_007540	0.0979	0.17	179.535	387.955	0.58	0.46	Same
Actin, beta cytoplasmic (ACTB)	NM_007393	2.242	3.922	268.94	364.185	0.57	0.74	Same
Neuropeptide Y, Preproneuropeptide Y	NM_023456	0.532	1.044	92.78	377.62	0.51	0.25	Same
Protein kinase C epsilon type	NM_011104	0.0869	0.182	164.11	587.81	0.48	0.28	Same
Neuropeptide Y receptor type 2 (Npy2r)	NM_008731	0.385	0.901	21.405	130.79	0.43	0.16	Same
Egr1 (zif/268)	NM_007913	0.184	0.454	212.54	525.57	0.41	0.40	Same
AMPA1 (alpha1) Glutamate Receptor, ionotropic	NM_008165	0.336	1.007	656.78	1728.635	0.33	0.38	Same
AMPA2 (alpha2) Glutamate Receptor, ionotropic	NM_013540	0.453	1.371	294.395	824.135	0.33	0.36	Same
Protein kinase C, gamma (Prkcc)	NM_011102	0.105	0.414	172.26	1487.21	0.25	0.12	Same

d. Comparison with the GDS1406 GEO data set for the C57BL/6J strain: 83.3% similarity

		Microarray		GDS1406		Microarray	GDS 1406	Comparison
Gene Name	**ID, NCBI**	**Brainstem**	**Hippocampus**	**Brainstem**	**Hippocampus**	**FC in Brainstem**	**FC in Brainstem**	**of results**
Tyrosine hydroxylase	NM_009377	0.825	0.31	348.225	75.745	2.66	4.60	Same
Proteinase-activated receptor 1 PAR1, F2r	NM_010169	0.452	0.198	83.415	78.645	2.28	1.06	Different
JNK2 Oligo1	NM_016961	1.68	0.828	545.24	320.35	2.03	1.70	Same
Ubiquitin C (housekeeping)	NM_019639	9.881	6.217	5332.58	4415.38	1.59	1.21	Different
Heat shock protein 70kD protein 5	NM_022310	1.142	0.729	963.935	706.905	1.57	1.36	Same
Heat shock protein 72 (HSP72)	NM_008301	0.142	0.218	97.645	262.955	0.65	0.37	Same
MAP kinase 1 (=Erk2): mitogen-activated protein kinase 1, Transcript variant 2	NM_011949	0.262	0.443	37.825	65.025	0.59	0.58	Same
MAP kinase 1 (=Erk2): mitogen-activated protein kinase 1, Transcript variant 1	NM_011949	0.158	0.267	37.825	65.025	0.59	0.58	Same
Mus musculus actin, beta, cytoplasmic (Actb), mRNA	NM_007393	2.284	3.879	279.25	284.69	0.59	0.98	Same
Brain derived neurotrophic factor (BDNF)	NM_007540	0.0979	0.17	194.79	472.3	0.58	0.41	Same
Actin, beta cytoplasmic (ACTB)	NM_007393	2.242	3.922	279.25	284.69	0.57	0.98	Different
Neuropeptide Y, Preproneuropeptide Y	NM_023456	0.532	1.044	93.76	619.8	0.51	0.15	Same
Protein kinase C epsilon type	NM_011104	0.0869	0.182	128.35	472.47	0.48	0.27	Same
Neuropeptide Y receptor type 2 (Npy2r)	NM_008731	0.385	0.901	11.585	140.635	0.43	0.08	Same
Egr1 (zif/268)	NM_007913	0.184	0.454	255.72	786.305	0.41	0.33	Same
AMPA1 (alpha1) Glutamate Receptor, ionotropic	NM_008165	0.336	1.007	415.77	1258.195	0.33	0.33	Same
AMPA2 (alpha2) Glutamate Receptor, ionotropic	NM_013540	0.453	1.371	199.465	690.82	0.33	0.29	Same
Protein kinase C, gamma (Prkcc)	NM_011102	0.105	0.414	119.29	1528.635	0.25	0.08	Same

e. Comparison with the GDS1406 GEO data set for the DBA/2J strain: 77.8% similarity

		Microarray		GDS1406		Microarray	GDS 1406	Comparison
Gene Name	**ID, NCBI**	**Brainstem**	**Hippocampus**	**Brainstem**	**Hippocampus**	**FC in Brainstem**	**FC in Brainstem**	**of results**
Tyrosine hydroxylase	NM_009377	0.825	0.31	339.975	115.885	2.66	2.93	Same
Proteinase-activated receptor 1 PAR1, F2r	NM_010169	0.452	0.198	96.3	98.69	2.28	0.98	Different
JNK2 Oligo1	NM_016961	1.68	0.828	459.27	296.805	2.03	1.55	Same
Ubiquitin C (housekeeping)	NM_019639	9.881	6.217	6223.38	3879.245	1.59	1.60	Same
Heat shock protein 70kD protein 5	NM_022310	1.142	0.729	895.76	845.655	1.57	1.06	Different
Heat shock protein 72 (HSP72)	NM_008301	0.142	0.218	133.195	245.525	0.65	0.54	Same
MAP kinase 1 (=Erk2): mitogen-activated protein kinase 1, Transcript variant 2	NM_011949	0.262	0.443	41.53	45.09	0.59	0.92	Different
MAP kinase 1 (=Erk2): mitogen-activated protein kinase 1, Transcript variant 1	NM_011949	0.158	0.267	41.53	45.09	0.59	0.92	Different
Mus musculus actin, beta, cytoplasmic (Actb), mRNA	NM_007393	2.284	3.879	152.22	229.22	0.59	0.66	Same
Brain derived neurotrophic factor (BDNF)	NM_007540	0.0979	0.17	181.685	347.915	0.58	0.52	Same
Actin, beta cytoplasmic (ACTB)	NM_007393	2.242	3.922	152.22	229.22	0.57	0.66	Same
Neuropeptide Y, Preproneuropeptide Y	NM_023456	0.532	1.044	106.275	454.915	0.51	0.23	Same
Protein kinase C epsilon type	NM_011104	0.0869	0.182	120.72	414.35	0.48	0.29	Same
Neuropeptide Y receptor type 2 (Npy2r)	NM_008731	0.385	0.901	15.83	102.375	0.43	0.15	Same
Egr1 (zif/268)	NM_007913	0.184	0.454	173.78	493.335	0.41	0.35	Same
AMPA1 (alpha1) Glutamate Receptor, ionotropic	NM_008165	0.336	1.007	501.13	1953.865	0.33	0.26	Same
AMPA2 (alpha2) Glutamate Receptor, ionotropic	NM_013540	0.453	1.371	227.415	808.79	0.33	0.28	Same
Protein kinase C, gamma (Prkcc)	NM_011102	0.105	0.414	199.1	1526.41	0.25	0.13	Same

f. Comparison with the GDS1406 GEO data set for the FVB/NJ strain: 77.8% similarity

		Microarray		GDS1406		Microarray	GDS 1406	Comparison
Gene Name	**ID, NCBI**	**Brainstem**	**Hippocampus**	**Brainstem**	**Hippocampus**	**FC in Brainstem**	**FC in Brainstem**	**of results**
Tyrosine hydroxylase	NM_009377	0.825	0.31	567.42	122.20	2.66	4.64	Same
Proteinase-activated receptor 1 PAR1, F2r	NM_010169	0.452	0.198	94.69	94.70	2.28	1.00	Different
JNK2 Oligo1	NM_016961	1.68	0.828	384.48	296.92	2.03	1.29	Same
Ubiquitin C (housekeeping)	NM_019639	9.881	6.217	5654.23	4364.03	1.59	1.30	Same
Heat shock protein 70kD protein 5	NM_022310	1.142	0.729	1013.70	1080.57	1.57	0.94	Different
Heat shock protein 72 (HSP72)	NM_008301	0.142	0.218	66.96	197.17	0.65	0.34	Same
MAP kinase 1 (=Erk2): mitogen-activated protein kinase 1, Transcript variant 2	NM_011949	0.262	0.443	35.89	39.00	0.59	0.92	Different
MAP kinase 1 (=Erk2): mitogen-activated protein kinase 1, Transcript variant 1	NM_011949	0.158	0.267	35.89	39.00	0.59	0.92	Different
Mus musculus actin, beta, cytoplasmic (Actb), mRNA	NM_007393	2.284	3.879	243.38	359.20	0.59	0.68	Same
Brain derived neurotrophic factor (BDNF)	NM_007540	0.0979	0.17	217.00	397.63	0.58	0.55	Same
Actin, beta cytoplasmic (ACTB)	NM_007393	2.242	3.922	243.38	359.20	0.57	0.68	Same
Neuropeptide Y, Preproneuropeptide Y	NM_023456	0.532	1.044	92.44	414.08	0.51	0.22	Same
Protein kinase C epsilon type	NM_011104	0.0869	0.182	103.46	483.88	0.48	0.21	Same
Neuropeptide Y receptor type 2 (Npy2r)	NM_008731	0.385	0.901	28.54	115.66	0.43	0.25	Same
Egr1 (zif/268)	NM_007913	0.184	0.454	199.17	383.60	0.41	0.52	Same
AMPA1 (alpha1) Glutamate Receptor, ionotropic	NM_008165	0.336	1.007	540.14	2104.34	0.33	0.26	Same
AMPA2 (alpha2) Glutamate Receptor, ionotropic	NM_013540	0.453	1.371	228.06	730.55	0.33	0.31	Same
Protein kinase C, gamma (Prkcc)	NM_011102	0.105	0.414	169.36	1683.14	0.25	0.10	Same

2.4.3 Hippocampus vs. cortex hybridizations

In this experiment, we compared the expression levels of the 230 genes of interest in the hippocampus and in the cortex of 3 control NMRI mice, which had not been subjected to any surgery. The scatter plots of the raw signals were well aligned on the midline, with most genes located between the 2 fold change lines. The scatter plots of the normalized values showed similar features (Figure 11). Both the raw and normalized signals were filtered on a volcano plot in order to select the genes, which had a 1.5 times higher expression in one of the analyzed part of the brain, and a P Value lower than 0.05 (Figure11). The analysis of the raw signals revealed that 14 genes were significantly differentially more expressed in the hippocampus. No genes had a higher expression in the cortex. The same analysis performed on the normalized signals showed that 3 genes were significantly differentially expressed between the two parts of the brain. Neuropeptide Y appeared to be 1.9 times more expressed in the cortex, whereas the AMPA1 ionotropic glutamate receptor and the Neuropeptide Y receptor type 2 showed respectively a 2.3 and a 3.6 higher expression in the hippocampus.

2.4.3.1 Hippocampus vs. cortex hybridizations, raw signals comparisons

In the low-density microarray analysis of the raw signals, 14 genes appeared to be more expressed in the hippocampus. As previously, we compared the intensities and the fold changes of these genes with data, which had been published on the GDS1406 GEO data set for 6 different inbred mice strains. According to our microarray analysis, both the vanilloid receptor 1 (VR1) and the vanilloid receptor 5 (TrpV5) appeared to be 1.5 times more expressed in the hippocampus than in the cortex. However, no data could be found on the GEO datasets for these genes.

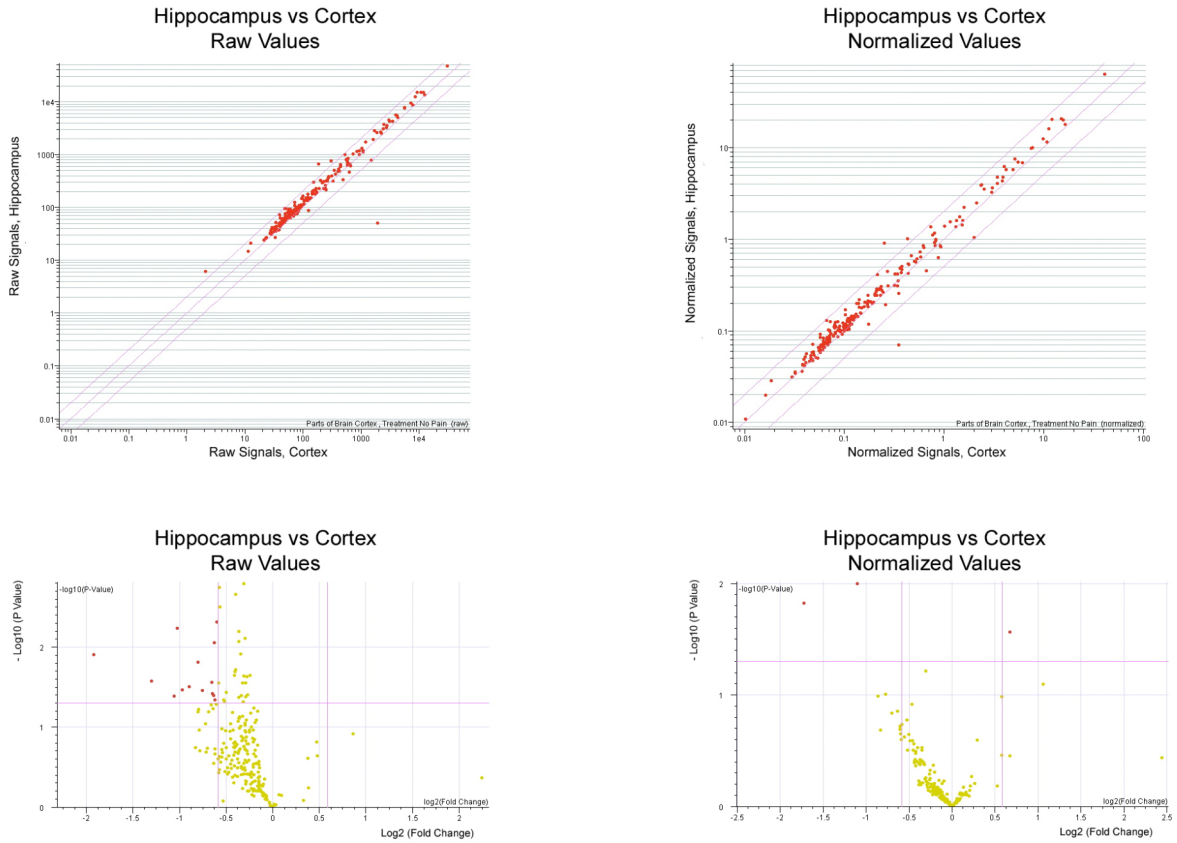

Figure 11: Scatter plots and volcano plots comparing the expression levels on the 230 genes of interest in the hippocampus and in the cortex of 3 non-operated NMRI mice. The scatter plots of both the raw and the normalized signals showed genes, which were more regulated in one part of the brain. The volcano plots were used to filter the genes, which had a 1.5 times or more higher signal in one part of the brain, and a P Value lower than 0.05. The positive genes were highlighted in red. 14 genes were significantly differentially expressed according to the raw signals, and 3 genes were significantly differentially expressed according to the normalized values.

In the 3 following mice strains: 129S6/SvEvTac, A/J and C3H/HeJ, 3 genes showed a different expression profile on the 2 platforms. The Tissue Plasminogen Activator, which was 1.52 times more expressed in the hippocampus according to our microarray data, appeared to be about 1.3 times more expressed in the cortex of these 3 inbred mice strains. The low-density microarray revealed, that the Neuropeptide Y receptor type 6 was 1.56 times more expressed in the hippocampus of the 3 NMRI mice we tested. However, in the GDS1406 datasets for the 129S6/SvEvTac and the C3H/HeJ, the expression of this gene was similar in both parts. In A/J mice, the Neuropeptide Y receptor type 6 was 1.96 times more regulated in the cortex. Similarly, the expression of the Brain Derived Neurotrophic Factor (BDNF) was 1.75 times higher in the hippocampus than in the cortex, but the GEO dataset for the 129S6/SvEvTac, A/J and the C3H/HeJ revealed a respectively 1.44, 1.58 and 2.15 times higher expression in the cortex. For these three strains, the similarity in the behavior of the 14 regulated genes was 57%, however, if we considered only the genes which could be verified on the GEO datasets, and

exclude the false positive which appeared in our results, the similarity jumped to 72.7%.

The GDS1406 dataset for both the C57BL/6J and the DBA/2J strains showed that the expression of the Tissue Plasminogen Activator shows were similar in the cortex and the hippocampus. However, our microarray data reported a 1.52 times higher expression in the hippocampus. A similar discrepancy was seen in these strains for BDNF and the Neurotrophin-3 (NT-3) genes. In the C57BL/6J strain, the BDNF and NT-3 genes were respectively 1.3 and 1.2 times upregulated in the cortex, and in the DBA/2J strains, these genes were respectively 2.37 and 1.04 times more expressed in the cortex. Our low-density microarray showed a 1.75 times higher expression in the hippocampus of both these genes.

In addition to those differences, 2 other genes could not be confirmed, when comparing the microarray results with the GDS1406 data for the C57BL/6J strain. The Neuropeptide Y receptor Type 6 and the P2x Purinoceptor 7 both showed a 1.56 times higher expression in the hippocampus than in the cortex, according to our microarray results. The GEO set for the Neuropeptide Y receptor type 6 in the strain mentioned above showed a 1.87 times higher expression in the cortex. For the P2x Purinoceptor 7, a 1.34 times higher expression in the cortex was reported. Taken together, 43% of the 14 genes, which appeared regulated in our microarray results, behaved the same way in the GDS1409 sets for the C57BL/6J strain. However, if we did not consider the obvious false positive, and the 2 genes, for which no data could be found in the GEO sets, the percentage of similarity increased to 54.5%.

In the DBA/2J strain, one additional gene showed a different behavior, than what we had measured on our microarray. Our data showed that the serotonin receptor 5-HTr5(B) had a 1.54 times higher expression in the hippocampus than in the cortex. However, the GDS1406 dataset of the DBA/2J strain reported no differences in the expression of that gene in the two regions of interest. The Neuropeptide Y receptor type 6 also showed a different behavior in the GDS1406 of the DBA/2J mice strains. According to that dataset, this gene was 2.34 times more expressed in the cortex. Our microarray results reported the opposite in NMRI mice. The comparisons of the behavior of the 14 significantly regulated genes on the microarray, with the GDS1406 dataset for the DBA/2J strain showed 43% similarity. But just as mentioned above, the percentage of similarity increased to 54.5% if we did not consider the obvious false positive, and the 2 genes, for which no data could be found in the GEO sets.

In the FVB/NJ strain, only 2 genes, out of the 14 significantly regulated genes from our microarray study showed a different expression profile in the GDS1406 GEO data set. According to our microarray results, the Serotonin Receptor 5-HTr5(B), the Neuropeptide Y Receptor type 6 and BDNF were respectively 1.54 times, 1.56 times and 1.75 times more expressed in the

hippocampus than in the cortex. In the GDS1406 dataset for the FVB/NJ strain, the Serotonin Receptor 5-HTr5(B) levels were equal in both parts of the brain, and the Neuropeptide Y receptor type 6 and BDNF were respectively 1.21 and 1.64 times more expressed in the cortex. Overall, 50% of the 14 significantly differentially expressed genes in the low-density microarray experiment could be confirmed in the GDS1406 data set for the FVB/NJ strain. However, if we did not include the randomly generated negative control 4 and the 2 genes, for which no data could be found in the GEO sets, the percentage of similarity increased to 63.6%. The list of differentially expressed genes between the hippocampus and the cortex, as well as the comparisons with the GDS1406 GEO datasets for each of the 6 inbred mice strains can be seen in Table .9

Table 9: Differentially expressed genes between the hippocampus and the cortex obtained in the raw data microarray analysis. Comparison of the signals and the fold changes of these genes, with their expression profiles published on the GDS1406 GEO data sets for 6 inbred mice strains.

a. Comparison with the GDS1406 GEO data set for the 129S6/SvEvTac strain: 57% similarity

		Microarray		GDS1406		Microarray	GDS 1406	Comparison
Gene Name	**ID, NCBI**	**Cortex**	**Hippocampus**	**Cortex**	**Hippocampus**	**FC in Cortex**	**FC in Cortex**	**of results**
Tissue plasminogen activator (Plat)	NM_008872	96.67	146.5	293.265	216.165	0.66	1.36	Different
Vanilloid-1 receptor (VR1) Oligo 3	NM_001001445	55.5	86.11			0.64		No Data
Vanilloid-receptor TrpV5	NM_001007572	59.75	92.19			0.65		No Data
Serotonin receptor: 5-HTr5(B)	NM_010483	71.28	110.2	48.89	60.53	0.65	0.81	Same
P2X purinoceptor 7	NM_011027	39.67	62.72	99.64	151.56	0.63	0.66	Same
Neuropeptide Y receptor type 6 (Npy6r)	NM_010935	48.42	75.78	10.735	9.845	0.64	1.09	Different
Randomly generated negative control 4		12.44	21.04			0.59		False Positive
Brain derived neurotrophic factor (BDNF)	NM_007540	71.44	125.6	637.77	442.755	0.57	1.44	Different
Neurotrophin-3 (NT-3)	NM_008742	50.03	94.14	25.145	27.805	0.53	0.90	Same
AMPA2 (alpha2) Glutamate Receptor, ionotropic	NM_013540	521.9	1'006	433.255	797.485	0.52	0.54	Same
Protein kinase C, gamma (Prkcc)	NM_011102	150.4	304.1	132.305	1532.34	0.49	0.09	Same
Mus musculus tubulin, alpha 6 (Tuba6), mRNA, Oligo 2	NM_009448	47.11	95.81	3109.225	4539.28	0.49	0.68	Same
AMPA1 (alpha1) Glutamate Receptor, ionotropic	NM_008165	302.6	765.6	1001.865	1734.975	0.40	0.58	Same
Neuropeptide Y receptor type 2 (Npy2r)	NM_008731	181.5	666.9	81.19	278.865	0.27	0.29	Same

b. Comparison with the GDS1406 GEO data set for the A/J strain: 57% similarity

		Microarray		GDS1406		Microarray	GDS 1406	Comparison
Gene Name	**ID, NCBI**	**Cortex**	**Hippocampus**	**Cortex**	**Hippocampus**	**FC in Cortex**	**FC in Cortex**	**of results**
Tissue plasminogen activator (Plat)	NM_008872	96.67	146.5	293.04	228.1	0.66	1.28	Different
Vanilloid-1 receptor (VR1) Oligo 3	NM_001001445	55.5	86.11			0.64		No Data
Vanilloid-receptor TrpV5	NM_001007572	59.75	92.19			0.65		No Data
Serotonin receptor: 5-HTr5(B)	NM_010483	71.28	110.2	51.84	52.935	0.65	0.98	Same
P2X purinoceptor 7	NM_011027	39.67	62.72	116.98	140.2	0.63	0.83	Same
Neuropeptide Y receptor type 6 (Npy6r)	NM_010935	48.42	75.78	27.12	13.825	0.64	1.96	Different
Randomly generated negative control 4		12.44	21.04			0.59		False Positive
Brain derived neurotrophic factor (BDNF)	NM_007540	71.44	125.6	728.21	461.74	0.57	1.58	Different
Neurotrophin-3 (NT-3)	NM_008742	50.03	94.14	32.04	38.56	0.53	0.83	Same
AMPA2 (alpha2) Glutamate Receptor, ionotropic	NM_013540	521.9	1'006	558.45	882.02	0.52	0.63	Same
Protein kinase C, gamma (Prkcc)	NM_011102	150.4	304.1	111.54	1443.905	0.49	0.08	Same
Mus musculus tubulin, alpha 6 (Tuba6), mRNA, Oligo 2	NM_009448	47.11	95.81	2830.79	4814.15	0.49	0.59	Same
AMPA1 (alpha1) Glutamate Receptor, ionotropic	NM_008165	302.6	765.6	951.44	1887.585	0.40	0.50	Same
Neuropeptide Y receptor type 2 (Npy2r)	NM_008731	181.5	666.9	84.82	400.38	0.27	0.21	Same

c. Comparison with the GDS1406 GEO data set for the C3H/HeJ strain: 57% similarity

		Microarray		GDS1406		Microarray	GDS 1406	Comparison
Gene Name	**ID, NCBI**	**Cortex**	**Hippocampus**	**Cortex**	**Hippocampus**	**FC in Cortex**	**FC in Cortex**	**of results**
Tissue plasminogen activator (Plat)	NM_008872	96.67	146.5	269.305	217.045	0.66	1.24	Different
Vanilloid-1 receptor (VR1) Oligo 3	NM_001001445	55.5	86.11			0.64		No Data
Vanilloid-receptor TrpV5	NM_001007572	59.75	92.19			0.65		No Data
Serotonin receptor: 5-HTr5(B)	NM_010483	71.28	110.2	32.8	50.385	0.65	0.65	Same
P2X purinoceptor 7	NM_011027	39.67	62.72	109.395	143.85	0.63	0.76	Same
Neuropeptide Y receptor type 6 (Npy6r)	NM_010935	48.42	75.78	18.9	16.94	0.64	1.12	Different
Randomly generated negative control 4		12.44	21.04			0.59		
Brain derived neurotrophic factor (BDNF)	NM_007540	71.44	125.6	834.775	387.955	0.57	2.15	Different
Neurotrophin-3 (NT-3)	NM_008742	50.03	94.14	15.58	35.32	0.53	0.44	Same
AMPA2 (alpha2) Glutamate Receptor, ionotropic	NM_013540	521.9	1'006	647.45	824.735	0.52	0.79	Same
Protein kinase C, gamma (Prkcc)	NM_011102	150.4	304.1	132.535	1487.21	0.49	0.09	Same
Mus musculus tubulin, alpha 6 (Tuba6), mRNA, Oligo 2	NM_009448	47.11	95.81	2816.85	4535.595	0.49	0.62	Same
AMPA1 (alpha1) Glutamate Receptor, ionotropic	NM_008165	302.6	765.6	1083.025	1728.635	0.40	0.63	Same
Neuropeptide Y receptor type 2 (Npy2r)	NM_008731	181.5	666.9	79.77	331.22	0.27	0.24	Same

d. Comparison with the GDS1406 GEO data set for the C57BL/6J strain: 43% similarity

		Microarray		GDS1406		Microarray	GDS 1406	Comparison
Gene Name	**ID, NCBI**	**Cortex**	**Hippocampus**	**Cortex**	**Hippocampus**	**FC in Cortex**	**FC in Cortex**	**of results**
Tissue plasminogen activator (Plat)	NM_008872	96.67	146.5	217.065	227.425	0.66	0.95	Different
Vanilloid-1 receptor (VR1) Oligo 3	NM_001001445	55.5	86.11			0.64		No Data
Vanilloid-receptor TrpV5	NM_001007572	59.75	92.19			0.65		No Data
Serotonin receptor: 5-HTr5(B)	NM_010483	71.28	110.2	49.555	71.12	0.65	0.70	Same
P2X purinoceptor 7	NM_011027	39.67	62.72	152.61	113.485	0.63	1.34	Different
Neuropeptide Y receptor type 6 (Npy6r)	NM_010935	48.42	75.78	23.565	12.57	0.64	1.87	Different
Randomly generated negative control 4		12.44	21.04			0.59		
Brain derived neurotrophic factor (BDNF)	NM_007540	71.44	125.6	612.565	472.3	0.57	1.30	Different
Neurotrophin-3 (NT-3)	NM_008742	50.03	94.14	27.2	23.605	0.53	1.15	Different
AMPA2 (alpha2) Glutamate Receptor, ionotropic	NM_013540	521.9	1'006	395.045	690.82	0.52	0.57	Same
Protein kinase C, gamma (Prkcc)	NM_011102	150.4	304.1	111.1	1528.635	0.49	0.07	Same
Mus musculus tubulin, alpha 6 (Tuba6), mRNA, Oligo 2	NM_009448	47.11	95.81	2966.765	5407.045	0.49	0.55	Same
AMPA1 (alpha1) Glutamate Receptor, ionotropic	NM_008165	302.6	765.6	926.875	1258.195	0.40	0.74	Same
Neuropeptide Y receptor type 2 (Npy2r)	NM_008731	181.5	666.9	92.75	416.41	0.27	0.22	Same

e. Comparison with the GDS1406 GEO data set for the DBA/2J strain: 43% similarity

		Microarray		GDS1406		Microarray	GDS 1406	Comparison
Gene Name	**ID, NCBI**	**Cortex**	**Hippocampus**	**Cortex**	**Hippocampus**	**FC in Cortex**	**FC in Cortex**	**of results**
Tissue plasminogen activator (Plat)	NM_008872	96.67	146.5	246.55	200.26	0.66	1.23	Different
Vanilloid-1 receptor (VR1) Oligo 3	NM_001001445	55.5	86.11			0.64		No Data
Vanilloid-receptor TrpV5	NM_001007572	59.75	92.19			0.65		No Data
Serotonin receptor: 5-HTr5(B)	NM_010483	71.28	110.2	50.77	53.455	0.65	0.95	Different
P2X purinoceptor 7	NM_011027	39.67	62.72	118.785	134.925	0.63	0.88	Same
Neuropeptide Y receptor type 6 (Npy6r)	NM_010935	48.42	75.78	33.51	14.33	0.64	2.34	Different
Randomly generated negative control 4		12.44	21.04			0.59		
Brain derived neurotrophic factor (BDNF)	NM_007540	71.44	125.6	826.03	347.915	0.57	2.37	Different
Neurotrophin-3 (NT-3)	NM_008742	50.03	94.14	33.235	31.805	0.53	1.04	Different
AMPA2 (alpha2) Glutamate Receptor, ionotropic	NM_013540	521.9	1'006	541.23	808.79	0.52	0.67	Same
Protein kinase C, gamma (Prkcc)	NM_011102	150.4	304.1	116.1	1526.41	0.49	0.08	Same
Mus musculus tubulin, alpha 6 (Tuba6), mRNA, Oligo 2	NM_009448	47.11	95.81	2742.35	5258.19	0.49	0.52	Same
AMPA1 (alpha1) Glutamate Receptor, ionotropic	NM_008165	302.6	765.6	895.95	1953.865	0.40	0.46	Same
Neuropeptide Y receptor type 2 (Npy2r)	NM_008731	181.5	666.9	120.95	304.84	0.27	0.40	Same

f. Comparison with the GDS1406 GEO data set for the FVB/NJ strain: 50% similarity

		Microarray		GDS1406		Microarray	GDS 1406	Comparison
Gene Name	**ID, NCBI**	**Cortex**	**Hippocampus**	**Cortex**	**Hippocampus**	**FC in Cortex**	**FC in Cortex**	**of results**
Tissue plasminogen activator (Plat)	NM_008872	96.67	146.5	204.995	315.825	0.66	0.65	Same
Vanilloid-1 receptor (VR1) Oligo 3	NM_001001445	55.5	86.11			0.64		No Data
Vanilloid-receptor TrpV5	NM_001007572	59.75	92.19			0.65		No Data
Serotonin receptor: 5-HTr5(B)	NM_010483	71.28	110.2	44.105	45.95	0.65	0.96	Different
P2X purinoceptor 7	NM_011027	39.67	62.72	126.79	166.995	0.63	0.76	Same
Neuropeptide Y receptor type 6 (Npy6r)	NM_010935	48.42	75.78	17.315	14.335	0.64	1.21	Different
Randomly generated negative control 4		12.44	21.04			0.59		False Positive
Brain derived neurotrophic factor (BDNF)	NM_007540	71.44	125.6	650.43	397.625	0.57	1.64	Different
Neurotrophin-3 (NT-3)	NM_008742	50.03	94.14	15.13	31.755	0.53	0.48	Same
AMPA2 (alpha2) Glutamate Receptor, ionotropic	NM_013540	521.9	1'006	596.32	730.55	0.52	0.82	Same
Protein kinase C, gamma (Prkcc)	NM_011102	150.4	304.1	125.78	1683.14	0.49	0.07	Same
Mus musculus tubulin, alpha 6 (Tuba6), mRNA, Oligo 2	NM_009448	47.11	95.81	2696.43	5372.495	0.49	0.50	Same
AMPA1 (alpha1) Glutamate Receptor, ionotropic	NM_008165	302.6	765.6	948.37	2104.34	0.40	0.45	Same
Neuropeptide Y receptor type 2 (Npy2r)	NM_008731	181.5	666.9	94.715	381.44	0.27	0.25	Same

2.4.3.2 Hippocampus vs. cortex hybridizations, normalized signals comparisons

The filtering on volcano plot of the normalized signals revealed that 3 genes were differentially expressed between the hippocampus and the cortex. One gene had a 1.91 times higher expression level in the cortex: Neuropeptide Y. The two other genes were the AMPA1 Glutamate Ionotropic Receptor, and the Neuropeptide Y Receptor Type 2, and they respectively had a 2.32 times and a 3.57 times higher expression in the hippocampus. In the 5 strains, the GDS1406 GEO dataset for Neuropeptide Y showed a different expression profile than what was observed in the low-density microarray analysis. In the 129S6/SvEvTac, A/J, DBA/2J and FVB/NJ, the expression levels of that gene were identical in the hippocampus and in the cortex and in the C57BL/6J strain, it was 1.32 times higher in the hippocampus. However, in the C3H/HeJ strain, Neuropeptide Y had a 1.32 higher expression level in the cortex, thereby confirming the observation made on the low-density microarray.

In all 6 inbred strains of the GDS1406 GEO dataset, the expression profile observed for the AMPA1 Glutamate Ionotropic Receptor, and the Neuropeptide Y Receptor Type 2 were similar to what was observed in the microarray measurements for these genes. Both genes appeared to be more expressed in the hippocampus on both platforms and in all strains. This means the expression profiles of 3 regulated genes, showed a 100% similarity in the microarray results and in the GDS1406 dataset for the C3H/HeJ strain and 66.7% similarity with the GDS1406 of the 5 other strains. The list of genes, as well as the signal comparisons with between the microarray measurements and the GDS1406 data can be seen in Table 10.

Table 10: Differentially expressed genes between the hippocampus and the cortex obtained in the 10 data microarray analysis. Comparison of the signals and the fold changes of these genes, with their expression profiles published on the GDS1406 GEO data sets for 6 inbred mice strains.

a. Comparison with the GDS1406 GEO data set for the 129S6/SvEvTac strain: 66.7% similarity

		Microarray		GDS1406		Microarray	GDS 1406	Comparison
Gene Name	**ID, NCBI**	**Cortex**	**Hippocampus**	**Cortex**	**Hippocampus**	**FC in Cortex**	**FC in Cortex**	**of results**
Neuropeptide Y, Preproneuropeptide Y	NM_023456	1.996	1.044	394.595	476.415	1.91	0.83	Different
AMPA1 (alpha1) Glutamate Receptor, ionotropic	NM_008165	0.429	1.007	1001.865	1734.975	0.43	0.58	Same
Neuropeptide Y receptor type 2 (Npy2r)	NM_008731	0.249	0.901	81.19	278.865	0.28	0.29	Same

b. Comparison with the GDS1406 GEO data set for the A/J strain: 66.7% similarity

		Microarray		GDS1406		Microarray	GDS 1406	Comparison
Gene Name	**ID, NCBI**	**Cortex**	**Hippocampus**	**Cortex**	**Hippocampus**	**FC in Cortex**	**FC in Cortex**	**of results**
Neuropeptide Y, Preproneuropeptide Y	NM_023456	1.996	1.044	442.62	376.765	1.91	1.17	Different
AMPA1 (alpha1) Glutamate Receptor, ionotropic	NM_008165	0.429	1.007	951.44	1887.585	0.43	0.50	Same
Neuropeptide Y receptor type 2 (Npy2r)	NM_008731	0.249	0.901	84.82	400.38	0.28	0.21	Same

c. Comparison with the GDS1406 GEO data set for the C3H/HeJ strain: 100% similarity

		Microarray		GDS1406		Microarray	GDS 1406	Comparison
Gene Name	**ID, NCBI**	**Cortex**	**Hippocampus**	**Cortex**	**Hippocampus**	**FC in Cortex**	**FC in Cortex**	**of results**
Neuropeptide Y, Preproneuropeptide Y	NM_023456	1.996	1.044	497.315	377.62	1.91	1.32	Same
AMPA1 (alpha1) Glutamate Receptor, ionotropic	NM_008165	0.429	1.007	1083.025	1728.635	0.43	0.63	Same
Neuropeptide Y receptor type 2 (Npy2r)	NM_008731	0.249	0.901	79.77	331.22	0.28	0.24	Same

d. Comparison with the GDS1406 GEO data set for the C57BL/6J strain: 66.7% similarity

		Microarray		GDS1406		Microarray	GDS 1406	Comparison
Gene Name	**ID, NCBI**	**Cortex**	**Hippocampus**	**Cortex**	**Hippocampus**	**FC in Cortex**	**FC in Cortex**	**of results**
Neuropeptide Y, Preproneuropeptide Y	NM_023456	1.996	1.044	471.685	619.8	1.91	0.76	Different
AMPA1 (alpha1) Glutamate Receptor, ionotropic	NM_008165	0.429	1.007	926.875	1258.195	0.43	0.74	Same
Neuropeptide Y receptor type 2 (Npy2r)	NM_008731	0.249	0.901	92.75	416.41	0.28	0.22	Same

e. Comparison with the GDS1406 GEO data set for the DBA/2J strain: 66.7% similarity

		Microarray		GDS1406		Microarray	GDS 1406	Comparison
Gene Name	**ID, NCBI**	**Cortex**	**Hippocampus**	**Cortex**	**Hippocampus**	**FC in Cortex**	**FC in Cortex**	**of results**
Neuropeptide Y, Preproneuropeptide Y	NM_023456	1.996	1.044	411.495	454.915	1.91	0.90	Different
AMPA1 (alpha1) Glutamate Receptor, ionotropic	NM_008165	0.429	1.007	895.95	1953.865	0.43	0.46	Same
Neuropeptide Y receptor type 2 (Npy2r)	NM_008731	0.249	0.901	120.95	304.84	0.28	0.40	Same

f. Comparison with the GDS1406 GEO data set for the FVB/NJ strain: 66.7% similarity

		Microarray		GDS1406		Microarray	GDS 1406	Comparison
Gene Name	**ID, NCBI**	**Cortex**	**Hippocampus**	**Cortex**	**Hippocampus**	**FC in Cortex**	**FC in Cortex**	**of results**
Neuropeptide Y, Preproneuropeptide Y	NM_023456	1.996	1.044	368.86	414.075	1.91	0.89	Different
AMPA1 (alpha1) Glutamate Receptor, ionotropic	NM_008165	0.429	1.007	948.37	2104.34	0.43	0.45	Same
Neuropeptide Y receptor type 2 (Npy2r)	NM_008731	0.249	0.901	94.715	381.44	0.28	0.25	Same

2.5 Real-Time PCR Measurements, Telemetric Apparatus Pain model

The low-density microarray experiments did not reveal any significant gene regulation linked to pain in the analyzed parts of the brain, which could be confirmed by Real-Time PCR. In order to see whether our microarray protocol was not sensitive enough to detect subtle gene expression changes linked to nociception, we selected 27 genes from our database based on their relevancy in pain research, and assessed their expression profile in the surgical pain model by Real-Time PCR. These genes are listed in Table 11.

The amount of animals tested was increased to 6 operated animals and 6 controls for statistical robustness. The surgical pain model was the same as previously described. The operated animals were anesthetized with Sevofluorane, subjected to a telemetric apparatus implantation, and treated twice daily a subcutaneous injection of Flunixin. The control animals, on the other hand, did not undergo surgery. They were only anesthetized, and treated twice daily with analgesics. After a careful observation of the mice behaviors, aspect and nest's state, the decision was taken to sacrifice the animals one day post surgery, to be able to analyze their gene expression in a post recovery timepoint, at which this behavioral analysis indicated that the animals were still in an acute phase of recovery.

The CNS of each animal was dissected, and the total RNA from brainstem, the hippocampus and the cortex as well as from 6 lumbar dorsal root ganglias was extracted. The mRNA of each of these parts was reversed in cDNA, which was used for the Real-Time PCR analysis. Given that Real-Time PCR is a more sensitive method to analyze gene expression changes than microarray, the fold changes were considered as significant when they were higher than 2. In each part of the CNS, the IL-6 Real-Time PCR reactions did not run optimally. The signals for the samples were inconsistent and appeared in the last cycles of the reaction with the signals of the negative controls. This tends to signal a problem in the PCR reaction of that gene. The fold changes observed for this gene were therefore not taken in consideration.

Table 11A: Statistics of the ΔCt values obtained in the bainstems of the operated and the control mice.

Gene		Group	N	Mean	SD	SEM	FC IN THE OPERATED ANIMALS	P Value obtained on T-test	
5HTr1D	Average Delta Ct	Control	6	8,69	,636	,260		Variances equal	,226
		Operated	6	9,08	,379	,155	-1.31	Variances different	,232
5HTr1A	Average Delta Ct	Control	6	,64	,273	,111		Variances equal	,473
		Operated	6	,51	,310	,127	1.09	Variances different	,473
5HTr2C	Average Delta Ct	Control	6	5,51	,353	,144		Variances equal	,394
		Operated	6	4,77	1,996	,815	-1.05	Variances different	,412
5HTr3A	Average Delta Ct	Control	6	2,72	,581	,237		Variances equal	,773
		Operated	6	2,83	,671	,274	-1.08	Variances different	,773
5HTr4	Average Delta Ct	Control	6	7,76	,365	,149		Variances equal	,766
		Operated	6	7,49	2,103	,858	1.20	Variances different	,771
BDNF	Average Delta Ct	Control	6	10,93	,441	,180		Variances equal	,418
		Operated	6	10,29	1,824	,745	-1.06	Variances different	,433
Creb3	Average Delta Ct	Control	6	1,02	,084	,034		Variances equal	,982
		Operated	6	1,02	,171	,070	1.00	Variances different	,982
Dream	Average Delta Ct	Control	6	4,79	,617	,252		Variances equal	,484
		Operated	6	4,58	,406	,166	1.16	Variances different	,487
Gabrg2	Average Delta Ct	Control	6	-1,30	,275	,112		Variances equal	,478
		Operated	6	-1,12	,503	,205	-1.13	Variances different	,483
HSP70	Average Delta Ct	Control	6	3,21	,335	,137		Variances equal	,137
		Operated	6	3,65	,574	,234	-1.36	Variances different	,144
IL6	Average Delta Ct	Control	6	5,06	15,967	6,518		Variances equal	,250
		Operated	6	13,15	2,809	1,147	-	Variances different	,273
LIF	Average Delta Ct	Control	6	5,84	,856	,349		Variances equal	,230
		Operated	6	4,86	1,682	,687	1.24	Variances different	,239
MapK1	Average Delta Ct	Control	6	-,19	,319	,130		Variances equal	,684
		Operated	6	-,13	,123	,050	-1.04	Variances different	,689
NPY	Average Delta Ct	Control	6	10,25	,855	,349		Variances equal	,927
		Operated	6	10,29	,455	,186	-1.03	Variances different	,927
Npy5r	Average Delta Ct	Control	6	-1,77	,403	,165		Variances equal	,822
		Operated	6	-1,71	,461	,188	-1.04	Variances different	,822
Npy6r	Average Delta Ct	Control	6	11,34	1,286	,525		Variances equal	,677
		Operated	6	11,11	,441	,180	1.18	Variances different	,682
NTRK3	Average Delta Ct	Control	6	-2,04	,184	,075		Variances equal	,717
		Operated	6	-2,09	,278	,113	1.04	Variances different	,718
Oprd1	Average Delta Ct	Control	6	4,87	,493	,201		Variances equal	,793
		Operated	6	4,96	,581	,237	-1.06	Variances different	,793
Oprm1	Average Delta Ct	Control	6	6,95	1,477	,603		Variances equal	,754
		Operated	6	7,19	1,025	,418	-1.18	Variances different	,754
Oprs1	Average Delta Ct	Control	6	-,51	,233	,095		Variances equal	,842
		Operated	6	-,48	,253	,103	-1.02	Variances different	,842
Pomc	Average Delta Ct	Control	6	,65	3,214	1,312		Variances equal	,355
		Operated	6	2,51	3,440	1,404	-3.64	Variances different	,355
Prkcc	Average Delta Ct	Control	6	-2,69	1,159	,473		Variances equal	,780
		Operated	6	-2,51	1,041	,425	-1.13	Variances different	,780
Runx1	Average Delta Ct	Control	6	9,20	,863	,352		Variances equal	,985
		Operated	6	9,19	,631	,257	1.01	Variances different	,985
Slc6a1	Average Delta Ct	Control	6	1,89	,175	,071		Variances equal	,202
		Operated	6	1,77	,121	,050	1.09	Variances different	,206
Tac1	Average Delta Ct	Control	6	-1,48	,447	,183		Variances equal	,783
		Operated	6	-1,41	,427	,174	-1.05	Variances different	,783
TacR1	Average Delta Ct	Control	6	6,79	,362	,148		Variances equal	,812
		Operated	6	6,84	,389	,159	-1.04	Variances different	,812
TrpV2	Average Delta Ct	Control	6	,88	,204	,083		Variances equal	,555
		Operated	6	,82	,137	,056	1.04	Variances different	,557

Table 11B: Statistics of the ΔCt values obtained in the cortices of the operated and the control mice.

Gene		Group	N	Mean	SD	SEM	FC IN THE OPERATED ANIMALS	P Value obtained on T-test	
5-HTr1D	Average Delta	Control	0	.	.	.		Variances equal	-
	Ct	Operated	0	.	.	.	-	Variances different	-
5HTr1A	Average Delta	Control	6	4,50	,324	,132		Variances equal	,012
	Ct	Operated	6	3,35	,854	,349	2.19	Variances different	,020
5HTr2C	Average Delta	Control	6	-2,16	,529	,216		Variances equal	,645
	Ct	Operated	5	-2,36	,855	,382	1.15	Variances different	,663
5HTr3A	Average Delta	Control	6	-,12	,493	,201		Variances equal	,473
	Ct	Operated	5	-,30	,236	,105	1.13	Variances different	,450
5HTr4	Average Delta	Control	6	8,31	,928	,379		Variances equal	,389
	Ct	Operated	6	7,24	2,774	1,133	1.51	Variances different	,402
BDNF	Average Delta	Control	6	6,83	,454	,185		Variances equal	,096
	Ct	Operated	5	8,03	1,521	,680	2.30	Variances different	,154
Creb3	Average Delta	Control	6	-1,02	,253	,103		Variances equal	,563
	Ct	Operated	4	-1,22	,808	,404	1.16	Variances different	,648
Dream	Average Delta	Control	0	.	.	.		Variances equal	-
	Ct	Operated	0	.	.	.	-	Variances different	-
Gabrg2	Average Delta	Control	6	2,17	,248	,101		Variances equal	,276
	Ct	Operated	5	1,90	,512	,229	1.20	Variances different	,321
HSP70	Average Delta	Control	6	-2,54	,519	,212		Variances equal	,707
	Ct	Operated	5	-2,66	,513	,230	1.09	Variances different	,707
IL6	Average Delta	Control	0	.	.	.		Variances equal	-
	Ct	Operated	0	.	.	.	-	Variances different	-
LIF	Average Delta	Control	6	9,80	,779	,318		Variances equal	,339
	Ct	Operated	6	9,26	1,075	,439	1.46	Variances different	,342
MapK1	Average Delta	Control	5	3,05	,333	,149		Variances equal	,188
	Ct	Operated	3	2,66	,412	,238	1.31	Variances different	,242
NPY	Average Delta	Control	6	2,37	,215	,088		Variances equal	,035
	Ct	Operated	5	1,88	,425	,190	1.40	Variances different	,060
Npy5r	Average Delta	Control	6	5,03	,261	,106		Variances equal	,076
	Ct	Operated	6	3,94	1,312	,536	1.20	Variances different	,100
Npy6r	Average Delta	Control	0	.	.	.		Variances equal	-
	Ct	Operated	0	.	.	.	-	Variances different	-
NTRK3	Average Delta	Control	6	-4,82	,403	,165		Variances equal	,065
	Ct	Operated	5	-5,46	,619	,277	1.57	Variances different	,086
Oprd1	Average Delta	Control	6	2,06	,342	,139		Variances equal	,889
	Ct	Operated	5	2,02	,558	,250	1.03	Variances different	,895
Oprm1	Average Delta	Control	0	.	.	.		Variances equal	-
	Ct	Operated	0	.	.	.	-	Variances different	-
Oprs1	Average Delta	Control	6	2,87	,495	,202		Variances equal	,184
	Ct	Operated	5	2,45	,477	,213	1.34	Variances different	,184
Pomc	Average Delta	Control	5	5,10	2,426	1,085		Variances equal	,884
	Ct	Operated	4	5,35	2,433	1,217	-1.19	Variances different	,884
Prkcc	Average Delta	Control	4	-2,19	,431	,216		Variances equal	,159
	Ct	Operated	5	-2,74	,568	,254	1.46	Variances different	,147
Runx1	Average Delta	Control	6	8,72	1,103	,450		Variances equal	,708
	Ct	Operated	5	8,49	,779	,348	1.17	Variances different	,699
Slc6a1	Average Delta	Control	5	-,98	,272	,121		Variances equal	,134
	Ct	Operated	4	-1,45	,551	,275	1.39	Variances different	,189
Tac1	Average Delta	Control	6	-2,65	1,270	,518		Variances equal	,269
	Ct	Operated	5	-3,62	1,483	,663	1.97	Variances different	,280
TacR1	Average Delta	Control	6	5,79	1,111	,453		Variances equal	,565
	Ct	Operated	5	5,28	1,685	,753	1.42	Variances different	,585
TrpV2	Average Delta	Control	6	,89	,420	,171		Variances equal	,195
	Ct	Operated	4	1,21	,146	,073	-1.24	Variances different	,138

Table 11C: Statistics of the ΔCt values obtained in the hippocampi of the operated and the control mice.

Gene		Group	N	Mean	SD	SEM	FC IN THE OPERATED ANIMALS	P Value obtained on T-test	
5-HTr1D	Average Delta	Control	6	7,65	3,469	1,416		Variances equal	,417
	Ct	Operated	6	9,63	4,591	1,874	-3.97	Variances different	,419
5HTr1A	Average Delta	Control	5	-,63	1,086	,486		Variances equal	,403
	Ct	Operated	6	-,12	,837	,342	-1.32	Variances different	,419
5HTr2C	Average Delta	Control	6	2,86	,705	,288		Variances equal	,413
	Ct	Operated	6	3,48	1,642	,670	-1.54	Variances different	,422
5HTr3A	Average Delta	Control	6	-1,05	,666	,272		Variances equal	,540
	Ct	Operated	6	-1,33	,813	,332	1.21	Variances different	,541
5HTr4	Average Delta	Control	6	8,65	,293	,120		Variances equal	,393
	Ct	Operated	6	9,22	1,538	,628	-1.48	Variances different	,410
BDNF	Average Delta	Control	6	7,25	,621	,253		Variances equal	,502
	Ct	Operated	6	7,83	1,946	,795	-1.50	Variances different	,512
Creb3	Average Delta	Control	6	2,57	1,145	,467		Variances equal	,594
	Ct	Operated	6	2,87	,743	,303	1.09	Variances different	,596
Dream	Average Delta	Control	6	,54	1,157	,472		Variances equal	,496
	Ct	Operated	6	,90	,443	,181	-1.28	Variances different	,505
Gabrg2	Average Delta	Control	6	-,96	,418	,171		Variances equal	,396
	Ct	Operated	6	-1,20	,524	,214	1.18	Variances different	,397
HSP70	Average Delta	Control	6	-2,22	,486	,198		Variances equal	,902
	Ct	Operated	6	-2,17	,651	,266	-1.03	Variances different	,902
IL6	Average Delta	Control	6	10,37	2,216	,905		Variances equal	,670
	Ct	Operated	6	9,83	2,019	,824	1.45	Variances different	,670
LIF	Average Delta	Control	6	7,27	1,252	,511		Variances equal	,569
	Ct	Operated	6	6,79	1,567	,640	1.40	Variances different	,569
MapK1	Average Delta	Control	6	-5,77	1,063	,434		Variances equal	,394
	Ct	Operated	6	-5,27	,872	,356	-1.41	Variances different	,395
NPY	Average Delta	Control	6	-3,11	,957	,391		Variances equal	,847
	Ct	Operated	6	-3,21	,777	,317	1.07	Variances different	,847
Npy5r	Average Delta	Control	6	,58	1,249	,510		Variances equal	,383
	Ct	Operated	6	1,11	,629	,257	-1.03	Variances different	,390
Npy6r	Average Delta	Control	6	8,98	1,283	,524		Variances equal	,317
	Ct	Operated	6	10,10	2,267	,926	-2.17	Variances different	,324
NTRK3	Average Delta	Control	6	-6,12	1,224	,500		Variances equal	,431
	Ct	Operated	6	-5,63	,801	,327	-1.40	Variances different	,434
Oprd1	Average Delta	Control	6	3,69	1,122	,458		Variances equal	,957
	Ct	Operated	6	3,74	1,913	,781	-1.04	Variances different	,957
Oprm1	Average Delta	Control	6	6,54	,433	,177		Variances equal	,390
	Ct	Operated	6	6,88	,813	,332	-1.26	Variances different	,396
Oprs1	Average Delta	Control	6	2,65	,526	,215		Variances equal	,926
	Ct	Operated	6	2,62	,583	,238	1.02	Variances different	,926
Pomc	Average Delta	Control	6	2,26	3,399	1,388		Variances equal	,563
	Ct	Operated	6	3,23	2,088	,853	-1.49	Variances different	,566
Prkcc	Average Delta	Control	6	-10,64	,916	,374		Variances equal	,789
	Ct	Operated	6	-10,51	,700	,286	-1.09	Variances different	,790
Runx1	Average Delta	Control	6	8,51	,884	,361		Variances equal	,361
	Ct	Operated	6	8,04	,823	,336	1.39	Variances different	,361
Slc6a1	Average Delta	Control	6	-2,53	1,077	,440		Variances equal	,394
	Ct	Operated	6	-2,10	,514	,210	-1.35	Variances different	,402
Tac1	Average Delta	Control	6	-,51	1,746	,713		Variances equal	,563
	Ct	Operated	6	,02	1,327	,542	-1.45	Variances different	,564
TacR1	Average Delta	Control	6	7,31	,916	,374		Variances equal	,792
	Ct	Operated	6	7,43	,663	,271	-1.09	Variances different	,792
TrpV2	Average Delta	Control	6	-,14	,542	,221		Variances equal	,521
	Ct	Operated	6	-,37	,633	,258	1.17	Variances different	,521

Table 11D: Statistics of the ΔCt values obtained in the dorsal root ganglia of the operated and the control mice.

Gene		Group	N	Mean	SD	SEM	FC IN THE OPERATED ANIMALS	P Value obtained on T-test	
5-HTr1D	Average Delta	Control	5	6,77	1,341	,600		Variances equal	,142
	Ct	Operated	4	5,58	,497	,249	1.30	Variances different	,125
5HTr1A	Average Delta	Control	5	3,49	,535	,239		Variances equal	,680
	Ct	Operated	4	3,36	,311	,156	1.19	Variances different	,662
5HTr2C	Average Delta	Control	2	6,86	2,258	1,596		Variances equal	,346
	Ct	Operated	3	5,40	,724	,418	1.04	Variances different	,524
5HTr3A	Average Delta	Control	5	-4,66	1,474	,659		Variances equal	,938
	Ct	Operated	5	-4,72	,546	,244	1.15	Variances different	,940
5HTr4	Average Delta	Control	2	7,96	1,603	1,133		Variances equal	,258
	Ct	Operated	3	6,14	1,337	,772	1.18	Variances different	,319
BDNF	Average Delta	Control	2	10,03	2,122	1,500		Variances equal	,259
	Ct	Operated	3	8,34	,659	,381	1.40	Variances different	,454
Creb3	Average Delta	Control	5	-1,39	,954	,426		Variances equal	,367
	Ct	Operated	4	-1,86	,142	,071	1.15	Variances different	,335
Dream	Average Delta	Control	5	3,26	,925	,413		Variances equal	,545
	Ct	Operated	4	2,90	,690	,345	1.03	Variances different	,531
Gabrg2	Average Delta	Control	6	3,16	,486	,198		Variances equal	,180
	Ct	Operated	6	2,57	,883	,360	1.51	Variances different	,188
HSP70	Average Delta	Control	5	,20	,315	,141		Variances equal	,099
	Ct	Operated	5	-,17	,317	,142	-2.30	Variances different	,099
IL6	Average Delta	Control	5	6,89	5,315	2,377		Variances equal	,436
	Ct	Operated	5	8,94	1,733	,775	1.11	Variances different	,451
LIF	Average Delta	Control	2	6,23	3,286	2,324		Variances equal	,299
	Ct	Operated	3	4,03	,406	,235	-1.19	Variances different	,516
MapK1	Average Delta	Control	5	1,73	,779	,348		Variances equal	,793
	Ct	Operated	4	1,86	,581	,291	-1.20	Variances different	,785
NPY	Average Delta	Control	6	4,59	1,747	,713		Variances equal	,261
	Ct	Operated	6	5,79	1,741	,711	-1.09	Variances different	,261
Npy5r	Average Delta	Control	5	2,08	4,621	2,066		Variances equal	,380
	Ct	Operated	4	4,34	1,389	,695	1.31	Variances different	,347
Npy6r	Average Delta	Control	2	9,66	1,645	1,163		Variances equal	,987
	Ct	Operated	2	9,60	4,395	3,108	2.27	Variances different	,988
NTRK3	Average Delta	Control	5	-3,85	1,248	,558		Variances equal	,661
	Ct	Operated	4	-4,19	,917	,458	1.39	Variances different	,649
Oprd1	Average Delta	Control	5	4,89	,514	,230		Variances equal	,939
	Ct	Operated	5	4,84	1,078	,482	1.09	Variances different	,939
Oprm1	Average Delta	Control	5	5,33	1,676	,749		Variances equal	,999
	Ct	Operated	4	5,32	3,722	1,861	1.00	Variances different	,999
Oprs1	Average Delta	Control	5	-2,19	,795	,355		Variances equal	,622
	Ct	Operated	5	-2,38	,314	,141	1.27	Variances different	,629
Pomc	Average Delta	Control	5	6,96	,967	,432		Variances equal	,213
	Ct	Operated	4	5,53	2,099	1,049	-1.17	Variances different	,276
Prkcc	Average Delta	Control	5	2,46	1,768	,791		Variances equal	,847
	Ct	Operated	4	2,70	1,650	,825	1.28	Variances different	,846
Runx1	Average Delta	Control	5	3,95	,664	,297		Variances equal	,230
	Ct	Operated	5	3,47	,506	,226	4.60	Variances different	,232
Slc6a1	Average Delta	Control	5	3,43	,944	,422		Variances equal	,729
	Ct	Operated	4	3,69	1,279	,640	3.24	Variances different	,741
Tac1	Average Delta	Control	5	-5,06	,914	,409		Variances equal	,687
	Ct	Operated	5	-5,26	,529	,236	3.53	Variances different	,689
TacR1	Average Delta	Control	5	6,60	1,635	,731		Variances equal	,801
	Ct	Operated	5	6,36	1,293	,578	2.75	Variances different	,801
TrpV2	Average Delta	Control	5	-1,43	,554	,248		Variances equal	,297
	Ct	Operated	5	-2,21	1,446	,647	1.04	Variances different	,314

In the brainstem, only one gene was downregulated in operated animals: the Pro-opiomelanocortine (Pomc). This gene was 3.7 times more expressed in the control animals. The rest of the genes showed no regulation linked to nociception in this part of the brain. In the cortex, 3 genes were more expressed in the operated animals than in the control ones: Tachikinin 1, the serotonin receptor 5-HTr1A and BDNF. All these genes had a 2 times higher expression in the operated animals. In the hippocampus, 2 genes were regulated: the Neuropeptide receptor Npy6r, and the 5-HTr1D, which were respectively 1.2 and 4 times more expressed in the control animals. The results obtained in the dorsal root ganglia indicated that the 5-Htr1D, 5-HTr4, 5HTr2C serotonin receptors, DREAM, LIF and BDNF were all 2.3 to 4.6 times more expressed expressed in the operated animals. On the other hand, the

Neuropeptide Y gene was 2.3 times more expressed in the dorsal root ganglia of the control animals.

A t-test with a confidence interval of 95% was applied to the ΔCt values measured in the operated and the control animals values for each gene. In the brainstem, no genes showed a significant difference, as illustrated by the boxplots of Figure 12A. The difference 3.7 times upregulation we observed in the control animals could not be confirmed by the t-test of the ΔCt values. Indeed, the P value of that gene was 0.355. In the cortex, only the 5HTr1A serotonin receptor showed a significant difference (P value = 0.012). BDNF was 2.3 times more expressed in the brainstem of the operated animals according to our Real-Time PCR data, but the differences between the ΔCt values of that gene in the operated animals and the control ones were not significant according to the t-test (P value = 0.096). The boxplots on Figure 12B graphically illustrate the ΔCt values in the cortex. In the hippocampus, no significant differences could be observed. The P Values for the 5HTr1D serotonin receptor and the Npy6r genes had a respective value of 0.42, and 0.32, which shows that the different observed was not significant. (Figure 12C). The differences observed in the dorsal root ganglia were also not significant, as the P Values obtained for the 5-Htr1D, 5-HTr4, 5HTr2C serotonin receptors, DREAM, LIF, BDNF and NPY genes are all higher than 0.05. The boxplots from Figure 12D illustrate the ΔCt values measured in the dorsal root ganglia. Table 11 A, B, C and D sum up the genes analyzed, their fold change in the operated animals vs. the control ones measured by Real-Time PCR in the brainstems, cortices, hippocampi and the dorsal root ganglias respectively and give all the descriptive and group statistics of the Ct values.

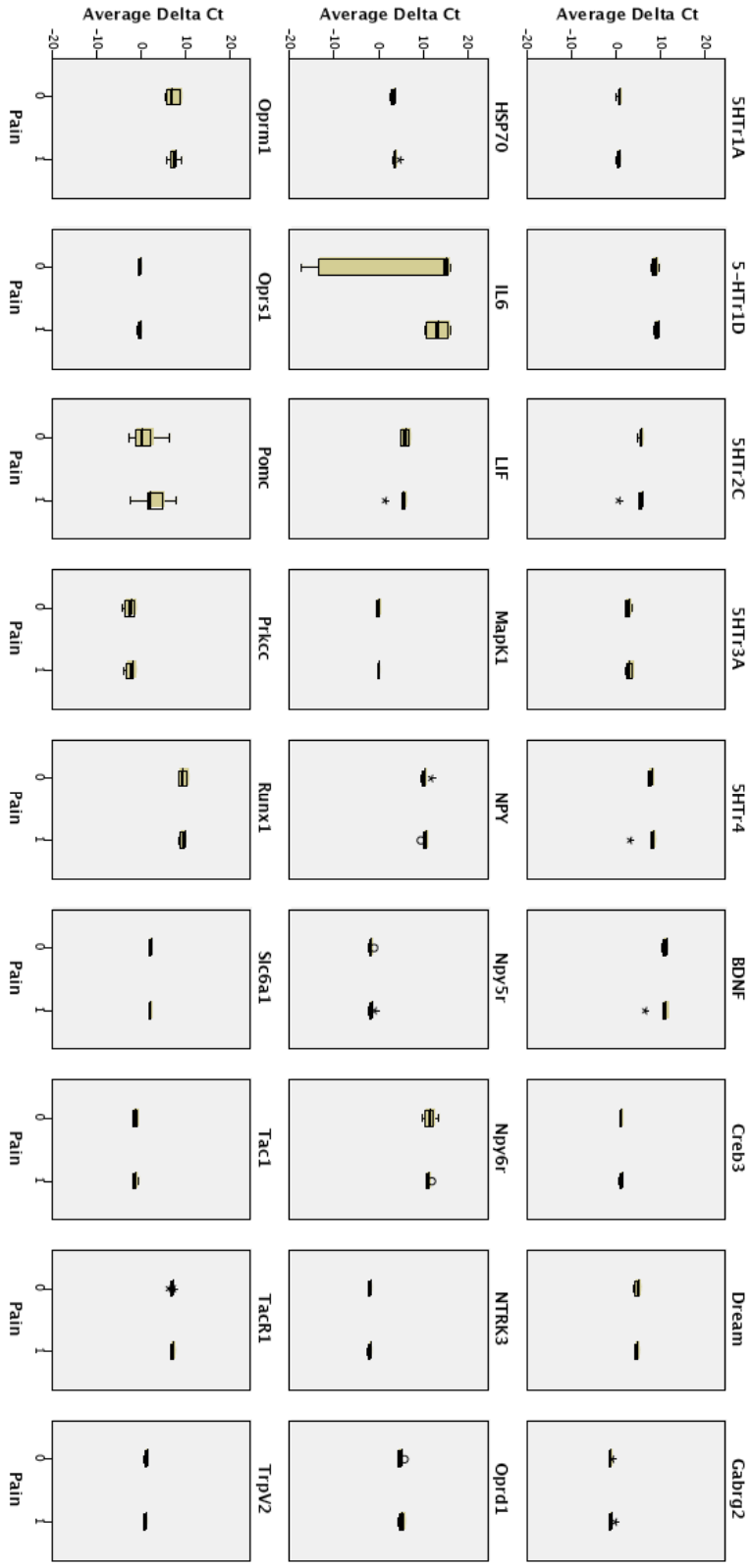

Figure 12A: Boxplots of the ΔCt values obtained in the brainstems of 6 operated mice (Pain =1 on the figure), and 6 Control mice (Pain = 0 on the figure). No significant difference could be observed.

Figure 12B: Boxplots of the ΔCt values obtained in the cortices of 6 operated mice (Pain =1 on the figure), and 6 Control mice (Pain = 0 on the figure). The only significant difference can be observed for 5HTr1A (P Value=0.012)

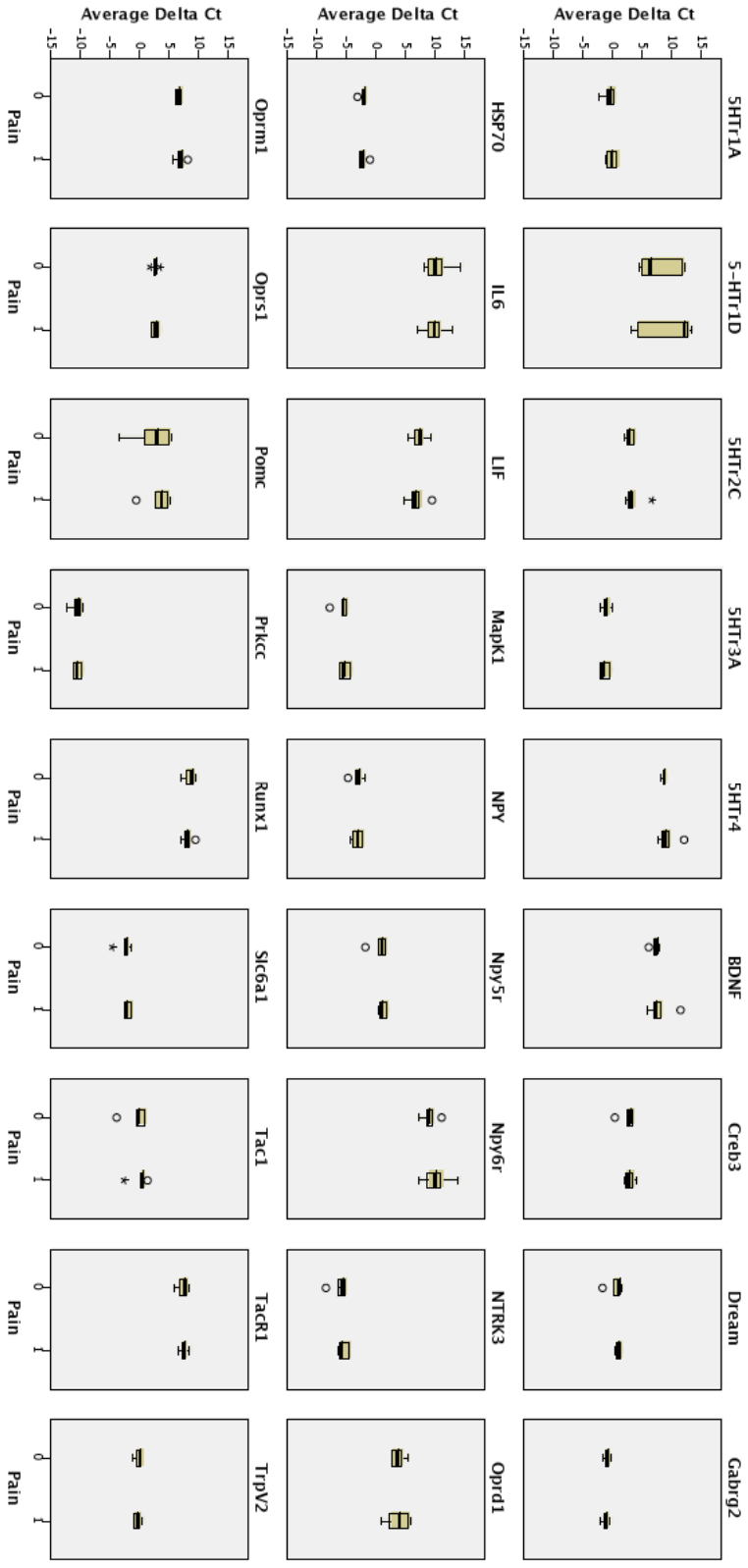

Figure 12C: Boxplots of the ΔCt values obtained in the hippocampi of 6 operated mice (Pain =1 on the figure), and 6 Control mice (Pain = 0 on the figure). No significant difference could be observed.

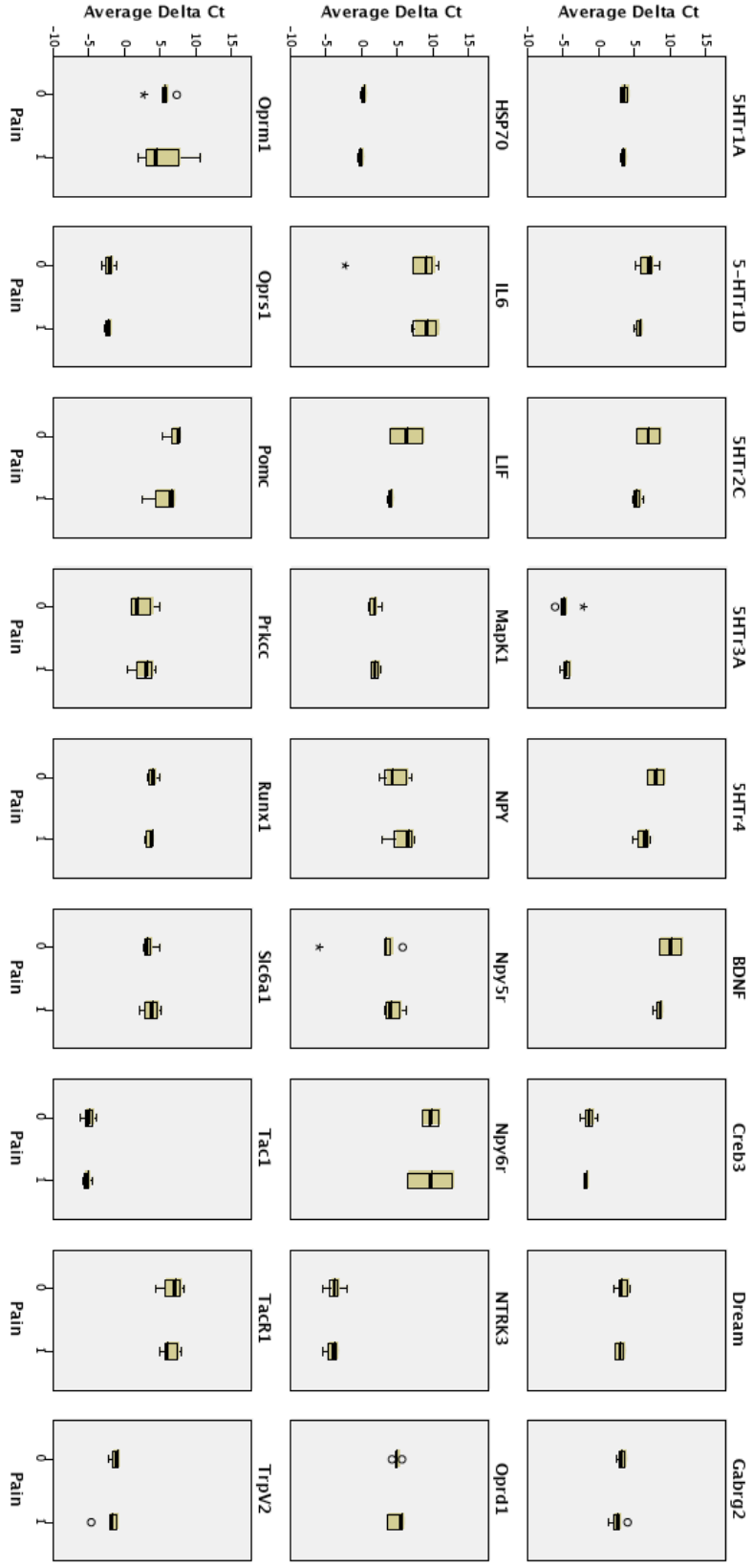

Figure 12D: Boxplots of the ΔCt values obtained in the dorsal root ganglia of 6 operated mice (Pain =1 on the figure), and 6 Control mice (Pain = 0 on the figure). No significant difference could be observed.

2.6 Real-Time PCR Measurements, inflammatory pain model

In order to test whether the lack of differences observed in gene expression was due to the pain model, the expression profiles of the 27 genes were tested in an inflammatory pain model. In this experiment, 6 mice received an intraperitoneal injection of BHV-1 immunization solution in Complete Feund's Adjuvent, and 6 control animals received an intraperitoneal injection of vehicle solution, which does not cause inflammation. All animals were sacrificed 3 days after the injection. For each animal, the cortex and spinal cord were dissected and analyzed by Real-Time PCR.

In the cortex, the PCRs for Interleukin 6, the 5-HTr1D serotonin receptor, the opioid receptor μ 1 and the Neuropeptide Y receptor type 6 did not run optimally, and their results for these genes could not be considered in the analysis. Similarily, the reactions for LIF, BDNF, the serotonin receptors 5-HTr4 and 5-HTr2C and the neuropeptide Y receptor type 6 in the spinal cord samples did not run properly and were excluded from the study.

Out of the 27 genes tested, Proopiomelanocortin (Pomc) is the only gene, which shows a regulation linked to the inflammatory pain. It appears to be 2.5 times upregulated in the cortices of the animals, who were subjected to the CFA injection. Interestingly, this gene behaves in the opposite way in the spinal cords of these animals, in which it appears to be 1.8 times downregulated after the CFA treatment. This downregulation could be caused by a difference in Pomc-expressing cell numbers between the treated and the control spinal cords. Indeed, the CFA injection might have triggered the migration of dendritic cells in the spinal cords. This process would have decreased the proportion of cells expressing Pomc in the spinal cords of treated animals, and would appear as a downregulation of the gene, when compared with controls in which no migration of dendritic cells would have happened.

The ΔCt values measured in the treated and the control animals were subjected to a T-test with a confidence interval of 95% to test the significance of the fold changes observed. The 2.5 times upregulation and the 1.8 downregulation of the Pomc gene observed in the cortices and the spinal cords of the immunized animals were not significant according to the T-Test (P Value = 0.26 and 0.072, respectively). Interestingly, the T-test showed that a significant difference could be seen between the ΔCt values of the Slc6a1 gene measured in the spinal cords of the immunized and the control animals (P Value = 0.02). However, the Real-Time PCR analysis indicated a fold change of 1.2 for Pomc, which means that the result of the T-test was a false positive. The boxplots of the ΔCt values in the cortices and the spinal cords of the treated and the control animals can be seen on Figure 13A and 13B. Table 12A and 12 B sum up the genes analyzed, their fold change in the treated animals vs. the control ones measured by Real-Time PCR in the cortex

and the spinal cord respectively and give all the descriptive and group statistics of the Ct values.

Table 12 A Statistics of the ΔCt values obtained in the cortices of the immunized (treated) and the control mice.

Gene		Group	N	Mean	SD	SEM	FC IN THE TREATED ANIMALS	P Value obtained on T-test	
5HTr1D	Average Delta	Control	0	.	.	.		Variances equal	-
	Ct	Treated	0	.	.	.	-	Variances different	-
5HTr1A	Average Delta	Control	6	4,07800	,476757	,194635		Variances equal	,782
	Ct	Treated	6	4,16400	,566826	,231406	-1.06	Variances different	,782
5HTr2C	Average Delta	Control	6	2,90033	,576472	,235344		Variances equal	,116
	Ct	Treated	6	3,50300	,633747	,258726	-1.52	Variances different	,116
5HTr3A	Average Delta	Control	6	1,74983	1,233703	,503657		Variances equal	,534
	Ct	Treated	6	2,10250	,521991	,213102	-1.28	Variances different	,540
5HTr4	Average Delta	Control	6	6,84033	,680712	,277899		Variances equal	,197
	Ct	Treated	6	7,34033	,566970	,231464	-1.41	Variances different	,198
BDNF	Average Delta	Control	6	3,62450	,434160	,177245		Variances equal	,623
	Ct	Treated	6	3,46300	,649021	,264962	1.12	Variances different	,625
Creb3	Average Delta	Control	6	2,92667	,219670	,089680		Variances equal	,781
	Ct	Treated	6	3,00967	,678190	,276870	-1.06	Variances different	,785
Dream	Average Delta	Control	6	-,86383	,219768	,089720		Variances equal	,479
	Ct	Treated	6	-,11883	2,468994	1,007962	1.17	Variances different	,494
Gabrg2	Average Delta	Control	6	4,54533	,486546	,198631		Variances equal	,443
	Ct	Treated	6	4,76850	,482179	,196849	-1.17	Variances different	,443
HSP70	Average Delta	Control	6	-2,20350	1,285059	,524623		Variances equal	,198
	Ct	Treated	6	-1,46750	,243896	,099570	-1.67	Variances different	,223
IL6	Average Delta	Control	0	.	.	.		Variances equal	-
	Ct	Treated	0	.	.	.	-	Variances different	-
LIF	Average Delta	Control	6	6,49550	,820426	,334938		Variances equal	,341
	Ct	Treated	6	6,91317	,611124	,249490	-1.34	Variances different	,343
MapK1	Average Delta	Control	6	2,00533	,316134	,129061		Variances equal	,407
	Ct	Treated	5	2,26720	,656281	,293498	-1.20	Variances different	,448
NPY	Average Delta	Control	6	4,97033	,549733	,224428		Variances equal	,577
	Ct	Treated	6	5,15633	,568757	,232194	-1.14	Variances different	,577
Npy5r	Average Delta	Control	6	4,04500	,235980	,096338		Variances equal	,996
	Ct	Treated	6	4,04300	,826955	,337603	1.00	Variances different	,996
Npy6r	Average Delta	Control	0	.	.	.		Variances equal	-
	Ct	Treated	0	.	.	.	-	Variances different	-
NTRK3	Average Delta	Control	6	,69083	,145432	,059373		Variances equal	,148
	Ct	Treated	5	,82460	,131747	,058919	-1.10	Variances different	,145
Oprd1	Average Delta	Control	6	6,22750	,599907	,244911		Variances equal	,971
	Ct	Treated	6	6,23883	,437504	,178610	-1.01	Variances different	,971
Oprm1	Average Delta	Control	0	.	.	.		Variances equal	-
	Ct	Treated	0	.	.	.	-	Variances different	-
Oprs1	Average Delta	Control	6	-,67300	,805235	,328736		Variances equal	,378
	Ct	Treated	6	-,27633	,677347	,276526	-1.24	Variances different	,378
Pomc	Average Delta	Control	6	6,05067	2,859423	1,167355		Variances equal	,258
	Ct	Treated	6	3,81317	3,565783	1,455725	2.47	Variances different	,259
Prkcc	Average Delta	Control	6	-2,11133	,190549	,077791		Variances equal	,686
	Ct	Treated	6	-1,99700	,645800	,263647	-1.08	Variances different	,692
Runx1	Average Delta	Control	6	9,12950	,640605	,261526		Variances equal	,897
	Ct	Treated	6	9,20517	1,239485	,506018	-1.05	Variances different	,898
Slc6a1	Average Delta	Control	6	3,44333	,262467	,107152		Variances equal	,954
	Ct	Treated	6	3,42867	,541737	,221163	1.01	Variances different	,954
Tac1	Average Delta	Control	6	-,45867	,576235	,235247		Variances equal	,678
	Ct	Treated	6	-,28950	,780758	,318743	1.07	Variances different	,679
TacR1	Average Delta	Control	6	5,05783	,760495	,310471		Variances equal	,496
	Ct	Treated	6	5,35383	,689788	,281605	-1.23	Variances different	,496
TrpV2	Average Delta	Control	6	4,50517	,459103	,187428		Variances equal	,313
	Ct	Treated	5	4,84480	,597511	,267215	-1.27	Variances different	,331

Table 12 B: Statistics of the ΔCt values obtained in the spinal cords of the immunized (treated) and the control mice.

Gene		Group	N	Mean	SD	SEM	FC IN THE TREATED ANIMALS	P Value obtained T-test	
5-HTr1D	Average Delta Ct	Control	6	10,34	,661	,270		Variances equal	,596
		Treated	6	10,12	,744	,304	1.17	Variances different	,596
5HTr1A	Average Delta Ct	Control	6	5,49	,186	,076		Variances equal	,135
		Treated	6	5,30	,221	,090	1.14	Variances different	,136
5HTr2C	Average Delta Ct	Control	0	.	.	.		Variances equal	-
		Treated	0	.	.	.	-	Variances different	-
5HTr3A	Average Delta Ct	Control	6	,23	,212	,086		Variances equal	,597
		Treated	6	,16	,208	,085	-1.01	Variances different	,597
5HTr4	Average Delta Ct	Control	0	.	.	.		Variances equal	-
		Treated	0	.	.	.	-	Variances different	-
BDNF	Average Delta Ct	Control	0	.	.	.		Variances equal	-
		Treated	0	.	.	.	-	Variances different	-
Creb3	Average Delta Ct	Control	6	,53	,308	,126		Variances equal	,425
		Treated	6	,67	,299	,122	-1.02	Variances different	,425
Dream	Average Delta Ct	Control	6	6,26	,174	,071		Variances equal	,046
		Treated	6	5,97	,265	,108	1.23	Variances different	,050
Gabrg2	Average Delta Ct	Control	6	1,04	,296	,121		Variances equal	,454
		Treated	6	1,14	,162	,066	-1.08	Variances different	,459
HSP70	Average Delta Ct	Control	6	-4,19	,200	,082		Variances equal	,096
		Treated	6	-4,36	,116	,047	1.13	Variances different	,104
IL6	Average Delta Ct	Control	6	7,83	,980	,400		Variances equal	,756
		Treated	6	7,63	1,148	,469	1.15	Variances different	,756
LIF	Average Delta Ct	Control	0	.	.	.		Variances equal	-
		Treated	0	.	.	.	-	Variances different	-
MapK1	Average Delta Ct	Control	6	,78	,169	,069		Variances equal	,343
		Treated	6	,64	,302	,123	1.10	Variances different	,349
NPY	Average Delta Ct	Control	6	-1,37	,167	,068		Variances equal	,875
		Treated	6	-1,35	,306	,125	-1.02	Variances different	,876
Npy5r	Average Delta Ct	Control	6	2,82	,511	,209		Variances equal	,926
		Treated	6	2,85	,363	,148	-1.02	Variances different	,926
Npy6r	Average Delta Ct	Control	0	.	.	.		Variances equal	-
		Treated	0	.	.	.	-	Variances different	-
NTRK3	Average Delta Ct	Control	6	-1,72	,507	,207		Variances equal	,466
		Treated	6	-1,53	,339	,139	-1.14	Variances different	,468
Oprd1	Average Delta Ct	Control	6	3,85	,620	,253		Variances equal	,677
		Treated	6	3,73	,310	,126	1.09	Variances different	,680
Oprm1	Average Delta Ct	Control	6	8,93	,818	,334		Variances equal	,140
		Treated	6	8,21	,714	,292	1.64	Variances different	,140
Oprs1	Average Delta Ct	Control	6	-,76	,168	,068		Variances equal	,780
		Treated	6	-,78	,141	,058	1.02	Variances different	,780
Pomc	Average Delta Ct	Control	6	8,25	,535	,218		Variances equal	,072
		Treated	6	9,11	,905	,370	-1.82	Variances different	,079
Prkcc	Average Delta Ct	Control	6	1,43	,188	,077		Variances equal	,336
		Treated	6	1,57	,293	,119	-1.10	Variances different	,340
Runx1	Average Delta Ct	Control	6	6,94	,394	,161		Variances equal	,864
		Treated	6	6,99	,495	,202	-1.03	Variances different	,864
Slc6a1	Average Delta Ct	Control	6	1,50	,177	,072		Variances equal	,020
		Treated	6	1,22	,173	,070	1.21	Variances different	,020
Tac1	Average Delta Ct	Control	6	-2,41	,212	,086		Variances equal	,405
		Treated	6	-3,83	3,994	1,631	-1.16	Variances different	,424
TacR1	Average Delta Ct	Control	6	,34	,280	,114		Variances equal	,606
		Treated	6	,52	,800	,326	-1.18	Variances different	,613
TrpV2	Average Delta Ct	Control	6	-1,89	,176	,072		Variances equal	,465
		Treated	6	-1,76	,375	,153	-1.09	Variances different	,472

Figure 13A: Boxplots of the ΔCt values obtained in the cortices of 6 immunized mice (Pain =1) on the figure), and 6 Control mice (Pain = 0 on the figure). No significant difference could be observed.

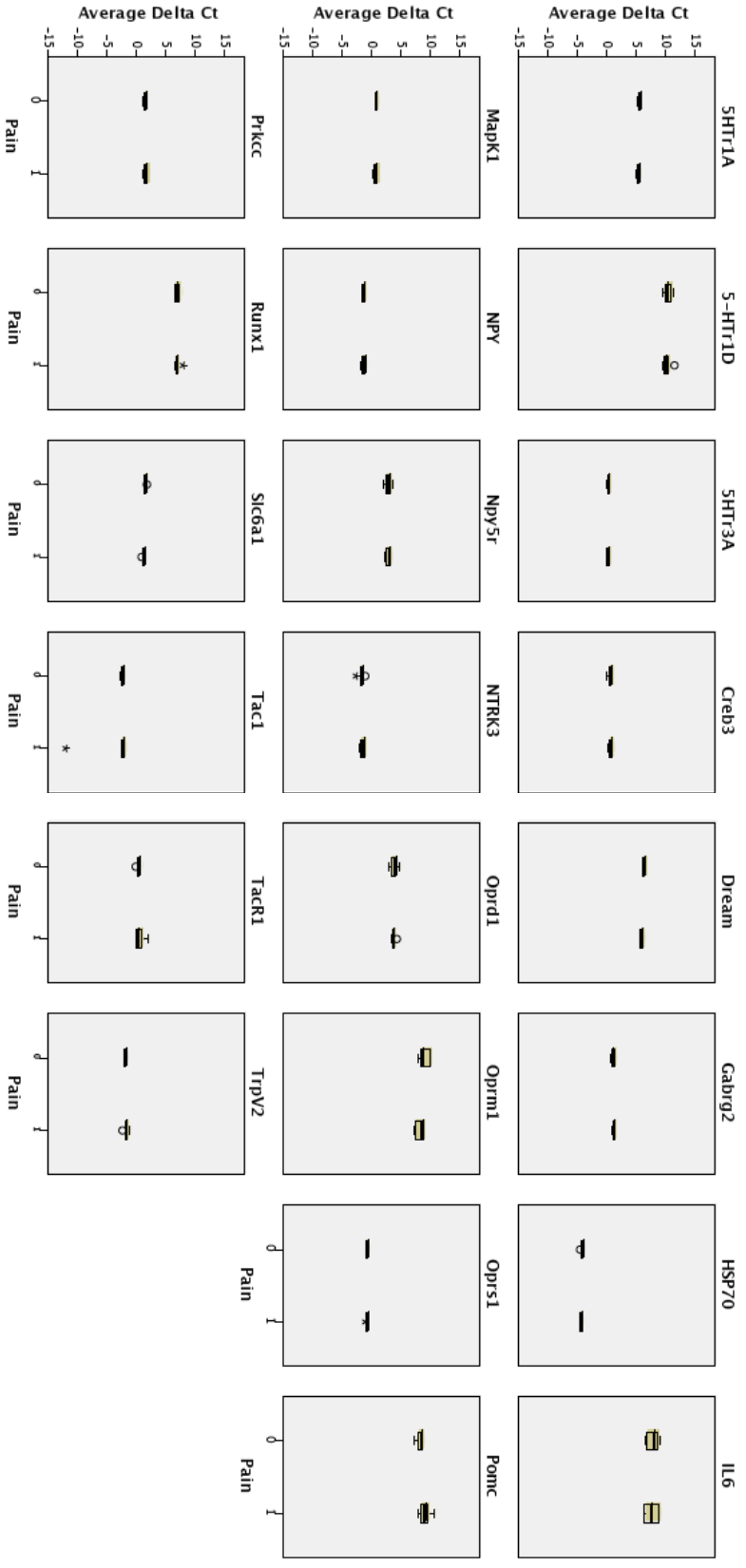

Figure 13B: Boxplots of the ΔCt values obtained in the Spinal cords of 6 immunized mice (Pain =1) on the figure), and 6 Control mice (Pain = 0 on the figure). No significant difference could be observed. Slc6a1 was a false positive with a FC = 1.2 and a P value = 0.02. No other significant difference could be observed.

2.7 Whole genome experiment in the spinal cord, Telemetric Apparatus

In order to have a further understanding of the gene expression changes linked to nociception, which occur in the post-operative recuperation phase in NMRI mice, we carried a whole genome microarray analysis. In this experiment, we worked with GeneChip® Mouse Exon 1.0 ST Arrays, which allow to study the behavior of all the exons of each gene of the murine organism. The surgical protocol was the same as previously described: 6 NMRI mice were anesthetized with Sevofluorane, subjected to a Telemetric Apparatus Implantation, and treated twice daily with 80 µl Flunixin (Conc.) injected intra-peritonealy during the recovery phase. The 6 control animals were subjected to the same anesthesia and analgesia, but did not undergo surgery. After a careful observation of each animal's behavior, aspect, coat, posture, cage and nest, the decision to sacrifice them 24 hours post surgery was taken. At the time of sacrifice, the operated animals showed clear differences in their behavior when compared to the control ones. They did not groom, adopted an arched back position, and their nests were poorly elaborated, when compared to the control animals. These observations led to the assumption that the operated animals were indeed experiencing pain at this time. After sacrifice, the spinal cords were dissected, and the total RNA was extracted, reverse transcribed, amplified and labeled for hybridization on the GeneChip® Mouse Exon 1.0 ST Arrays.

On the GeneChip® Mouse Exon 1.0 ST Arrays, 4 probes for the same exon are included in one probeset. In most cases, one probeset covers one exon, however more probesets cover long exons. In our experiments, 4.5×10^6 probesets were differentially expressed between the operated animals and the control ones. A general asymmetry of the regulations was observed, with about 37% of the exon expression level changes being upregulations, and 63% of them being downregulations. For our analyses, we worked with the 37000 probesets, which showed the most significant fold changes. Two types of analysis were carried out. The first one consisted in understanding, which genes tend to show a complete differential expression, and to cluster them to understand their function. The second analysis consisted in identifying genes, which were most likely to have splice variants between the two conditions.

2.7.1 Whole gene regulations

The goal of this analysis, was to understand, which genes have 3 or more probesets, which were either upregulated or downregulated in the operated animals and to define, which processes they might be linked to. For study of the downregulations, we analyzed the 4000 most significantly differentially expressed probesets. Out of these 4000 exons, 2823 were known and defined, and 1177 were not annotated sequences. We excluded genes, which had

two or less downregulated probesets, as well as probesets recognizing single intronic sequences and intergenic sequences. This filtering showed that 166 genes had 3 or more exons, which were downregulated in the spinal cords of the operated animals. After a literature search, and a search on Entrez (NCBI), the genes were then classified according to their function. The results can be seen in table 13.

Interestingly, 68 genes were linked to cell motility. These genes are typical cytoskeleton components, often implicated in skeletal muscle cell function: such as Actin alpha 1, or Myosin, heavy polypeptide 2. Out of this category, the gene, which had the most downregulated exons was the Titin gene. This gene had 301 probesets, which showed a 2 to 4 times downregulation. According to Ensembl, this gene is 278567 bp long, and has 363 exons, which explains the high number of probesets present. Another noticeable feature is that 7 genes, which had many downregulated exons in the spinal cords of the operated animals, are involved in neurogenesis. Taken together, this data could lead to the supposition that synaptic plasticity processes are happening in the spinal cord of the operated animals. It could also reflect microglia activation in the spinal cord. The activation of the immune system in the central nervous system also requires cellular motility, and could be explain the downregulations described above.

Our analysis showed that 30 genes involved in inflammation, such as Interleukin receptor 8 beta or Annexin A1 are downregulated in the spinal cords of the operated mice. The other main represented categories are genes involved in the cell cycle (21 genes), and genes encoding channels or recepors (12 genes). The complete list of genes, which have at least 3 downregulated exons in the spinal cords of the operated animals, can be seen in Appendix 6.

Table 13: Classification of the 166 genes, which had 3 or more downregulated exons in the lumbar spinal cords of the operated animals.

Not Annotated	1177	
Gene with minimum of 3 downregulated exons	166	
		Examples
Cell Motility	68	Acta1, Actn2, Diap3, Myh2, Trpm2, Ttn
Inflammation	30	Il8rb, Anxa1, Fcrla, Lirb4
Cell Cycle	21	Ccna2, Bub1
Neurogenesis	7	Aspm, Comp
Channels and receptors	12	Scn10a, Scn11a
Cell differenciation	6	Mcm4, S100a4, s100a8
ATPase	5	Atp2a1, Atp6v0d2
Protein degradation	6	Bckdhb
GPI coupled receptors or related	6	Gpr128, Gpr141
Apoptosis	1	Birc5
Heterochromatin formation	1	Baz1a
Cancer	3	Cox8b, Hmmr, Fap

For the study of the upregulated genes, we increased the number of screened genes, because of the asymmetry between the upregulated and downregulated genes. We therefore considered the 18000 most significantly upregulated probesets. Out of this list, 8932 were located in not annotated sequences, and 9068 were in exons of known genes. After excluding the genes, which had two or less upregulated probeset, and the probesets recognizing single intronic sequences or intergenic sequences, we obtained a list of 96 genes, which had 3 or more upregulated probesets. After a literature search and a screening on Entrez, we classified the 96 genes according to their function.

In the list of genes, which had at least 3 upregulated exons in the spinal cords of the operated animals, 22 genes were directly involved in axonal guidance and synaptic plasticity. Interestingly, 4 members of the EphA receptors family (Epha3, Epha4, Epha5 and Epha6), and 6 members of the Semaphorin family (Sema3F, Sema4A, Sema5A, Sema6A, Sema6C and Sema6D) were upregulated. EphA receptors are involved in the growth cone guidance of spinal motor neurons, and Semaphorins are one of the most important families of genes involved in the maintenance of neuronal networks and in axonal guidance.

Two other noticeable functions among the 96 genes, which have 3 or more upregulated exons are the neuronal development (13 genes), and cell interaction and adhesion (8 genes). In our experiment, one of the most important upregulated genes in the category of neuronal development is Dab1. This gene is an important element of the Reelin Dab1 pathway, which regulates neuronal positioning during the development. This pathway is also involved in Pain perception. In our microarray analysis, Reelin was downregulated in the operated animals. This tends to show, that the Reelin-Dab1 pathway is active in our surgical pain model. In the cell interaction and adhesion category, Neural Cell Adhesion Molecule 1 and 2 are two important elements, as these molecules are involved the establishment of synapses

Two genes directly linked to nociceptive processes had at least 3 upregulated exons in the spinal cords of the operated mice: Gabrb2 and Oprm1. Interestingly, Oprm1 was present on the low-density microarray, but did not show any regulation in any other experiments, even in the Spinal cord. The other 2 key categories, which were present, were Glycosylation and Inflammation. These are both known to be influencing synaptic generation. All the classifications of the genes, which have at least 3 upregulated exons in the post operative phase are described in Table 14, and Appendix 7 is the complete list of the 96 with more than 2 upregulated exons.

Table 14: Classification of the 96 genes, which had 3 or more upregulated exons in the spinal cords of the operated animals.

Non Attributed	8932	
Gene with a minimum of 2 upregulated probesets	96	
		Examples
Axonal guidance and Synaptic formation	22	Epha3, Epha4, Erc5, Pcdha6, Sema5a
Neuronal Development	13	Plxdc2, Med12l, Pax6, Immp21, Dach1
Cell cell interaction and adhesion	8	Ctnna1, Ncam1, Ncam2
Glycosylation	3	Ext1, Gtdc1, Alg13
Solute carrier	8	Slc25a37, Slc25a40, Slc26a3, Slc27a2
G Protein coupled receptor	2	Lphn2, Lphn3
Inflammation	3	Pibf1, Ilf3, Pros1
Signal Transmission	6	Map4k5, Odz4, Plcl1
CNS disorders	4	Auts2, Brunol14, Hnt
Potassium channel	2	Kcnab1, Kcnc2
Exocytosis Endocytosis	2	Exoc6b, Sgip1
Nociception	2	Gabrb2, Oprm1
Cancer	4	Ptprz1, Gtf2h1, Gtf2h2, Gtf2i
Others (chaperone, mitochondrial protein...)	17	Lace1, Fads1, Dnajc2, Bai1

2.7.2 Clustering analysis

We performed a bi-clustering meta-analysis using Genevestigator, in order to better understand the mechanisms in which the regulated genes from our study might be involved in. The lists of up- and downregulated genes, were clustered in Genevestigator, according to the "Stimulus" criterion. In this procedure, the software searches how the genes of the proposed list reacted to a specific stimulus in published microarrays, and performs a bi-clustering analysis to group genes, which showed similar regulation after specific stimulations. Specific cellular effects are caused by each stimulus listed in Genevestigator. By understanding which cellular process is triggered by the stimulation, one can gain information about the subset of genes, which is clustered according to this stimulus.

2.7.2.1 Bi-clustering analysis of the downregulated genes

The first clustering was performed on the 166 genes, which had 3 or more downregulated exons in the spinal cords of the operated animals. The goal was to find subsets from this gene list, which were also downregulated after specific stimuli. This analysis revealed that a cluster of 21 genes from our list, represented by 29 probesets, was also downregulated in 4 different types of experimental stimulations: two different experiments involving lipopolysaccharides, an experiment with Trichostatin A3, and a myoblast to myotubule in-vitro differentiation. The list of the clustered probesets and their corresponding genes can be seen in Table 15. The clusters can be seen in Figure 12 A.

Table15: Bi-clustering analysis of the 166 downregulated genes. 29 clustered probesests, which are all downregulated after Lipopolysaccharide 4, Lipopolysaccharide 5, Trichostatin A3, myoblast to myotubule differentiation stimuli.

Probe Set ID	Gene Symbol	Gene Title	Entrez Gene ID
1415945_at	Mcm5	minichromosome maintenance deficient 5, cell division cycle 46 (S. cerevisiae)	17218 Entrez gene
1416961_at	Bub1b	budding uninhibited by benzimidazoles 1 homolog, beta (S. cerevisiae)	12236 Entrez gene
1417910_at	Ccna2	cyclin A2	12428 Entrez gene
1417911_at	Ccna2	cyclin A2	12428 Entrez gene
1418264_at	Cenpk	centromere protein K	60411 Entrez gene
1422814_at	Aspm	asp (abnormal spindle)-like, microcephaly associated (Drosophila)	12316 Entrez gene
1424046_at	Bub1	budding uninhibited by benzimidazoles 1 homolog (S. cerevisiae)	12235 Entrez gene
1424060_at	Neil3	nei like 3 (E. coli)	234258 Entrez gene
1424118_a_at	Spc25	SPC25, NDC80 kinetochore complex component, homolog (S. cerevisiae)	66442 Entrez gene
1424278_a_at	Birc5	baculoviral IAP repeat-containing 5	11799 Entrez gene
1427161_at	Cenpf	centromere protein F	108000 Entrez gene
1427276_at	Smc4	structural maintenance of chromosomes 4	70099 Entrez gene
1429172_a_at	Ncapg	on-SMC condensin I complex, subunit G	54392 Entrez gene
1434767_at	C79407	expressed sequence C79407	217653 Entrez gene
1435306_a_at	Kif11	kinesin family member 11	16551 Entrez gene
1436186_at	E2f8	E2F transcription factor 8	108961 Entrez gene
1439695_a_at	Kif20b	kinesin family member 20B	240641 Entrez gene
1440924_at	Kif20b	kinesin family member 20B	240641 Entrez gene
1444319_at	E2f8	E2F transcription factor 8	108961 Entrez gene
1447363_s_at	Bub1b	budding uninhibited by benzimidazoles 1 homolog, beta (S. cerevisiae)	12236 Entrez gene
1449171_at	Ttk	Ttk protein kinase	22137 Entrez gene
1450157_a_at	Hmmr	hyaluronan mediated motility receptor (RHAMM)	15366 Entrez gene
1450692_at	Kif4	kinesin family member 4	16571 Entrez gene
1452314_at	Kif11	kinesin family member 11	16551 Entrez gene
1452315_at	Kif11	kinesin family member 11	16551 Entrez gene
1452459_at	Aspm	asp (abnormal spindle)-like, microcephaly associated (Drosophila)	12316 Entrez gene
1453748_a_at	Kif23	kinesin family member 23	71819 Entrez gene
1455990_at	Kif23	kinesin family member 23	71819 Entrez gene
1456280_at	Clspn	claspin homolog (Xenopus laevis)	269582 Entrez gene
1458447_at	Cenpf	centromere protein F	108000 Entrez gene

Lipopolysaccharide injections are known to stimulate the immune system, and have been shown to enhance axonal sprouting in injured spinal cords of rats (CITE Chen Q, Exp Neurol 2008). Trichostatin A3 is known to inhibit class I and II histone deacetylases and has been shown to differentiate neuro2a cells into neurons, which can form neural networks (Inokoshi et al., 1999) (cite Biochem Biophys Res Commun., Inokoshi J 1999).

The second clustering was performed in order to find subsets of the 166 downregulated genes, which were upregulated after specific stimuli in other experiments. This analysis showed that a cluster of 21 genes from our list, represented by 31 probesets, was upregulated after 4 different types of stimulations: 2 experiments involving 1-fluoro-2,4 dinitrobenzene, one involving ovalbumin, and one, in which a combination of ovalbumin and particulate matter was used. These 21 genes are therefore downregulated in our experiment, but upregulated after the 4 stimuli mentioned above. The list of the clustered probesets and their corresponding genes can be seen in Table 16, and the clusters can be seen in Figure 12 B.

Table 16: Bi-clustering analysis of the 166 downregulated genes. 31 clustered probesests, which are all upegulated after the 1-fluoro-2,4 dinitrobenzene, 1-fluoro-2,4 dinitrobenzene 2, ovalbumin, and ovalbumin / particulate matter stimuli.

Probe Set ID	Gene Symbol	Gene Title	Entrez Gene ID
1415945_at	Mcm5	minichromosome maintenance deficient 5, cell division cycle 46 (S. cerevisiae)	17218 Entrez gene
1416961_at	Bub1b	budding uninhibited by benzimidazoles 1 homolog, beta (S. cerevisiae)	12236 Entrez gene
1417256_at	Mmp13	matrix metallopeptidase 13	17386 Entrez gene
1417910_at	Ccna2	cyclin A2	12428 Entrez gene
1417911_at	Ccna2	cyclin A2	12428 Entrez gene
1420394_s_at	Gp49a	glycoprotein 49 A	14727 Entrez gene
	Lilrb4	leukocyte immunoglobulin-like receptor, subfamily B, member 4	14728 Entrez gene
1422016_a_at	Cenph	centromere protein H	26886 Entrez gene
1422814_at	Aspm	asp (abnormal spindle)-like, microcephaly associated (Drosophila)	12316 Entrez gene
1422944_a_at	Diap3	diaphanous homolog 3 (Drosophila)	56419 Entrez gene
1422978_at	Cybb	cytochrome b-245, beta polypeptide	13058 Entrez gene
1424046_at	Bub1	budding uninhibited by benzimidazoles 1 homolog (S. cerevisiae)	12235 Entrez gene
1424118_a_at	Spc25	SPC25, NDC80 kinetochore complex component, homolog (S. cerevisiae)	66442 Entrez gene
1424278_a_at	Birc5	baculoviral IAP repeat-containing 5	11799 Entrez gene
1427161_at	Cenpf	centromere protein F	108000 Entrez gene
1429172_a_at	Ncapg	on-SMC condensin I complex, subunit G	54392 Entrez gene
1434767_at	C79407	expressed sequence C79407	217653 Entrez gene
1435306_a_at	Kif11	kinesin family member 11	16551 Entrez gene
1436186_at	E2f8	E2F transcription factor 8	108961 Entrez gene
1436778_at	Cybb	cytochrome b-245, beta polypeptide	13058 Entrez gene
1436779_at	Cybb	cytochrome b-245, beta polypeptide	13058 Entrez gene
1436808_x_at	Mcm5	minichromosome maintenance deficient 5, cell division cycle 46 (S. cerevisiae)	17218 Entrez gene
1439695_a_at	Kif20b	kinesin family member 20B	240641 Entrez gene
1440924_at	Kif20b	kinesin family member 20B	240641 Entrez gene
1447363_s_at	Bub1b	budding uninhibited by benzimidazoles 1 homolog, beta (S. cerevisiae)	12236 Entrez gene
1449366_at	Mmp8	matrix metallopeptidase 8	17394 Entrez gene
1452314_at	Kif11	kinesin family member 11	16551 Entrez gene
1453748_a_at	Kif23	kinesin family member 23	71819 Entrez gene
1455990_at	Kif23	kinesin family member 23	71819 Entrez gene
1456280_at	Clspn	claspin homolog (Xenopus laevis)	269582 Entrez gene
1458374_at	C79407	expressed sequence C79407	217653 Entrez gene
1460218_at	Cd52	CD52 antigen	23833 Entrez gene

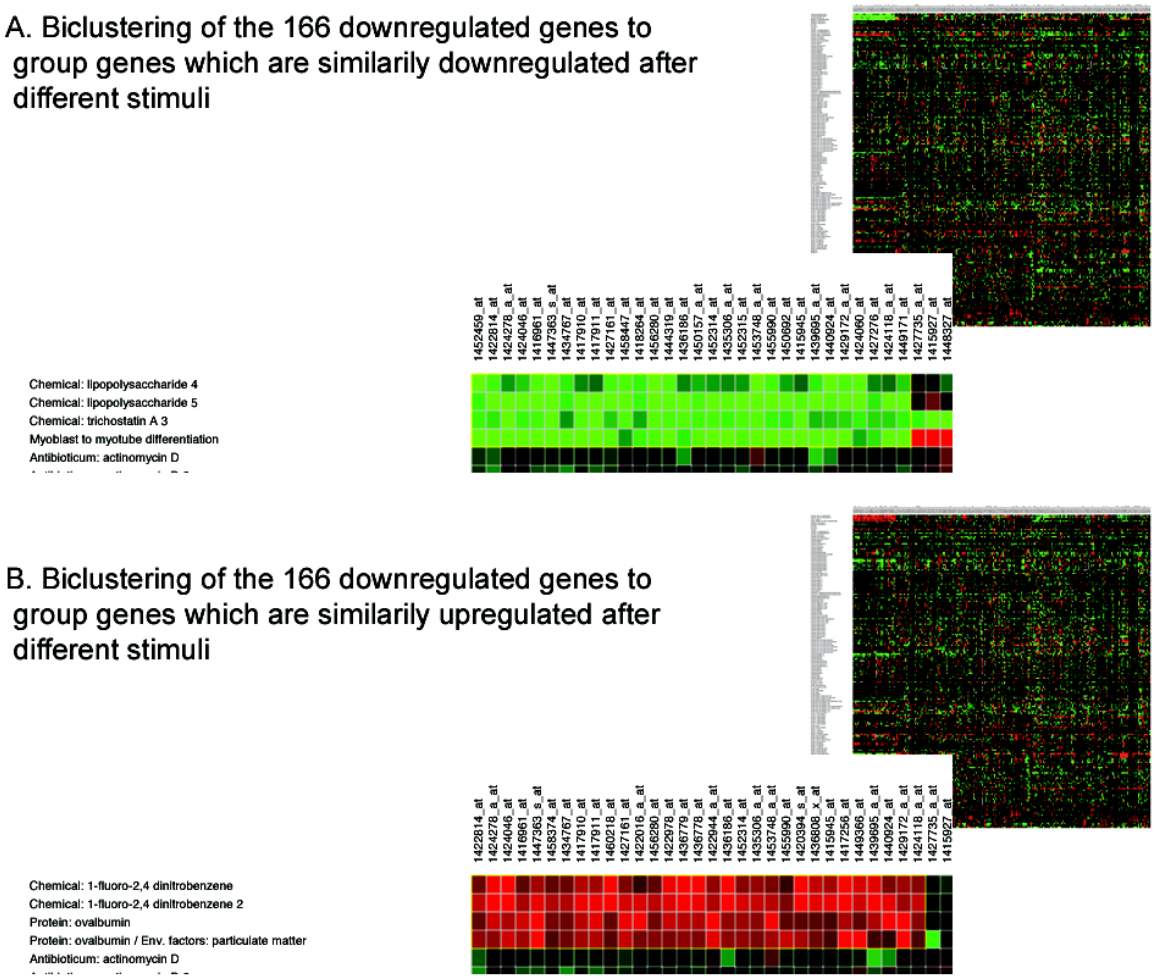

Figure 12: Bi-clustering meta-analysis of the 166 genes with more than 3 downregulated exons in the spinal cords of the operated animals. The list of genes was clustered according to the "stimulus" criteria in Genevestigator, and two searches were perormed. **A**. Clustering in order to find subsets of the 166 genes list, which are downregulated after specific stimuli. 29 probesets, corresponding to 21 genes are similarily downregulated in after Lipopolysaccharide 4, Lipopolysaccharide 5, Trichostatin A3, myoblast to myotubule differentiation. **B.** Clustering in order to find subsets of the 166 genes list, which are upregulated after specific stimuli. 31 probesets, corresponding to 21 genes are similarily upregulated in after 1-fluoro-2,4 dinitrobenzene, 1-fluoro-2,4 dinitrobenzene 2, ovalbumin, and ovalbumin / particulate matter stimuli.

2.7.2.2 Bi-clustering analysis of the upregulated genes

The 96 genes, which had at least 3 upregulated exons in our microarray analysis, were clustered according to the criteria "Stimulus". The first clustering consisted in finding subsets from this gene list, which were downregulated after specific stimuli in other experiments. The analysis revealed that a cluster of 19 probesets representing 17 genes, which were upregulated in our experiment, was downregulated after a chemical stimulation with 1.5-naphtalenediamine 2 and with N-(1-naphthyl)ethylenediamine dihydrochloride 2. The list of the clustered probesets and their corresponding genes can be seen in Table 17. The clusters can be seen in Figure 13 A.

Table 17: Bi-clustering analysis of the 96 upregulated genes. 19 clustered probesests, which are all downregulated after the Chemical 1.5-naphtalenediamine 2 and N-(1-naphthyl)ethylenediamine dihydrochloride 2 stimuli.

Probe Set ID	Gene Symbol	Gene Title	Entrez Gene ID
1418912_at	Plxdc2	plexin domain containing 2	67448 Entrez gene
1419271_at	Pax6	paired box gene 6	18508 Entrez gene
1420557_at	Epha5	Eph receptor A5	13839 Entrez gene
1421929_at	Epha4	Eph receptor A4	13838 Entrez gene
1422162_at	Dcc	deleted in colorectal carcinoma	13176 Entrez gene
1425840_a_at	Sema3f	sema domain, immunoglobulin domain (Ig), short basic domain, secreted, (semaphorin) 3F	20350 Entrez gene
1425960_s_at	Pax6	paired box gene 6	18508 Entrez gene
1427307_a_at	Dab1	disabled homolog 1 (Drosophila)	13131 Entrez gene
1430698_a_at	Pibf1	progesterone immunomodulatory binding factor 1	52023 Entrez gene
1431675_a_at	Gtf2i	general transcription factor II I	100044121 Entrez gene
	LOC100044121	similar to transcription factor TFII-I-gamma	14886 Entrez gene
1431680_a_at	Ptprk	protein tyrosine phosphatase, receptor type, K	19272 Entrez gene
1436904_at	Med13	mediator complex subunit 13	327987 Entrez gene
1439757_s_at	Epha4	Eph receptor A4	13838 Entrez gene
1448955_s_at	Cadps	Ca2+-dependent secretion activator	27062 Entrez gene
1449958_a_at	Fgf14	fibroblast growth factor 14	14169 Entrez gene
1451898_a_at	Sema6c	sema domain, transmembrane domain (TM), and cytoplasmic domain, (semaphorin) 6C	20360 Entrez gene
1455258_at	Kcnc2	potassium voltage gated channel, Shaw-related subfamily, member 2	268345 Entrez gene
1455266_at	Kif5c	kinesin family member 5C	16574 Entrez gene

N-(1-naphthyl)ethylenediamine dihydrochloride 2 is used in research to measure Nitric Oxide concentrations (Ignarro et al., 1987). Nitric oxide has been shown to be a vasodilatator, but recent studies have also shown, that it has a role in cell proliferation, neuronal motility and synaptic maturation (Tegenge and Bicker, 2009).

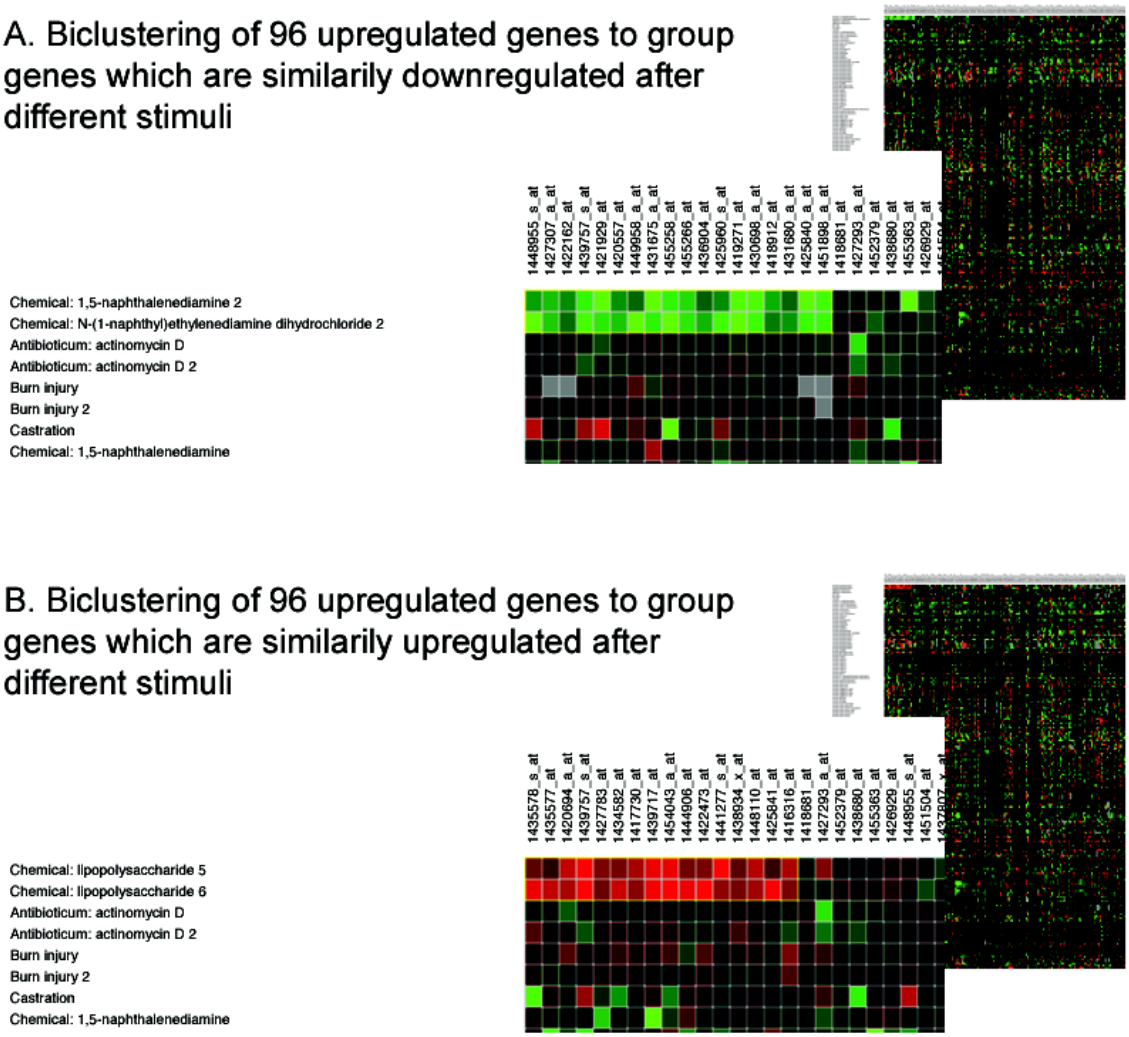

Figure 13: Bi-clustering meta-analysis of the 96 genes with more than 3 upegulated exons in the spinal cords of the operated animals. The list of genes was clustered according to the "stimulus" criteria in Genevestigator, and two searches were perormed. **A**. Clustering in order to find subsets of the 96 genes list, which are downregulated after specific stimuli. 19 probesets, corresponding to 17 genes are similarily downregulated in after 1.5-naphtalenediamine 2 and N-(1-naphthyl)ethylenediamine dihydrochloride 2 stimulations. **B.** Clustering in order to find subsets of the 96 genes list, which are upregulated after specific stimuli. 17 probesets, corresponding to 15 genes are similarily upregulated after lipopolysaccharide 5 and lipopolysaccharide 6 stimulations.

Another clustering was performed in order to find, which subset of the 96 upregulated genes was also upregulated after specific stimuli in other experiments. This analysis showed, that 17 probesets, corresponding to 15 genes were upregulated in our experiment, but also after stimulations with Lipopolysaccharide 5 and 6. Lipopolysaccharides are known to trigger inflammation, and have been shown to allow axonal sprouting in injured rat spinal chords (Chen et al., 2008). The list of the clustered probesets and their corresponding genes can be seen in Table 18. The clusters can be seen in Figure 13 B.

Table 18: Bi-clustering analysis of the 96 upregulated genes. 17 clustered probesests, which are all upregulated after Lipopolysaccharide 5 and Lipoplysaccharide 6 stimuli.

Probe Set ID	Gene Symbol	Gene Title	Entrez Gene ID
1416316_at	Slc27a2	solute carrier family 27 (fatty acid transporter), member 2	26458 Entrez gene
1417730_at	Ext1	exostoses (multiple) 1	14042 Entrez gene
1420694_a_at	Dach1	dachshund 1 (Drosophila)	13134 Entrez gene
1422473_at	Pde4b	phosphodiesterase 4B, cAMP specific	18578 Entrez gene
1425841_at	Slc26a7	solute carrier family 26, member 7	208890 Entrez gene
1427783_at	Erbb4	v-erb-a erythroblastic leukemia viral oncogene homolog 4 (avian)	13869 Entrez gene
1434582_at	Erc2	ELKS/RAB6-interacting/CAST family member 2	238988 Entrez gene
1435577_at	Dab1	disabled homolog 1 (Drosophila)	13131 Entrez gene
1435578_s_at	Dab1	disabled homolog 1 (Drosophila)	13131 Entrez gene
1438934_x_at	Sema4a	sema domain, immunoglobulin domain, transmembrane domain and short cytoplasmic domain,	20351 Entrez gene
1439717_at	Gabrg3	gamma-aminobutyric acid (GABA-A) receptor, subunit gamma 3	14407 Entrez gene
1439757_s_at	Epha4	Eph receptor A4	13838 Entrez gene
1441277_s_at	Ptprk	protein tyrosine phosphatase, receptor type, K	19272 Entrez gene
1444906_at	LOC100048050	similar to calcium-independent alpha-latrotoxin receptor homolog 2	100048050 Entrez gene
	Lphn2	latrophilin 2	99633 Entrez gene
1448110_at	Sema4a	sema domain, immunoglobulin domain, transmembrane domain and short cytoplasmic domain,	20351 Entrez gene
1454043_a_at	Kcnab1	potassium voltage-gated channel, shaker-related subfamily, beta member 1	16497 Entrez gene

2.7.3 Splice variant analysis

The GeneChip® Mouse Exon 1.0 ST Arrays show expression level changes of each exon of the murine genome. It is therefore possible to monitor which genes show alternative splicing events. The genes, for which the fold changes of all the exons have a high standard deviation, are likely to be subjected to splicing events.

To monitor which genes are differentially spliced between the operated mice and the control mice among the 37000 most significantly regulated probesets, the standard deviation of the various signals obtained for each gene was calculated, after exclusion of unspecific intronic or intergenic probesets, which add artefactual variability. This procedure led to a list of 1310 genes, which can be seen in Appendix 7, along with their Ensembl Gene identifier and their standard deviation. Among these genes, 389 were known registered in Ensemble as sequences encoding unknown proteins, and 59 were only defined with their Riken gene identifiers. The threshold, at which the standard deviation of the signals was considered as a significant indicator of alternative splicing events, was set at 0.4. The genes, which had a higher standard deviation than the threshold, were selected, and a list of 410 genes was established. This list corresponds the first 410 genes of Appendix 7.

An analysis on the g:Profiler software was carried in order to gain more information about the 410 genes, which showed alternative splicing events. This software allows to group subsets from a gene list, according to their described biological functions. Table 19 lists the functions in which the genes, which have spice variants in our microarray experiment, are involved in.

Most of the differentially spliced genes between the spinal cords of the operated mice and the ones of the controls are involved in catalytic activity (152 genes), are proteins from the plasma membrane (85 genes) or have a

hydroxylase activity (85 genes). Another high proportion of genes are involved in nucleotide binding or ATP binding.

In accordance with what was observed for the genes, which have more than 3 up or down regulated exons, many functional categories, which regroup up to 39 genes, are linked to cell adhesion, extracellular matrix, cytoskeleton, and actin or myosin contraction. This tends to show, that cellular motility, which might be either linked to inflammation, or to synaptic rearrangements takes place, and involves various splice variants of specific genes. For instance, the microarray experiment reported signals with a standard deviation of 1.25 for Semaphorin 3F. This gene is involved in axonal guidance, and has splice variants, which are involved in a temporal and regional regulation during the maturation of the murine CNS (Kusy et al., 2003).

Table 18: Functional grouping of the genes, which have different alternative splicing events in the spinal cords of the operated and the control animals.

Functional Category	Total number of genes in the specific category	Category Domain	Number of analyzed genes which belong to this category	P Value
catalytic activity	5817	Molecular Function	152	2.66E-05
plasma membrane	2761	Cell Component	85	1.45E-05
hydrolase activity	2568	Molecular Function	85	8.08E-07
non-membrane-bounded organelle	2245	Cell Component	75	3.06E-06
intracellular non-membrane-bounded organelle	2245	Cell Component	75	3.06E-06
nucleotide binding	2257	Molecular Function	73	1.33E-05
purine nucleotide binding	1967	Molecular Function	68	3.09E-06
ribonucleotide binding	1882	Molecular Function	66	2.74E-06
purine ribonucleotide binding	1882	Molecular Function	66	2.74E-06
adenyl nucleotide binding	1638	Molecular Function	65	4.12E-08
adenyl ribonucleotide binding	1553	Molecular Function	63	3.09E-08
ATP binding	1529	Molecular Function	62	4.12E-08
protein complex	1817	Cell Component	61	2.64E-05
cytoskeleton	1231	Cell Component	58	5.54E-10
organ development	1555	Biological Process	56	8.20E-06
plasma membrane part	1375	Cell Component	55	4.17E-07
calcium ion binding	959	Molecular Function	53	1.08E-11
transmembrane transporter activity	1052	Molecular Function	41	2.60E-05
biological adhesion	674	Biological Process	39	2.03E-09
cell adhesion	674	Biological Process	39	2.03E-09
cytoskeletal part	786	Cell Component	37	9.89E-07
MI:mmu-miR-466b-5p	1059	miRBase	37	7.57E-05
MI:mmu-miR-466e-5p	1054	miRBase	37	6.87E-05
system process	821	Biological Process	36	6.93E-06
MI:mmu-miR-324-3p	922	miRBase	33	1.20E-04
cytoskeletal protein binding	441	Molecular Function	32	2.59E-10
MI:hsa-miR-648	831	miRBase	31	9.21E-05
MI:mmu-miR-742	769	miRBase	31	2.18E-05
actin binding	306	Molecular Function	29	3.10E-12
actin cytoskeleton	278	Cell Component	23	8.05E-09
contractile fiber	90	Cell Component	23	1.51E-19
myofibril	85	Cell Component	23	3.63E-20
contractile fiber part	82	Cell Component	21	5.61E-18
sarcomere	77	Cell Component	21	1.34E-18
cell surface	305	Cell Component	20	3.07E-06
extracellular matrix	331	Cell Component	20	1.04E-05
proteinaceous extracellular matrix	317	Cell Component	20	5.48E-06
Muscle contraction	51	REACTOME	18	5.48E-16
Striated Muscle Contraction	51	REACTOME	18	5.48E-16
Release Of ADP From Myosin	51	REACTOME	18	5.48E-16
Calcium Binds Troponin-C	51	REACTOME	18	5.48E-16
Myosin Binds ATP	51	REACTOME	18	5.48E-16
ATP Hydrolysis By Myosin	51	REACTOME	18	5.48E-16
Focal adhesion	193	KEGG	17	3.23E-07
actin filament-based process	193	Biological Process	15	7.11E-06
actin cytoskeleton organization	181	Biological Process	14	1.51E-05
muscle system process	78	Biological Process	14	3.50E-10
muscle contraction	75	Biological Process	14	2.02E-10
I band	46	Cell Component	11	1.10E-09
myosin complex	62	Cell Component	11	3.17E-08
ECM-receptor interaction	80	KEGG	11	5.70E-07
striated muscle contraction	37	Biological Process	9	3.16E-08
Z disc	39	Cell Component	8	7.72E-07
actomyosin structure organization	31	Biological Process	7	1.93E-06
myosin II complex	18	Cell Component	7	2.92E-08
muscle myosin complex	16	Cell Component	7	1.08E-08
A band	10	Cell Component	6	1.12E-08
myosin filament	15	Cell Component	6	2.45E-07
striated muscle thick filament	15	Cell Component	6	2.45E-07
striated muscle cell development	20	Biological Process	5	3.54E-05
myofibril assembly	20	Biological Process	5	3.54E-05
Response to activity	7	Biological Process	4	4.99E-06
cardiac myofibril assembly	6	Biological Process	4	2.17E-06
striated muscle thin filament	10	Cell Component	4	2.86E-05
myosin light chain kinase activity	3	Molecular Function	3	7.63E-06

3. Discussion

3.1. Low-density microarray

3.1.1 Whole brain microarray experiments

The first protocol we established consisted in competitive hybridizations of a sample labeled with Alexa-555 (green) and a sample labeled with Alexa-647 (red). These experiments were performed to analyze whether it was possible to detect expression level changes between whole brains of operated and control mice (see chapter 5.2 for the protocol). To do so, we labeled all our experimental samples – whether from operated animals or controls – with Alexa-555 and a reference mouse brain aRNA with Alexa-647.

The data revealed a general bias towards the Alexa-555 signal, which particularly affected the genes with signals lower than 1000. This effect was observed regardless of whether the sample labeled in green was from an operated animal or from a control one (Figure 2). The quality of the hybridization was however very good, with mean background values below 50 as well as a good intraslide and interslides reproducibility between the replicates and the samples. To assess whether this bias came from a biological regulation, which could enhance the gene expression levels in the brain of handled animals compared to the reference naïve animals, we performed a dye swap experiment. On one slide, the hybridized sample contained equal amounts of brain19 aRNA, which was derived from an operated animal, and labeled with Alexa-555 and of reference mouse brain aRNA labeled with Alexa-647. On the other slide, the sample mixture had equal amounts of brain 16 aRNA labeled with Alexa-647, and of reference mouse brain aRNA labeled with Alexa-555. On both slides, the sample labeled with Alexa-555 had higher signals, which meant that this effect was due to a dye imbalance (Figure 4). Had the effect been caused by a generally higher genetic expression in the brain 19 sample, the second slide would have had higher Alexa-647 signals.

Such dye effects have been reported in previous studies (Dombkowski et al., 2004; Tseng et al., 2001; Yang and Speed, 2002). Dombkowski et al. have shown by performing dye swap experiments on comparisons of gene expression changes between cells from breast cancer tumors at various stages, that dye effects influence the results obtained on 2 color arrays. According to their results, the comparison of ratios of the Cy3/Cy5 signals, with the reference samples labeled with the same dye on all slides is not robust enough to bypass dye artifacts. They postulate that all genes do not incorporate dyes with the same efficiency, and that a same gene can incorporate dyes differently from one labeling reaction to another. This could explain the general dye biases, and the need for appropriate normalization protocols. (Dombkowski et al., 2004). Similar observations have been made in

studies using a custom-made microarrays to measure gene expression changes in bacteria. The authors attributed the dye discrepancies to different chemical stability, incorporation rates, and scanning efficiency for the two dyes (Tseng et al., 2001).

Our analysis of the raw data showed no significant gene expression differences between the expression levels in the brains of the operated and the control animals. To see whether this was due to the dye imbalance, we normalized our values using the locally weighed scatter plot smoothing (Loess) normalization, which is commonly used in the analysis of two color microarray data (Colantuoni et al., 2002; Workman et al., 2002; Yang et al., 2002). This method gives robust results in the normalization of gene datasets with more than 1000 genes (Chiogna et al., 2009). In order to be able to use this normalization, only a relatively small proportion of the genes has to show significant expression level differences between the two co-hybridized aRNA samples or there has to be symmetry in the expression levels of the up/down-regulated genes (Yang et al., 2002). This assumption cannot be true when less than 1000 genes are analyzed, and one has to be aware that the Loess normalization might give unreliable results in such a case. Given that our microarray had less than 1000 genes, this normalization was not optimal. On the scatter plots, it did seem to correct the dye imbalance, however no significant gene expression differences could be observed between the operated and the control animals. This experiment showed that this hybridization and normalization model was not suitable to detect relevant gene expression changes.

Another possible explanation for the lack of relevant differences is the fact that the analyses were carried out with RNA extracted from the whole brain. Gene expression profiles are not constant between the various parts of the brain (Hovatta et al., 2005; Nelson et al., 2006). This means that if a gene expression change occurs in one part of the brain, it might not be detected in a whole brain analysis, as normal expression levels in the rest of the brain could compensate the difference. Moreover, the integration of the noxious signal in the brain involves specific areas of the "pain matrix" as well as the regions, which activate the descending pathways such as the PAG-RVM in the brainstem (Albe-Fessard et al., 1985; Apkarian et al., 2005; Fields, 1985, 2000). We therefore decided to optimize the hybridization protocol to bypass all possible dye imbalances and to carry a more precise analysis of smaller parts of the central nervous system.

3.1.2 One-color model hybridization protocol validation

To bypass any dye imbalance, we developed a one-color microarray protocol in which all the samples were labeled with Cy5, and single hybridizations were performed separately. Although two color hybridization models are widely used for custom-made microarrays, hybridization with a

single color protocols with Cy5 have also been developed and used for other arrays such as the CodeLink Bioarrays (GE Healthcare) (Severgnini et al., 2006). The Affymetrix microarrays are all also based on a single-channel model. In order to test the relevancy of a single color hybridization protocol, a validation experiment was carried out.

The brain of 3 naïve NMRI was dissected, and hybridizations were performed to compare the expression levels differences between the hippocampus, the brainstem and the cortex. After the data acquisition, two analyses were performed: one on the raw data, and one on the data normalized according to a set of ubiquitously expressed positive control genes. The results obtained were compared with the ones obtained by Hovatta et al. in their microarray study on anxiety (Hovatta et al., 2005). In their study, they assessed the gene expression level differences between various parts of the brain in 6 inbred mice strains: A/J, 129S6/SvEvTac, C3H/HeJ, C57BL/6J, DBA/2J, and FVB/NJ, and made their data publically available in the GEO dataset n°: GDS1406. We compared the results we obtained before and after normalization with the results they obtained. We primarily focused on their measurements for the A/J strain, because our observations were highly similar to what they measured in this strain. We nevertheless also compared our data with what they had observed for the other strains they analyzed (see chapter 3.4).

When assessing whether the differentially expressed genes in our microarray experiments were also showing such expression level differences in the GDS 1406 GEO datasets for the A/J mouse strain, we obtained high levels of similarities. We first considered the raw data, and observed that 73% of the genes, which were differentially expressed between the cortex and the brainstem according to our results, had similar expression level differences on the GDS1406 data. In this experiment only two genes showed different regulations across the two platforms: Pomc and the serotonin receptor 5HTr5B, which were both more expressed in the brainstem according to our data (Figure 9 and Table 5). In the comparisons between the brainstem and the hippocampus, 90% of the genes, which were regulated on the microarray showed similar regulations on the GEO datasets, with only one gene behaving differently on the two platforms: Par1, the proteinase-activated receptor 1 (Figure 10 and Table 7). When considering the comparisons between the hippocampus and the cortex, on both platforms the similarity was somewhat lower. Indeed, 57% of the regulated genes on the one-color microarray model showed a similar behavior. In fact, out of the 14 differentially expressed genes on the microarray, only 3 had different regulations on both platforms, but two other genes were not analyzed on the GDS1406 dataset, and one gene was a control gene (Figure 11 and Table 9).

The analysis of the regulations observed on the GDS1406 A/J strain dataset for the differentially expressed genes on our microarray after normalization revealed even higher similarities. In the brainstem against cortex hybridizations, 100% of the differentially expressed genes in our experiment

behaved the same way on the GEO set (Table 6). For the brainstem against hippocampus analysis, 88.9% of the differentiated genes behaved the same way on both platforms. Only two genes had a different expression profile: Par1 and the heat shock 70kD protein 5, which were more expressed in the brainstem according to our data, but were not differentially expressed in these two parts of the brain on the GDS1406 dataset (Table 8). For the hippocampus vs. cortex hybridizations, 3 genes were differentially expressed in our experiment, and one of these genes, behaved differently on the GEO dataset: Neuropeptide Y. This brought the similarity between the two platforms for this experiment to 66.7% (Table 10).

We performed the same comparisons, with the data for the 5 other inbred strains analyzed in the GDS1406 dataset. The detailed comparison tables are listed in chapter 3.4 (Tables 5 to 10).

Overall, most of the gene expression level differences we observed between the cortex, brainstem and hippocampus could get confirmed in the analysis of the GDS1406 GEO dataset. The lowest similarity rates were observed mostly in the raw data of the hippocampus vs. cortex hybridization. This is due to the fact that two genes, which appeared to be differentially expressed in our microarray had not been analyzed in the GEO dataset, and that one gene of our microarray was a false positive.

The differences obtained with the normalized values had high similarity rates (between 66.7 and 100%) with the differences observed in the GDS1406 values. For the raw data, the similarity rates were ranged between 43 and 100%. The differences observed between our microarray data, and the GDS1406 data can partly be explained by the fact that different strains were analyzed on both platforms. NMRI mice are an outbred mice strain, whereas the A/J, 129S6/SvEvTac, C3H/HeJ, C57BL/6J, DBA/2J, and FVB/NJ are all inbred strains. The genetic background of these strains presents fundamental differences, which can influence gene expression profiles in the brain. This sometimes underlies strain specific behavioral phenotypes (Holmes, 2008). It has for instance been shown that BALB/cJ and DBA/2J inbred mouse strains that carry a specific mutation of the tryptophan hydroxylase type 2 (1473G allele of the Tph2 gene) exhibit significantly less serotonin expression in the frontal cortex and striatum compared to the C57BL/6J and 129X1/SvJ mice, which carry the 1473C allele of that gene (Hackler et al., 2006; Zhang et al., 2004). Such inter-strain differences could explain the variations we observe between the results obtained on our microarrays performed with material from outbred NMRI mice, and the results available on the GDS1406 dataset, which are derived from 6 different inbred strains.

Another explanation for the variation observed can be the fact that 2 different platforms were used to measure the gene expression differences. Our experiments were carried out on a custom made microarray, and the GEO set experiments from Hovatta et al, were performed on Affymetrix

Murine Genome U74 Version 2 arrays (Affymetrix, Inc.) A study performed by Hester et al. addressed this issue of reproducibility of microarray data across various platforms. They studied the detection efficiency of 3 genomic DNA amplifications and 5 deletions in the genome of HL-60 leukemia cells on 6 different platforms: Agilent, Affymetrix 500K, Affymetrix U1333 Plus 2.0, Illumina and RPCI 19K Bac arrays. Their results showed that although all the platforms detected the genetic modifications, only two of the five tested platforms were able to detect 10 other new genetic modifications (Hester et al., 2009). These differences of detection could be attributed to different sensitivities of the probes, as well as the different normalization procedures.

Considering the fact that our protocol was able to detect gene expression changes, which could be in majority confirmed on a different platform and in different mouse strains, we could conclude that our hybridization protocol was able to detect relevant expression level changes in the central nervous system. Our analysis showed that the data normalized according to the set of positive control genes had higher similarity rates with the GDS1406 data, but the raw data also mainly detected expression changes, which could be confirmed in the comparison. Therefore, a dual analysis of both the raw and normalized data obtained with our microarray leads to relevant results.

3.1.3 Microarray experiments on specific regions of the central nervous system

The one-color hybridization protocol was followed to detect gene expression changes in the cortices, brainstems, hippocampi, cerebelli and spinal cords between 3 operated mice, and 3 controls. In the cortex and in the hippocampus analysis, no difference could be detected with the raw or on the normalized values.

3.1.3.1 Microarray experiments on the brainstem

In the analysis of the raw signals in the brainstem, one gene was 1.5 times upregulated in the operated animals: Neuropeptide receptor type 5 (Npy5r) (Table 2a). However, Real-Time PCR measurements could not confirm this overexpression. According to published histological studies performed on rats, the Npy5r is widely expressed in the brain. In the brainstem, it is particularly present in the Edinger-Westphal nucleus, the locus coeruleus and the mesencephalic trigeminal nucleus (Grove et al., 2000). Further studies on axotomized rats have shown that the Neuropeptide Y expression increases in the mesencephalic trigeminal suggesting that this Neuropeptide Y and it receptors could have a role in pain processing by the brainstem (Arvidsson et al., 1994).

The results obtained with the normalized signals showed that 6 genes were more expressed in the brainstems of the operated mice, but could not be

confirmed by Real-Time PCR (Table 2b). Amongst them, 2 were control genes, which were obviously false positives. Two genes from the vanilloid receptors family showed a 1.5 times higher expression in the brainstems of the control animals: TrpV5, and VR1, and two genes from the serotonergic system also: 5Htr6 and 5Htr4.

The transient receptor potential vanilloid channel 5 plays an important role in Ca^{2+} homeostasis, and has been shown to be implicated in many cellular functions such as the regulation of cytoskeleton binding proteins, transcriptional control, and modulation of surface receptors in the blood and immune system cells (Semenova et al., 2009). Real-Time PCR studies performed in Balb/c mice have revealed that TrpV5 is mostly expressed in the lung and the kidney but it is also expressed in the brain. However more studies would be needed to identify the role of this gene in pain processing (Kunert-Keil et al., 2006). The VR1 receptor is commonly known as the noxious heat receptor at the periphery, however patch clamp recordings performed in rats have shown that VR1 receptors are expressed in the paraventricular nucleus, where they activate glutamatergic synaptic inputs (Li et al., 2004).

No studies have identified a precise expression of the 5HTr4 serotonin receptor in the brainstem, however, it has been shown by immunocytochemistry combined with a yeast-2 hybrid system assay, that this receptor is expressed in the striatum, the cortex, the amygdala and the hippocampus, and interacts with P11, a protein, which has been shown to have antidepressant properties (Warner-Schmidt et al., 2009). Similarly, recent clinical studies on polymorphisms of the 5HTr6 receptors have shown its implication in major depressions (Illi et al., 2009). Taken together with the downregulations we observed on our microarray results, one could postulate that a downregulation of these 2 receptors in the brainstems of the operated mice could be indicative of a depressive state linked to the post-operative pain.

3.1.3.2 Microarray experiments on the cerebellum.

The raw data obtained on the microarray comparisons of the cerebelli the 3 operated mice and the 3 control ones revealed that 17 genes were differentially expressed (Table 3a), among which 15 were upregulated and 2 were downregulated in the operated animals. Among the upregulated genes, the neuropeptide Y receptor Npy5r is 4 times more expressed in the operated animals. Interestingly, in the analysis of the normalized signals in the cerebellum, only one gene showed a differential expression between the operated and the control animals: the neuropeptide receptor type 6 Npy6r, which appeared to be 5.5 times more expressed in the operated animals (Table 3b). However all these genes appeared unchanged, when a real-time PCR analysis was performed on the same samples. The fold changes observed on the microarray could therefore not be confirmed.

While Npy5r has been shown to play a role in appetite as well as seizures (Lin et al., 2004), Npy6r has been identified in mice, but no real studies have shown its function in the brain. In general, neuropeptide receptors, especially Npy1r, have been shown to have an anxiolytic effect when activated (Lin et al., 2004). This could be the case in our study too. Indeed, the cerebellum is not only involved in motor processes, but also in emotional and behavioral ones (Bloedel and Bracha, 1997), and behavioral studies have shown an increase of exploratory behavior after a low anxiolytic dose of diazepam in the ANT rat line that carries a natural point mutation in a cerebellum-specific GABAA receptor subunit making their motor behavior abnormally sensitive to benzodiazepine agonists (Vekovischeva et al., 1999). This tends to show that the cerebellum is also involved in anxiety and fear. The upregulation of Npy6r that is observed in the cerebelli of the operated animals could therefore be linked to anxiety.

Interestingly, the sodium- and chloride-dependant GABA transporter 1 (Slc6a1) showed a 2 times higher expression in the cerebelli of the operated animals according to the raw data (Table 3A). This could be a further indication of an anxiolytic effect. Indeed, Slc6a1 knockout mice have reduced rates of GABA clearance in the synapses of the cerebellum, which lead to slower decay of spontaneous inhibitory post-synaptic currents in cerebellar granule cells. This causes motor disorders, gait abnormality, tremor and anxiety, as evidenced by lower percentages of inhibition in the prepulse inhibtion test for the knockout animals (Chiu et al., 2005). The upregulation of Slc6a1 in the cerebelli of the operated animals could therefore have a calming effect on mice in their post-operative phase.

The α_{2C} adrenergic receptor showed a 1.8 times higher expression in the cerebelli of implanted mice (Table 3a). This could be due to some impaired locomotor activity in the recovery phase. Schambra et al. have shown by in-situ hybridization, that adrenergic receptors are expressed in the human cerebellum (Schambra et al., 2005). In the rat, α_{2C} adrenergic receptor is more precisely present in nuclei, which are involved in motor function (Scheinin et al., 1994).

The serotonin recetptor 5-HTr4 was 1.7 times downregulated in the animals, which underwent surgery. No study has focused on the expression pattern of this receptor in the cerebellum. However, it has been shown pharmacologically and by histochemistry on primary mouse neuron cultures, that the activation of this receptor activates the ERK pathway by a G-coupled protein-independent mechanism (Barthet et al., 2007). Interestingly, Mapk1 is 2.1 times more expressed in the operated animals according to our microarray data, which indicates this pathway might be also active in the pain processes. Moreover, CREB3 is also 1.7 times less expressed in the operated animals. Western blot analysis performed with protein extracts from mice cerebellar neurons have shown the activation of GABAB receptor leads to Mapk1 phosphorylation, which in turn induces the activation of CREB (Tu et

al., 2007). Taken together, this data shows that these genes are present in the cerebellum, and the regulations observed on the microarray could indicate that these pathways are also active in the postoperative phase in our surgical pain model.

3 other genes were upregulated in the operated animals were the NMDA1 receptor, the Somatostatin Receptor 1, the Cytochrome P450, and the guanine nucleotide binding protein $\alpha 0$. Electrophysiological studies on Guinea Pig cerebellar slices have shown that anandamid, an endogenous ligand of cannabinnoid receptors, can modulate the activity of NMDA1 receptors, by eliciting a reduced cannabinoid-induced Ca^{2+} flux. This process could be involved in pain modulation (Hampson et al., 1998). Interestingly, NMDA glutamate receptors and Ca^{2+} fluctuation control granule cell migration during the cerebellar development, a process which is accelerated by endogenous somatostatin (Yacubova and Komuro, 2003). However, no study has ever shown the role of somatostatin and its receptor in pain processing. The role of Cytochrome P450 in the cerebellum has also not been widely studied, but gene profiling experiments have shown that it is expressed in the human cerebellum, where it could be linked to anandamide signaling and possibly to pain modulation through the cannabinoid receptors (Stark et al., 2008). Another player in the cannabinoid mediated pain modulation might be the guanine nucleotide binding protein $\alpha 0$. While no studies have shown that this protein is linked to pain in the mouse brain, in situ hybridization on the brain of rats, which had received an injection of a synthetic cannabinoid receptor ligand, have shown that this treatment led to decreased levels of guanine nucleotide binding protein $\alpha 0$ in the cortex, and of guanine nucleotide binding protein $\alpha 1$ in the cerebellum (Rubino et al., 1997).

The two last upregulated genes in the cerebellum of the mice in pain were the coagulation factor II receptor-like 2 (F2rl2), proopiomelanocortin and NGF. No data could be found on the role of F2rl2 in the cerebellum, and more studies could possibly be done to verify whether this gene is expressed in the cerebellum and whether it plays a role in nociception. While no real experiments have demonstrated the role of cerebellar NGF levels and pain, it has been demonstrated that high levels of NGF are linked to neuronal survival in the central nervous system and can induce hyperalgesia (Seidel et al., 2009).

The microarray analysis of the raw data showed that the proopiomelanocortin gene is 1-7 times more expressed in the cerebelli of unoperated animals. Although no articles have demonstrated a real involvement in cerebellar melanocortin levels and pain, it has been published, Crhr1 receptor to ACTH is expressed in the cerebellum and that ACTH knockout mice exhibit reduced anxiety behaviors (Timpl et al., 1998). Therefore, the lower expression observed in the cerebelli of the mice in pain seems somewhat surprising, given that these mice should be experiencing

more anxiety than the control ones. This data was not verified by real-time PCR, due to unsufficient extracted material. These observations therefore still remain to be validated.

3.1.3.3 Microarray experiments on the spinal cords.

The microarray analysis performed on the spinal cords of the operated and control animals revealed that 6 genes were downregulated in the operated animals according to the raw data (Table 4a), and 3 only according to the normalized values (Table 4b). However, the fold changes observed were very high. They ranged between 245.1 and 1488.1 for the raw values, and between 18.3 and 61.7 for the normalized ones. Such high fold changes are quite untypical for microarray results, and given the poor quality of the scatter plots, we concluded that these differences were artefactual and insignificant. We however decided to perform a more detailed analysis of the possible gene regulations in the spinal cord using GeneChip® Mouse Exon 1.0 ST Arrays from Affymetrix in the final part of this project.

3.1.4 General conclusions, low density microarray experiments

Although the microarray analyses gave the results described above, none of them could be validated by Real-Time PCR. This means that at least a proportion of these changes were artefactual. Another explanation could be that the regulated genes actually underwent some alternative splicing events, and that the exon to which the microarray probes hybridized were differently regulated than the ones which are amplified in the Real-Time PCR reaction. However, it seems quite doubtful that alternative splicing events would happen in all the regulated genes from our microarray experiments.

Preliminary experiments had been made before starting this project (Cinelli et al., 2006). A first batch of low-density microarray had been produced with 130 genes, to test hybridization conditions and detect whether signals could be detected. For these experiments, the slides were spotted by Operon AG, according to a proprietary spotting protocol, and a similar 2-color hybridization model had been followed, with Cy3 and Cy5 dyes instead of Alexa dyes. This experiment compared the brains of 3 implanted mice with the brains of 3 control mice. The analysis of the raw signals detected expression level differences, but these differences were never confirmed by Real-Time PCR, and had not been reproduced. Our project was started to study at a deeper level whether some gene regulations associated to nociception could be detected in the central nervous system, reproduced across platforms, and used to build a diagnostic tool to monitor pain. Our data obtained with 2 different hybridization protocols as well as on Real-Time PCR shows that the signal differences detected in the preliminary phase of this project were probably artefactual. Indeed, microarray is a sensitive technique, and hybridization can give artefactual results if the GC content of the probes varies strongly from one probe to the other. Moreover, cross

hybridization problems can also influence the results. Normalizing the data and performing Real-Time PCR for the differentially expressed genes according to the microarray is an essential step in the validation of an experiment. Our microarray data as well as the subsequent real-time PCR data have shown that no expression changes could be reliably used for a diagnostic based on the microarray we had developed and on the models that we had studied.

3.2. Real-Time PCR measurements on 27 candidate genes

Given that the microarray results could not be confirmed in the Real-Time PCR measurements, we chose to test whether our microarray was not sensitive enough to detect some changes, which might indeed be happening. We therefore selected the most promising 27 genes of our list. These genes were characteristic members of the various gene categories present on our slide. The sample sizes were increased to 6 animals per condition for statistical robustness. The experiments on the telemetric apparatus implantation surgical pain model were carried out in four parts of the central nervous system: the brainstem, the cortex, the hippocampus, and the dorsal root ganglia.

In the surgical pain model, only one of the observed gene expression differences was statistically significant. The serotonin receptor 5-HTr1A was 2.2 times more expressed in the cortices of the operated mice (P Value=0.12) (Table 11B and Figure 12B). It has been shown that this gene is expressed in axon terminals of the serotoninergic neurons, where it acts as an autoreceptor. Experiments on rat striatum slices have shown that serotonin stimulates the 5-HTr1A receptor and thereby induces an activation of the cholinergic system, which is responsible for antinociception (Galeotti et al., 1997; Gillet et al., 1985). 5HT1A receptors have been identified in the superficial laminae of the spinal dorsal horn, the dorsal and medial raphe nuclei, limbic areas of the hippocampus and lateral septum, and in the cortex as well (Barnes and Sharp, 1999). Our data therefore suggests that the significant increase observed in the operated animals is caused by central analgesic mechanism activation to mediate the postoperative pain.

To see if the genes showed more expression level differences in another pain model, we performed similar Real-Time PCR measurements on central nervous system RNA from the mice subjected to the BHV-1 inflammatory pain model. In this round of experiments, we compared the expression levels in cortices and spinal cords of 6 immunized and 6 control animals. None of the genes tested showed a significant expression level difference in these parts of the central nervous system in this pain model.

Taken together, the microarray and Real-Time PCR data showed that the vast majority of the commonly defined pain and anxiety genes do not show any expression level changes in the central nervous system and can therefore not

be used to monitor nociception for an objective diagnosis of pain. Most of the data on these genes comes from studies on transgenic animals (Lacroix-Fralish et al., 2007), but the fact that a pain-related phenotype is observed in a knockout animal for a specific gene does not necessarily mean that this gene will exhibit expression level changes in wt animals. The research on the transient receptor potential melastin 8 channel (TRPM8) is a good example of this problematic paradox in pain research. Although behavioral tests and electrophysiological measurements have demonstrated that this receptor is involved in the transmission of noxious cold, and that its activation disminishes the pain sensation linked to heat (Bautista et al., 2007; Colburn et al., 2007), no regulation in the expression levels of this gene after a noxious cold stimulation could be demonstrated in wt animals. However, it has been shown that knockout TRPM8$^{-/-}$ mice do not benefit from the analgesic effect associated with this receptor's activation after a formalin injection in the hindpaw (Dhaka et al., 2007), and based on these results this gene is considered as a "pain gene".

Our data has shown that the genes, which are commonly associated to pain processes based on the results of transgenic studies are not regulated in the central nervous system of wt mice subjected to a surgical or inflammatory pain models. This observation raises the question of the suitability of monitoring nociception by measuring gene expression changes. Indeed, the activation of a protein involved in the transmission of a nociceptive signal is not necessarily linked to a differential expression of the gene encoding it. On the other hand, it is possible that the common "pain genes" are not the ones which are regulated during the transmission of a nociceptive signal. To verify this hypothesis, further experiments have therefore to be performed to identify the genes, which are really regulated by nociception in the central nervous system and which could be good candidates for the monitoring of nociception in laboratory animals.

3.3 Whole Genome experiment on the spinal cord

No differential expression could be observed in the genes we selected for our study. Even if these genes had been established as being linked to a pain phenotype in transgenic animal models, our microarray and real-time PCR results have shown that they cannot be used to monitor nociception in the central nervous system of wt mice because their expression remains unaltered in the pain models we have studied. In order to observe which genes show a differential expression due to nociceptive processes and to find potential new genes, which would show a regulation linked the transmission of the nociceptive signal we performed a whole genome analysis.

Our experiment compared the spinal cords of 6 mice, which underwent the telemetric apparatus implantation with those of 6 control mice. We used GeneChip® Mouse Exon 1.0 ST Arrays for this analysis, to be able to detect not

only whole gene regulations, but also possible alternative splicing events. 63% of the regulations observed in the operated animals were downregulations, therefore, in the analysis of the whole gene regulations, the most significant 4000 downregulated probesets, and the 18000 most significant upregulated probesets were considered. We excluded the probesets, which had intronic or intergenic regulated sequences because they consist in undefined regions, which are located near an exon and could probably be regulated like this exon. However, they have not yet been defined as exons. We also excluded non-annotated sequences, which correspond to unknown putative probesets found bioinformatically. Among the first 4000 downregulated genes, 166 had a minimum of 3 downregulated exons. Among the first 18000 upregulated genes, only 96 had at least 3 upregulated exons. A search for the signals of the 230 genes, which we studied on the low-density microarray, confirmed that these genes do not show any expression level difference between the operated and the control mice. These genes are therefore not good candidates for the establishment of a microarray diagnostic tool for the monitoring of nociception in laboratory animals.

In order to identify which of these genes show similar regulations in other experimental conditions, we performed a bi-clustering meta-analysis using Genevestigator® (Nebion AG) on the 166 downregulated genes. The goal was to find which stimuli had induced either a downregulation or an upregulation of these genes in other experiments. The analysis of the downregulated genes revealed that 29 probesets corresponding to 21 genes were also downregulated in 4 different stimuli experiments: 2 experiments involving lipopolysaccharide stimulations, one with trichostatin A3 stimulation, and one consisting in myoblast to myotubule differentiation (Table 15 and Figure 12a). Lipopolysaccharide has been shown to enhance axonal sprouting in spinal cords of rats, after a lesion. This effect can even be seen in a lipopolysaccharide injection performed 4 months after the lesion (Chen et al., 2008). Trichostatine A3 is a cell cycle inhibitor, which deactivates class I and II histone deacetylases, and can be used with butyrolactone I to differentiate neuro2a cells into neurons capable of forming functional neural networks (Inokoshi et al., 1999). The fact, that the 21 of the genes, which had more than 3 downregulated exons in our microarray study were also downregulated following these stimulations, tends to show that processes linked to neuronal rearrangements were also happening in the spinal cords, during the post operative phase of our surgical pain model.

The clustering of the 166 downregulated genes, to find which stimulus had induced an upregulation of these genes, revealed that a cluster from 21 genes had been upregulated after 4 other experimental stimulations: two different experiments in which stimulations with 1-fluoro-2,4 dinitrobenzene (DNFB) were applied, one where ovalbumin was used, and one where a combination of ovalbumin and particulate matter was applied (Table 16 and Figure 12b). Both ovalbumin and 1-fluoro-2,4 dinitrobenzene are causing inflammation. ovalbumin is commonly used to study airway inflammation.

DNFB is known to induce inflammation and enhance contact hypersensitivity, and it has been postulated, that a key element in this process is the migration of dendritic cells to lymph nodes. This migration involves called plexins, which have a high similarity to semaphorins (Walzer et al., 2005). Interestingly, sproteins are essential keyplayers in axonal guidance.

The most interesting feature of this bi-clustering analysis is that the 21 genes are identical in both lists. This means that these 21 genes, which are amongst the 166 genes with more than 3 downregulated exons in the operated animals, are downregulated after the Lipopolysaccharide 4, Lipopolysaccharide 5, Trichostatin A3, myoblast to myotubule differentiation stimuli, and upregulated after the 1-fluoro-2,4 dinitrobenzene, 1-fluoro-2,4 dinitrobenzene 2, ovalbumin, and ovalbumin / particulate matter. All these stimuli involve cell migration, either in neurons, dendritic cells, or muscle cells. This tends to show, that these 21 genes are also involved in cell migration or cellular movements in the spinal cord of the mice used in our experiments, during the post-operative phase.

Two other clusterings were performed on 96 genes, which showed a complete upregulation in the spinal cords of the operated mice, to see which genes among these had been down- or up- regulated in previous stimulation experiments. The first clustering showed that a cluster of 17 genes represented by 19 probesets had been downregulated after a chemical stimulation with 1.5-naphtalenediamine and with N-(1-naphthyl)ethylenediamine dihydrochloride, which is usually used to measure nitric oxide concentration (Table 17 and Figure 13a). In the central nervous system, nitric oxide is involved in neuronal motility and synaptic formation. Indeed, in the human neuronal precursor cell line NT2, the use of a nitric oxide synthase inhibitor blocks migration, and on the contrary, the application of a nitric oxide donor or a cGMP analog, the migration is enhanced. This tends to show that the NO-cGMP-PKG signaling cascade is essential for the appropriate cell migration in the developing human brain (Ignarro et al., 1987; Tegenge and Bicker, 2009).

The clustering of the 96 upregulated genes to find subsets of genes, which were also upregulated in other experiments showed that 15 genes represented by 17 probesets were upregulated in 2 experiments using lipopolysaccharide as a stimulus (Table 18 and Figure 13b). As previously mentioned, lipopolysaccharide can induce axonal sprouting after an injury (Chen et al., 2008).

The comparison of the two lists obtained after the clustering revealed that 3 genes, which are upregulated in our experiment, are present in both clusters: the EPH receptor A 4 (Epha4), Disabled Homolog 1 (Dab1), and Protein Tyrosine Phosphatase Receptor type K (Ptprk). Epha4 has been shown to be involved in adult neurogenesis, and soluble versions of Ptprk are known stimulate neurite outgrowth (Drosopoulos et al., 1999). Dab1 is a key member

of the Reelin-Dab1 pathway. This pathway regulates neuronal positioning during development, and has recently been shown to differentially contribute to acute and persistant pain (Akopians et al., 2008). Interestingly, our microarray also revealed that Reelin was downregulated in the spinal cords of the operated mice. Taken together, these results tend to show that the Dab1-Reelin pathway is also activated in the spinal cord of these animals.

The final part of the analysis consisted in finding which categories of genes were exhibiting alternative splicing events in the spinal cords of the operated animals. To do so, we calculated the standard deviations of all the probe signals for each of the top 37000 probesets were calculated. After exclusion of the non-annotated sequences, as well as the genes, which contained intergenic and intronic probesets, we obtained a list of 1310 probesets. From this list, we selected the genes for which, the standard deviation of the signals was higher than 0.4, and we obtained a final list of 410 probesets, which showed alternative splicing events. A functional profiling analysis revealed that the main roles of these genes were catalytic, and hydroxylase activities. 20,7% of these genes, were plasma membrane proteins, and interestingly, 10% of the alternatively spliced genes were linked to cell adhesion, cytoskeleton, actin, and myosin contraction. This tends to show, that cellular motility, which might be either linked to inflammation, or to synaptic rearrangements takes place, and involves various splice variants of specific genes. For instance, the microarray experiment reported signals with a standard deviation of 1.25 for Semaphorin 3F. This gene is involved in axonal guidance, and has splice variants, which are involved in a temporal and regional regulation during the maturation of the murine central nervous system (Kusy et al., 2003).

Taken together, the results of the whole genome microarrays have shown that gene expression changes happen in the spinal cord in the surgical pain model. Genes linked to cell motility, cell-cell adhesions, cytoskeleton and extracellular matrix seem to be highly regulated, or alternatively spliced. This could be explained by the migration of cells fro the immune system, or by a neuronal rearrangements linked to synaptic plasticity. Cell motility in pain is a growing field of research. It has for instance recently been shown in vitro, that morphine increases microglial migration via an interaction between the μ-opioid and P2X(4) receptors, a process which could be underlying the tolerance hyperalgesic side effect of morphine (Horvath and DeLeo, 2009). Synaptic plasticity also occurs in the spinal cord, and contributes to an enhanced responsiveness of motoneurons in the central nervous system. This process is called central sensitization (Ikeda et al., 2009; Woolf and Salter, 2000). The expression level changes observed in the spinal cord during post-operative phase could therefore be mediating central sensitization states, which contribute to pain maintenance.

Taken together, our data shows that the gene expression changes linked to nociception are subtle and complicated. The altered pain related phenotypes observed in transgenic animals do not necessarily reflect the

physiological expression regulations, which occur in wild-type animals experiencing pain. The gene expression changes do not occur in genes, which are directly involved in the transmission of the nociceptive message such as channels or receptor. We observed them for genes, which are involved in other processes such as neuronal circuit rearrangements or inflammation. These observations could not only lead to diagonostic tools for the monitoring of nociception and pain, but they could also help to better understand the processes and the key players involved in the generation the pain sensation.

4. Conclusions and Outlook

Longer lasting pain like the one that occurs after a surgery involves processes, which could modify the expression levels of genes, to maintain the nociceptive message transmission in the CNS. Therefore, monitoring expression level changes in the brain or the spinal cord of mice in a post-operative recovery phase could possibly help to objectively detect changes linked to pain. If these changes were reproducible and characteristic of pain, microarrays could be used in every day laboratory work to detect pain.

To identify potential genes involved in pain mechanisms, we screened the literature and established a set of 230 genes. Half of these genes were also defined by Lacroix-Fralish et al. as the commonly known "pain genes" (Lacroix-Fralish et al., 2007), the other half consisted in genes linked to stress and anxiety (see Appendix 1). Most of these genes induced pain-related behaviors in transgenic animal models, and therefore represented good candidates for the monitoring of nociception. In the first part of this project, we have established a low-density microarray hybridization and normalization protocol in one color, which bypassed dye imbalances that occur in two-color models. This protocol was followed to detect gene expression changes between the hippocampus, the brainstem and the cortex in 3 naïve NMRI mice. The genes regulations obtained in this experiment were compared to publically available microarray data of a gene profiling study carried out in the brain for 6 inbred mice strains (Hovatta et al., 2005). Our results were highly similar to the ones obtained in this experiment, despite strains and experimental platforms differences. The microarray protocol was therefore able to detect relevant gene expression changes in the CNS, and could therefore be applied in future experiments.

We then applied this microarray protocol to detect potential gene expression changes in the brainstem, cortex, hippocampus, cerebellum and spinal cords of mice, which were in the postoperative phase after a telemetric apparatus implantation. In previous experiments, these mice exhibited higher heart rates, which were indicative of pain (Arras, 2007; Arras et al., 2007). The microarrays detected some regulations in the brainstem, the cerebellum and the spinal cords. These regulations albeit interesting, could not be confirmed by Real-Time PCR measurements, and were therefore probably artefactual. Further Real-Time PCR measurements to evaluate the genetic regulations in the brainstem, the hippocampus, the cortex and the DRGs on the 26 more potent candidate genes confirmed this tendency, as only one of them showed a significant upregulation in the cortices of the operated animals. This gene was the serotonin receptor 5HTr1A. We performed similar Real-Time PCR experiments in the cortices and the spinal cords of mice, which had been immunized against the BHV-1 virus, and which were experiencing inflammatory pain. None of the 26 genes showed a significant, regulation.

Our data generally shows, that all the commonly known "pain genes" except the 5HTr1A receptor are not regulated in the surgical or the in inflammatory pain model, although they all induce a pain-associated phenotype in transgenic mice. They can therefore not be used for a diagnostic tool of pain based on gene expression level assessments.

Further studies should however be performed on other animal models for pain to test whether the 5HTr1A upregulation observed in the cortices of the animals in pain can be reproduced in other pain models. We were able to observe it in our surgical pain model, but not in the inflammatory one. One could measure the expression levels of the 5-HTr1A receptor by Real-Time PCR in chronic pain models such as nerve ligations to understand better if the expression levels of this gene only increase in longer lasting pain. Recent clinical studies on elderly people who had suffered from a hip fracture have shown that higher 5-HTr1A are linked to a higher risk of post-traumatic depression characterized by a lower general activity (Lenze et al., 2008). Other studies have shown that certain alleles of that gene are associated with a higher risk of depression (Kishi et al., 2009). Therefore, the higher expression we have measured in the cortices of the operated mice was maybe a sign of a depressive state caused by a post-operative distress. In that sense, measuring the expression levels of that gene after an experimental procedure could give some indication of the level of suffering experienced by the animal.

In the final part of the project we performed whole genome microarray analyses to detect regulations that occur at the exon level. The experiments were performed in the spinal cords of mice, which had been subjected to our surgical pain model. The goal of this experiments was to identify, which genes have a differential expression or are subjected to alternative splicing events, during the transmission of a longer-lasting nociceptive signal. The results first confirmed that the 230 genes on which we had focused in the beginning do not show any regulation. However, we were able to show, that significant and relevant whole gene expression changes, as well as alternative splicing events happen in the spinal cords of the operated animals.

We identified 166 genes, which were downregulated in the post-operative phase. Among these, 21 genes had also been down- or up-regulated in stimulation experiments, which induce cell motility and axonal sprouting. The second analysis revealed 96 upregulated genes in the operated animals. Among these, 19 had been downregulated in previous stimulation experiments, which enhance neuronal motility, and 17 had been upregulated in previous experiments, which induce axonal growth. Moreover, a functional classification revealed that the main regulated genes were linked the cytoskeleton, cell motility and extracellular matrix. The 5HTr1A serotonin receptor that was upregulated in the cortex of the operated mice during our low-density microarray experiment showed no expression level changes in the spinal cord in this experiment. The 166 downregulated genes and the 96

upregulated ones which were revealed in this experiment could potentially be good candidates for building a diagnostic tool based on pain. Technology advancements have allowed the establishment of high throughput real-time PCR measurements (Schmittgen et al., 2008). This method could be used to measure precisely the expression levels of these genes in other parts of the CNS, as well as in other pain models, to determine whether they can really be used as indicators for the levels of pain experiences by an animal. Comparative studies of the expression profiles in various parts of the CNS could then determine whether some signature patterns are characteristic of some specific pain models.

Our data has shown that the most important 410 genes, which underwent alternative splicing were linked to cell motility, cytoskeletal processes as well as inflammation. The role of alternative splicing in pain is a growing field of research. It has been shown that various splice variants of the Prrxl1 gene contribute to the development of the murine nociceptive system (Rebelo et al., 2009). This gene also appeared in our experiments, as being subjected to some alternative splicing linked to pain in the spinal chords of the operated mice. Deep sequencing experiments of all the splice variants of the top 410 genes, which came out of our experiments could provide us with better information on the exons of each genes, which are alternatively spliced during the transmission of the nociceptive signal. This could open the door the the generation of transgenic animals, which would either over express or not express at all certain splice variants of a gene. Studying their responses to common behavioral tests for pain could allow us to reach a further understanding of the role of splice variants in the generation and the transmission of a nociceptive signal.

Taken together, our data shows that cell motility probably contributes to the nociceptive signal, and could be an interesting parameter to study, to possibly monitor nociception. This migration could be linked to neuronal rearrangements, or the movements of dendritic cells, or components of the immune system. Further functional experiments on cell migration, and its role on nociception are needed to understand in what extent synaptic plasticity, and neuronal rearrangements, and general cell motion contribute to the maintenance of pain, in surgical and inflammatory models. Prager-Khoutorsky et al. have recently shown on Aplysia neurons, that actin-perturbing drugs such as cytochalasin B, latrunculin A, or jasplakinolide inhibit axonal motility by blocking neurite retraction (Prager-Khoutorsky and Spira, 2009). It could be interesting to submit mice to spinal injections of these drugs, and to test how these animals respond to common behavioral tests for pain such as the hot plate tests. Such experiments could give some indication on the eventual role of neuronal motility in the transmission of shorter lasting nociceptive signals.

The initial aim of this work was to establish a low density microarray which could be used as a diagnostic tool to evaluate pain in the central nervous system of laboratory animals. Our projects has shown that the genes

commonly refered to as the pain-genes based on the studies of transgenic animals do not show any characteristic gene expression changes in our surgical and inflammatory pain models. They were therefore good candidates for such the establishment the array. In that sense, the initial goal of this project was not reached. However, the second part of the project has revealed that gene expression changes occur in the spinal cord of mice subjected to our surgical protocol. All the regulated or alternatively spliced genes identified in this experiment could be important new candidate genes for the monitoring of nociception, and it would be interesting to test if the regulations in other pain models are similar to what we have observed, and to test precisely by real-time PCR, which of these genes would be the most relevant candidates for a diagnostic tool to monitor pain in laboratory animals. This tool could then be routinely used in animals, which are subjected to experimental procedures, or to new, uncharacterized transgenic animals to monitor nociception, and to take the appropriate analgesic measures to abolish their pain.

5. Material and methods

5.1 Low density microarray establishment

5.1.1 Gene selection and probes design

A litterature search was performed in order to screen genes, which were linked to nociception. The criterion of selection was their relevancy in pain research. The genes were related to pain induced behaviors in knockout animals, or in transgenic animals, which were either overexpressing the gene. Other genes were encoding proteins, which were expressed in nerve ligation models. In addition to these, signal transduction molecules were added, as well as genes for channels, and receptors. Table 1, in the results chapter sums up the various categories of genes present in the microarray design. A final set of 199 genes was selected for the analysis.

For slide orientation as well as for data normalization purposes, 19 positive control genes, which are ubiquitously expressed and 8 spikes sequences were also included in the probes design. 11 negative controls, which were either derived from the E. Coli genome or randomly generated, were also considered, in order to monitor the hybridization quality. This brought the final number of probes produced to 238.

The probes were designed and produced by Operon Biotechnologies GmbH in Germany. They were 70mer oligonucleotides, corresponding to a sequence located in the last 750 nucleotides at the 3' ending of each gene. Given that RNA degradation starts in the 5' ending of a gene, having probes, which recognize the 3' terminal of RNA can help to bypass due to degradation. Moreover, this technology offers the advantage of minimizing secondary structures, which have high melting temperatures, and therefore allows hybridization reactions to run at normal temperatures. The probes were synthesized without being coupled to an amino-linker, as it is not required for the coupling to epoxy slides. Amino linkers are easily subjected to oxidation, which disminishes the quality of the probes.

5.1.2 Spotting of oligos

The Lyophilized 70mer oligonucleotides were diluted in RNAse free water (Qiagen®) to bring them to a final concentration of 100μM. For the 2 first designs of the slide, the spotting was performed on a Perkin Elmer Piezzorray contact printer at the Functional Genomics center in Zürich. For this printing, the probes were diluted in 20x SSC to bring them to a final concentration of 20μM in 3x SSC (20μl 70mers 100μM, 20μl 20x SSC, 65μl Rnase free H_2O), and 40μl of each probe was then transferred to a 384 well plate, according to a specific design.

5.2 Animal handling and treatments

5.2.1 Animal housing

The experiments requiring a telemetric apparatus implantation were performed on male HsdHan:NMRI mice, which were obtained from a commercial supplier (Harlan, Horst, The Netherlands). The animals were 4 weeks old at arrival, and underwent the telemetric apparatus implantation after an adaptation period of 4 weeks. At the time of implantation, the animals had a weight ranging from 32g to 48g.

The experiments on inflammatory pain were performed on 12 male A129 mice obtained from a commercial supplier (Harlan, Horst, The Netherlands) All animals were 4 months old at the time of the immunization,

The housing conditions were identical for both strain used in this project. The mice were kept in type 3 filter-top clear-transparent plastic cages (425 mm × 266 mm × 150 mm, floor area 820 cm2) with autoclaved dust-free sawdust bedding (80–90 g/cage) and autoclaved hay (18–20 g/cage) as nesting material. They had unrestricted access to sterilized drinking water were fed a pelleted and extruded mouse diet (Kliba No. 3431, Provimi Kliba, Kaiseraugst, Switzerland) ad libitum. The dark/light cycle consisted of 12/12h. Each male was housed with an ovariectomized female, but after the surgery, they were housed individually, to avoid companion's actions on the readout.

5.2.2 Telemetric implantation

Mock TA10ETA-F20 telemetric transmitters (Data Sciences International, St. Paul, MN, USA), which have the same size, shape and weight as the original ones were implanted, when the mice were 8 weeks old. The mice were anesthetized by inhalation of the volatile anesthetic sevoflurane (Sevorane™, Abbott, Cham, Switzerland) at a concentration of 8-4.5% in 100% oxygen at a flow rate of 200 ml/min. The anesthetic gas was administered with a nose mask. This anesthesia protocol was performed on the operated animals as well as on the control ones. The surgery time was approximately of 1h per animal, and for each operated animal, one control was always kept under anesthesia during he same time. 20 min prior to the end of the anesthesia, the operated and the control animals received an intraperitoneal injection of 100µl Flunixin, 150µl Borgal and 1ml Ringer Lactate. After surgery, both the operated and the control animals were treated twice daily with a subcutaneous injection of 2µl/g body weight Flunixin (Biokema Flunixine™, Biokema SA, Crissier-Lausanne, Switzerland) until sacrifice.

For each operated animals, the surgery consisted in a mid line laparotomy was performed to open the abdominal cavity, in which the telemetric transmitter's body was implanted. One telemetry lead was tunneled

subcutaneously from the thorax to the neck, and the wired electrode was fixed between the muscles located right of the trachea. The second wired loop was sutured to the xiphoid process with a silk thread. The muscles and skin were then closed with resorbable sutures.

For the whole brain microarray experiment, and for the microarray experiments performed on parts of brain, 3 mice were operated, and 3 mice were used as control, and 2 mice were used as reserve animals. All animals were sacrifieced 2 days post surgery. For the Real Time PCR experiments on parts of the Central Nervous System, and for the GeneChip® Mouse Exon 1.0 ST microarray on the Spinal Cords: 6 animals were operated, 6 were used as controls, and 2 were reserve animals. The 12 animals used for the Real-Time PCR measurements were sacrificed 2 days after the surgery, and those used for the whole genome microarray experiment were sacrificed 1 day after surgery. In each case, the mice were sacrificed by cervical dislocation.

5.2.3 Inflammation model

All the 12 mice used in that experiment were implanted as previously described with TA10ETA-F20 telemetric transmitters (Data Sciences International, St. Paul, MN, USA) at 10 weeks of age. The post-implantation convalescence period was set at 8 weeks. The mice were then randomly divided into two groups: 6 mice were subjected to the BHV-1 immunization protocol, and 6 underwent a control injection.

The BHV-1 immunization solution consisted of UV-inactivated BHV-1 (corresponding to the antigenic mass of 10^7 $TCID_{50}$ live BHV-1) in 50 µl cell culture medium (DMEM supplemented with 2% FBS, 100 units/ml Penicillin G, and 75 units/ml Streptomycin), which was emulsified with 50 µl CFA (Sigma-Aldrich Corp. St. Louis, MO, USA, F-5881, Lot 014K8927). 100 µl of the freshly prepared solution was injected to each of the 6 immunized mice. For the 6control animals, the vehicle solution (100 µl, DMEM supplemented with 1% FBS, 50 units / ml Penicillin G, and 37.5 units / ml Streptomycin), containing neither BHV-1 nor FA, was injected intraperitoneally.

The injected and the control animals were all sacrificed 3 days after the injection. For each animal, the Cortex and Spinal Cord were dissected and analyzed by Real-Time PCR.

5.3 Central nervous system dissection, and tissue preservation

5.3.1 Brain dissection

Immediately after having been sacrificed by cervical dislocation, the heads of the mice were cut with scissors at the cervical level. The brain extractions were performed fast to avoid RNA degradation. After a complete removal of the skin and muscle to reveal the mouse skull, the interparietal bone was cut surgical scissors in the middle until the Lambda, and carefully removed, with forceps to reveal the cerebellum. Two cuts were performed along the jaw and the mandibule of the animals, and the parietal bone was then cut in half along the sagittal suture with surgical scissors, from the Lambda to the Bregma. The coronal suture was then cut transversally, and the two halves of the parietal bone were carefully removed with a forceps. The brain was then taken out with a forceps, after cutting the optical nerves. It was placed on a Parafilm M (American National Can™, cut in half along the fissura longitudinalis cerebri, and preserved in 2ml RNAlater solution (Qiagen®) at 4°C overnight, and were then further dissected for the experiments performed on parts of the central nervous system, or were then stored at -80°C.

For the experiments performed on parts of the central nervous system, each half brain was dissected as follows. The cerebellum was first removed from each brain half with a forceps, and the cortex was carefully pealed off, revealing the hippocampus, which was then cut away. The brainstem was then removed, by dissecting the Pons along the Fissura Transversa Cerebri, and the Fissura Posterolateralis. Each of these parts immediately stored in 2ml RNAlater solution (Qiagen®) at 4°C overnight, and then kept at -80°C.

5.3.2 Spinal cord dissection

Directly after the cut in the cervical region to remove the head, the mouse was fixed by pinning each paw to the surface. The skin was cut longitudinally from the neck to the tail of the animal, the muscles were cut and removed and another transversal cut was performed in the sacral region with strong surgical scissors, to expose the of the spinal cord. A laminectomy was performed by cutting each vertebra longitudinally with sharp small surgical scissor, on each side, and by removing the upper lamina progressively with forceps until the beginning of the spine curve. At this point, the dorsal lamina was removed, to expose the lumbar part of the spinal cord. Forceps were used to delicately remove the spinal cord, which was immediately placed in 2ml RNALater solution (Qiagen®).

5.3.3 Dorsal root ganglia dissection

After the removal of the spinal cord, 6 lumbar dorsal root dorsal root ganglia were explanted from the vertebrae with a forceps, and their afferents were cut. They were then stored in 1ml RNALater solution (Qiagen®).

5.4 RNA extraction

5.4.1 Whole brain RNA extraction

For this RNA extraction, the RNeasy® Mini kit from Qiagen® was used. The extraction was performed on the right hemisphere of the Brains. Each hemisphere was transferred to 8ml RLT buffer 10% β-Mercaptoethanol (Sigma-Aldrich®) and was homogenized for 30s with a Rotor-Stator. 600µl from each homogenate were then transferred in 1.5 microfuge tubes (Eppendorf AG) and centrifuged 3 minutes at maximum speed, while the rest the homogenate was stored at -80°C for further possible use. The centrifuged supernatant was then precipitated with 600µl 70% Ethanol (Sigma-Aldrich®), and successively applied on 2 RNeasy columns, and the RNeasy® Mini kit protocol for animal tissues was performed to extract the total RNA. In the final step, the RNA was eluted in 50µl RNase-free water (Qiagen®). The RNA quality was controled on a Bioanalyzer 2100 Nano Chip (Agilent®) according to the manufacturer's instructions, and the concentration was measured on a Nanodrop ND 1000 spectrophotometer (Thermo Scientific®). Each total RNA sample was stored at -80°C until use.

5.4.2 Parts of brain RNA extraction

The RNA from all the analyzed parts of brain were extracted using the RNeasy® Mini kit (Qiagen®). The cortices, cerebelli, brainstems were all homogenized in 1.2 ml RLT buffer 10% β-Mercaptoethanol (Sigma-Aldrich®). The Hippocampi were homogenized in 600µl of the same buffer. All the parts were homogenized with the Mixer Mill MM 300 after having placed a stainless steel bead (Qiagen®) in the respective microfuge tubes (Eppendorf AG). For each cerebelli, brainstems, and hippocampi, 4 homogenization cycles of 2 min at 20 Hz were performed. For the cortices, 8 homogenization cycles of 2 min at 20 Hz were necessary. For all the homogenates, the extraction process was the same: 300µl homogenate were centrifuged for 3 minutes at full speed, while the rest of the homogenate was stored at -80°C for further use. After centrifugation, the supernatant was transferred to another microfuge tube, and were precipitated with 300µl 70% Ethanol (Sigma-Aldrich®). The 600µl of precipitated homogenate were then successively transferred to RNeasy columns, and the RNeasy® Mini kit protocol for animal tissues with DNase digestion was followed for the total RNA purification. In the final step, the

volume of RNas-free water used for the elution was 50µl (Qiagen®). The RNA quality was assessed on a Bioanalyzer 2100 Nano Chip (Agilent®) according to the manufacturer's instructions, and the concentration was measured on a Nanodrop ND 1000 spectrophotometer (Thermo Scientific®). All the total RNA samples were then kept at -80°C until use.

5.4.3 Spinal cord RNA extraction

The Spinal cord RNA was extracted with the RNeasy® Mini kit (Qiagen®). They were transferred in 1.2ml RLT buffer 10% β-Mercaptoethanol (Sigma-Aldrich®). A stainless steel bead (Qiagen®) was added to each sample, and 6 homogenization cycles of 2 min at 20Hz were performed on the Mixer Mill MM300. The homogenates were then centrifuged at maximum speed for 3min, after which 350µl were transferred to a new microfuge tube and precipitated with 350µl 70% Ethanol (Sigma-Aldrich®). The rest of the homogenate was stored at -80°C. The precipitated homogenate were then applied successively to their respective RNeasy column, and the RNeasy® Mini kit (Qiagen®) for animal tissues with DNase digestion protocol was followed to extract the total RNA. The elution step was performed with 50µl RNase-Free water. The total RNA concentration of each sample was measured on a Nanodrop spectrophotometer (Thermo Scientific®), and the RNA quality was checked on a Bioanalyzer 2100 Nano Chip (Agilent®) following to the manufacturer's instructions. The Spinal Cord total RNA samples were then stored at -80°C until use.

5.4.4 Dorsal root ganglia RNA extraction

This RNA extraction was performed with the RNeasy® Mini kit from Qiagen®. The dorsal root ganglia were transferred in 350µl RLT buffer 10% β-Mercaptoethanol (Sigma-Aldrich®). A stainless bead was added to each microfuge tube, and 4 homogenization rounds of 2 min at 20hz were performed. The samples were then centrifuged at full speed for 3 min, and the supernatant were transferred to new microfuge tubes (Eppendorf AG). The RNA precipitation was achieved by adding 350µl 70% Ethanol (Sigma-Aldrich®). After that step, the precipitated homogenates were successively applied to their respective RNeasy column, and the rest of the extraction was done according the animal tissue protocol with DNase digestion from the RNeasy® Mini kit (Qiagen®). The RNA quality was assessed with a Bioanalyzer 2100 Nano Chip (Agilent®) following to the manufacturer's guidelines, and the concentration was measured by spectrophotometry on a NanoDrop ND 1000 (Thermo Scientific®). The samples were then stored at -80°C until use.

5.5 aRNA amplification for low density microarray hybridization

The Ambion Amino Allyl MessageAmp™ II aRNA Amplification Kit (Applied Biosystems®) was used to amplify every aRNA sample hybridized on the low-density microarray. For the amplification reactions of the aRNA derived from whole brains, the hippocampi, cerebelli, cortices and brainstems, 1μg of total RNA was used at the beginning of the reaction. For the amplification reactions of the aRNA derived from the spinal cords and the dorsal root ganglia, 500ng of total RNA was used to start the reaction.

All the reactions were followed according to the protocol provided by the manufacturer. The first step consisted in a reverse transcription of the mRNA into cDNA. Depending on which part of the central nervous system was studied, samples of 1μg or 500ng total RNA were aliquoted. 1μl of T7 Oligo(dT) Primers were added, and the volume of each sample was then completed to 12μl with RNase free Water. The samples were incubated 10 min at 70°C for the annealing of the Oligo (dT) Primers. 8μl Reverse transcription Master Mix containing 2μl 10x First Strand Buffer, 4μl dNTP Mix, 1μl RNase Inhibitor and 1μl ArrayScript were added to each sample. The reverse transcription reaction was carried at 42°C during 2h, and the samples were placed on ice.

For the synthesis of the second strand cDNA, 80μl Second Strand Master Mix containing 63μl RNase free water, 10μl 10x Second Strand Buffer, dNTP Mix, 2μl DNA Polymerase and 1μl RNase H, were added to each sample. The reaction was carried out at 16°C during 2h, and the cDNA was then purified according to the manual's instructions, and each cDNA sample was eluted twice in 9 μl RNAse free water at 50°C, which brought the final cDNA volume to approximatively 14μl, as some water does not flow through the column.

The in vitro transcription of the RNA was carried out directly after the cDNA purification. In the case of the total brain and the spinal cord samples, 26μl in vitro transcription Master Mix, containing 3μl amino-allyl UTP (50mM), 12μl ATP, CTP, GTP Mix (25mM), 3μl UTP (50mM) 4μl T7 10x Reaction Buffer, 4μl T7 Enzyme Mix, were added to each sample, and the reaction was carried out overnight at 37°C. For the invitro transcriptions of the cerebellum, brainstem, hippocampus and cortex aRNA, 26μl in vitro transcription Master Mix, containing 12μl ATP, CTP, GTP Mix (25mM), 6μl UTP (50mM) 4μl T7 10x Reaction Buffer, 4μl T7 Enzyme Mix, were added to and the reaction was also carried out overnight at 37°C.

At the end of all in vitro transcription reactions 60μl RNase-free water were added to the samples. The manufacturer's protocol was followed to purify the aRNA. The elution was performed with 100μl Nuclease heated at 55°C. After purification, the aRNA quality was assessed on a Bioanalyzer Nano Chip (Agilent®) following to the manufacturer's instructions and the concentration

was measured by spectrophotometry on a NanoDrop ND 1000 (Thermo Scientific®).

5.6 aRNA labeling

5.6.1 Whole brain and spinal cord aRNA labelling

The aRNA amplified from the whole brains mRNA or from the spinal cord mRNA were labelled with Molecular Probes™ Alexa Fluor® Succinimidyl Esther dyes from Invitrogen™. For each labelling reaction, 15µg of aRNA were vacuum dried on an Eppendorf™ Concentrator 5301 at RT, and resuspended in 9µl Coupling Buffer. The Alexa Fluor® were resuspended in 11µl DMSO and added to the resuspended aRNA. The mixes were incubated for 30 min at room temperature in the dark, after which 4.5µl 4M Hydroxylamine were added to quench the labeling reaction. After a 15 min long incubation at room temperature in the dark, 5.5µl RNase free water was added to each tube. The labeled aRNA solutions were then purified by according to the manufacturer protocol, and immediately used for hybridization.

For the microarray experiments performed on whole brains, the aRNA samples derived from the Brains of the 3 operated and the 3 control animals were labeled with Alexa Fluor®-555 dyes (Invitrogen™) and the aRNA derived from the brains of 3 naive NMRI mice were labeled with Alexa Fluor®-647 (Invitrogen™). For the microarray measurements done on spinal cords, all the samples were labeled with Alexa Fluor®-555 (Invitrogen™) solely.

For the dye swap experiments, 2 aRNA samples from brain n°19, which was extracted from one of our operated animals were respectively labeled with Alexa Fluor®-555 (Invitrogen™) and Alexa Fluor®-647, and 2 reference brains aRNA samples, derived from naive NMRI mice were respectively labeled with Alexa Fluor®-555 (Invitrogen™) and Alexa Fluor®-647 (Invitrogen™).

5.6.2 Parts of brain aRNA labelling

The aRNA amplified from the mRNA purified extracted from the cerebelli, cortices, hippocampi and brainstems were labeled with Cy5-ULS dyes, using ULS™ aRNA Fluorescent Labelling Kit from Kreatech™ Biotechnology. The labeling mixes contained of 2µg Cy5, 2µl 10x Labelling solution, and were completed to a final volume of 20µl with RNAse free water. The samples were then incubated for 15 min at 85°C to allow the dye coupling reaction. At the end of the reaction, 80µl RNAase free water was added to each sample, and the labelled aRNA was purified following the RNA Cleanup protocol of the RNeasy® Mini kit from Qiagen®. The elution step was performed with 30µl RNase free water.

5.7 aRNA Hybridization

5.7.1 Whole brain aRNA hybridization

Prior to the hybridization, the labeled aRNA and the Ambion SlideHyb™ Glass Array Hybridization Buffer #1 (Applied Biosystems®) were heated 10 min at 70°C for linearization. The aRNA concentration and the dye incorporation were then measured by spectrophotometry on a Nanodrop ND 1000 (Thermo Scientific®). The six samples to hybridize on the slides were prepared by mixing 1.5µg brain of interest aRNA (from either an operated or a control mouse) labeled with Alexa Fluor®-555 (Invitrogen™), 1.5µg reference brain aRNA (from naïve NMRI mice) labeled with Alexa Fluor®-647 and by completing the volume to 150µl with SlideHyb™ Glass Array Hybridization Buffer #1 (Applied Biosystems®) (Applied Biosystems®), which prevented the unspecific binding of the sample to the slide.

For the dye swap experiment, 2 samples were prepared. The first one contained 1.5µg brain 19 aRNA (derived from an operated mouse) labeled with Alexa Fluor®-555 (Invitrogen™) and 1.5µg reference brain aRNA (from naïve NMRI mice) labeled with Alexa Fluor®-647 in a final volume of 150µl SlideHyb™ Glass Array Hybridization Buffer #1 (Applied Biosystems®) (Applied Biosystems®). The second one contained 1.5µg brain 19 aRNA (derived from an operated mouse) labeled with Alexa Fluor®-647 (Invitrogen™) and 1.5µg Reference Brain aRNA (from naïve NMRI mice) labeled with Alexa Fluor®-555 in a final volume of 150µl SlideHyb™ Glass Array Hybridization Buffer #1 (Applied Biosystems®) (Applied Biosystems®).

All the hybridization were performed according to the following protocol

The spotted sciCHIP Epoxy slides (Scienion, Art. SE-011) were placed in a Tecan Hybridization Station 4800 (Tecan, Männedorf, Switzerland) and washed as follows:

- 1min 30s at 10°C in 2x SSC, 0.5% SDS
- 30s at 23°C in 0.5x SSC, 0.5% SDS
- 30s at 23°C in 0.1x SSC

The slides were then blocked in 50 mM Ethanolamine (Sigma-Aldrich®), 0.1 M Tris (pH 9) for 30min, and washed as follows:

- 4min at 23°C in RNase Free Water
- 30 s at 23°C in 2x SSC, 0.5% SDS

After this step, the aRNA sample mixes were injected to their respective chambers, and the hybridization reaction was carried out at 42°C during 16h. The slides were then washed as follows:

- 30 s at 23°C in 2x SSC, 0.5% SDS, 4 times
- 30 s at 23°C in 0.5x SSC, 0.5% SDS, 4 times
- 30s at 23°C in 0.1x SSC, 2 times

At the end of the hybridization, the slides were dried with N_2 during 4min 30s at 30°C, and scanned immediately.

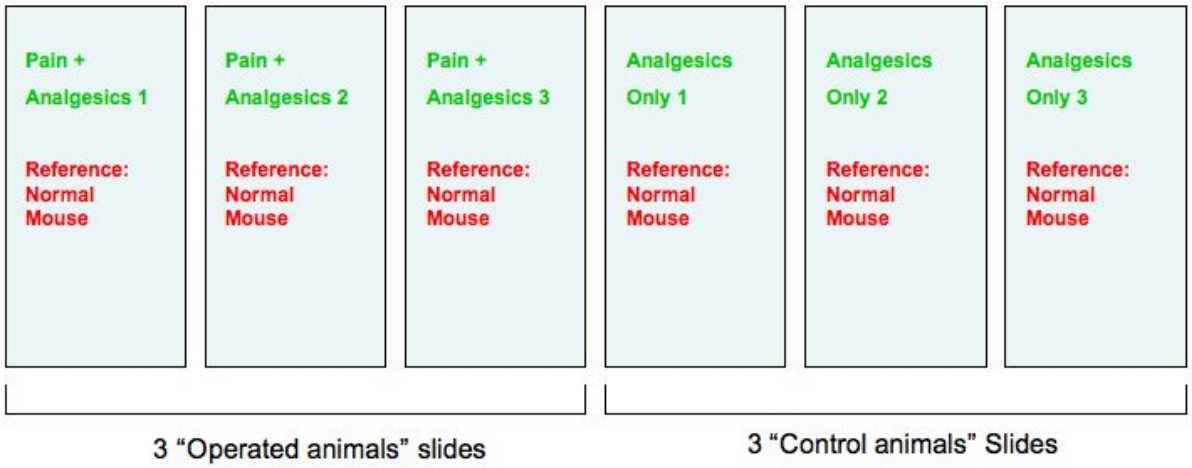

Figure 1: Scheme of the hybridized samples in the 2 color hybridizations of the whole Brain aRNA

5.7.2 Spinal cord aRNA hybridization

The labeled spinal cord aRNA and the Ambion SlideHyb™ Glass Array Hybridization Buffer #1 (Applied Biosystems®) were heated 10 min at 70°C for linearization before the sample preparation. The dye incorporation and the aRNA concentration were measured on a Nanodrop ND 1000 (Thermo

Scientific®) spectrophotometer. The six samples to hybridize on the slides were prepared. Each sample had a volume of 150µl and contained 1.5µg spinal cord aRNA (from either an operated or a control mouse) labeled with Alexa Fluor®-647 (Invitrogen™) in SlideHyb™ Glass Array Hybridization Buffer #1 (Applied Biosystems®) (Applied Biosystems®), which prevented the unspecific binding of the sample to the slide.

The spotted sciCHIP Epoxy slides (Scienion, Art. SE-011) were placed in a Tecan Hybridization Station 4800 (Tecan, Männedorf, Switzerland), and the washing, blocking and hybridization steps were identical as for the whole Brain aRNA hybridization. At the end of the hybridization, the slides were dried with N_2 during 4min 30s at 30°C, and scanned immediately.

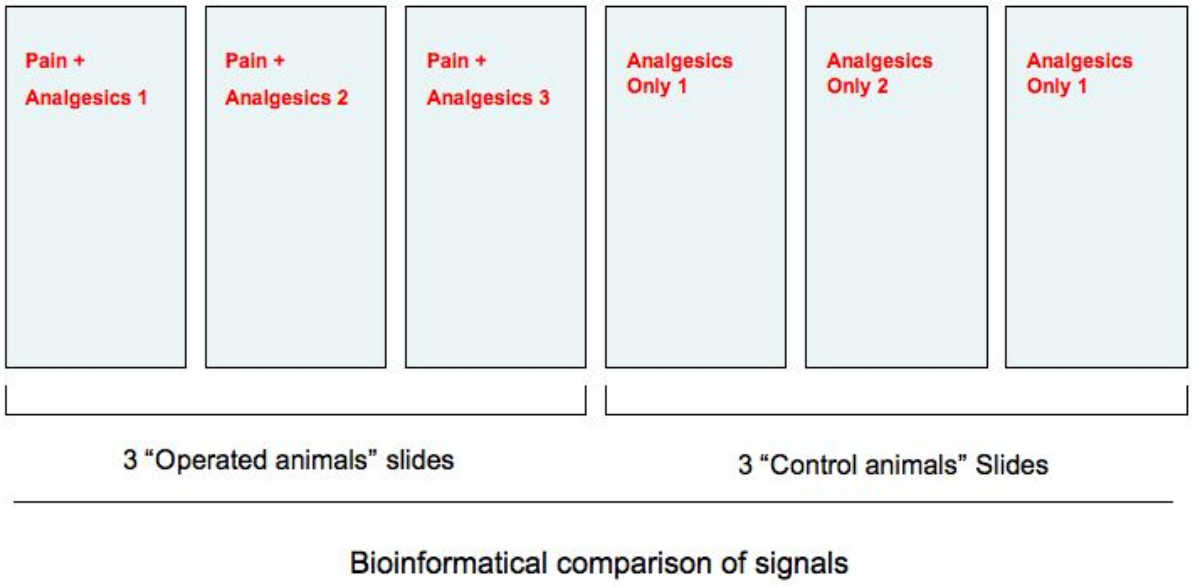

Figure 2: Scheme of the hybridized samples in the 1 color hybridizations performed for the Spinal Cord and the parts of Brain aRNA.

5.7.3 Parts of brain aRNA hybridization

Before the beginning of the hybridization, the samples and the KreaBlock Buffer (Kreatech™ Biotechnology) were heated 10min at 70°C. The dye

incorporation and the aRNA concentration were then measured on a Nanodrop ND 1000 (Thermo Scientific®) spectrophotometer. The samples were then prepared by mixing 1.5µg part of brain of interest aRNA (from either an operated or a control mouse), ¼ of the final volume KreaBlock Buffer (Kreatech™ Biotechnology), and by completing with RNase free water to a final volume of 160µl.

The spotted sciCHIP Epoxy slides (Scienion, Art. SE-011) were placed in a Tecan Hybridization Station 4800 (Tecan, Männedorf, Switzerland). 160µl 50 mM Ethanolamine (Sigma-Aldrich®), 0.1 M Tris (pH 9) were injected in each chamber, and the blocking reaction was carried out for 30 min at 50°C. The slides were then washed as follows:

- 30s at 23°C in RNase free water, 3 times
- 30s at 50°C in 4x SSC, 0.1% SDS, 4 times
- 30s at 23°C in RNase free water, 3 times

The slides were then boiled during 1min in MiliQ water (Milipore™) to denature any denature any secondary structure of the probes, and placed again in the Tecan Hybridization Station 4800 (Tecan, Männedorf, Switzerland). The following washing steps were performed:

- 30s at 10°C in 2x SSC, 0.5% SDS
- 30s at 23°C in 0.5x SSC, 0.5% SDS
- 30s at 23°C in 0.1x SSC

After washing, the labeled aRNA samples were injected to their respective chambers, and the hybridization reaction was performed at 42°C during 16h. The slides were then washed as follows:

- 30 s at 23°C in 2x SSC, 0.5% SDS, 5 times
- 30 s at 23°C in 0.5x SSC, 0.5% SDS, 5 times
- 30s at 23°C in 0.1x SSC, 2 times

At the end of the hybridization, the slides were dried with N_2 during 4min 30s at 30°C, and scanned immediately.

5.7.4 Slide scanning and data quantification

The hybridized microarrays were scanned using the Agilent DNA Microarray Scanner and Feature Extraction Software (Agilent Technologies Inc., Santa Clara CA, United States). The quantification of the pixel intensity of each spot with local background correction the slides was done using Genespotter (MicroDiscovery GmbH, Berlin, Germany).

5.8 Low density microarray data analysis and normalization

All the data interpretion and statistical analysis were performed on GeneSpring GX 7.3.1 (Agilent Technologies Inc., Santa Clara CA, United States).

5.8.1 Whole brain hybridization data

The Alexa Fluor®-555 signal values were labeled as "Signal", and the Alexa Fluor®-647 values were labeled as "Control". The normalization chosen for these experiments was the Loess normalization (locally weighted scatterplot smoothing), which combines linear least square regression with non-linear regression to normalize all the points of the plots independently, to align the curve of highest density.

Two analyses were run in parallel: one on the raw values of the "Signal" and the "Control", and one on their normalized values. In each case, a scatter plot of one "Signal" in function of its corresponding "Control" was observed, to assess the quality of the hybridization.

One parameter was set: "Pain" and "Non Pain". For the values from the 3 slides on which aRNA derived from the brain of an operated mouse was hybridized, the "Pain" parameter was set. For the values from the 3 slides on which aRNA derived from the brain of a control mouse was hybridized, the "Non Pain" parameter was set. An analysis of variance (P value = 0.1) was then performed according to the "Pain"/"Non Pain" parameter to detect possibly differentially expressed genes.

5.8.2 Spinal cord and parts of brain hybridization data

In this case, all the samples were labeled with only one dye: Alexa Fluor®-647 for the spinal cord aRNA, and Cy5 for the parts of Brain aRNA. In each case the data processing was the same. The values were all labeled as "Signal", and for each gene, the signals measured on the slides on which some aRNA derived from an operated animal was hybridized, were parametered as "Pain", and the signals measured on the slides on which some aRNA derived from a control animal was hybridized were labeled as "Non Pain".

The normalization chosen for all these experiments was the "normalize to a set of positive control genes". The identifiers of the 19 ubiquitously expressed positive control genes was uploaded, and the normalization consisted in fitting the positive controls to the curve of highest density, and to normalize all the other signals accordingly.

Two analyses were run in parallel: one for the raw values, and one for the normalized values. In both cases, a scatter plot of the "Pain" values in function of the "Non Pain" values was established to control the hybridization's quality. After that, volcano plots, which plot for each gene's -log10(P Value) in function of the log2(Fold Change) were used to filter the genes which had a Fold Change>1.5 and a P Value<0.05.

5.8.3 Comparison between parts of brain hybridization data

In this analysis, the "Pain" parametered values were excluded. For all the "Non Pain" parametered signals, a new parameter was set: "Parts of CNS", for which 3 different possibilities were entered: "Brainstem", "Cortex", "Hippocampus".

The normalization chosen for all these experiments was the "normalize to a set of positive control genes". The identifiers of the 19 ubiquitously expressed positive control genes was uploaded, and the normalization consisted in fitting the positive controls to the curve of highest density, and to normalize all the other signals accordingly.

For each part of central nervous system comparison, two analyses were run in parallel: one for the raw values, and one for the normalized values. In both cases, a scatter plot of the values of one of the "Parts of central nervous system" in function of the values of another "Parts of central nervous system" was established to control the hybridization's quality. After that, volcano plots, which plot for each gene's -log10(P Value) in function of the log2(Fold Change) were used to filter the genes which had a Fold Change>1.5 and a P Value<0.05.

5.9 Low-density microarray protocol validation

The protocol validation was carried out on the genes, which showed different expression profiles between the brainstem, the hippocampus, and the cortex. For each comparison, the list of differentially expressed genes was established according for the analyses made on both the raw and the normalized values. The fold changes of the differentially expressed genes were calculated and compared with the Fold obtained by Hovatta & al in their published model for mouse anxiety (Hovatta et al., 2005). In their study, they have assessed the expression profiles of the whole genome in parts of the central nervous sytem of 6 inbred mice strains: 129S6/SvEvTac, A/J, C3H/HeJ, C57BL/6J, DBA/2J, and FVB/NJ. They have worked with Affymetrix Murine Genome U74 Version 2 Arrays, and their results are stored in the GEO dataset, under the following ID number: GDS1406.

The fold changes of the differentially expressed genes in the low-density microarray experiments on parts of the bain were then compared to the fold

changes published in the GDS1406 GEO data set for the same genes in the same parts of the Brain in 6 inbred mice strains. A gene was considered differentially expressed, when his fold change was higher than 1.3 on the dataset. The comparison results were labeled as "Same", when the fold changes obtained on the low-density experiment and the GDS1406 dataset were both upregulated or downregulated, and as "Different" if one platform showed the gene to be upregulated and the other showed it to be downregulated or unchanged. For each comparison a percentage of similarity was calculated with the number of "Same" obtained.

5.10 Quantitative Real Time PCR analysis

5.10.1. Reverse transcription of total RNA

Prior to every Quantitative Real-Time PCR reaction, the sample's mRNA was reverse transcribed into cDNA. For all the total RNA samples extracted from the hippocampus, brainstem, cortex and cerebellum, the procedure was the same. The samples were prepared by mixing 0.5μg Total RNA, 2μl 10mM dNTP Mix (Invitrogen™), 1μg Oligo (dT)$_{12-18}$ Primer (Invitrogen™), and by completing with RNase-free water to a final volume 26μl. All the reaction mixes were then heated at 65°C for 5 min

A reverse transcription Master Mix was added to every sample. It contained 8μl 5x First Strand Buffer (Invitrogen™), 2μl 0.1M DTT (Invitrogen™), 2μl RNAsin® 40 U/μl (Promega™), 2μl Superscript III Reverse Transcriptase (Invitrogen™) (200U/μl) To control the efficiency of the reverse transcription, negative control samples (RT NEG Control cDNA) were prepared for every reaction. They consisted of the same samples, to which the following Master Mix was added: 8μl 5x First Strand Buffer (Invitrogen™), 2μl 0.1M DTT (Invitrogen™), 2μl RNAsin® 40 U/μl (Promega™), 2μl RNase-Free water.

All the samples and the negative controls were then incubated for 2h at 50°C and 15 min at 70°C, for the reverse transcription reaction.

5.10.2 Quantitative Real-Time PCR analysis of the differentially expressed genes in the low density microarray experiment

All the primers were designed using the Clone Manager 7 software (Sci-Ed Software™) in order to amplify a 300-400bp PCR product close to the 3' terminal of the mRNA of the differentially expressed genes from the low-density microarray data. Table 1 contains a list of the primers designed for the Real-Time PCR measurements. All the primers were synthesized commercially (Microsynth AG)

For each reaction, the protocol followed was the same. The primers were diluted to a final concentration of 10mM, And the cDNAs obtained after the reverse transcription were diluted 20x. For each part of the brain, 6 samples were prepared (3 derived from operated mice, and 3 coming from control mice). Each sample contained 2μl cDNA 1/20, 10μl QuantiTect™ SYBR® Green PCR Master Mix (Qiagen®), 1μl Forward (FWD) Primer, 1μl Backwards (BKD) Primer and 6μl H_2O.

For each Real-Time PCR reaction, 3 Reverse Transcription negative control samples, and one Real-Time PCR Negative Control sample were pipetted. Each of the 3 Reverse Transcription negative control samples contained 2μl RT NEG Control cDNA 1/20, 10μl QuantiTect™ SYBR® Green PCR Master Mix (Qiagen®), 1μl Forward (FWD) Primer, 1μl Backwards (BKD) Primer and 6μl H_2O. The Real-Time PCR Negative Control sample contained 10μl QuantiTect™ SYBR® Green PCR Master Mix (Qiagen®), 1μl Forward (FWD) Primer, 1μl Backwards (BKD) Primer and 8μl H_2O.

For every Real-Time PCR round, the reactions were carried on all the samples and negative controls for the gene of interest, and also for the β-Actin gene. The β-Actin Real-Time PCR signals of each sample were used for normalization purposes. Each sample, and negative controls were pipetted in triplicates.

Table 1: Primes used in the Real-Time PCR measurements performed to verify the low-density microarray data. The primers are noted in the 5'- 3' direction.

Gene Name	Primer Names	Primer Sequence
	Neuropeptide Y FWD	GCTAGGTAACAAGCGAATGG
Neuropeptide Y	Neuropeptide Y BKD	GATGAGATGAGGGTGGAAAC
	Vanilloid Receptor TrpV5 FWD	GACCTGCCAATTACAGAGTG
Vanilloid Receptor TrpV5	Vanilloid Receptor TrpV5 BKD	GCTATTGCTGCTTAGGGATG
	Vanilloid 1 Receptor VR1 FWD	TCCTGTTACTGGCCTATGTG
Vanilloid Receptor VR1	Vanilloid 1 Receptor VR1 BKD	TGCTATGCCTATCTCGAGTG
	5HTr4 FWD	TCCTCTGGCTTGGCTATATC
Serotonin Receptor 5HTr4	5HTr4 BKD	CTTAGGACTGGCTTCGTTTC
	Npy5r FWD	AAGCAGAAGCGACCGCACTC
Neuropeptide Y Receptor 5	Npy5r BKD	CTACGCTGCCTCTATAGTCC
	NPY6r FWD	ACTCCAACTCCAGGGAATAG
Neuropeptide Y Receptor 6	NPY6r BKD	TAGGTGTTGGCTGGTTTGTG
	MapK1 FWD	CTGCATACTGGTGTCATTGG
MAP Kinase 1 (Erk 2)	MapK1 BKD	CTATGTGGCATGCAGTGTAG
	Sodium and Chloride dependent GABA Transporter 1 FWD	CTCGTGCCGTAGCTTCTTAG
Sodium and Chloride dependent GABA Transporter 1	Sodium and Chloride dependent GABA Transporter 1 BKD	GGGAAGAGCTGGTAGATTGC
	Guanine nucleotide binding protein alpha 1 FWD	CCGACTACGATGGACCTAAC
Guanine nucleotide binding protein alpha 1	Guanine nucleotide binding protein alpha 1 BKD	TGCAAGCCTCATGCCTTTGG
	Nerve Growth Factor alpha (NGF) FWD	TGCTGTGCCTCAAGCCAGTG
Nerve Growth Factor alpha (NGF)	Nerve Growth Factor alpha (NGF) BKD	CAGTGATGTTGCGGGTCTGC
	Alpha 2C Adrenergic Receptor FWD	CCAGCCAGCTCTTCAACTTC
Alpha 2C Adrenergic Receptor	Alpha 2C Adrenergic Receptor BKD	GGCTCATGTGTCCCTCTCAG
	NMDA Receptor 1 FWD	AGCAACGCAAGCCCTGTGAC
NMDA Receptor 1	NMDA Receptor 1 BKD	ATCCGCTTCGACTCGCTACG
	Creb3 FWD	GTGTTCTGGTCCTCGTGTTC
Creb3	Creb3 BKD	GAAGGGCTGTGGTTAGGTTG
	Pomc FWD	GGCCTGACACGTGGAAGATG
Pomc	Pomc BKD	CAGCACTGCTGCTGTTCCTG
	Actin FWD	CAGCCAGGCTGTGCTGTCCCTGTATGC
β-Actin	Actin BKD	GATCTTCATGGTGCTAGGAGCCAGAGC

All the PCR reactions were performed on a Rotor-Gene 6000 (Corbett Research™) Real-Time PCR machine. For every reaction, the same program was used:

- 15min 95°C

- 45 repeats cycles:
  - 15s denaturation at 94°C
  - 30s annealing at 60°C
  - 30s elongation at 72°C

- melt from 72°C to 95°C, with 5s hold at each step

5.10.3 Quantitative Real-Time PCR analysis of 27 selected genes

These Real-Time PCR measurements were performed on the brainstems, cortices, hippocampi, cerebelli and dorsal root ganglia of 6 operated and 6 control mice for the surgical pain model, as well as on the cortices and the spinal cords of 6 mice, which underwent an intraperitoneal injection of CFA, ans 6 control mice, which received an intraperitoneal injection with medium, for the inflammatory pain model. All the mRNA samples were reverse transcribed into cDNA as previously described.

The primers of the 27 genes analyzed in these Real-Time PCR measurements are listed in Table 2. Each primer was diluted to a final concentration of 10mM.

In a 96 well plate (BRAND), the cDNAs were diluted 20 times. All the wells from the column contained 20µl 1/20 cDNA of one specific sample. For each sample, the PCR master mixes were prepared as follows: 500µl QuantiTect™ SYBR® Green PCR Master Mix (Qiagen®), 50µl Forward (FWD) Primer, 50µl Backwards (BKD) Primer. Each Master Mix was specific for a gene and was then distributed in the 8 wells of a 96 well plate column (BRAND), at a volume of 65µl Master Mix / well.

The content of the cDNA 96-well plates and the Master Mixes 96-well plates were then mixed in a 384-well plate (Genetix®) by a Beckman FX plate pipetting robot according to a specific design. Basically, each well contained 8µl cDNA 1/20 and 12 µl Real-Time PCR MasterMix. Every well across the same row of the plate contained the same cDNA. And every well across a same column contained a Master Mix specific for one gene. Every column was pipetted in duplicates. With this design, every sample and negative controls were pipetted in duplicates, to bettor monitor eventual artifacts in the reaction.

Gene Name	Primer Names	Primer Sequence
	IL6_FWD	CCAACAGACCTGTCTATACC
Interleukin 6 IL6	IL6_BKD	GGACTCTGGCTTTGTCTTTC
	HSP70_FWD	GTGACAGCTGAAGACAAAGG
Heat Shock Protein HSP70	HSP70_BKD	GGCTTTCCAGCCATTCAATC
	5HTr3A_FWD	TACAGCGGCCAGTACCTGAC
Serotonin Receptor 5-HTr3A	5HTr3A_BKD	AGTGGCGGATGGAGGATAGC
	Tac1_FWD	ACCAGATCAAGGAGGCAATG
Tachykinin 1 Tac1	Tac1_BKD	ACTGCTCACTGACACAGATG
	TacR1_FWD	GCCCTGGGAACCTATAACTG
Tachykinin Receptor 1 TacR1	TacR1_BKD	CAACAAGAGCGATGGCACTG
	Runx1_FWD	CCAGGGACATTCGGTCTTAG
Runt related transcription factor 1Runx1	Runx1_BKD	TACCGACCTGGCTGAAAGAG
	Oprs1_FWD	AGCTGCAGTGGGTATTTGTG
Opioid receptor sigma 1 Oprs1	Oprs1_BKD	AAGTGTCGGCTAGTGCAAAG
	OprD1_FWD	CAAGGCTGTGCTCTCCATTG
Opioid receptor delta 1Oprd1	OprD1_BKD	GCAGTAGCATGAGGCCATAG
	Gabrg2_FWD	CCTGACATCGGAGTGAAACC
GABA A receptor, subunit gamma 2 Gabrg2	Gabrg2_BKD	GCAGGAGTGTTCATCCATTG
	Npy_FWD	GCTAGGTAACAAGCGAATGG
Neuropeptide Y	Npy_BKD	GATGAGATGAGGGTGGAAAC
	TprV2_FWD	TCCTCACCTACGTCCTACTG
Transient receptor potential cation channel, subfamily V, member 2 TrpV2	TprV2_BKD	CCTCTGAGGCACTGTTCTTC
	Npy5r_FWD	AAGCAGAAGCGACCGCACTC
Neuropeptide Y Receptor Type 5 NPY5R	Npy5r_BKD	CTACGCTGCCTCTATAGTCC
	Slc6a1_GABAtr1_FWD	CTCGTGCCGTAGCTTCTTAG
Solute carrier family 6 (neurotransmitter transporter, GABA), member 1	Slc6a1_GABAtr1_BKD	GGGAAGAGCTGGTAGATTGC
	MapK1_FWD	CTGCATACTGGTGTCATTGG
Map Kinase 1 (Erk2)	MapK1_BKD	CTATGTGGCATGCAGTGTAG
	Pomc_FWD	GGCCTGACACGTGGAAGATG
Proopiomelanocortin	Pomc_BKD	CAGCACTGCTGCTGTTCCTG
	5HTr1d_FWD	TGGGTGCTGGTGGGTGTTTC
Serotonin Receptor 5HTr1d	5HTr1d_BKD	TGTCCTGCTGACGGCTTTGC
	Creb3_FWD	GTGTTCTGGTCCTCGTGTTC
cAMP responsive element binding protein 3 Creb3	Creb3_BKD	GAAGGGCTGTGGTTAGGTTG
	5HTr1A_FWD	CCCTTCAGCTGTATCTTTCC
Serotonin Receptor 5-HTr1A	5HTr1A_BKD	GTGCGTCTTCTCCACAGAAC
	Oprm1_FWD	ACGGCTAATACAGTGGATCG
Opioid Receptor mu 1 Oprm1	Oprm1_BKD	AACACGCAATACGGCAAACC
	NTRK3_FWD	GCATGTCCAGGGACGTCTAC
neurotrophic tyrosine kinase, receptor, type 3 NTRK3	NTRK3_BKD	TAGGGCAGACTCTGGGTCTC
	Prkcc_FWD	AGCTGTGGCCATCTGCAAAG
Protein Kinase C Gamma Prkcc	Prkcc_BKD	GCATCTGGGTGCACGAAGTC
	DREAM_FWD	GATAAGGGAGGTCCTTAGAG
Kv channel interacting protein 3, calsenilin Dream	DREAM_BKD	TAAGGGATGCAGCAGGTTAG
	LIF_FWD	CCACGGCAACCTCATGAACC
Leukemia Inhibiting Factor LIF	LIF_BKD	TTGCACAGACGGCAAAGCAC
	BDNF_FWD	CAGGCAGAATGAGCAATGTC
Brain Derived Neurotrophic Factor BDNF	BDNF_BKD	CCATAGAAGTGAGGGACTCA
	5HTr4_FWD	TCCTCTGGCTTGGCTATATC
Serotonin Receptor 5-HTr4	5HTr4_BKD	CTTAGGACTGGCTTCGTTTC
	5HTr2C_FWD	CCTGTCTCTGCTTGCAATTC
Serotonin Receptor 5-Htr2C	5HTr2C_BKD	GTCATTGAGCACGCAGGTAG
	NPY6r_FWD	ACTCCAACTCCAGGGAATAG
Neuropeptide Y Receptor Type 6 NPY6r	NPY6r_BKD	TAGGTGTTGGCTGGTTTGTG

Table 1: Primers used for the Real-Time PCR of 27 selected genes. The primers are noted in the 5'- 3' direction.

5.10.4 Data interpretation

In all the Real-Time PCR reactions, the Ct value of each sample was normalized to the Ct value of the β-Actin gene for the same sample, to obtain the sample's ΔCt value. The mean of the normalized Ct values of the 6 operated animals, as well as the one of the 6 control animals were then calculated. The ΔΔCt was then calculated as follows:

$\Delta\Delta Ct = Mean(\Delta Ct_{OPERATED\ ANIMALS}) - Mean(\Delta Ct_{CONTROL\ ANIMALS})$

The fold change (FC) of each gene's expression level in the operated animals was calculated as follows:

$FC = 2^{-(\Delta\Delta Ct)}$

5.11 GeneChip® Mouse Exon 1.0 ST Arrays

5.11.1 cRNA preparation

The quality of the isolated RNA was determined with a NanoDrop ND 1000 (NanoDrop Technologies, Delaware, USA) and a Bioanalyzer 2100 (Agilent, Waldbronn, Germany). The cDNA was prepared from total RNA using a primer mix and reverse transcriptase (RT) (WTOvation Pico System, NuGEN, 3300-12). The primers have a DNA portion that hybridizes either to the 5' portion of the poly (A) sequence or randomly across the transcript. SPIA amplification, a linear isothermal DNA amplification process, was used to prepare single-stranded cDNA in the antisense direction of the mRNA starting material. Single-stranded cDNA quality and
quantity was determined using NanoDrop ND 1000 and Bioanalyzer 2100. Single-stranded cDNA (3ug) was converted into sense target cDNA (ST-cDNA) using WT-Ovation™ Exon (Cat # 2000-12). Fragmented and biotin-labeled ST-cDNA targets were generated with the FL- Ovation cDNA Biotin Module V2 (NuGEN, 4200-12).

5.11.2 Hybridization and data processing

Biotin-labeled single-stranded cDNA targets (5ug) were mixed in 220 µl of Hybridization Mix (Affymetrix Inc., P/N 900720) containing a Hybridization Controls and Control Oligonucleotide B2 (Affymetrix Inc., P/N 900454). Samples were hybridized to Affymetrix Mouse Exon 1.0 ST Arrays for 18h at 45°C. Arrays were then washed using an Affymetrix Fluidics Station 450 FS450 0001 protocol. An Affymetrix GeneChip Scanner 3000 (Affymetrix Inc.) was used to measure the fluorescent intensity emitted by the labeled target.

Raw data processing was performed using the Affymetrix AGCC software. After hybridization and scanning, probe cell intensities were calculated and summarized for the respective probe sets using Exon Level: All: RMA Sketch.

5.11.3 Data analysis and Normalization

The raw data from the microarrays have been summarized using RNA algorithm as implemented in "affy" package of BioConductor (Gentleman et al., 2004) and then analyzed using the "exonmap" package (Okoniewski and Miller, 2008; Okoniewski et al., 2007) connected to the X:MAP database (Yates et al., 2008)

The report including all 1.2M probesets with the genes to which they are assigned was created. Each probeset was identified according to genome and Ensembl genes matching as:

- Exonic: matching a known exon in a unique way
- Intronic: matching a known gene in a unique way, but not matching any of known exons
- Intergenic: not matching any of known genes
- Multitarget: matching the genome in more than one place at least with a part of probes belonging to the probeset. Multitarget probesets with several matches to the genome are most likely matching a protein domain, those with many (ca >5) are considered repetitive matches and their expression measurements are usualy close to the saturation level.

For each probeset, the fold change (log2 ratio) and p-value of the t-test have been calculated to filter out the most up and -downregulated probesets. Multi-exonic genes with several probesets showing consistently significant fold change (eg FC(log2) >1) have been selected as a potential targets for furter investigation. For genes with small number of exons, just one probesets is Enough to consider regard the gene as significantly expressed.

5.11.4 Clustering analysis

A bi-clustering using Genevestigator® (Nebion™) (Hruz, 2008) was performed. The lists of up- and downregulated genes were uploaded in the Clustering toolset, and clustered according to the "Stimulus" criterion. The meta analysis was carried out on the data obtained with Affymetrix Mouse 430_2: 40k Arrays. A total of 2974 datasets were included in the study among which 2591 were GEO datasets, 157 came from the ArrayExpress database, 208 from the Neuroscience Microarray Consortium, and 18 from other sources. All the data were normalized according to the GCOS algorithm (GeneChip® Operating Software, Affymetrix™). In the clusterings, the BiMax algorithm grouped genes, which showed similar regulation profiles after specific stimuli listed in Genevestigator.

Two clusterings were performed for the genes, which had 3 or more downregulated exons on the microarray analysis: one to group the genes,

which were similarly upregulated after specific stimuli, and one to group the genes, which were similarly upregulated after specific stimuli. Similar clusterings were performed for the genes, which had 3 or more downregulated exons on the microarray analysis. A literature search was then performed to understand which cellular process was triggered by the stimuli, to which the clustered genes reacted.

6. Literature

Akitsuki, Y., and Decety, J. (2009). Social context and perceived agency affects empathy for pain: an event-related fMRI investigation. Neuroimage *47*, 722-734.

Akopians, A.L., Babayan, A.H., Beffert, U., Herz, J., Basbaum, A.I., and Phelps, P.E. (2008). Contribution of the Reelin signaling pathways to nociceptive processing. Eur J Neurosci *27*, 523-537.

Albe-Fessard, D., Berkley, K.J., Kruger, L., Ralston, H.J., 3rd, and Willis, W.D., Jr. (1985). Diencephalic mechanisms of pain sensation. Brain Res *356*, 217-296.

Antony, V.B., Sahn, S.A., Antony, A.C., and Repine, J.E. (1985). Bacillus Calmette-Guerin-stimulated neutrophils release chemotaxins for monocytes in rabbit pleural spaces and in vitro. J Clin Invest *76*, 1514-1521.

Apkarian, A.V., Bushnell, M.C., Treede, R.D., and Zubieta, J.K. (2005). Human brain mechanisms of pain perception and regulation in health and disease. Eur J Pain *9*, 463-484.

Arras, M. (2007). Improvement of Pain Therapy in laboratory mice.
Laboratory Mice ALTEX, 3.

Arras, M., Rettich, A., Cinelli, P., Kasermann, H.P., and Burki, K. (2007). Assessment of post-laparotomy pain in laboratory mice by telemetric recording of heart rate and heart rate variability. BMC Vet Res *3*, 16.

Arvidsson, J., Raappana, P., Diez, M., and Hokfelt, T. (1994). Expression of neuropeptides in the rat mesencephalic trigeminal nucleus after peripheral axotomy. Neuroreport *5*, 1269-1272.

Barnes, N.M., and Sharp, T. (1999). A review of central 5-HT receptors and their function. Neuropharmacology *38*, 1083-1152.

Barthet, G., Framery, B., Gaven, F., Pellissier, L., Reiter, E., Claeysen, S., Bockaert, J., and Dumuis, A. (2007). 5-hydroxytryptamine 4 receptor activation of the extracellular signal-regulated kinase pathway depends on Src activation but not on G protein or beta-arrestin signaling. Mol Biol Cell *18*, 1979-1991.

Bautista, D.M., Siemens, J., Glazer, J.M., Tsuruda, P.R., Basbaum, A.I., Stucky, C.L., Jordt, S.E., and Julius, D. (2007). The menthol receptor TRPM8 is the principal detector of environmental cold. Nature *448*, 204-208.

Bessou, P., Burgess, P.R., Perl, E.R., and Taylor, C.B. (1971). Dynamic properties of mechanoreceptors with unmyelinated (C) fibers. J Neurophysiol *34*, 116-131.

Bhutta, A.T., Rovnaghi, C., Simpson, P.M., Gossett, J.M., Scalzo, F.M., and Anand, K.J. (2001). Interactions of inflammatory pain and morphine in infant rats: long-term behavioral effects. Physiol Behav *73*, 51-58.

Bloedel, J.R., and Bracha, V. (1997). Duality of cerebellar motor and cognitive functions. Int Rev Neurobiol *41*, 613-634.

Burnstock, G. (1981). Review lecture. Neurotransmitters and trophic factors in the autonomic nervous system. J Physiol *313*, 1-35.

Burstein, R., Cliffer, K.D., and Giesler, G.J., Jr. (1990a). Cells of origin of the spinohypothalamic tract in the rat. J Comp Neurol *291*, 329-344.

Burstein, R., Dado, R.J., and Giesler, G.J., Jr. (1990b). The cells of origin of the spinothalamic tract of the rat: a quantitative reexamination. Brain Res *511*, 329-337.

Carrion, A.M., Mellstrom, B., and Naranjo, J.R. (1998). Protein kinase A-dependent derepression of the human prodynorphin gene via differential binding to an intragenic silencer element. Mol Cell Biol *18*, 6921-6929.

Casey, K.L., Svensson, P., Morrow, T.J., Raz, J., Jone, C., and Minoshima, S. (2000). Selective opiate modulation of nociceptive processing in the human brain. J Neurophysiol *84*, 525-533.

Caterina, M.J., Leffler, A., Malmberg, A.B., Martin, W.J., Trafton, J., Petersen-Zeitz, K.R., Koltzenburg, M., Basbaum, A.I., and Julius, D. (2000). Impaired nociception and pain sensation in mice lacking the capsaicin receptor. Science *288*, 306-313.

Caterina, M.J., Rosen, T.A., Tominaga, M., Brake, A.J., and Julius, D. (1999). A capsaicin-receptor homologue with a high threshold for noxious heat. Nature *398*, 436-441.

Caterina, M.J., Schumacher, M.A., Tominaga, M., Rosen, T.A., Levine, J.D., and Julius, D. (1997). The capsaicin receptor: a heat-activated ion channel in the pain pathway. Nature *389*, 816-824.

Chen, Q., Smith, G.M., and Shine, H.D. (2008). Immune activation is required for NT-3-induced axonal plasticity in chronic spinal cord injury. Exp Neurol *209*, 497-509.

Cheng, H.Y., Pitcher, G.M., Laviolette, S.R., Whishaw, I.Q., Tong, K.I., Kockeritz, L.K., Wada, T., Joza, N.A., Crackower, M., Goncalves, J.*, et al.* (2002). DREAM is a critical transcriptional repressor for pain modulation. Cell *108*, 31-43.

Chiogna, M., Massa, M.S., Risso, D., and Romualdi, C. (2009). A comparison on effects of normalisations in the detection of differentially expressed genes. BMC Bioinformatics *10*, 61.

Chiu, C.S., Brickley, S., Jensen, K., Southwell, A., McKinney, S., Cull-Candy, S., Mody, I., and Lester, H.A. (2005). GABA transporter deficiency causes tremor, ataxia, nervousness, and increased GABA-induced tonic conductance in cerebellum. J Neurosci *25*, 3234-3245.

Cinelli, P., Arras, M., and Buerki, K. (2006). Detection of pain and stress by monitoring gene expression. ALTEX *23 Suppl*, 416-419.

Clark, T.A., Schweitzer, A.C., Chen, T.X., Staples, M.K., Lu, G., Wang, H., Williams, A., and Blume, J.E. (2007). Discovery of tissue-specific exons using comprehensive human exon microarrays. Genome Biol *8*, R64.

Colantuoni, C., Henry, G., Zeger, S., and Pevsner, J. (2002). SNOMAD (Standardization and NOrmalization of MicroArray Data): web-accessible gene expression data analysis. Bioinformatics *18*, 1540-1541.

Colburn, R.W., Lubin, M.L., Stone, D.J., Jr., Wang, Y., Lawrence, D., D'Andrea, M.R., Brandt, M.R., Liu, Y., Flores, C.M., and Qin, N. (2007). Attenuated cold sensitivity in TRPM8 null mice. Neuron *54*, 379-386.

Collins, W.R., Jr., Nulsen, F.E., and Randt, C.T. (1960). Relation of peripheral nerve fiber size and sensation in man. Arch Neurol *3*, 381-385.

Corey, D.P., and Garcia-Anoveros, J. (1996). Mechanosensation and the DEG/ENaC ion channels. Science *273*, 323-324.

Costigan, M., and Woolf, C.J. (2002). No DREAM, No pain. Closing the spinal gate. Cell *108*, 297-300.

Couture, R., Harrisson, M., Vianna, R.M., and Cloutier, F. (2001). Kinin receptors in pain and inflammation. Eur J Pharmacol *429*, 161-176.

Cox, J.J., Reimann, F., Nicholas, A.K., Thornton, G., Roberts, E., Springell, K., Karbani, G., Jafri, H., Mannan, J., Raashid, Y*., et al.* (2006). An SCN9A channelopathy causes congenital inability to experience pain. Nature *444*, 894-898.

Dhaka, A., Murray, A.N., Mathur, J., Earley, T.J., Petrus, M.J., and Patapoutian, A. (2007). TRPM8 is required for cold sensation in mice. Neuron *54*, 371-378.

Djouhri, L., Bleazard, L., and Lawson, S.N. (1998). Association of somatic action potential shape with sensory receptive properties in guinea-pig dorsal root ganglion neurones. J Physiol *513 (Pt 3)*, 857-872.

Djouhri, L., and Lawson, S.N. (2001). Differences in the size of the somatic action potential overshoot between nociceptive and non-nociceptive dorsal root ganglion neurones in the guinea-pig. Neuroscience *108*, 479-491.

Dombkowski, A.A., Thibodeau, B.J., Starcevic, S.L., and Novak, R.F. (2004). Gene-specific dye bias in microarray reference designs. FEBS Lett *560*, 120-124.

Drosopoulos, N.E., Walsh, F.S., and Doherty, P. (1999). A soluble version of the receptor-like protein tyrosine phosphatase kappa stimulates neurite outgrowth via a Grb2/MEK1-dependent signaling cascade. Mol Cell Neurosci *13*, 441-449.

Enthoven, L., de Kloet, E.R., and Oitzl, M.S. (2008). Differential development of stress system (re)activity at weaning dependent on time of disruption of maternal care. Brain Res *1217*, 62-69.

Fields, H.L. (1985). Nociceptive Transmission: The Pain System. Science *228*, 1522.

Fields, H.L. (2000). Pain modulation: expectation, opioid analgesia and virtual pain. Prog Brain Res *122*, 245-253.

Fields, H.L., Bry, J., Hentall, I., and Zorman, G. (1983). The activity of neurons in the rostral medulla of the rat during withdrawal from noxious heat. J Neurosci *3*, 2545-2552.

Fields, H.L., Malick, A., and Burstein, R. (1995). Dorsal horn projection targets of ON and OFF cells in the rostral ventromedial medulla. J Neurophysiol *74*, 1742-1759.

Fu, K.Y., Tan, Y.H., Sung, B., and Mao, J. (2009). Peripheral formalin injection induces unique spinal cord microglial phenotypic changes. Neurosci Lett *449*, 234-239.

Galeotti, N., Ghelardini, C., and Bartolini, A. (1997). 5-HT1A agonists induce central cholinergic antinociception. Pharmacol Biochem Behav *57*, 835-841.

Garcia-Anoveros, J., and Corey, D.P. (1996). Touch at the molecular level. Mechanosensation. Curr Biol *6*, 541-543.

Garcia-Anoveros, J., Ma, C., and Chalfie, M. (1995). Regulation of Caenorhabditis elegans degenerin proteins by a putative extracellular domain. Curr Biol *5*, 441-448.

Garcia-Anoveros, J., Samad, T.A., Zuvela-Jelaska, L., Woolf, C.J., and Corey, D.P. (2001). Transport and localization of the DEG/ENaC ion channel BNaC1alpha to peripheral mechanosensory terminals of dorsal root ganglia neurons. J Neurosci *21*, 2678-2686.

Geha, P.Y., Baliki, M.N., Chialvo, D.R., Harden, R.N., Paice, J.A., and Apkarian, A.V. (2007). Brain activity for spontaneous pain of postherpetic neuralgia and its modulation by lidocaine patch therapy. Pain *128*, 88-100.

Gentleman, R.C., Carey, V.J., Bates, D.M., Bolstad, B., Dettling, M., Dudoit, S., Ellis, B., Gautier, L., Ge, Y., Gentry, J.*, et al.* (2004). Bioconductor: open software development for computational biology and bioinformatics. Genome Biol *5*, R80.

Gillet, G., Ammor, S., and Fillion, G. (1985). Serotonin inhibits acetylcholine release from rat striatum slices: evidence for a presynaptic receptor-mediated effect. J Neurochem *45*, 1687-1691.

Green, G.M., Scarth, J., and Dickenson, A. (2000). An excitatory role for 5-HT in spinal inflammatory nociceptive transmission; state-dependent actions via dorsal horn 5-HT(3) receptors in the anaesthetized rat. Pain *89*, 81-88.

Grove, K.L., Campbell, R.E., Ffrench-Mullen, J.M., Cowley, M.A., and Smith, M.S. (2000). Neuropeptide Y Y5 receptor protein in the cortical/limbic system and brainstem of the rat: expression on gamma-aminobutyric acid and corticotropin-releasing hormone neurons. Neuroscience *100*, 731-740.

Hackler, E.A., Airey, D.C., Shannon, C.C., Sodhi, M.S., and Sanders-Bush, E. (2006). 5-HT(2C) receptor RNA editing in the amygdala of C57BL/6J, DBA/2J, and BALB/cJ mice. Neurosci Res *55*, 96-104.

Hampson, A.J., Bornheim, L.M., Scanziani, M., Yost, C.S., Gray, A.T., Hansen, B.M., Leonoudakis, D.J., and Bickler, P.E. (1998). Dual effects of anandamide on NMDA receptor-mediated responses and neurotransmission. J Neurochem *70*, 671-676.

Heinricher, M.M., Haws, C.M., and Fields, H.L. (1991). Evidence for GABA-mediated control of putative nociceptive modulating neurons in the rostral ventromedial medulla: iontophoresis of bicuculline eliminates the off-cell pause. Somatosens Mot Res *8*, 215-225.

Heinricher, M.M., and Kaplan, H.J. (1991). GABA-mediated inhibition in rostral ventromedial medulla: role in nociceptive modulation in the lightly anesthetized rat. Pain *47*, 105-113.

Heinricher, M.M., Morgan, M.M., and Fields, H.L. (1992). Direct and indirect actions of morphine on medullary neurons that modulate nociception. Neuroscience *48*, 533-543.

Heinricher, M.M., Morgan, M.M., Tortorici, V., and Fields, H.L. (1994). Disinhibition of off-cells and antinociception produced by an opioid action within the rostral ventromedial medulla. Neuroscience *63*, 279-288.

Hermann, D.M., Luppi, P.H., Peyron, C., Hinckel, P., and Jouvet, M. (1997). Afferent projections to the rat nuclei raphe magnus, raphe pallidus and reticularis gigantocellularis

pars alpha demonstrated by iontophoretic application of choleratoxin (subunit b). J Chem Neuroanat *13*, 1-21.

Hester, S.D., Reid, L., Nowak, N., Jones, W.D., Parker, J.S., Knudtson, K., Ward, W., Tiesman, J., and Denslow, N.D. (2009). Comparison of comparative genomic hybridization technologies across microarray platforms. J Biomol Tech *20*, 135-151.

Hohmann, A.G., Suplita, R.L., Bolton, N.M., Neely, M.H., Fegley, D., Mangieri, R., Krey, J.F., Walker, J.M., Holmes, P.V., Crystal, J.D.*, et al.* (2005). An endocannabinoid mechanism for stress-induced analgesia. Nature *435*, 1108-1112.

Holloway, A.J., van Laar, R.K., Tothill, R.W., and Bowtell, D.D. (2002). Options available--from start to finish--for obtaining data from DNA microarrays II. Nat Genet *32 Suppl*, 481-489.

Holmes, A. (2008). Genetic variation in cortico-amygdala serotonin function and risk for stress-related disease. Neurosci Biobehav Rev *32*, 1293-1314.

Horvath, R.J., and DeLeo, J.A. (2009). Morphine enhances microglial migration through modulation of P2X4 receptor signaling. J Neurosci *29*, 998-1005.

Hovatta, I., Tennant, R.S., Helton, R., Marr, R.A., Singer, O., Redwine, J.M., Ellison, J.A., Schadt, E.E., Verma, I.M., Lockhart, D.J.*, et al.* (2005). Glyoxalase 1 and glutathione reductase 1 regulate anxiety in mice. Nature *438*, 662-666.

Hruz (2008). Genevestigator V3: a reference expression database for the meta-analysis of transcriptomes. Advances in Bioinformatics *420747*

Ignarro, L.J., Buga, G.M., Wood, K.S., Byrns, R.E., and Chaudhuri, G. (1987). Endothelium-derived relaxing factor produced and released from artery and vein is nitric oxide. Proc Natl Acad Sci U S A *84*, 9265-9269.

Ikeda, H., Kiritoshi, T., and Murase, K. (2009). Synaptic plasticity in the spinal dorsal horn. Neurosci Res *64*, 133-136.

Illi, A., Setala-Soikkeli, E., Viikki, M., Poutanen, O., Huhtala, H., Mononen, N., Lehtimaki, T., Leinonen, E., and Kampman, O. (2009). 5-HTR1A, 5-HTR2A, 5-HTR6, TPH1 and TPH2 polymorphisms and major depression. Neuroreport *20*, 1125-1128.

Inokoshi, J., Katagiri, M., Arima, S., Tanaka, H., Hayashi, M., Kim, Y.B., Furumai, R., Yoshida, M., Horinouchi, S., and Omura, S. (1999). Neuronal differentiation of neuro 2a cells by inhibitors of cell cycle progression, trichostatin A and butyrolactone I. Biochem Biophys Res Commun *256*, 372-376.

Ito, A., Kumamoto, E., Takeda, M., Shibata, K., Sagai, H., and Yoshimura, M. (2000). Mechanisms for ovariectomy-induced hyperalgesia and its relief by calcitonin: participation of 5-HT1A-like receptor on C-afferent terminals in substantia gelatinosa of the rat spinal cord. J Neurosci *20*, 6302-6308.

Ji, R.R., Samad, T.A., Jin, S.X., Schmoll, R., and Woolf, C.J. (2002). p38 MAPK activation by NGF in primary sensory neurons after inflammation increases TRPV1 levels and maintains heat hyperalgesia. Neuron *36*, 57-68.

Johnson, G.L., and Lapadat, R. (2002). Mitogen-activated protein kinase pathways mediated by ERK, JNK, and p38 protein kinases. Science *298*, 1911-1912.

Julius, D., and Basbaum, A.I. (2001). Molecular mechanisms of nociception. Nature *413*, 203-210.

Kafatos, F.C., Jones, C.W., and Efstratiadis, A. (1979). Determination of nucleic acid sequence homologies and relative concentrations by a dot hybridization procedure. Nucleic Acids Res *7*, 1541-1552.

Kato, A., and Touhara, K. (2009). Mammalian olfactory receptors: pharmacology, G protein coupling and desensitization. Cell Mol Life Sci.

Kenney, A.M., and Kocsis, J.D. (1998). Peripheral axotomy induces long-term c-Jun amino-terminal kinase-1 activation and activator protein-1 binding activity by c-Jun and junD in adult rat dorsal root ganglia In vivo. J Neurosci *18*, 1318-1328.

Kishi, T., Tsunoka, T., Ikeda, M., Kawashima, K., Okochi, T., Kitajima, T., Kinoshita, Y., Okumura, T., Yamanouchi, Y., Inada, T.*, et al.* (2009). Serotonin 1A receptor gene and major depressive disorder: an association study and meta-analysis. J Hum Genet.

Koerber, H.R., Druzinsky, R.E., and Mendell, L.M. (1988). Properties of somata of spinal dorsal root ganglion cells differ according to peripheral receptor innervated. J Neurophysiol *60*, 1584-1596.

Kohno, T., Wang, H., Amaya, F., Brenner, G.J., Cheng, J.K., Ji, R.R., and Woolf, C.J. (2008). Bradykinin enhances AMPA and NMDA receptor activity in spinal cord dorsal horn neurons by activating multiple kinases to produce pain hypersensitivity. J Neurosci *28*, 4533-4540.

Koltai, H., and Weingarten-Baror, C. (2008). Specificity of DNA microarray hybridization: characterization, effectors and approaches for data correction. Nucleic Acids Res *36*, 2395-2405.

Koltzenburg, M., Stucky, C.L., and Lewin, G.R. (1997). Receptive properties of mouse sensory neurons innervating hairy skin. J Neurophysiol *78*, 1841-1850.

Krishtal, O.A., Marchenko, S.M., Obukhov, A.G., and Volkova, T.M. (1988). Receptors for ATP in rat sensory neurones: the structure-function relationship for ligands. Br J Pharmacol *95*, 1057-1062.

Kunert-Keil, C., Bisping, F., Kruger, J., and Brinkmeier, H. (2006). Tissue-specific expression of TRP channel genes in the mouse and its variation in three different mouse strains. BMC Genomics *7*, 159.

Kusy, S., Funkelstein, L., Bourgais, D., Drabkin, H., Rougon, G., Roche, J., and Castellani, V. (2003). Redundant functions but temporal and regional regulation of two alternatively spliced isoforms of semaphorin 3F in the nervous system. Mol Cell Neurosci *24*, 409-418.

Kwan, K.Y., Glazer, J.M., Corey, D.P., Rice, F.L., and Stucky, C.L. (2009). TRPA1 modulates mechanotransduction in cutaneous sensory neurons. J Neurosci *29*, 4808-4819.

Lacroix-Fralish, M.L., Ledoux, J.B., and Mogil, J.S. (2007). The Pain Genes Database: An interactive web browser of pain-related transgenic knockout studies. Pain *131*, 3 e1-4.

Landau, W., and Bishop, G.H. (1953). Pain from dermal, periosteal, and fascial endings and from inflammation; electrophysiological study employing differential nerve blocks. AMA Arch Neurol Psychiatry *69*, 490-504.

Lawson, S.N. (1979). The postnatal development of large light and small dark neurons in mouse dorsal root ganglia: a statistical analysis of cell numbers and size. J Neurocytol *8*, 275-294.

Lawson, S.N., and Biscoe, T.J. (1979). Development of mouse dorsal root ganglia: an autoradiographic and quantitative study. J Neurocytol *8*, 265-274.

Lawson, S.N., Crepps, B.A., and Perl, E.R. (1997). Relationship of substance P to afferent characteristics of dorsal root ganglion neurones in guinea-pig. J Physiol *505 (Pt 1)*, 177-191.

Lawson, S.N., and Waddell, P.J. (1991). Soma neurofilament immunoreactivity is related to cell size and fibre conduction velocity in rat primary sensory neurons. J Physiol *435*, 41-63.

Lazarewicz, J.W., Wroblewski, J.T., and Costa, E. (1990). N-methyl-D-aspartate-sensitive glutamate receptors induce calcium-mediated arachidonic acid release in primary cultures of cerebellar granule cells. J Neurochem *55*, 1875-1881.

Leenaars, M., Koedam, M.A., Hendriksen, C.F., and Claassen, E. (1998). Immune responses and side effects of five different oil-based adjuvants in mice. Vet Immunol Immunopathol *61*, 291-304.

Leith, J.L., Wilson, A.W., Donaldson, L.F., and Lumb, B.M. (2007). Cyclooxygenase-1-derived prostaglandins in the periaqueductal gray differentially control C- versus A-fiber-evoked spinal nociception. J Neurosci *27*, 11296-11305.

Lenze, E.J., Shardell, M., Ferrell, R.E., Orwig, D., Yu-Yahiro, J., Hawkes, W., Fredman, L., Miller, R., and Magaziner, J. (2008). Association of serotonin-1A and 2A receptor promoter polymorphisms with depressive symptoms and functional recovery in elderly persons after hip fracture. J Affect Disord *111*, 61-66.

Li, D.P., Chen, S.R., and Pan, H.L. (2004). VR1 receptor activation induces glutamate release and postsynaptic firing in the paraventricular nucleus. J Neurophysiol *92*, 1807-1816.

Lidow, M.S., Song, Z.M., and Ren, K. (2001). Long-term effects of short-lasting early local inflammatory insult. Neuroreport *12*, 399-403.

Lin, S., Boey, D., and Herzog, H. (2004). NPY and Y receptors: lessons from transgenic and knockout models. Neuropeptides *38*, 189-200.

Lingueglia, E., de Weille, J.R., Bassilana, F., Heurteaux, C., Sakai, H., Waldmann, R., and Lazdunski, M. (1997). A modulatory subunit of acid sensing ion channels in brain and dorsal root ganglion cells. J Biol Chem *272*, 29778-29783.

Loeser, J.D., and Treede, R.D. (2008). The Kyoto protocol of IASP Basic Pain Terminology. Pain *137*, 473-477.

Loyd, D.R., and Murphy, A.Z. (2009). The role of the periaqueductal gray in the modulation of pain in males and females: are the anatomy and physiology really that different? Neural Plast *2009*, 462879.

Lyons, P. (2003). Advances in spotted microarray resources for expression profiling. Brief Funct Genomic Proteomic *2*, 21-30.

Ma, Q., Jones, D., Borghesani, P.R., Segal, R.A., Nagasawa, T., Kishimoto, T., Bronson, R.T., and Springer, T.A. (1998). Impaired B-lymphopoiesis, myelopoiesis, and derailed cerebellar neuron migration in CXCR4- and SDF-1-deficient mice. Proc Natl Acad Sci U S A *95*, 9448-9453.

Mantyh, P.W., DeMaster, E., Malhotra, A., Ghilardi, J.R., Rogers, S.D., Mantyh, C.R., Liu, H., Basbaum, A.I., Vigna, S.R., Maggio, J.E*., et al.* (1995). Receptor endocytosis and dendrite reshaping in spinal neurons after somatosensory stimulation. Science *268*, 1629-1632.

Mantyh, P.W., Rogers, S.D., Honore, P., Allen, B.J., Ghilardi, J.R., Li, J., Daughters, R.S., Lappi, D.A., Wiley, R.G., and Simone, D.A. (1997). Inhibition of hyperalgesia by ablation of lamina I spinal neurons expressing the substance P receptor. Science *278*, 275-279.

Marshall, G.E., Shehab, S.A., Spike, R.C., and Todd, A.J. (1996). Neurokinin-1 receptors on lumbar spinothalamic neurons in the rat. Neuroscience *72*, 255-263.

McKemy, D.D., Neuhausser, W.M., and Julius, D. (2002). Identification of a cold receptor reveals a general role for TRP channels in thermosensation. Nature *416*, 52-58.

Mensah-Nyagan, A.G., Meyer, L., Schaeffer, V., Kibaly, C., and Patte-Mensah, C. (2009). Evidence for a key role of steroids in the modulation of pain. Psychoneuroendocrinology.

Moore, K.A., Kohno, T., Karchewski, L.A., Scholz, J., Baba, H., and Woolf, C.J. (2002). Partial peripheral nerve injury promotes a selective loss of GABAergic inhibition in the superficial dorsal horn of the spinal cord. J Neurosci *22*, 6724-6731.

Morales, M., Battenberg, E., and Bloom, F.E. (1998). Distribution of neurons expressing immunoreactivity for the 5HT3 receptor subtype in the rat brain and spinal cord. J Comp Neurol *402*, 385-401.

Muller, U., Steinhoff, U., Reis, L.F., Hemmi, S., Pavlovic, J., Zinkernagel, R.M., and Aguet, M. (1994). Functional role of type I and type II interferons in antiviral defense. Science *264*, 1918-1921.

Nagy, I., and Rang, H. (1999). Noxious heat activates all capsaicin-sensitive and also a sub-population of capsaicin-insensitive dorsal root gangion neurons.
. Neuroscience *88*, 3.

Nakamura, F., and Strittmatter, S.M. (1996). P2Y1 purinergic receptors in sensory neurons: contribution to touch-induced impulse generation. Proc Natl Acad Sci U S A *93*, 10465-10470.

Nelson, S.B., Hempel, C., and Sugino, K. (2006). Probing the transcriptome of neuronal cell types. Curr Opin Neurobiol *16*, 571-576.

Nishida, K., Kuchiiwa, S., Oiso, S., Futagawa, T., Masuda, S., Takeda, Y., and Yamada, K. (2008). Up-regulation of matrix metalloproteinase-3 in the dorsal root ganglion of rats with paclitaxel-induced neuropathy. Cancer Sci *99*, 1618-1625.

Okoniewski, M.J., and Miller, C.J. (2008). Comprehensive analysis of affymetrix exon arrays using BioConductor. PLoS Comput Biol *4*, e6.

Okoniewski, M.J., Yates, T., Dibben, S., and Miller, C.J. (2007). An annotation infrastructure for the analysis and interpretation of Affymetrix exon array data. Genome Biol *8*, R79.

Olave, M.J., and Maxwell, D.J. (2003). Axon terminals possessing the alpha 2c-adrenergic receptor in the rat dorsal horn are predominantly excitatory. Brain Res *965*, 269-273.

Paller, C.J., Campbell, C.M., Edwards, R.R., and Dobs, A.S. (2009). Sex-based differences in pain perception and treatment. Pain Med *10*, 289-299.

Persson, A.K., Gebauer, M., Jordan, S., Metz-Weidmann, C., Schulte, A.M., Schneider, H.C., Ding-Pfennigdorff, D., Thun, J., Xu, X.J., Wiesenfeld-Hallin, Z.*, et al.* (2009). Correlational analysis for identifying genes whose regulation contributes to chronic neuropathic pain. Mol Pain *5*, 7.

Pohl, A.A., Sugnet, C.W., Clark, T.A., Smith, K., Fujita, P.A., and Cline, M.S. (2009). Affy Exon Tissues: Exon Levels in Normal Tissues in Human, Mouse, and Rat. Bioinformatics.

Polgar, E., Hughes, D.I., Arham, A.Z., and Todd, A.J. (2005). Loss of neurons from laminas I-III of the spinal dorsal horn is not required for development of tactile allodynia in the spared nerve injury model of neuropathic pain. J Neurosci *25*, 6658-6666.

Polgar, E., and Todd, A.J. (2008). Tactile allodynia can occur in the spared nerve injury model in the rat without selective loss of GABA or GABA(A) receptors from synapses in laminae I-II of the ipsilateral spinal dorsal horn. Neuroscience *156*, 193-202.

Potrebic, S.B., Fields, H.L., and Mason, P. (1994). Serotonin immunoreactivity is contained in one physiological cell class in the rat rostral ventromedial medulla. J Neurosci *14*, 1655-1665.

Prager-Khoutorsky, M., and Spira, M.E. (2009). Neurite retraction and regrowth regulated by membrane retrieval, membrane supply, and actin dynamics. Brain Res *1251*, 65-79.

Price, M.P., Lewin, G.R., McIlwrath, S.L., Cheng, C., Xie, J., Heppenstall, P.A., Stucky, C.L., Mannsfeldt, A.G., Brennan, T.J., Drummond, H.A.*, et al.* (2000). The mammalian sodium channel BNC1 is required for normal touch sensation. Nature *407*, 1007-1011.

Price, M.P., McIlwrath, S.L., Xie, J., Cheng, C., Qiao, J., Tarr, D.E., Sluka, K.A., Brennan, T.J., Lewin, G.R., and Welsh, M.J. (2001). The DRASIC cation channel contributes to the detection of cutaneous touch and acid stimuli in mice. Neuron *32*, 1071-1083.

Priest, B.T., Murphy, B.A., Lindia, J.A., Diaz, C., Abbadie, C., Ritter, A.M., Liberator, P., Iyer, L.M., Kash, S.F., Kohler, M.G.*, et al.* (2005). Contribution of the tetrodotoxin-resistant voltage-gated sodium channel NaV1.9 to sensory transmission and nociceptive behavior. Proc Natl Acad Sci U S A *102*, 9382-9387.

Rebelo, S., Lopes, C., Lima, D., and Reguenga, C. (2009). Expression of a Prrxl1 alternative splice variant during the development of the mouse nociceptive system. Int J Dev Biol *53*, 1089-1095.

Reynolds, D.V. (1969). Surgery in the rat during electrical analgesia induced by focal brain stimulation. Science *164*, 444-445.

Ribeiro, R.A., Vale, M.L., Thomazzi, S.M., Paschoalato, A.B., Poole, S., Ferreira, S.H., and Cunha, F.Q. (2000). Involvement of resident macrophages and mast cells in the writhing nociceptive response induced by zymosan and acetic acid in mice. Eur J Pharmacol *387*, 111-118.

Ritter, A.M., and Mendell, L.M. (1992). Somal membrane properties of physiologically identified sensory neurons in the rat: effects of nerve growth factor. J Neurophysiol *68*, 2033-2041.

Rubino, T., Patrini, G., Parenti, M., Massi, P., and Parolaro, D. (1997). Chronic treatment with a synthetic cannabinoid CP-55,940 alters G-protein expression in the rat central nervous system. Brain Res Mol Brain Res *44*, 191-197.

Ruda, M.A., Ling, Q.D., Hohmann, A.G., Peng, Y.B., and Tachibana, T. (2000). Altered nociceptive neuronal circuits after neonatal peripheral inflammation. Science *289*, 628-631.

Sauer, U., Bodrossy, L., and Preininger, C. (2009). Evaluation of substrate performance for a microbial diagnostic microarray using a four parameter ranking. Anal Chim Acta *632*, 240-246.

Sawada, Y., Hosokawa, H., Hori, A., Matsumura, K., and Kobayashi, S. (2007). Cold sensitivity of recombinant TRPA1 channels. Brain Res *1160*, 39-46.

Schaefer, D.C., Asner, I.N., Seifert, B., Burki, K., and Cinelli, P. (2009). Analysis of physiological and behavioural parameters in mice after toe clipping as newborns. Lab Anim.

Schambra, U.B., Mackensen, G.B., Stafford-Smith, M., Haines, D.E., and Schwinn, D.A. (2005). Neuron specific alpha-adrenergic receptor expression in human cerebellum: implications for emerging cerebellar roles in neurologic disease. Neuroscience *135*, 507-523.

Scheinin, M., Lomasney, J.W., Hayden-Hixson, D.M., Schambra, U.B., Caron, M.G., Lefkowitz, R.J., and Fremeau, R.T., Jr. (1994). Distribution of alpha 2-adrenergic receptor subtype gene expression in rat brain. Brain Res Mol Brain Res *21*, 133-149.

Schena, M., Shalon, D., Davis, R.W., and Brown, P.O. (1995). Quantitative monitoring of gene expression patterns with a complementary DNA microarray. Science *270*, 467-470.

Schmidt, M.V., Levine, S., Oitzl, M.S., van der Mark, M., Muller, M.B., Holsboer, F., and de Kloet, E.R. (2005). Glucocorticoid receptor blockade disinhibits pituitary-adrenal activity during the stress hyporesponsive period of the mouse. Endocrinology *146*, 1458-1464.

Schmittgen, T.D., Lee, E.J., and Jiang, J. (2008). High-throughput real-time PCR. Methods Mol Biol *429*, 89-98.

Scholz, J., and Woolf, C.J. (2002). Can we conquer pain? Nat Neurosci *5 Suppl*, 1062-1067.

Seagrove, L.C., Suzuki, R., and Dickenson, A.H. (2004). Electrophysiological characterisations of rat lamina I dorsal horn neurones and the involvement of excitatory amino acid receptors. Pain *108*, 76-87.

Seidel, M.F., Herguijuela, M., Forkert, R., and Otten, U. (2009). Nerve Growth Factor in Rheumatic Diseases. Semin Arthritis Rheum.

Semenova, S.B., Vassilieva, I.O., Fomina, A.F., Runov, A.L., and Negulyaev, Y.A. (2009). Endogenous expression of TRPV5 and TRPV6 calcium channels in human leukemia K562 cells. Am J Physiol Cell Physiol *296*, C1098-1104.

Severgnini, M., Bicciato, S., Mangano, E., Scarlatti, F., Mezzelani, A., Mattioli, M., Ghidoni, R., Peano, C., Bonnal, R., Viti, F*., et al.* (2006). Strategies for comparing gene expression profiles from different microarray platforms: application to a case-control experiment. Anal Biochem *353*, 43-56.

Shichida, Y., and Morizumi, T. (2007). Mechanism of G-protein activation by rhodopsin. Photochem Photobiol *83*, 70-75.

Sonohata, M., Furue, H., Katafuchi, T., Yasaka, T., Doi, A., Kumamoto, E., and Yoshimura, M. (2004). Actions of noradrenaline on substantia gelatinosa neurones in the rat spinal cord revealed by in vivo patch recording. J Physiol *555*, 515-526.

Stark, K., Dostalek, M., and Guengerich, F.P. (2008). Expression and purification of orphan cytochrome P450 4X1 and oxidation of anandamide. FEBS J *275*, 3706-3717.

Stills, H.F., Jr. (2005). Adjuvants and antibody production: dispelling the myths associated with Freund's complete and other adjuvants. ILAR J *46*, 280-293.

Story, G.M., Peier, A.M., Reeve, A.J., Eid, S.R., Mosbacher, J., Hricik, T.R., Earley, T.J., Hergarden, A.C., Andersson, D.A., Hwang, S.W*., et al.* (2003). ANKTM1, a TRP-like channel expressed in nociceptive neurons, is activated by cold temperatures. Cell *112*, 819-829.

Svensson, C.I., and Yaksh, T.L. (2002). The spinal phospholipase-cyclooxygenase-prostanoid cascade in nociceptive processing. Annu Rev Pharmacol Toxicol *42*, 553-583.

Sweitzer, S.M., Colburn, R.W., Rutkowski, M., and DeLeo, J.A. (1999). Acute peripheral inflammation induces moderate glial activation and spinal IL-1beta expression that correlates with pain behavior in the rat. Brain Res *829*, 209-221.

Tegenge, M.A., and Bicker, G. (2009). Nitric oxide and cGMP signal transduction positively regulates the motility of human neuronal precursor (NT2) cells. J Neurochem.

Timpl, P., Spanagel, R., Sillaber, I., Kresse, A., Reul, J.M., Stalla, G.K., Blanquet, V., Steckler, T., Holsboer, F., and Wurst, W. (1998). Impaired stress response and reduced anxiety in mice lacking a functional corticotropin-releasing hormone receptor 1. Nat Genet *19*, 162-166.

Todd, A.J. (2002). Anatomy of primary afferents and projection neurones in the rat spinal dorsal horn with particular emphasis on substance P and the neurokinin 1 receptor. Exp Physiol *87*, 245-249.

Todd, A.J., McGill, M.M., and Shehab, S.A. (2000). Neurokinin 1 receptor expression by neurons in laminae I, III and IV of the rat spinal dorsal horn that project to the brainstem. Eur J Neurosci *12*, 689-700.

Tominaga, M., Caterina, M.J., Malmberg, A.B., Rosen, T.A., Gilbert, H., Skinner, K., Raumann, B.E., Basbaum, A.I., and Julius, D. (1998). The cloned capsaicin receptor integrates multiple pain-producing stimuli. Neuron *21*, 531-543.

Tseng, G.C., Oh, M.K., Rohlin, L., Liao, J.C., and Wong, W.H. (2001). Issues in cDNA microarray analysis: quality filtering, channel normalization, models of variations and assessment of gene effects. Nucleic Acids Res *29*, 2549-2557.

Tu, H., Rondard, P., Xu, C., Bertaso, F., Cao, F., Zhang, X., Pin, J.P., and Liu, J. (2007). Dominant role of GABAB2 and Gbetagamma for GABAB receptor-mediated-ERK1/2/CREB pathway in cerebellar neurons. Cell Signal *19*, 1996-2002.

Vekovischeva, O.Y., Haapalinna, A., Sarviharju, M., Honkanen, A., and Korpi, E.R. (1999). Cerebellar GABA(A) receptors and anxiolytic action of diazepam. Brain Res *837*, 184-187.

Waldmann, R., and Lazdunski, M. (1998). H(+)-gated cation channels: neuronal acid sensors in the NaC/DEG family of ion channels. Curr Opin Neurobiol *8*, 418-424.

Walzer, T., Galibert, L., and De Smedt, T. (2005). Dendritic cell function in mice lacking Plexin C1. Int Immunol *17*, 943-950.

Wang, E., Miller, L.D., Ohnmacht, G.A., Liu, E.T., and Marincola, F.M. (2000). High-fidelity mRNA amplification for gene profiling. Nat Biotechnol *18*, 457-459.

Wang, E.T., Sandberg, R., Luo, S., Khrebtukova, I., Zhang, L., Mayr, C., Kingsmore, S.F., Schroth, G.P., and Burge, C.B. (2008). Alternative isoform regulation in human tissue transcriptomes. Nature *456*, 470-476.

Wang, H., Kohno, T., Amaya, F., Brenner, G.J., Ito, N., Allchorne, A., Ji, R.R., and Woolf, C.J. (2005). Bradykinin produces pain hypersensitivity by potentiating spinal cord glutamatergic synaptic transmission. J Neurosci *25*, 7986-7992.

Wang, X.M., Hamza, M., Wu, T.X., and Dionne, R.A. (2009). Upregulation of IL-6, IL-8 and CCL2 gene expression after acute inflammation: Correlation to clinical pain. Pain *142*, 275-283.

Warner-Schmidt, J.L., Flajolet, M., Maller, A., Chen, E.Y., Qi, H., Svenningsson, P., and Greengard, P. (2009). Role of p11 in cellular and behavioral effects of 5-HT4 receptor stimulation. J Neurosci *29*, 1937-1946.

Welch, J.M., Simon, S.A., and Reinhart, P.H. (2000). The activation mechanism of rat vanilloid receptor 1 by capsaicin involves the pore domain and differs from the activation by either acid or heat. Proc Natl Acad Sci U S A *97*, 13889-13894.

Westlund, K.N., Bowker, R.M., Ziegler, M.G., and Coulter, J.D. (1982). Descending noradrenergic projections and their spinal terminations. Prog Brain Res *57*, 219-238.

Widmann, C., Gibson, S., Jarpe, M.B., and Johnson, G.L. (1999). Mitogen-activated protein kinase: conservation of a three-kinase module from yeast to human. Physiol Rev *79*, 143-180.

Willis, W.D., Jr. (2007). The somatosensory system, with emphasis on structures important for pain. Brain Res Rev *55*, 297-313.

Woolf, C.J., Allchorne, A., Safieh-Garabedian, B., and Poole, S. (1997). Cytokines, nerve growth factor and inflammatory hyperalgesia: the contribution of tumour necrosis factor alpha. Br J Pharmacol *121*, 417-424.

Woolf, C.J., and Fitzgerald, M. (1983). The properties of neurones recorded in the superficial dorsal horn of the rat spinal cord. J Comp Neurol *221*, 313-328.

Woolf, C.J., Safieh-Garabedian, B., Ma, Q.P., Crilly, P., and Winter, J. (1994). Nerve growth factor contributes to the generation of inflammatory sensory hypersensitivity. Neuroscience *62*, 327-331.

Woolf, C.J., and Salter, M.W. (2000). Neuronal plasticity: increasing the gain in pain. Science *288*, 1765-1769.

Workman, C., Jensen, L.J., Jarmer, H., Berka, R., Gautier, L., Nielser, H.B., Saxild, H.H., Nielsen, C., Brunak, S., and Knudsen, S. (2002). A new non-linear normalization method for reducing variability in DNA microarray experiments. Genome Biol *3*, research0048.

Yacubova, E., and Komuro, H. (2003). Cellular and molecular mechanisms of cerebellar granule cell migration. Cell Biochem Biophys *37*, 213-234.

Yaksh, T.L., Yeung, J.C., and Rudy, T.A. (1976). Systematic examination in the rat of brain sites sensitive to the direct application of morphine: observation of differential effects within the periaqueductal gray. Brain Res *114*, 83-103.

Yang, Y.H., Dudoit, S., Luu, P., Lin, D.M., Peng, V., Ngai, J., and Speed, T.P. (2002). Normalization for cDNA microarray data: a robust composite method addressing single and multiple slide systematic variation. Nucleic Acids Res *30*, e15.

Yang, Y.H., and Speed, T. (2002). Design issues for cDNA microarray experiments. Nat Rev Genet *3*, 579-588.

Yates, T., Okoniewski, M.J., and Miller, C.J. (2008). X:Map: annotation and visualization of genome structure for Affymetrix exon array analysis. Nucleic Acids Res *36*, D780-786.

Yoshimura, M., and Jessell, T.M. (1989a). Membrane properties of rat substantia gelatinosa neurons in vitro. J Neurophysiol *62*, 109-118.

Yoshimura, M., and Jessell, T.M. (1989b). Primary afferent-evoked synaptic responses and slow potential generation in rat substantia gelatinosa neurons in vitro. J Neurophysiol *62*, 96-108.

Zhang, X., Beaulieu, J.M., Sotnikova, T.D., Gainetdinov, R.R., and Caron, M.G. (2004). Tryptophan hydroxylase-2 controls brain serotonin synthesis. Science *305*, 217.

Zhu, B., Ping, G., Shinohara, Y., Zhang, Y., and Baba, Y. (2005). Comparison of gene expression measurements from cDNA and 60-mer oligonucleotide microarrays. Genomics *85*, 657-665.

7. Acknowledgements

To Prof. Dr. Kurt Bürki: Thank you for giving me the opportunity to join the LTK, and for your support during the course of this project. I am very grateful for the chance you have given me to learn and to develop my scientific knowledge in your institute.

To Dr. Paolo Cinelli: Thank you so much for your trust and guidance through the course of this project. I am very grateful for everything! You have always been very involved and interested in my work and have supported me through the good and the difficult times of this project… Thank you also for the scientific conversations, and the friendly atmosphere you have created in your lab!

To Prof. Dr. Sonderegger and Prof. Dr. Hanns Ulrich Zeilhofer: Thank you for being part of my committee, for your interest in my work and for your interesting suggestions.

To Dr. Margarete Arras: Thank you for your guidance and your help throughout this project! Thank you also for all the surgeries you have performed for my analyses, and for having given me the opportunity to assist to them.

To Dr. Hans Peter Käsermann: Thank your for giving me the chance to join the Module 1 as a tutor. It was a fantastic experience! Thank you for the good atmosphere, for your interest in my work, and for your good advice.

I am fortunate enough to have the best family one could ever imagine! They were there for me at each step of the project, shared my joys, pains, and gave me the best guidance I could imagine…

To Jagoda Asner, my mother: Mama moja! Hvala ti na svemu! Je t'aime du fond du coeur et je te remercie pour tout ton soutien à travers ces années. Quel chemin parcouru!! Tu as constamment été là et tu as fait tout ton possible pour m'aider à surmonter les moments les plus durs. Merci! J'ai de la chance d'avoir la meilleure mère au monde! Volim te!!

To Sandra Asner, my sister: Sandra, ma soeur adorée! Merci pour ton soutien, tous les rires qu'on a partagé, et merci pour avoir été là dans des moments de doutes. J'ai toujours pu me confier à toi et ton avis m'a toujours été d'une grande aide. Merci pour les rires partagés à Genolier depuis toujours. Merci d'être là pour moi à chaque fois, et merci pour cette complicité unique qu'on partage. J'ai vraiment de la chance de t'avoir! Je t'aime très fort!

To Rajna Gibson-Brandon, my sister: Rajna, ma soeur que j'adore!! Merci pour toute la compréhension, et le soutien que tu m'as apporté pendant ces années. Tes conseils ont valu de l'or pour moi!! "La these, c'est un tunnel…" Merci pour tout ce que tu as fait pour moi! Merci aussi pour tous les dîners, les Starbucks, les rires, les larmes et tout ce qu'on partage au quotidien. Quel chance d'avoir une soeur comme toi! Je t'aime très fort!

To Jim Brandon, my brother in law: Jim, you're my best friend ever! Thank you for the endless conversations about everything. Thanks you for having taken time to talk to me, to encourage me, and to challenge me. Thank you also for kicking me in the ass when I was being a whiner! Thank you for always being there for me since my teenage years. I don't know where I would be without you! And you know what? Thank you for pushing me to do a PhD! Never thought you'd read that, huh?

To Tess Brandon, my wonderful niece: Tess! You were a baby when I first arrived in Zurich and look at you now: an amazing little girl! You're the sunshine in all our lives, and seeing your smile erases all traces of a bad day I might be having. I love you from the bottom of my heart and can't wait to see what beautiful surprises the future will bring you!

To Berislav Krizanic: Berislav, dragi moj! Hvala ti za tvoj interes I tvoju pomoc! Uvjek si se interesirao za mene i za moj posao. Nasi razgovori su mi uvjek dobro cinili i pomogli su mi da dobijem neku perspektivu kad mi je to naj vise trebalo.

In loving memory of my father, Fred Asner.

As anyone knows, doing a PhD is an adventure of its own and a vast learning process. I have the fondest memories of the years I have spent at the Institute of Laboratory Animal Science. I would therefore like to thank the following people for their friendship and constant support…

To Aline Widmer: Aline, meene Lekkerste! Thank you for everything!! I was lucky enough to meet my best friend in Zurich during the course of my PhD. You shared the best times with me, but you were also there through the toughest and most challenging times I had to face. I will never forget your support! For the Monday seminars, the "Léschär" products and the Labyrinth, but also for Amsterdam, Madonna, Dublin and Lady Gaga. The future has a lot to bring!!

To Elisa Casanova: Elisa, cara mia! What can I say?! You were with me from the beginning… Thank you so much for all the conversations and advice on scientific and not-so-scientific subjects. For all the laughs, the shared frustrations, and the help we have given to each other during in past 4 years. For the estrus controls, and for the long talks about… well… about everything really! Grazie Mille!! E a presto, no?

To Dr. Dagmar Schäfer: Dagmar! First and foremost, thank you for your friendship, and all our laughs at our coffee breaks. But also, thank you for the interesting work we have done together with our poor little mice! For the hours spent with hotplates, scoresheets and bat detectors, but also for our dinners and long scientific talks about everything but science…

To Fabienne Weber: Fabienne! Thank you for the fantastic atmosphere you have brought to the lab. It was always a pleasure to spend time with you! For the talks, the coffee breaks and also for the kirsch! Best of luck with your PhD!

To Urs Graf: Jo, ebbe Urs… Thank you very much for the laughs, the imitations, the great atmosphere you have created every day, and for the guitar tips! I wish you the best of luck with your PhD!

To Jon Paulin Zumthor: This Paulin… Thank you for all the shared laughs, the interesting conversations about the life's ups and downs, and for the unexpected encounters at parties!

To Nicole Konrad: Thank you for all the talks we had in the lab or around a cup of coffee. Thanks for the laughs despite the stressful times that research brings. Thank you also for your support during some the hardest parts of this project!

To Zsuzsi Pataki: Draga Zsuzsi! Hvala ti na svemu! I have always enjoyed our conversations, and will never forget your support throughout those years.

To Sameera Patel: Thank you for the nice talks, and the good laughs we have shared. Best of luck with your PhD!

To Dr. Rossana Scavelli, and Dr. Priska Lochmatter: Thanks for the great atmosphere you have created when I first joined the LTK! It was a pleasure to work with you!

To Gregor Fischer, Manuela Buholzer, Manuela Dittrich, Regula Dähler, Li Wegmann, Ursi Makanzu and everyone at the LTK: Thank you for all your support and the unique work atmosphere you have created every day!

To Catharine Aquino-Fournier: Thank you for your help with the spotting, the dyes, for taking time to talk to me when I was facing spot-smearing, dye imbalances, or any other events which makes the everyday life of microarray research. Thank you for your friendship, for the lovely dinners, and for your support. And last but not least, thank you for your help with the Exon arrays!

To Dr. Hubert Rehrauer and Dr. Michal Okoniewski: Thank you very much for all your help and guidance in bioinformatics and statistics!

To Prof. Dr. Burkhardt Seifert: Thank you very much for helping me with the statistical analysis of my Real-Time PCR data!

Last but not least… To my closest friends who have been here through all the phases of this project! I love each and every single one of you!

Valérie Moynat, Ludovic Amiguet, Roberto Greco, Daniele Pintaudi, Luc Jaccard, Bruno Stalder, Neven Jeremic, Olivier Freiburghaus, Mandoline Whittlesey, Simone Von Burg, Beat Käser, Martti Wichmann, Fridtjof Flucke, Nicole Greensil and Jean-Sebastien Clément.

And also…

To Dr. Gunhild Hoffmann: Thank you for everything.